NASA Conference Publication 2344

Global Scale Atmospheric Processes Research Program Review

Abstracts of a program review held at
the NASA Goddard Space Flight Center
Greenbelt, Maryland
August 8-10, 1984

NASA

NASA Conference Publication 2344

Global Scale Atmospheric Processes Research Program Review

Edited by
Barbara A Worley and Cindy Peslen
Goddard Space Flight Center

Abstracts of a program review sponsored by the Global Scale Atmospheric Processes Program, National Aeronautics and Space Administration, and held at NASA Goddard Space Flight Center
Greenbelt, Maryland
August 8–10, 1984

NASA
National Aeronautics
and Space Administration

Scientific and Technical Information Branch

1984

Page intentionally left blank

FOREWORD

This report documents the presentations at the NASA Global Scale Atmospheric Processes Research Program Review held at the Goddard Space Flight Center 8-10 August 1984. The purpose of the Review was to provide a forum for the evaluation of the Global Scale Atmospheric Processes Research Program by NASA Headquarters management. The ongoing in-house research program at Goddard primarily in the Global Modeling and Simulation Branch of the Laboratory for Atmospheric Sciences, as well as NASA-supported research at universities and other institutions was reviewed.

A synopsis of each research topic presented at the Review is contained in this document. The format has been standardized to highlight the research objectives, significant accomplishments, future plans, and relevant publications of each investigator. It is hoped that this report will provide a useful reference for the material presented at the Review.

Eugenia Kalnay
Head, Global Modeling and Simulation Branch
Goddard Space Flight Center

Page intentionally left blank

TABLE OF CONTENTS

VI. DYNAMICS OF PLANETARY WAVES

VII. FGGE DIAGNOSTIC STUDIES

VIII. NATIONAL RESEARCH COUNCIL RESEARCH ASSOCIATESHIP PROGRAM

AUTHOR INDEX

I. GLOBAL MODELING

Page intentionally left blank

GLAS FOURTH ORDER MODEL
(E. Kalnay-GSFC)

RESEARCH OBJECTIVE:

To develop and maintain a general circulation model for numerical weather prediction, analysis and forecast impact experiments, stratospheric analysis and extended range weather forecasting.

SIGNIFICANT ACCOMPLISHMENTS:

One of the two general circulation models (GCM's) presently available at the Global Modeling and Simulation Branch is the GLAS Fourth Order Model, originally described in Kalnay-Rivas et al. (1977) and Kalnay and Hoitsma (1979). The UCLA model, developed by Arakawa, Suarez, Randall and collaborators is also available at GLAS.

The GLAS Fourth Order Model has been extensively used in the GLAS Analysis/Forecast System, in satellite data assimilation and weather forecast impact studies. It has proven to be a reasonably accurate forecast model even at the coarse resolution of four degrees latitude by five degrees longitude and nine vertical levels, because of its higher order horizontal differences; its reproduction of the circulation of the atmosphere is comparable to some of the best currently used general circulation models. Figs. 1-6 present the average of the last 30 days of 45 days winter and summer integrations, started from ECMWF analysis for 15 December 1978 and 15 June 1979 respectively. For comparison, observed and climatological fields are also presented.

The model reproduces most of the atmospheric stationary circulations, both at sea level and at 500 mb, and in some cases, as could be expected, is closer to climatology than to the observed monthly averages for 1979. Some deficiencies in the simulations are also apparent. In January, we note excessive westerlies at sea level over western Europe and Canada, at 500 mb there is a gross underestimation of the Atlantic ridge, and the precipitation rate (hatched wherever it is larger than 4 mm/day) tends to be somewhat excessive and extends too much into the Saharan and Australian deserts. In the July integration the model has too intense surface lows over Labrador, central Europe and north of Japan. On the other hand, at 500 mb, the model has captured rather well the most important anomaly of the July 79 circulation: the intense blocking over central Europe and Scandinavia. In the summer precipitation, there is again some overestimation, especially in the extension of convective precipitation south of the equator over South America and Africa.

This baseline model used in the forecast experiments and in the above climatology, has been thoroughly documented (NASA Technical Memorandum 86064), including not only detailed descriptions of the hydrodynamics and physics formulations, but, equally important, sections devoted to user's guide and code management procedures. A "user friendly" system guides a new user into the procedures for running the model and modifying its code for experimental runs. The documentation also includes a thorough description of input climatological fields and the default output fields, both prognostic and diagnostic, and an indication on how to modify the choice of output diagnostic fields.

CURRENT RESEARCH AND FUTURE PLANS:

The model is also undergoing major developments: 1) A 2° x 2.5° x 9 level version has been developed by J. Pfaendtner and collaborators and the impact of several definitions of the orography is being studied. This version will be used for high resolution analysis/forecast experiments; 2) A new model of the PBL with higher vertical resolution and a Monin-Obukhov parameterization of surface fluxes and a second order closure scheme to describe turbulent vertical flux has been developed and is undergoing implementation by M. Helfand and collaborators; 3) A stratospheric-tropospheric version of the model has been developed by Geller, Chao, Takano and collaborators. It is used in the stratospheric-tropospheric analysis cycle and is presently being converted to the Cyber 205 computer.

The model described in the documentation is available to outside investigators who may want to use it for atmospheric dynamics research. NASA has recently funded a proposal to allow members of universities to take advantage of this opportunity and come to NASA for a period of up to a few months in order to become familiar with the model and its use. Examples of possible research are climate sensitivity studies, in which the boundary forcing is modified, changes in the parameterization, changes in the numerical schemes, weather prediction experiments, etc. Some of the studies of this type are already being performed, both within the branch and outside, and will be discussed at the meeting.

TECHNICAL PUBLICATIONS:

Kalnay, E., R. Balgovind, W. Chao, D. Edelmann, J. Pfaendtner, L. Takacs and K. Takano, 1983: Documentation of the GLAS Fourth Order General Circulation Model. 3 volumes. NASA Tech. Memo. 86064.

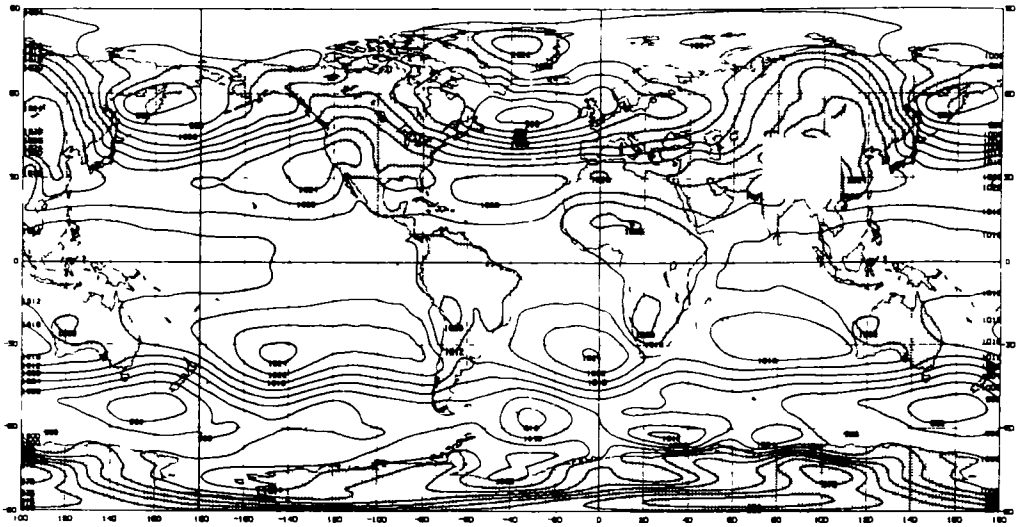

Simulated Sea Level Pressure (mb) - January

Fig. 1

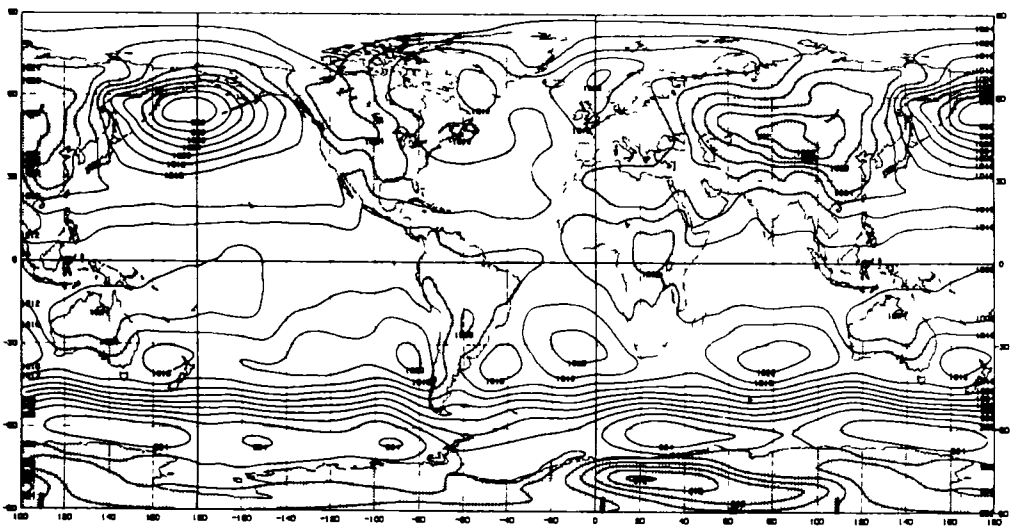

Observed Sea Level Pressure (mb) - January 1979

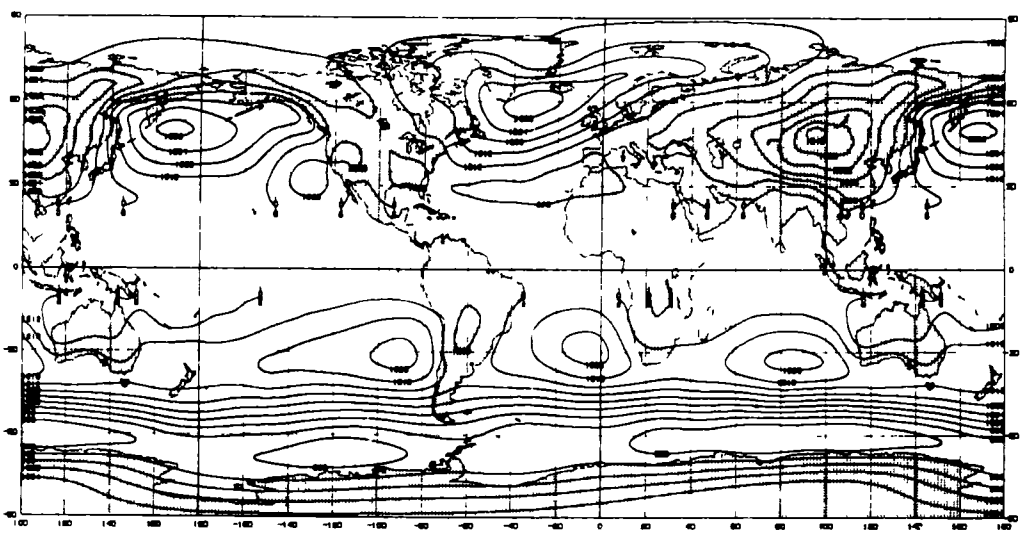

Climatological Sea Level Pressure (mb) - January
(no data between 20°N and 10°S)

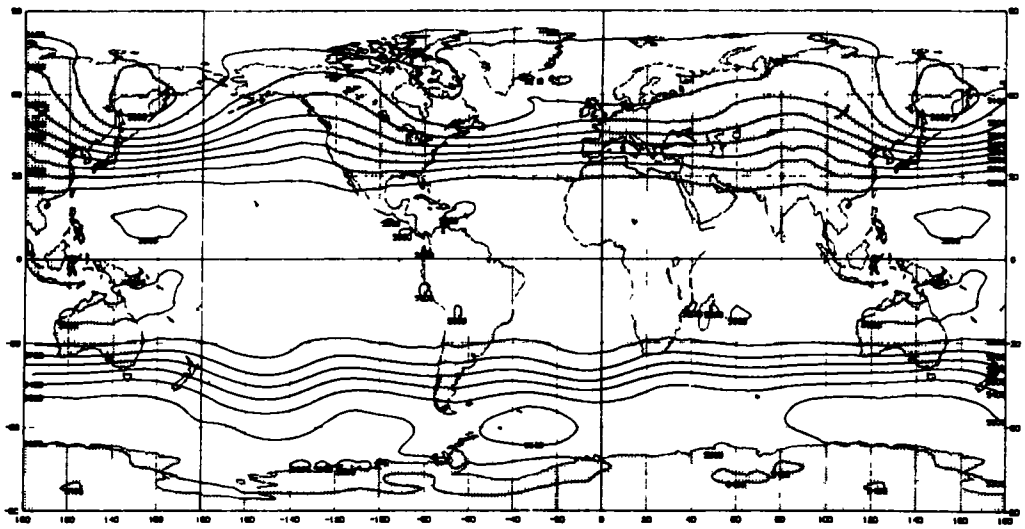

Simulated 500 mb Geopotential Height (m) - January

Fig. 2

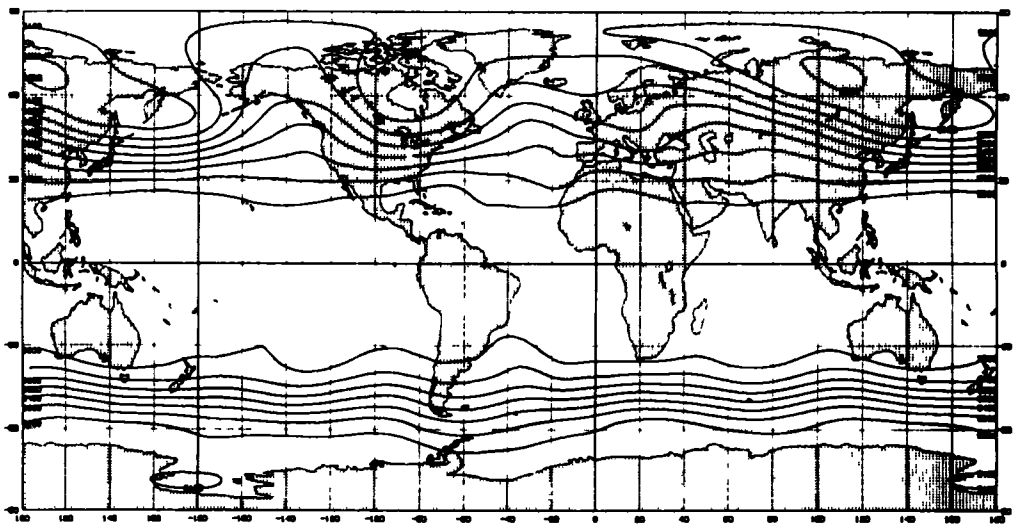

Observed 500 mb Geopotential Height (m) - January 1979

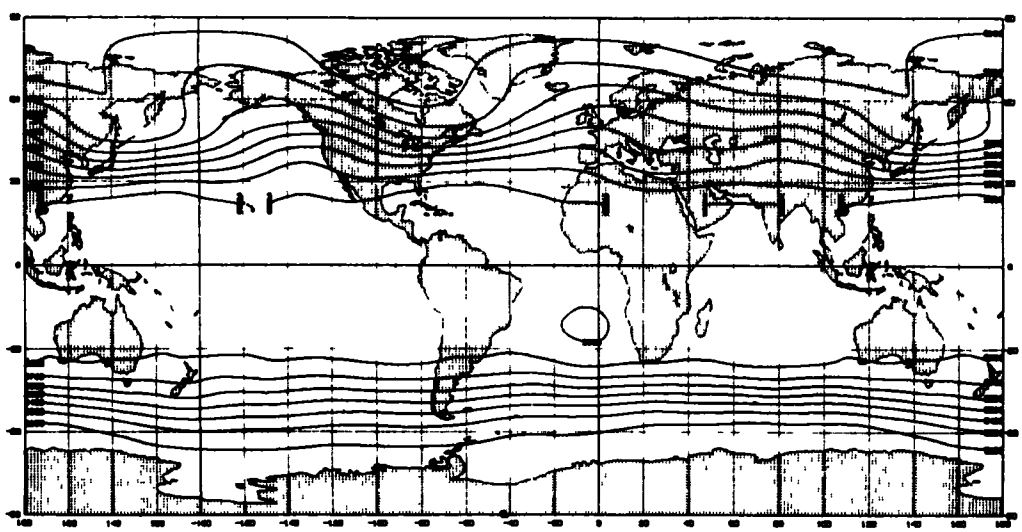

Climatological 500 mb Geopotential Height (m) - January
(no data between 20°N and 10°S)

Fig. 3

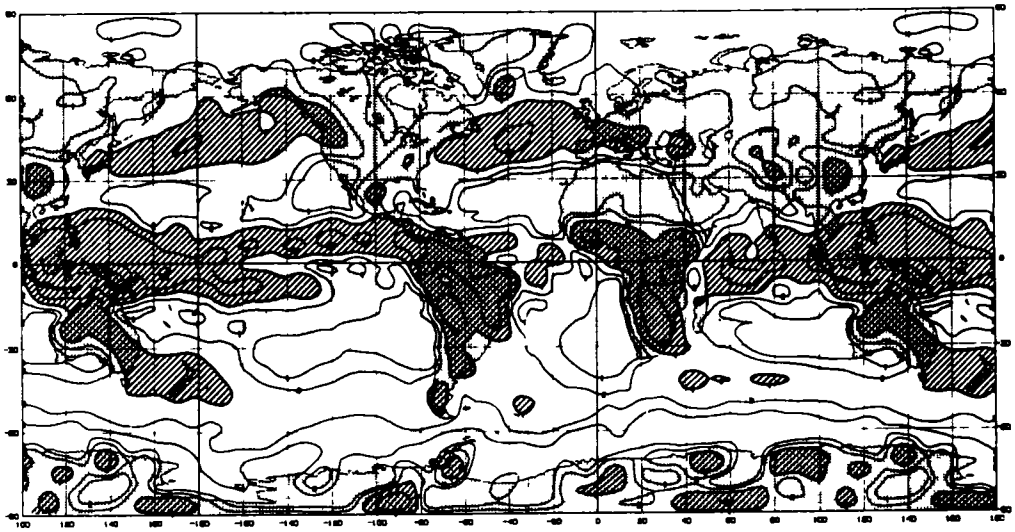

Simulated Precipitation Rate (mm/day) - January

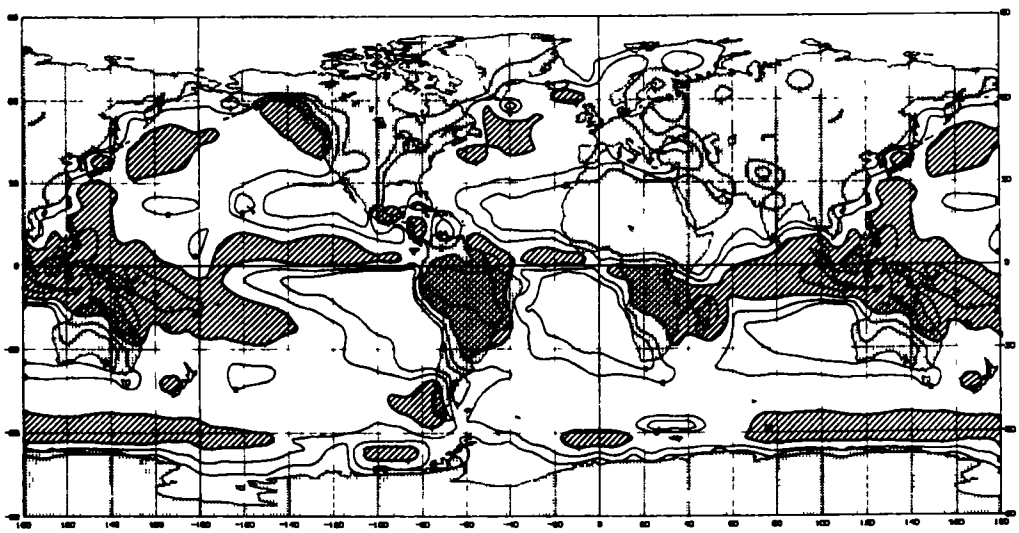

Climatological Precipitation Rate (mm/day) - January

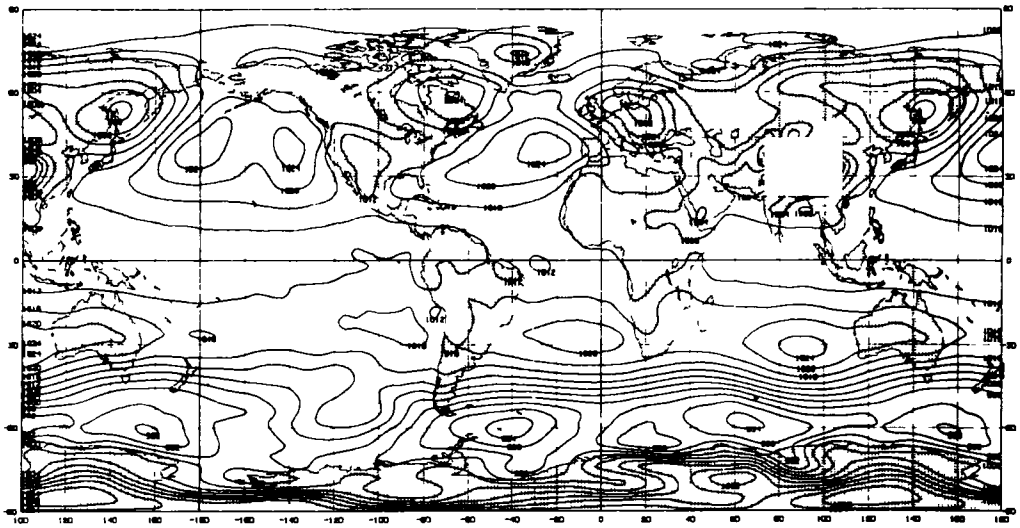

Simulated Sea Level Pressure (mb) - July

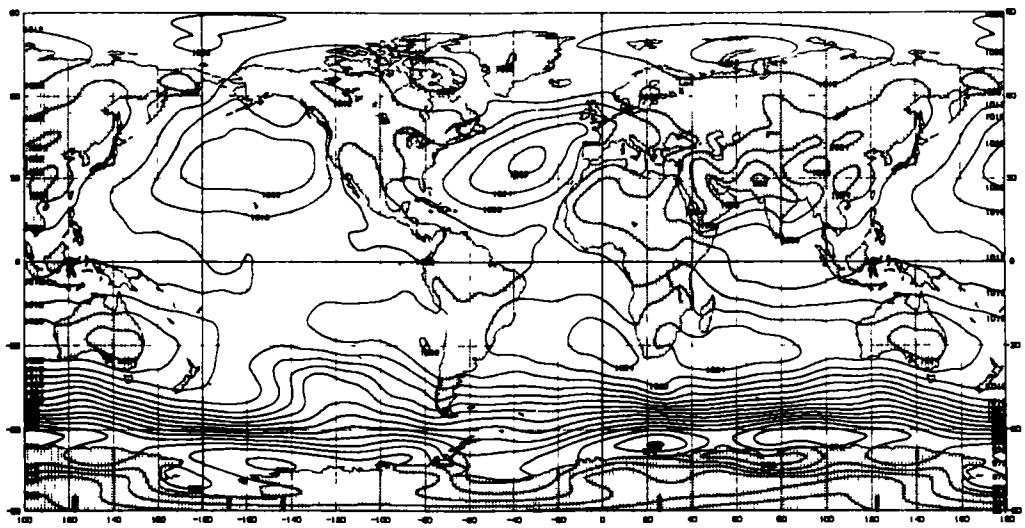

Observed Sea Level Pressure (mb) - July 1979

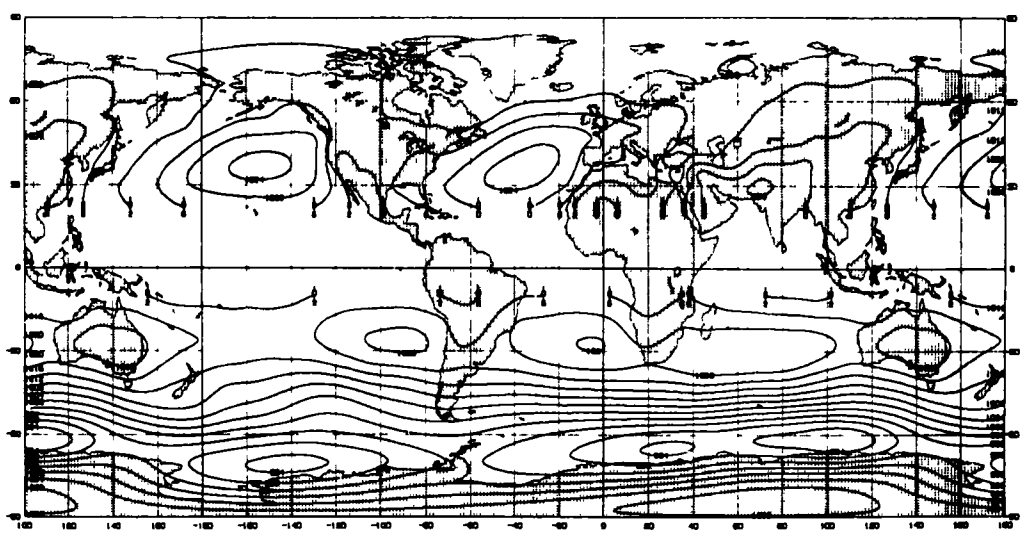

Climatological Sea Level Pressure (mb) - July
(no data between 20°N and 10°S)

Fig. 4

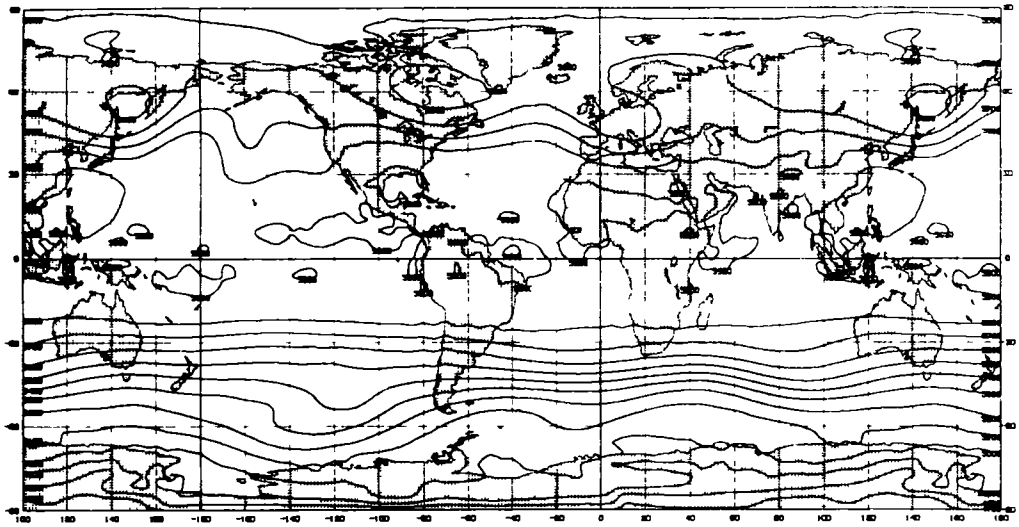

Fig. 5

Simulated 500 mb Geopotential Height (m) - July

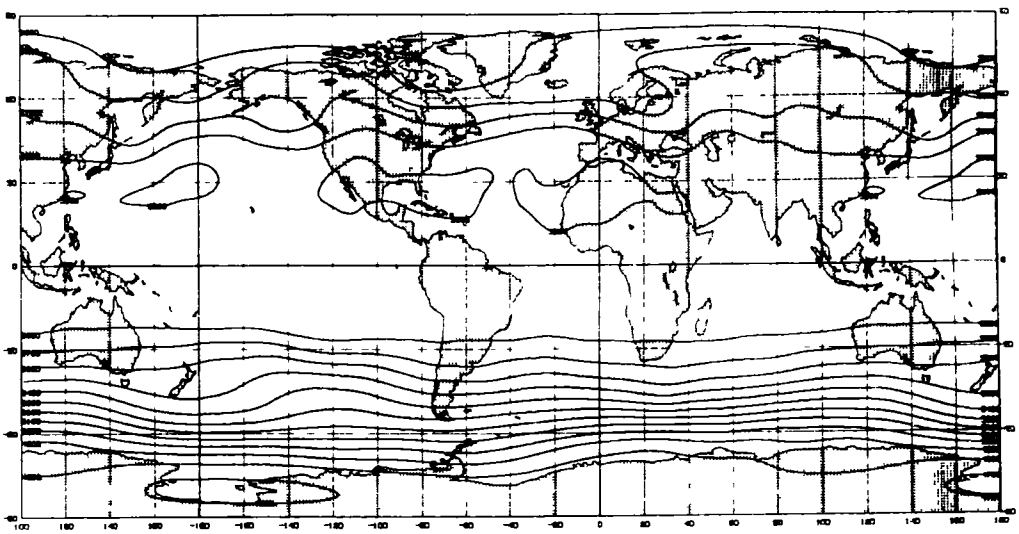

Observed 500 mb Geopotential Height (m) - July 1979

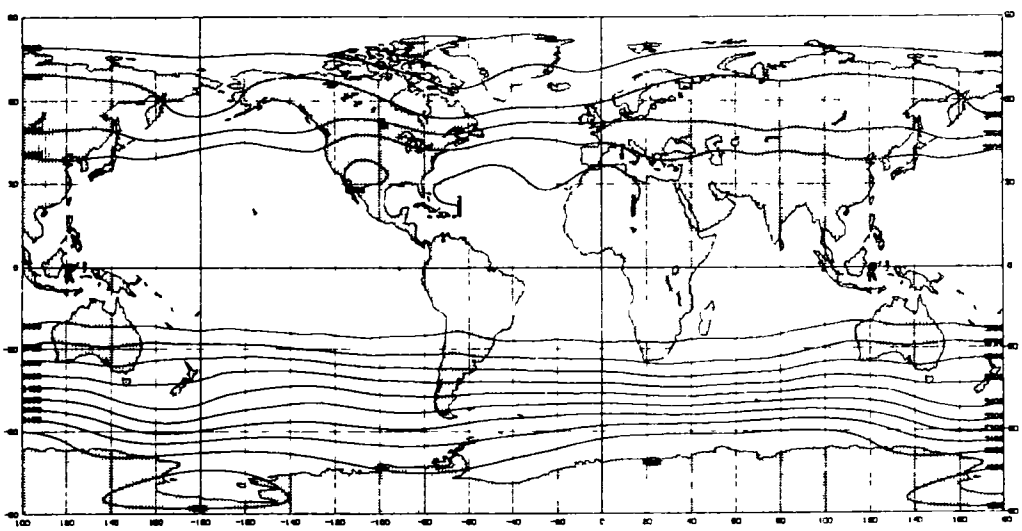

Climatological 500 mb Geopotential Height (m) - July
(no data between 20°N and 10°S)

Fig. 6

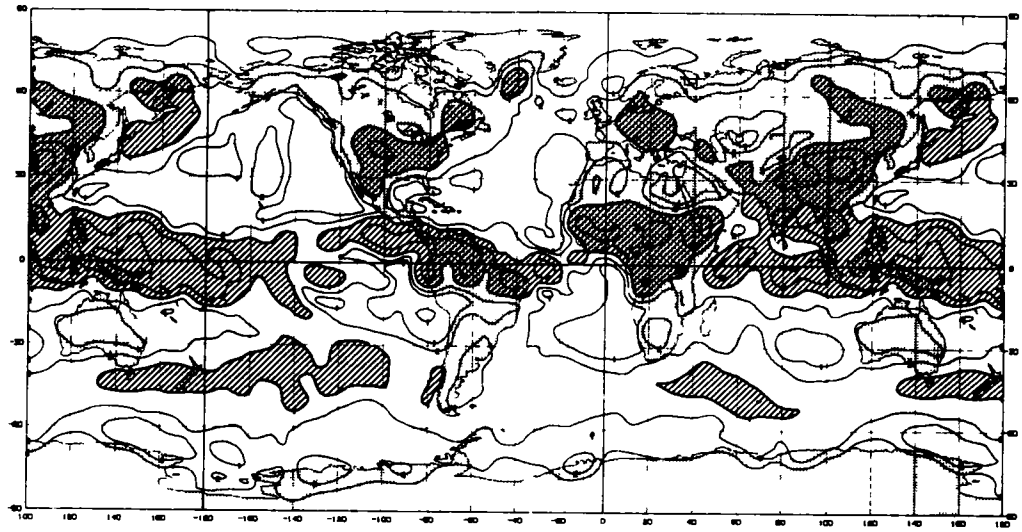

Simulated Precipitation Rate (mm/day) - July

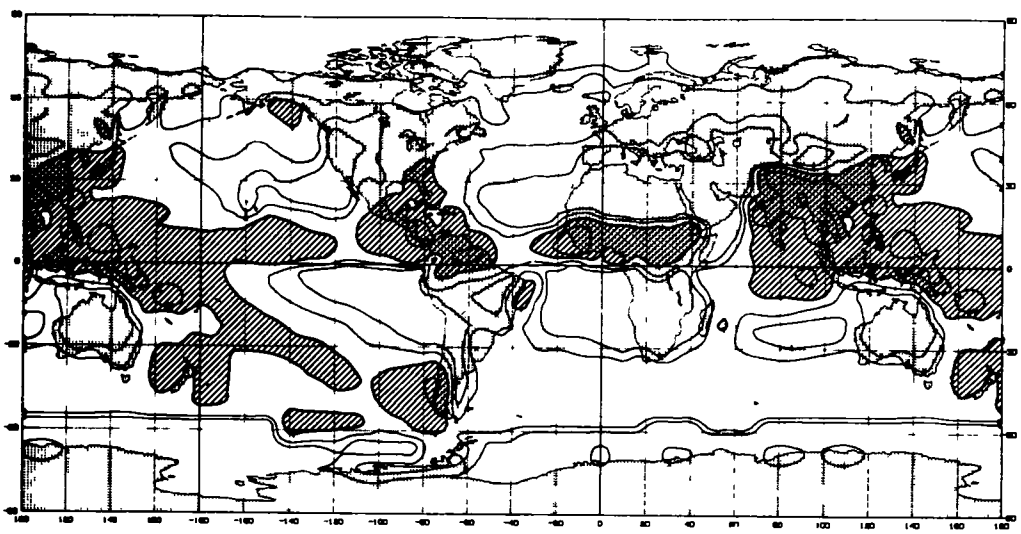

Climatological Precipitation Rate (mm/day) - July

OROGRAPHIC EFFECTS IN ATMOSPHERIC CIRCULATION
(D. G. Duffy-GSFC)

RESEARCH OBJECTIVES:

The objective of this investigation is to study the role of orography on the large-scale and regional atmospheric circulation, with special emphasis on lee cyclogenesis. These studies include effects observed in the actual atmosphere as well as in numerical weather prediction and general circulation models.

SIGNIFICANT ACCOMPLISHMENTS:

Using a new orographic field at a resolution of 10' by 10', several new topography fields have been generated for numerical experiments with the GLAS fourth-order GCM. These topographic fields differ in the manner in which small-scale fluctuations have been eliminated. Several five-day numerical forecasts with different topographies have been made and significant differences have been observed. Currently, we are trying to determine which form of the topography gives the best forecasts and the reason it does so.

Despite the tardiness of the data from the special experiment run over the Alps during March and April 1982 (ALPEX), we have completed formatting the special aircraft data and have begun to test this data in our analysis system. Furthermore, we have begun to calculate GLAS temperature sounds for the ALPEX region. These will be included in our analysis of ALPEX events.

FUTURE PLANS:

We plan to develop a regional SCM (successive correction method) analysis so that we can perform an analysis of the ALPEX region with these enhanced data. These will be used as initial conditions for several short (up to 48 h) forecasts over the ALPEX region. By shutting off several different physical parameterizations, we will determine what physical processes are important in lee cyclogenesis.

We intend to create envelope topographies for experiments with the 4th-order GCM. We have had difficulties in formulating one of these envelopes because the standard deviations of the fine-scale topography over the Andes Mountains is too large to produce a realistic envelope topography in that region. We will be working to eliminate this problem.

SPECTRAL GENERAL CIRCULATION MODEL DEVELOPMENT

(S. A. Orszag, R. L. McCrory, C. P. Verdon-Cambridge Hydrodynamics, Inc., Cambridge, MA)

RESEARCH OBJECTIVES:

We are developing a spectral general circulation model to run on the Cyber 205 computer system installed at the NASA Goddard Space Flight Center. This model should enhance the utility of satellite-based observation systems for accurate long-range numerical weather prediction.

SIGNIFICANT ACCOMPLISHMENTS:

The present code solves the primitive equations as formulated in the GLAS Fourth Order General Circulation Model (NASA Technical Memorandum 86064) and has been written to be compatible with the history files for the model which employs equally space θ- and ϕ-locations. The code is compatible with the physical process packages developed for the GLAS fourth-order GCM, so that newly improved physics packages should be 'plug-compatible' with our spectral GCM. The high resolution spectral GCM we have developed for the Cyber 205 incorporates vector spherical harmonic transforms (McCrory, Orszag and Verdon, 1984) which treat the pole problem (Orszag, 1974) in a completely natural way. The vector spherical harmonic transform packages have been vectorized for the Cyber 205 and use the FFT77 codes (multiple fast real periodic Fourier transforms) developed by Temperton for the Cyber 205. The code has been written in both in-core and out-of-core versions, the latter involving multiple buffering of 'super-layers' between central and secondary memory. This multiply buffered version has been designed to run with up to about 64 x 128 modes in each of up to about 40 horizontal layers.

Accuracy of the code, including the interpolation routines required to load the equally-spaced history file data, has been verified using normal model initial conditions (Chao and Geller 1982; Kasahara, 1976). Hough function initialization tests have been used to compare spectral- and pseudospectral-models for the code. We have determined that the pseudospectral model will probably give the most efficient GCM.

FUTURE PLANS:

Our next step is to use the spectral code in comparison runs with the GLAS Fourth Order GCM. A final determination of the desirability of 32 vs 64-bit arithmetic and pseudospectral methods will be made for the high-resolution code.

In addition to tests of the code on real data, several additional aspects of this development work are now under way. First, spectral methods to improve the vertical resolution for the GCM are under study. Second, we have shown how to use spectral patching and element methods to accomplish efficient limited area modeling. These techniques will be tested on specific atmospherical applications. Finally, a complete set of user documentation for both the in-core and out-of-core spectral GCMs will be completed over the next year.

TECHNICAL PUBLICATION:

McCrory, R. L., S. A. Orszag and C. P. Verdon, 1984: Pseudospectral and spectral general circulation models based on vector harmonics, CHI Report No. 84.

BIOSPHERE/ATMOSPHERE INTERACTIONS
(Y. Mintz-Univ. of Maryland)

The starting point, in this collaborative research effort by Y. Mintz, P. J. Sellers, Y. C. Sud and C. J. Willmott, was the recognition that vegetation influences the energy, mass and momentum exchange between land-surface and atmosphere and, in that way, may significantly affect weather and climate. The morphology and physiology of the vegetation determine the surface albedo, precipitation interception and interception loss, stomatal control of transpiration, moisture storage in the root zone and, through the vegetation roughness height, the aerodynamic resistance to the transfers of latent and sensible heat and momentum between land-surface and atmosphere.

That the albedo and soil moisture have a large influence on the atmospheric circulation and rainfall has been demonstrated in sensitivity experiments with general circulation models. (Eleven of such experiments, made with different GCMs, have been reviewed and compared by Mintz, 1984). Moreover, we can now show that through its effect on the convergence of the horizontal water vapor transport in the planetary boundary layer, the surface roughness height has a large influence on rainfall.

I.

Fig. 1, from the paper by Sud, Shukla and Mintz (1984), shows the change in the convergence of the horizontal water vapor transport in the lowest model layer, $[-\nabla \cdot \overline{vq}]_9$, (bottom panel), and the change in the precipitation (top panel), when, in the 1982 version of the GLAS climate model, the land-surface roughness height was changed from everywhere having about the average roughness height for all vegetation types, z_0 = 45 cm, to the roughness height of the oceans, z_0 = 0.02 cm. (This change in z_0 produces about the same relative reduction in surface stress as would a change from the value of z_0 for a tropical forest to the value of z_0 for a desert). In the subtropical and higher latitudes, the effect on the boundary layer convergence is due primarily to larger cross-isobaric flow when the surface roughness is larger. Near the equator, where the horizontal pressure gradient is very small and the coriolis acceleration vanishes, the change in the boundary layer convergence is due primarily to larger downstream reduction of the wind speed when the surface roughness is larger. The resulting change in rainfall, of up to 4 mm/day and more, exceeds the natural variability of this climate model.

Currently, Mintz and Sud are investigating how simulations and predictions of weather and climate with the GLAS 4th order GCM (Kalnay et al, 1983) will be affected when the land-surface drag coefficient in that model is changed to correspond with the vegetation roughness heights that are given by Baumgartner et al, (1977), where z_0 is less than 1 cm in the desert areas and more than 200 cm in the tropical rainforests.

II.

The strategy for parameterizing the biosphere for general circulation models was given in the technical memorandum by Mintz, Sellers and Willmott (1983).

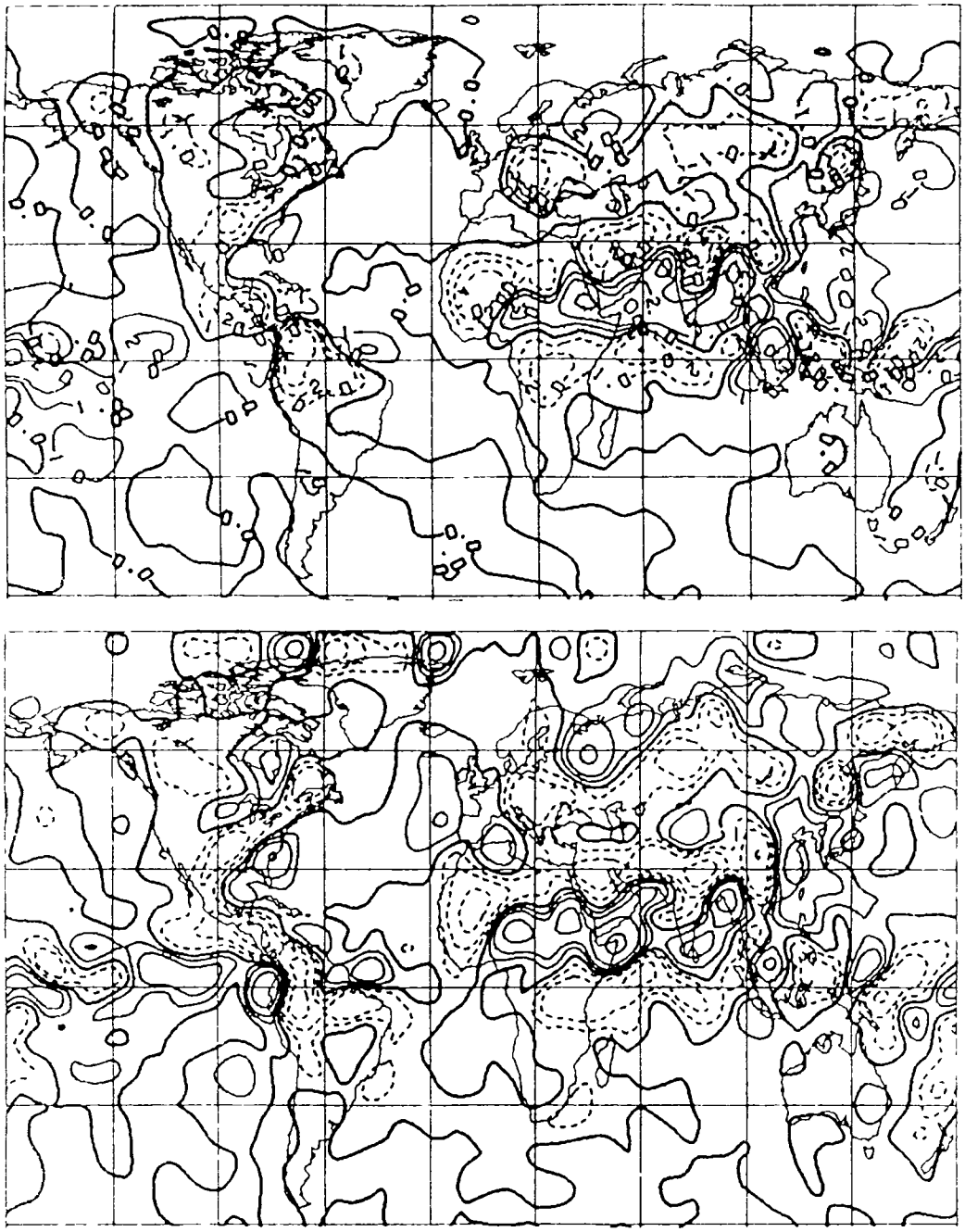

Fig. 1. Average for three Julys, when the land surface roughness height is changed from z_o = 45 cm to z_o = 0.02 cm.

Bottom panel difference in the convergence of the horizontal water vapor transport in the lowest model layer, $[-\nabla \cdot \rho q]_g$.

Top panel difference in the precipitation.

Each panel shows the smooth surface (z_o = 0.02 cm) case minus the rough surface (z_o = 45 cm) case. Contours for 0, $\pm$ 1, $\pm$ 2, $\pm$ 4, $\pm$ 8, $\pm$ 12, $\pm$ 16 (mm/day.) Heavy line is zero. Broken line contours show negative values.

The two fundamental design criteria were:

A: That the albedo, precipitation-interception capacity, stomatal control of transpiration, soil moisture storage capacity, and surface roughness height, shall not be independently prescribed parameters: but that all of them shall be functions of the morphological and physiological characteristics of the vegetation. Inasmuch as the vegetation physiology and morphology depend on the weather and climate, this will make the biosphere interactive with the atmosphere.

B: That the biosphere will be made interactive with the atmosphere in three phases:

Phase 1. a) the vegetation physiology will be interactive with the atmosphere and soil moisture, and b) vegetation morphology will be prescribed.

1:a means that the stomatal resistance will depend on the atmospheric state (i.e., on the incident photosynthetically active radiation, air temperature and air relative humidity) as well as on the soil moisture. Thus (unlike in the present "open bucket" land-surface formulations), there will be no transpiration at night and no very large transpiration when the air is very hot or very dry. 1:b means that the vegetation leaf area density as a function of height and the root length density as a function of depth will be completely prescribed as functions of location and time.

Phase 2. a) again, the vegetation physiology will be interactive with the atmosphere and soil moisture; and b) the morphology of the vegetation formations will be prescribed, but the phenological state of the vegetation morphology will be made interactive with the atmosphere and soil moisture. 2:b means that the phenological changes in leaf area density and root length density and, thereby, all of the landsurface properties that depend on them (albedo, precipitation interception, bulk stomatal resistance, soil moisture availability, and surface roughness height) will be interactive with the atmosphere and soil moisture.

Phase 3. (to be undertaken only if the two preceding phases are successful) All aspects of the vegetation physiology and morphology will be interactive with the atmosphere and soil moisture. This means that on the time scale of the order of 10^0 to 10^2 years the vegetation formations will be prognostic components of the climate model.

The formulation of the biosphere for Phase 1 has been nearly completed and will appear, shortly, in a technical memorandum by Sellers et al. (1984). A schematic of this simple biosphere (SiB) is shown in Fig. 2.

Sellers is currently testing the biosphere formulation offline, with atmospheric data taken from two field experiments: i) over a wheat and barley crop in Europe and ii) over a forest in the Amazon basin.

The next step will be to incorporate SiB into the GLAS 4th order GCM (Kalnay, et al., 1984). Initially, SiB will be allowed to respond to the atmospheric forcing taken from some preceding climate simulations with the GCM: which is to say, the atmosphere will be non-interactive and will not respond to the latent, sensible and upward longwave radiative heat transfers, nor to the momentum transfer, which SiB produces. Studying the behavior of SiB in this way

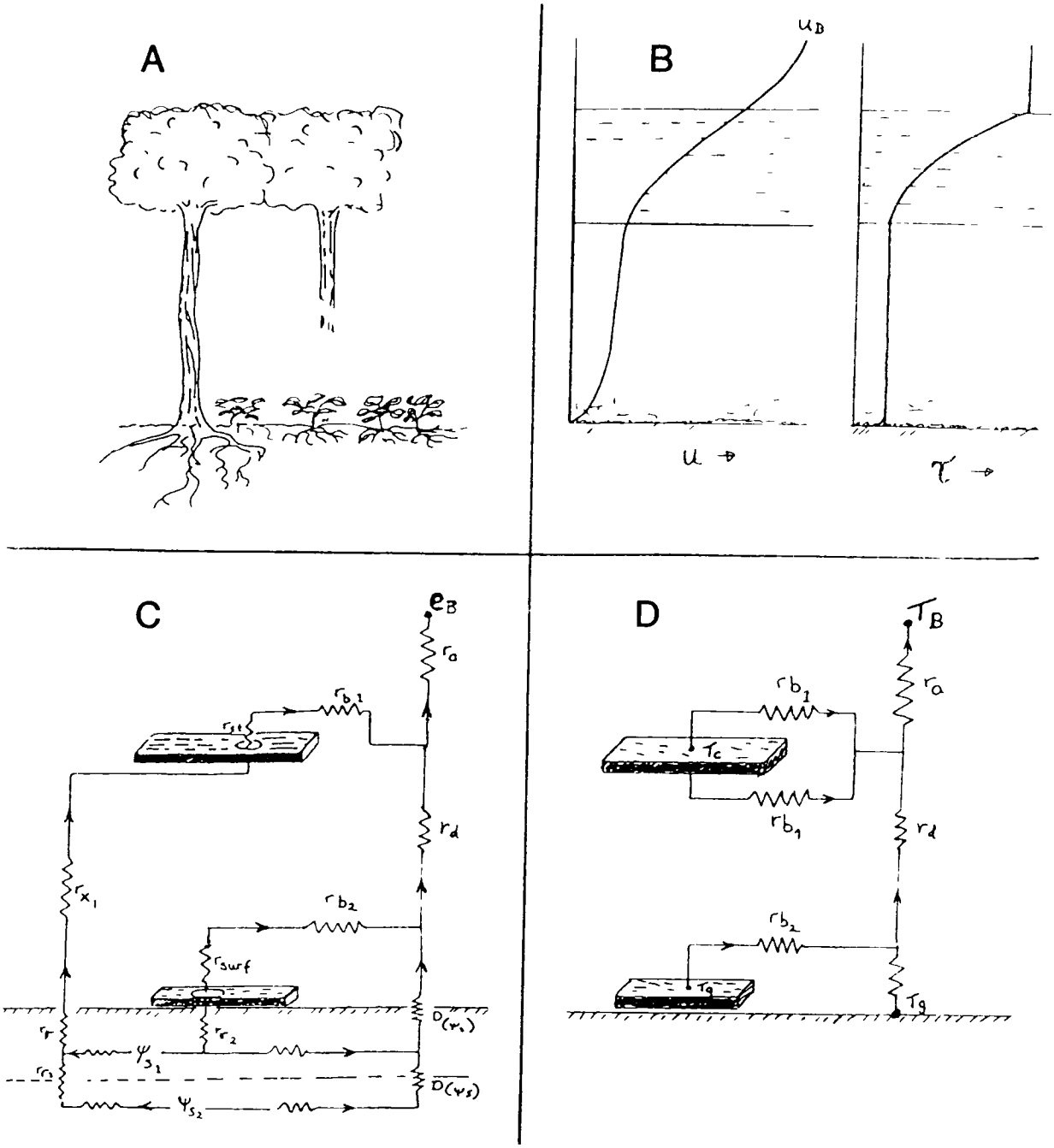

Fig. 2. Structure of the Simple Biosphere.

A Visual appearance of the canopy layer, groundcover, and roots.

B Derived vertical profiles of wind (u) and stress (τ)

C Pathway of water flux, from the soil (where ψ_{s_1} and ψ_{s_2} are the moisture potentials), through the roots, stems and leaves, to the atmospheric boundary layer (where e_B is the vapor pressure) Also shown is the pathway of the water flux from the soil surface (Subscripted r designate the several resistances to the water flux)

D Pathway of sensible heat flux, from the canopy (at temperature T_c), and from the groundcover and soil surface (at temperature T_g), to the atmospheric boundary layer (at temperature (T_B)

The absorption and emission of short wave and long wave radiation, (which depend on the vegetation morphology - the leaf distribution and leaf orientation - and on the temperatures, T_c and T_g) are not shown here

will be analogous to the study of the two off-line tests mentioned above. After that, the model atmosphere and biosphere will be allowed to interact with each other freely (first in the Phase 1 sense, and then in the Phase 2 sense) and from that we will try to learn how important, for weather and climate simulations and predictions, are the several influences of vegetation when they act together. Mintz, Sud and Sellers will make and evaluate these studies.

If suitable arrangements can be made, SiB will also be incorporated into other state-of-the-art GCMs. It is important to learn how SiB behaves in different GCMs, expecially those which have other physical and mathematical formulations for the atmospheric boundary layer.

III

An important problem, when making both deterministic weather predictions on the 3 to 10 day time scale and climate predictions (predictions of the time-averaged weather) on the bi-weekly to monthly and seasonal time scales, is how to initialize the moisture in the plant root zone of the soil. Mintz is preparing a report on his work in this area, which is being done in collaboration with J. Susskind and J. Dorman. It is expected that this will lead to a practical way of initializing the soil moisture from the information provided by existing satellite observing systems.

References

Baumgartner, A., H. Mayer and W. Metz, 1977: Weltweite Verteilund des Rauhigkeitsparameters z_0 mit Anwendung auf die Energiedissipation an der Erdoberfläche. Meteorol. Rdsch., 30, 43-48.

Kalnay, E., R. Balgovind, W. Chao, D. Edelmann, J. Pfaendtner, L. Takacs and K. Takano, 1983: Documentation of the GLAS Fourth Order General Circulation Model. Vol. I. Model documentation. Vol. II: Scalar Code. Vol. III: Vectorized Code for the Cyber 205. NASA/Goddard Space Flight Center, Technical Memorandum 86064, December 1983.

Mintz, Y., 1984 The Sensitivity of Numerically Simulated Climates to Land-Surface Boundary Conditions. Chapter 6 in The Global Climate. (J. T. Houghton, editor.) Cambridge University Press, Cambridge/London/New York, 1984. pp. 79-105.

Mintz, Y., P. J. Sellers and C. J. Willmott, 1983: On the Design of an Interactive Biosphere for the GLAS General Circulation Model. NASA/Goddard Space Flight Center, Technical Memorandum 84973, January 1983. 54 pp.

Sellers, P. J., Y. C. Sud and Y. Mintz, 1984: SiB: A Simple Biosphere for General Circulation Models. (In preparation for publication).

Sud, Y. C., J. Shukla and Y. Mintz, 1984: Influence of Land-Surface Roughness on Atmospheric Circulation and Rainfall: A GCM Sensitivity Experiment. (In preparation for publication).

FULLY IMPLICIT NUMERICAL METHODS FOR THE BAROCLINIC PRIMITIVE EQUATIONS
(S. E. Cohn and E. Isaacson-Courant Institute of Mathematical Sciences)

RESEARCH OBJECTIVES:

We are developing a fully implicit code to solve the three-dimensional primitive equations of atmospheric flow. The scheme is second order accurate in time and fourth order accurate in the horizontal and vertical directions. Furthermore, as a result of being fully implicit, the time step is not restricted by the mesh spacing near the poles, nor by the speed of inertia-gravity waves. Rather, the time step, Δt, is determined simply by the requirement that it be small enough to adequately resolve the atmospheric flow of interest. We expect our scheme to significantly improve upon the accuracy and efficiency of current models for fine grids.

This research is being carried out in collaboration with Drs. J. Augenbaum (GLAS/RRA), D. Dee (PUCRJ/BRAZIL), E. Kalnay (GLAS), and D. Marchesin (PUCRJ/BRAZIL) and with the assistance of G. Hsu (NYU) and Arlinda Silva de Moraes (PUCRJ/BRAZIL).

SIGNIFICANT ACCOMPLISHMENTS:

We have tested the factorization scheme on the one hand, and the improvement obtained with fourth order accurate vertical differencing on the other hand, for two different kinds of two-dimensional models [1, 2, 3, 4, 5, 6].

i) For a shallow water model over a spherical earth with and without orography.

Here we found that for a 3° by 3° grid, the implicit scheme was more efficient than an explicit scheme with Fourier filtering near the poles. The relative efficiency of the implicit scheme becomes still greater for finer grids. In figures a, b and c, we display the motion of an initial Haurwitz 8-wave. Wind vectors and contours of the height field are plotted:

a) at t=0
b) at t=24 hours, using t = 15 minutes, and
c) at t=24 hours, using t = 30 minutes.

Comparison of the two forecasts indicates that a one-half hour time step adequately resolves this flow, in which the maximum velocity is about 100 meters/second.

ii) For a baroclinic model of a vertical slice of the atmosphere taken along latitude 45°.

The table indicates the sizes of the relative root mean square errors for second order accurate and for fourth order accurate vertical differencing. Here we used a model whose simple exact solution we knew (see [4, 5]). We calculated the errors in the horizontal velocity, the vertical velocity, and the potential temperature after 12 hours had elapsed. Observe that the errors produced by the fourth order accurate scheme are at most 1/32

times the size of those of the second order accurate scheme. We believe that an appreciable improvement in the accuracy of current three dimensional forecast models, could be attained by introducing fourth-order accurate vertical differencing.

CURRENT RESEARCH:

The three-dimensional code is being written in a modular fashion so that the results of using explicit schemes and implicit schemes can be compared. The code is completely portable and is being run simultaneously at the NASA Goddard High Speed Computing Facility and at the Pontifical Catholic University of Rio de Janeiro, Brazil. See the report by J. Augenbaum in this volume for further details.

JOURNAL PUBLICATIONS:

Cohn, S. E., D. Dee, E. Isaacson, D. Marchesin and G. Zwas, 1983: A fully implicit scheme for the baroclinic primitive equations: Two-dimensional models. Submitted to Mon. Wea. Rev.

Marchesin, D., 1984: Using exact solutions to develop an implicit scheme for the baroclinic primitive equations. Mon. Wea. Rev., 112, 269-277.

TECHNICAL PUBLICATIONS:

Augenbaum, J. M., S. E. Cohn and D. Marchesin, 1984: The effect of compact implicit differencing in a baroclinic primitive equations model. Research Review-1983, NASA Tech. Memo. 86053, 87-89.

Cohn, S. E., D. Dee and D. Marchesin, 1982: Baroclinic models with fourth-order vertical accuracy: Preliminary report. CIMS-NYU, 13 pp.

Marchesin, D., 1982: A split-implicit scheme for the baroclinic primitive equations: Preliminary report. CIMS-NYU, 20 pp.

CONFERENCE PUBLICATION:

Isaacson, E., D. Marchesin and G. Zwas, 1979: Numerical methods for meteorology and climatology. Fourth NASA Weather and Climate Program Science Review, Conf. publ. 2076, pp. 183-190.

Table 1 Relative RMS Errors for Second Order and for Fourth Order vertical differencing schemes after 12 hours

RMS of Error / RMS of Exact Solution \ vertical differencing	Second Order scheme	Fourth order scheme
horizontal velocity	2.2%	0.068%
vertical velocity	8.5%	0.15%
potential temperature	0.089%	0.0012%

Fig. (a)

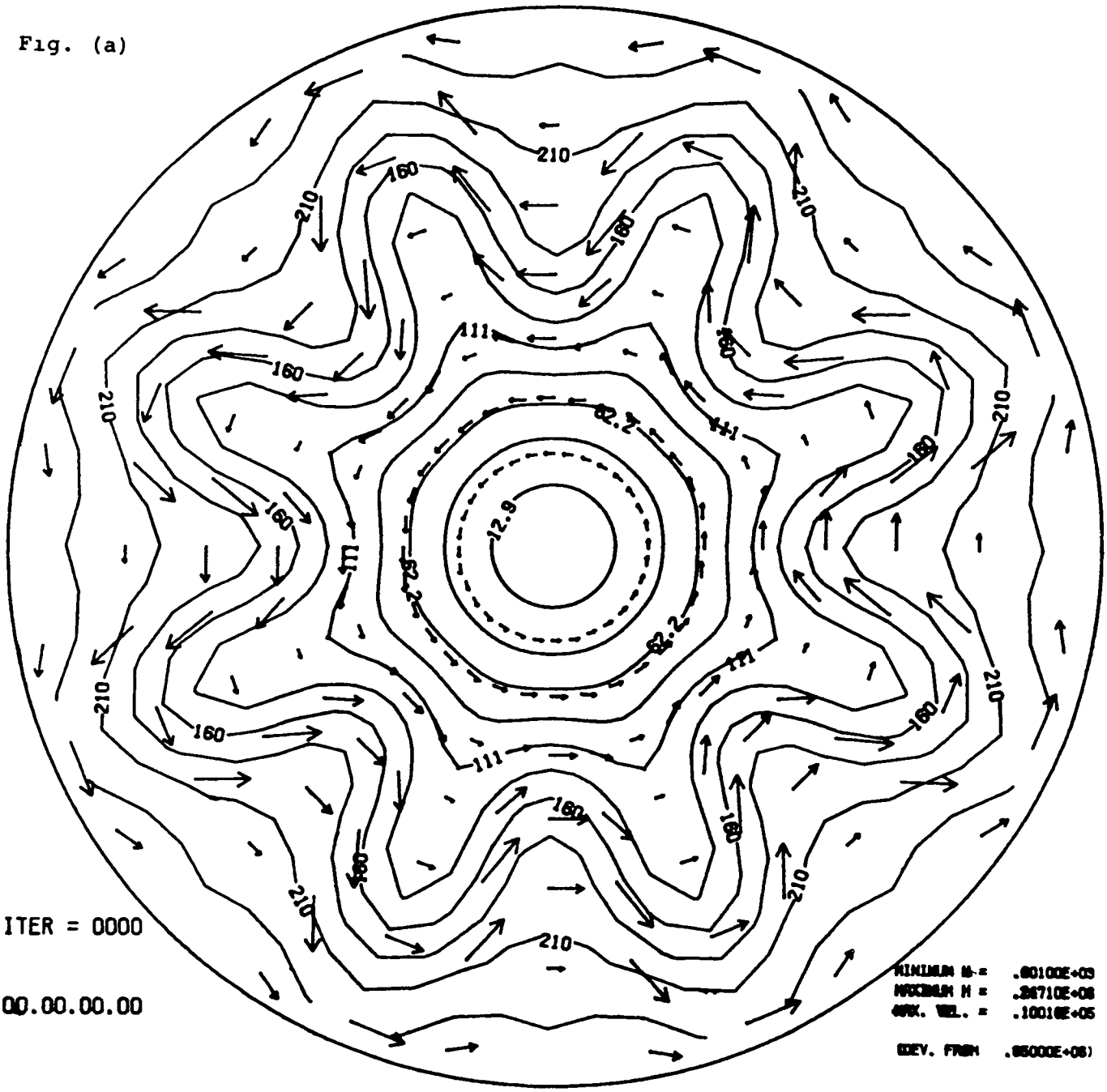
210
160
111
12.9
ITER = 0000
00.00.00.00
CONTOUR FROM 12920. TO .23488E+08 CONTOUR INTERVAL OF 2484Q. LABELS SCALED BY .10000E-02

Fig. (b)

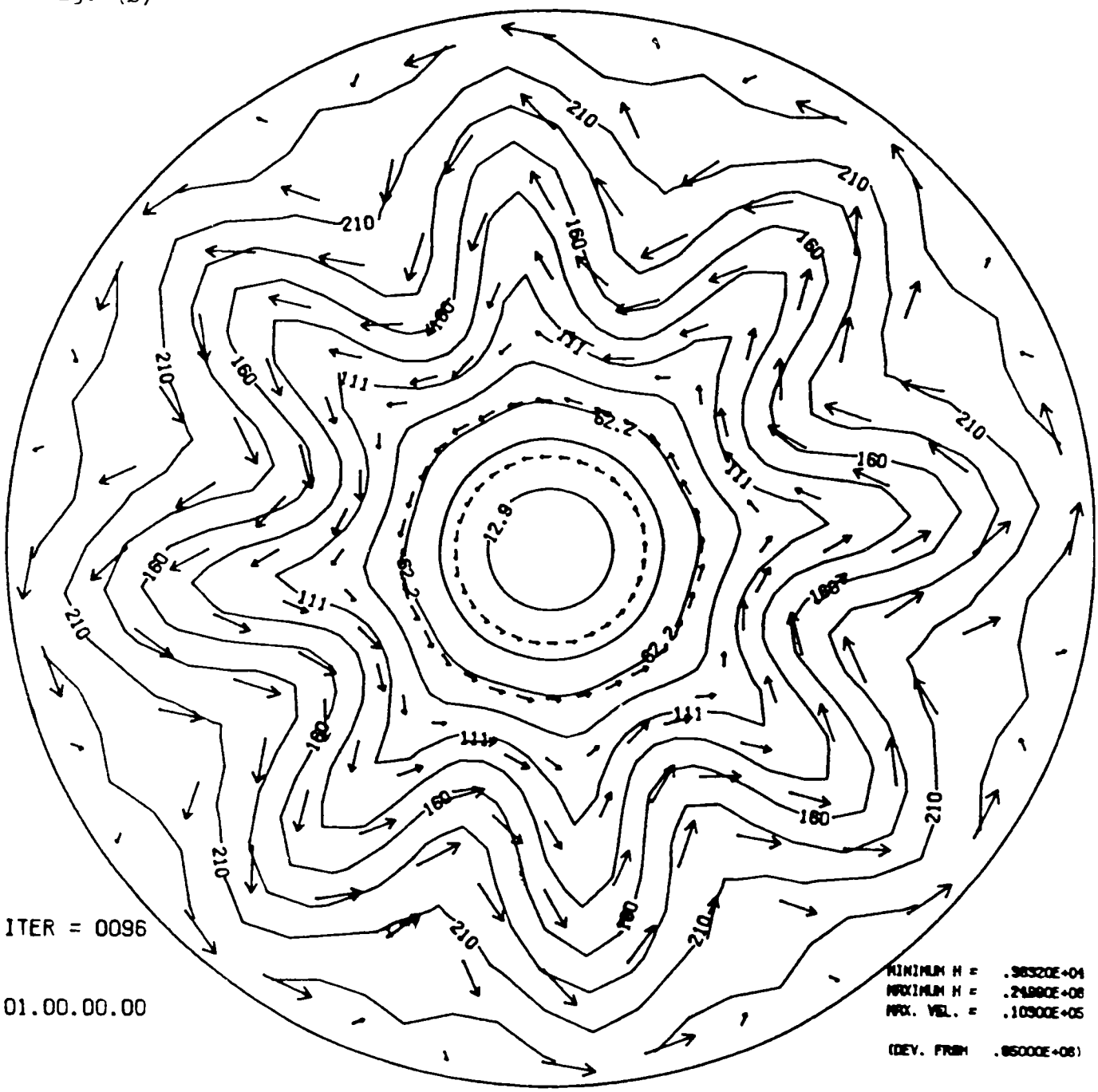
210
160
111
62.7
62.2
12.8
ITER = 0096
01.00.00.00
MINIMUM H = .98320E+04
MAXIMUM H = .21990E+05
MAX. VEL. = .10300E+05
(DEV. FROM .85000E+04)
CONTOUR FROM 12820. TO .29488E+05 CONTOUR INTERVAL OF 24840. LABELS SCALED BY .10000E-02

Fig. (c)

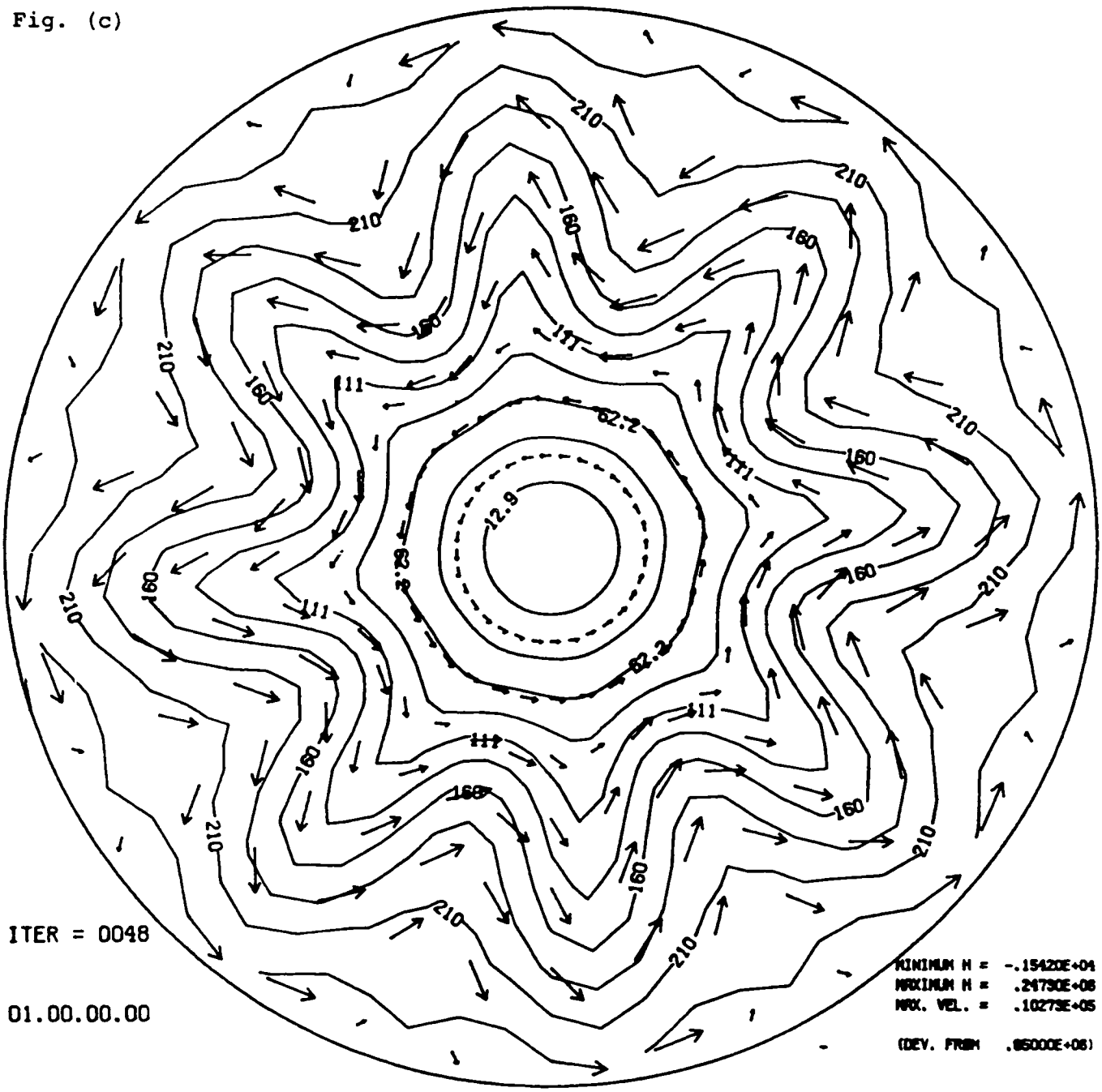
ITER = 0048
01.00.00.00
MINIMUM H = -.15420E+04
MAXIMUM H = .24790E+08
MAX. VEL. = .10273E+05
(DEV. FROM .85000E+08)
CONTOUR FROM 12920. TO .29480E+08 CONTOUR INTERVAL OF 24840. LABELS SCALED BY .10000E-02

MASSIVELY PARALLEL PROCESSOR
(M. Suarez-GSFC)

RESEARCH OBJECTIVES:

The main purpose has been to study the feasibility of using the Massively Parallel Processor (MPP) and possible future machines with parallel architecture for weather prediction and climate simulation.

The first objective of the project was to implement a shallow-water model (Kalnay and Takacs, 1981), and the second to implement a two-level primitive equations model (Held and Suarez, 1974).

SIGNIFICANT ACCOMPLISHMENTS:

The first objective is now completed. A 100% parallel shallow water model with a resolution of 2.8° longitude by 1.4° latitude (128 x 128 grid points: one per processor) was implemented using the MPP's machine language. This code ran three times faster than a comparable code on the CYBER 205.

CURRENT RESEARCH:

These results have encouraged us to the second objective--the implementation of the two-layer primitive equations model with simple parameterizations of physical processes. This model presents two new challenges to the machine and its user. It includes "non-ideal" types of calculations which may be minimized but not completely eliminated in GCMs. One of these is the solution of inherently non-local elliptic problems such as one encounters in using semi-implicit time differencing. Although not crucial for forecasting models, a practically useful machine should not place a prohibitive tax on such calculations. The second "non-ideal" task is unavoidable and concerns the single-instruction characteristic of the MPP. Processes such as radiation, precipitation, and subgrid scale convection are often highly branched. We've now built a grid-point version of the dynamics of the Held-Suarez model on the CYBER. In this version, care has been taken to make it suitable for conversion to the MPP.

Extensive testing of the grid-point two-level model is being conducted on the CYBER. We are also working on a half-precision (32-bit) version to make the comparison with the MPP as clean as possible. Work on the MPP itself has been waiting for a parallel Pascal compiler. One is now available and we have begun to experiment with it.

FUTURE PLANS:

To familiarize ourselves with the new compiler we plan to start by building a Pascal version of the shallow water model. We will then implement the dynamics part of the two-level model with simple forcing and finally a version with full physics. We should note that the two-level Held-Suarez model takes us beyond the point of a mere technical exercise in feasibility of use. If advantageously implemented on the MPP, it would be a valuable tool for atmospheric research.

A VERTICALLY RESOLVED PLANETARY BOUNDARY LAYER
(H. M. Helfand-GSFC)

RESEARCH OBJECTIVES:

Our objectives are to increase the vertical resolution of the GLAS Fourth Order GCM near the earth's surface and to install a new package of parameterization schemes for subgrid-scale physical processes so that the GLAS Model GCM will predict the resolved vertical structure of the planetary boundary layer (PBL) for all grid points.

SIGNIFICANT ACCOMPLISHMENTS:

1) Both the scalar and the vector versions of the Fourth Order GCM have been recoded so that they can have a variable vertical resolution which becomes finer as one approaches the earth's surface. In the recoded model this is now possible with an arbitrary number of vertical layers, but we anticipate running only with 9 and 15 layer versions.

2) A Monin-Obukhov layer similarity scheme has been developed which can reasonably predict the turbulent surface fluxes of momentum, heat and moisture even when the lowest model layer is as deep as 300 m.

3) A Level 2.5 second-order turbulent closure scheme has been developed by Helfand and Labraga (1984) and tested offline by Labraga and Helfand (1984) against data from the Wangara Experiment. The scheme predicts turbulent kinetic energy as a prognostic variable from which it computes the vertical turbulent fluxes of momentum, heat and moisture between the layers of the atmospheric model. The scheme is based on the work of Mellor and Yamada, but it has been considerably redesigned in order to assure the conditions of physical realizability.

CURRENT RESEARCH:

The variable vertical resolution version of the model is being implemented and tested to make sure that it is compatible with the most up-to-date version of the Fourth Order Model. Simultaneously, code for the Monin-Obukhov surface fluxes and for the Level 2.5 second-order closure scheme is being developed so that it can be interfaced with the variable vertical resolution version of the model. In addition, an algorithm is being developed to interactively predict the surface roughness length for open water surfaces as a function of predicted surface stresses.

FUTURE PLANS:

We plan both to refine the parameterization schemes described above and to embellish our treatment of the PBL by adding further sophistication to the treatment of land surfaces. The computational efficiency of the above schemes will be improved and steps will be taken to make sure the schemes remain numerically stable as the vertical resolution is increased. Special attention will

be paid to the dynamics of the region at the very top of the PBL where the turbulence vanishes. Also, the turning angle within the "constant flux" surface layer will be parameterized. In addition, ensemble averaging techniques will be used to account for the large discrepancy between the large size of a grid cell and the area of homogeneity surrounding a typical surface layer observation tower.

The treatment of land surfaces will include a ground heat condition model, a two-layer ground hydrology scheme, and an interactive snow-cover scheme. In addition, we will make our PBL fully interactive with the biospheric model being developed by Mintz, Sud and Sellers.

TECHNICAL PUBLICATIONS:

Helfand, H. M., and J. Labraga, 1983: A level 2.4 second-order closure model for the prediction of turbulence. Research Activities in Atmospheric and Oceanic Modelling. I. D. Rutherford, ed., GARP Working Group on Numerical Experimentation.

Labraga, J., and H. M. Helfand, 1983: Selection of a best candidate higher-order closure scheme for turbulence in the GLAS Fourth Order GCM. Research Activities in Atmospheric and Oceanic Modelling. I. D. Rutherford, ed., GARP Working Group on Numerical Experimentation.

JOURNAL PUBLICATIONS:

Helfand, H. M., and Labraga, J., 1984: Design of a nonsingular level 2.5 second-order closure model for the prediction of atmospheric turbulence. To be submitted to J. Atmos. Sci.

Labraga, J., and H. M. Helfand, 1984: Evaluation of a simple second-order turbulent closure model for use in the GLAS Fourth Order GCM. In preparation.

AN INVESTIGATION OF THE MARINE BOUNDARY LAYER DURING COLD AIR OUTBREAK
(S. A. Stage-Florida State University)

RESEARCH OBJECTIVES:

This project is designed to study various aspects of the marine atmospheric boundary layer (MABL) during cold air outbreak using data from the Mesoscale Air Sea Interaction Experiment (MASEX) and using a model for the MABL developed by Stage and Businger (1981a,b). Several areas have been identified for emphasis in this project:

A. Determination of the momentum budget and divergence of the MABL.

B. Development and testing of techniques for the remote determination of ocean surface sensible and latent heat fluxes by use of satellite data.

C. Use of MASEX data to evaluate various techniques for parameterizing layer turbulence, to determine the typical magnitudes of such parameters and to improve the MABL model.

D. Use of the resulting MABL model and understanding of layer parameters to develop and evaluate more sophisticated schemes for remotely sensing layer evolution and sea surface sensible and latent heat fluxes.

SIGNIFICANT ACCOMPLISHMENTS:

A. The MABL Momentum Budget: A study of the momentum balance of the MABL during cold air outbreak is in progress. It has been found that the flow can be divided into a quasi-geostrophic component and a departure from quasi-geostrophic. This provides a basis for scaling the equations. By neglecting small terms in the quasi-geostrophic departure equation it can be shown that the divergence within the boundary layer is the linear sum of the quasi-geostrophic divergence and a divergence which is due to boundary layer effects. The boundary layer effects are changed in surface roughness at the shore, inertial oscillations, and baroclinicity associated with the warming and deepening of the mixed layer as it moves over the water. During cold air outbreak these effects can be large and can give divergences which are comparable in magnitude to the quasi-geostrophic divergence imposed by the large scale flow.

B. Techniques for Remotely Determining Sensible and Latent Heat Fluxes. Don Allison is currently finishing a Master's thesis at Florida State University under my supervision which investigates a simple technique using satellite data which can be obtained with current technology to remotely estimate surface latent and sensible heat fluxes. We have found that the most promising set of variables which are currently available are either surface wind or stress and the sea surface temperature, the total integrated water vapor in the atmosphere, the total integrated liquid water in the atmosphere, and the cloud-top temperature. We assume that the MABL has well-mixed water vapor and equivalent potential temperature and we need to use a typical sounding for the temperature and relative humidity of the air above the mixed layer. Under these assumptions the satellite data can be inverted to find layer depth, potential temperature and humidity.

Surface heat and vapor fluxes can then be estimated using aerodynamic transfer relationships. We are still doing the analysis, however it appears that the sensible heat flux can be determined to within 24% with the major error being due to uncertainties in the surface wind or stress. The latent heat flux can be determined to within 82% with the principle error being due to integrated water vapor. If it were possible to remove the error in the integrated water vapor, then the latent heat flux could be determined to within 32%.

This technique rests on the assumption of a well-mixed MABL but does not rely on other features of the MABL model. Thus it is not just applicable to cold air outbreak situations but also to coastal stratus cloud layers whenever surface fluxes or cloud top radiative cooling are stong enough to thoroughly mix the layer. An additional bonus is that cloud top radiative cooling can be estimated using this technique although errors may be largely due to uncertainties in the soundings above the mixed layer.

C. Parameterization of Turbulence in the MABL: Surface-sensible and latent heat fluxes from the MASEX data are being analyzed to determine a suitable relationship to use for the aerodynamic transfer relationships for these fluxes. We have compared the flux formulations of Liu et al. (1979), a formulation based on Charnock's relationship and the assumption that the roughness lengths for momentum, heat and vapor are the same (This assumption was used by Stage and Businger in their model), and the data. Some preliminary results were reported by Stage (1984). Although errors in the two are of similar size, the Liu et al. formulation appears to be slightly better.

FUTURE PLANS:

Stage and Businger (1981a) modeled MABL entrainment and evolution of temperature and humidity but needed to rely on an external determination of divergence. They further found that it is difficult to obtain values for divergence which are adequate for model use. We are currently expanding the model to include the boundary layer momentum equations and will test it against the MASEX data and will study the comparative magnitudes of the various terms in the equations.

We will be further studying the MASEX data in the near future and will be making comparisons between the data and the MABL model including the momentum equations. We will also be using the model to study MABL evolution during cold air outbreak and to develop more sophisticated means of remotely estimating MABL parameters.

JOURNAL ARTICLES:

Stage, S. A., 1983: Boundary layer evolution in the region between the shore and cloud edge during cold-air outbreaks. J. Atmos. Sci., 40, 1453-1471.

CONFERENCE PAPERS:

Stage, S. A., 1984: An evaluation of a boundary layer model by comparison with MASEX data. Paper presented at the Fifth Conference on Ocean-Atmosphere Interaction, January 9-13, 1984, Miami Beach, Florida.

REFERENCES:

In addition to the articles and papers listed above, the following articles were referenced in this abstract:

Liu, W. T., K. B. Katsaros, and J. A. Businger, 1979: Bulk parameterization of air-sea exchanges of heat and water vapor including the molecular constraints at the interface. J. Atmos. Sci., 36, 1722-1735.

Stage, S. A. and J. A. Businger, 1981a: A model for entrainment into a cloud-topped marine boundary layer. Part I: Model description and application to a cold-air outbreak episode. J. Atmos. Sci., 38, 2213-2229.

_____ and _____, 1981b: A model for entrainment into a cloud-topped marine boundary layer. Part II: Discussion of model behavior and comparison with other models. J. Atmos. Sci., 38, 2230-2242.

STRUCTURE AND GROWTH OF THE MARINE BOUNDARY LAYER
(M. McCumber-GSFC)

RESEARCH OBJECTIVES:

Atlas and Chou recently used LANDSAT visible imagery and a one-dimensional Lagrangian boundary layer model to hypothesize the nature and the development of the marine boundary layer during a winter episode of strong seaward cold air advection. They suggested that over-water heating and moistening of the cold, dry continental air is estimable from linear relations involving horizontal gradients of the near-surface air temperature and humidity. A line of enhanced convection paralleling the Atlantic U.S. coast from south of New York Bay to the vicinity of Virginia Beach, VA was attributed to stronger convergence at low levels -- Atlas and Chou referred to this feature as characterizing a mesoscale "front."

During January of 1983 a cooperative field experiment (MASEX) between NASA, NOAA and the Johns Hopkins Applied Physics Laboratory was conducted off the U.S. east coast from Long Island, NY to the north to North Carolina to the south. Clouds and boundary layer structure were sampled from the coast seaward to the gulf stream (a distance of about 600 km from the shore). Data from four flight days were compiled to be used to study the actual behavior of the sea and atmospheric boundary layers and to both initialize and to validate numerical simulations of the cold air outbreak events.

Although the research aircraft provided a true description of the state of the atmosphere and the sea, areal coverage was severely limited by considerations of finite resources and time. It is also difficult to quantitatively assess the spatial characteristics of the marine PBL (Planetary Boundary Layer) using the one-dimensional Lagrangian model because horizontal dynamic and thermodynamic forcings cannot be accommodated.

With the assistance of a three-dimensional mesoscale boundary layer model, initialized with data obtained from the MASEX, the marine boundary layer can be mapped over the entire Atlantic coastal domain and the evolution of the boundary layer can be studied as a function of different characteristics of important surface level forcings. This research is concerned with the effects on boundary layer growth due to the magnitude and pattern of sea surface temperature, to the shape of the coastline, and to atmospheric conditions, such as the orientation of the prevailing wind.

SIGNIFICANT ACCOMPLISHMENTS:

A successful simulation for a northerly flow MASEX day (January 20, 1983) has been run on the CYBER 205. The model was initialized with the Atlantic City morning rawinsonde and the model was run for about seven hours to insure a nearly steady state for the atmosphere. Flow curvature over the ocean due to reduced surface momentum stress and coastline configuration was evident to the west and north in the MASEX domain. A zone of convergence extended southward from New York Bay along, but offshore from, the coast. This convergence is most probably a manifestation of differential heating between the long over-water fetch airstream to the east and the short over-water fetch

airstream to the west, which is cooler and less moist. The differential warming established a hydrostatic pressure gradient, which caused the horizontal wind to curve. This result confirms the hypothesis of Atlas and Chou who reached the same conclusion by examining cloud photographs and by applying a one-dimensional PBL model.

Another simulation was also run for January 19, 1979, a day characterized by a northwesterly low level synoptic flow. Mesoscale convergence was especially evident in and downwind from the Delaware Bay and to a lesser extent from the New York Bay. Warmer water in the bays (especially Delaware) was apparently the principal mechanism responsible for the enhanced convergence. The flow pattern appears to confirm the ocean wave studies of Walsh, where his data pointed to a wave source near the mouth of the Delaware Bay

CURRENT RESEARCH:

Efforts to initialize the model with multiple soundings in the highly baroclinic atmosphere which characterizes strong cold air outbreaks have met with little success. Therefore, the model has been initialized in the usual manner with a single sounding. The impact will be most significant where the synoptic flow deviates sharply from the coastal rawinsonde, such as in the eastern and northeastern part of the domain where the real winds are stronger and exhibit more curvature closer to the cyclone. Model results suggest too much southward and a likely spurious westward component to the low level winds in this area due to this error (the winds react to the hydrostatic pressure trough to the south and southeast with no compensation from a more westerly real synoptic flow). To insure that deviations from the observation (or anticipated) winds to the east and northeast are due only to initialization errors, tests are being made to change lateral boundary conditions from a simple condition (where the normal gradients of model variables are set to zero) to a radiation boundary condition (Sommerfeld-type). In this way cleaner solutions are obtained, effectively preventing the lateral boundaries from significantly impacting the solution in the interior of the domain. Work is also underway to improve the graphics, in particular to provide vertical projections of prognostic and diagnostic data fields.

FUTURE PLANS:

One or two more MASEX days will be selected for study. Effects of coastal geometry and sea surface temperature pattern will be determined by running the model with variations in each. The wind hodograph will also be rotated to better define the effect of wind orientation, all other forcings being held constant.

Relations between model-generated surface energy fluxes and boundary layer growth, as evidenced by cloud patterns and lidar signatures, will be determined and the results will be compared to the relationships derived in the Atlas-Chou study using a simpler PBL model. Predicted surface stresses will be compared with oceanographic data to determine their utility in ocean PBL research.

JOURNAL PUBLICATIONS:

McCumber, M., and D. Atlas, 1984: Numerical simulation of the coastal marine boundary layer during cold air outbreaks. To be submitted to Mon. Wea. Rev.

LØCAL TIME = 2.2 GEØSTRØPHIC WIND IS 9.9 M/SEC FRØM 20. DEG
DIVERGENCE ØF WIND AT 100. METERS

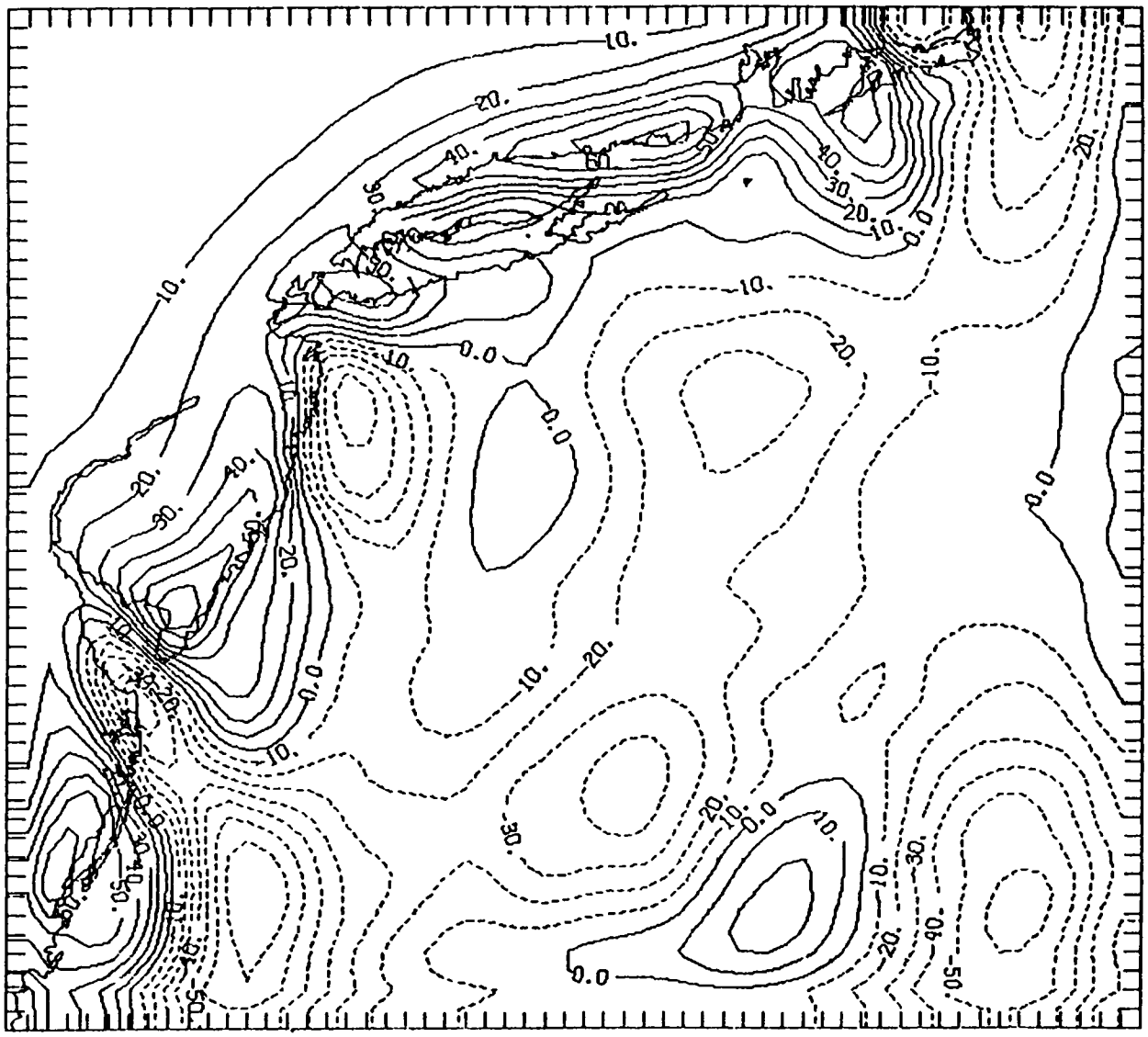

(CØNTØUR INTERVAL IS 10.0 X E - 6)
MASEX, JANUARY 20, 1983 ACY SØUNDING ØNLY / MAS3

Figure 1. Wind divergence at a height of 100 meters for the MASEX domain. Divergence has been multiplied by 10^6 and dashed contours indicate negative values. Simulation is for the northerly flow case, January 20. Note stronger convergence near Delaware Bay and New York Bay.

NUMERICAL MODELING OF THE ATMOSPHERE
(P. H. Stone-Massachusetts Institute of Technology)

RESEARCH OBJECTIVES:

The objective of this research is to use numerical models and numerical analyses of observations to improve our understanding of the physical processes important in global weather and climate.

SIGNIFICANT ACCOMPLISHMENTS:

(1) Results from a study of the effect of baroclinic waves on mid-latitude vertical temperature structure show that the waves' vertical eddy heat flux tend to eliminate the potential vorticity gradient near the steering level by causing the static stability to decrease rapidly with height in the lower troposphere above the boundary layer.

(2) An empirical study of the relationship between eddy heat fluxes and the meridional temperature gradient has been completed. The results indicate that the feedback in the flux-gradient system is comparable to dissipation on all time scales between the synoptic and the seasonal.

(3) We have generalized the definition of the Eliassen-Palm flux and the Eliassen-Palm and non-acceleration theorems to include eddy forcing of condensation. Calculations based on the generalized diagnostics showed that the annual mean eddy forcing of the zonal mean zonal wind is two and one half times stronger when the condensation effects are included.

CURRENT AND FUTURE RESEARCH:

The following projects have been proposed for the current year:

(1) Investigation of air-sea interactions on climate time scales using a numerical model developed at GMSB.

(2) Calculations from observations of the eddy forcing of the atmosphere's moisture field.

(3) Numerical simulation of how shear in a mean zonal flow affects quasi-geostrophic energy cascades.

JOURNAL PUBLICATIONS:

Zebiak, S. E., 1982: A simple atmospheric model of relevance to El Niño. J. Atmos. Sci., 39, 2017-2027.

Cane, M., 1982: The variability of equatorial currents. Recent Progress in Equatorial Oceanography (S. P. McCreary, D. W. Moore, J. Witte, Eds., Nova/NYIT Press, Ft. Lauderdale, Florida), pp. 197-206.

Cane, M. and E. S. Sarachik, 1982: Linear baroclinic response of equatorial oceans to periodic forcing. Recent Progress in Equatorial Oceanography (S. P. McCreary, D. W. Moore, J. Witte, Eds., Nova/NYIT Press, Ft. Lauderdale, Florida), pp. 365-372.

Stone, P. H., S. J. Ghan, D. Spiegel and S. Rambaldi, 1982: Short-term fluctuations in the eddy heat flux and baroclinic stability of the atmosphere. J. Atmos. Sci., 39, 1734-1746.

Cane, M. and Y. du Penhoat, 1982: On the effect of islands on low frequency equatorial motions. J. Mar. Res., 40, 937-962.

Cane, M. and E. S. Sarachik, 1983: Equatorial oceanography. Rev. Geophys. Space Phys., 21, 1137-1148.

Salustri, G. and P. H. Stone, 1983: A diagnostic study of the forcing of the Ferrell cell by eddies, with latent heat effects included. J. Atmos. Sci., 40, 1101-1109.

Ghan, S. J., 1983: Empirical models of the eddy heat flux and vertical shear on short time scales. J. Atmos. Sci., 41, 389-401.

Stone, P. H. and G. Salustri, 1984: Generalization of the quasi-geostrophic Eliassen-Palm flux to include eddy forcing of condensation heating. Submitted to J. Atmos. Sci.

II. SATELLITE DATA ASSIMILATION AND INITIALIZATION

Page intentionally left blank

COMPARISON OF OPTIMUM INTERPOLATION AND CRESSMAN ANALYSES

(W. E. Baker-GSFC, S. C. Bloom-GSFC/USRA, M. S. Nestler-Sigma Data)

RESEARCH OBJECTIVES:

The objective of this investigation is to develop a state-of-the art optimum interpolation (O/I) objective analysis procedure for use in numerical weather prediction studies.

SIGNIFICANT ACCOMPLISHMENTS:

A three-dimensional multivariate O/I analysis scheme has been developed. Some characteristics of the GLAS O/I compared with those of the NMC and ECMWF systems are summarized in Table 1. Some recent enhancements of the GLAS scheme include a univariate analysis of water vapor mixing ratio, a geographically dependent model prediction error correlation function and a multivariate oceanic surface analysis.

Figure 1 compares the 24 h and 48 h forecasts from 0000 GMT 13 January 1979 initial conditions provided by the O/I analysis scheme with forecasts from a successive correction method (SCM) of analysis developed earlier. As may be seen in Fig. 1, the forecast of the intensity and position of the cyclone which moves northeastward across the United States as well as the ridging which follows, is more accurate with the O/I than with the SCM.

FUTURE PLANS:

Future work includes completing vectorization of the O/I on the Cyber 205, a detailed comparison with the SCM, real and simulated data impact studies and experiments with normal mode initialization.

CONFERENCE PUBLICATION:

Bloom, S. C., W. E. Baker and M. S. Nestler, 1984: Multivariate optimum interpolation of surface pressure and winds over oceans. Preprints Tenth Conf. on Weather Forecasting and Analysis, 25-29 June, Amer. Meteor. Soc., Clearwater, Florida, 106-108.

TABLE 1. CHARACTERISTICS OF THE GLAS O/I COMPARED WITH THOSE OF OTHER SYSTEMS

SALIENT FEATURES	GLAS	NMC	ECMWF
APPROACH	3-D; MULTIVARIATE IN Z,U,V UNIVARIATE IN W	3-D; MULTIVARIATE IN Z,U,V UNIVARIATE IN RH	3-D, MULTIVARIATE IN Z,U,V UNIVARIATE IN Q
RESOLUTION	18 LEVELS; 4° x 5° (2-D) 12 LEVELS; 4° x 5° (3-D)	12 LEVELS; 3.75° UPPER AIR, 2.5° SURFACE	15 LEVELS; 1.875°
AUTOCORRELATION FUNCTION	DAMPED COSINE FOR Z DAMPED EXPONENTIAL FOR W	GAUSSIAN	BESSEL
CROSS-CORRELATION MODEL	GEOSTROPHIC (SCALED TO 0.0 AT EQUATOR)	SAME	SAME
ASSUMPTION OF ISOTROPY	Z (YES); U,V (NO)	SAME	SAME
GEOGRAPHICALLY DEPENDENT μ	YES	NO	YES (LATITUDINALLY DEPENDENT)
MULTIVARIATE SURFACE ANALYSIS	YES (EKMAN BALANCE)	YES (GEOSTROPHIC)	YES (GEOSTROPHIC AT 1000 MB)

Fig. 1. O/I and SCM Forecasts from 0000 GMT 13 January 1979

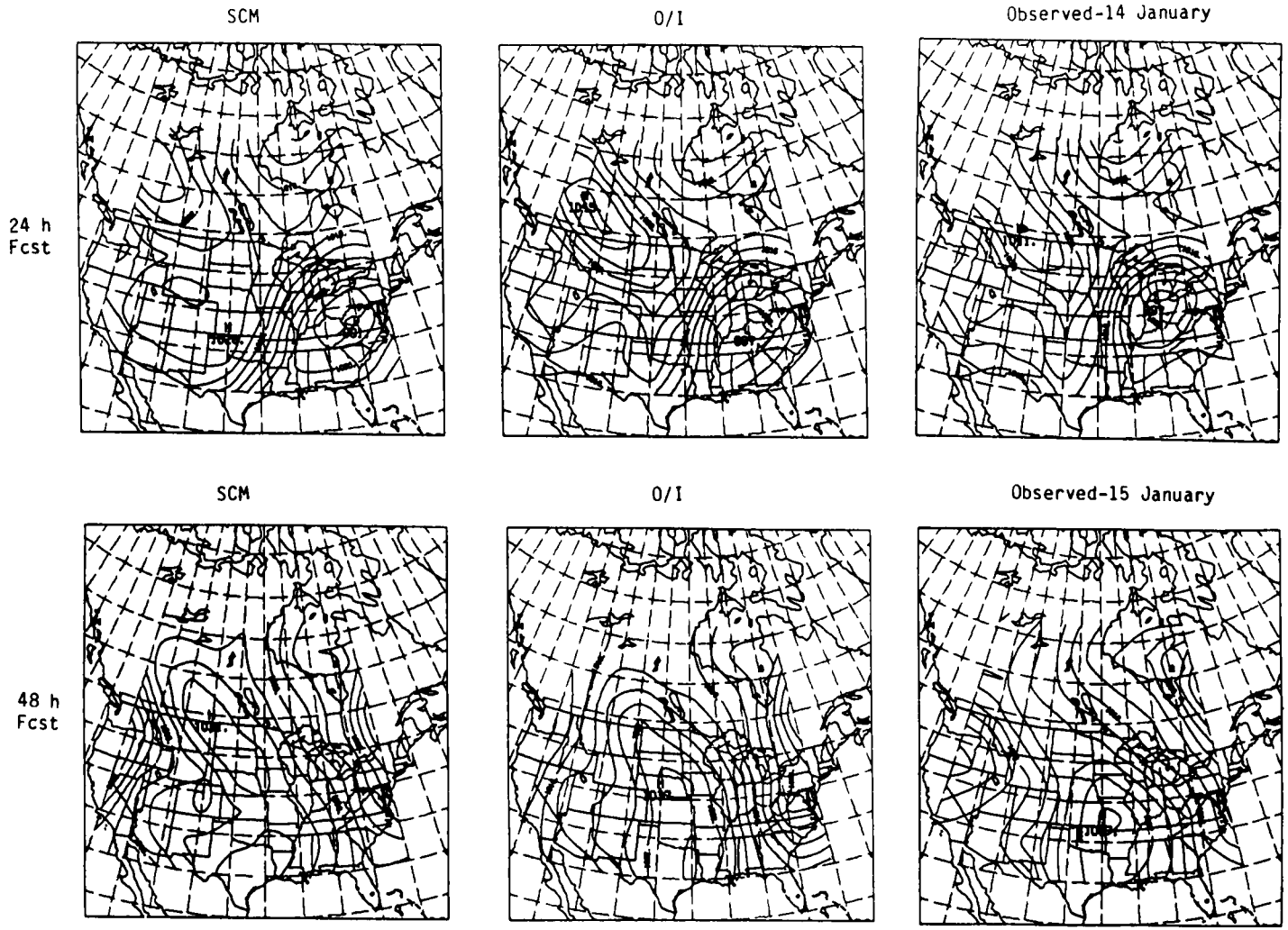

NORMAL MODE INITIALIZATION
(S. C. Bloom-GSFC/USRA

RESEARCH OBJECTIVES:

The objective of this research is the development and implementation of normal mode procedures for use with the GLAS analysis/forecast system. Specific tasks of this work include:

1) High latitude filtering of model fields to preserve the GLAS GCM's linear stability during integration.

2) Development of nonlinear normal mode initialization (NLNMI) processes, both adiabatic and diabatic. Using NLNMI to initialize GLAS analyses; investigation of the impact of normal mode initialization on the GLAS analysis/forecast system, especially in regard to data assimilation.

3) Diagnosis of the 1-3 day systematic forecast errors of the GLAS GCM.

SIGNIFICANT ACCOMPLISHMENTS:

To date, milestones reached with the normal modes project include:

1) The computation of the normal modes for the GLAS 4th order GCM (Bloom, 1983). Two sets of modes have been generated; one suitable for use with scalar code on the Amdahl V6, and a second one for use with vector code on the Cyber 205.

2) The development and testing of both scalar and vector forms of a linear normal mode projection (initialization) process (Bloom, 1984).

3) A preliminary study of an adiabatic NLNMI process using a shallow water model based on the GLAS GCM (Navon, Bloom and Takacs, 1984).

CURRENT RESEARCH:

Currently, two projects are underway:

1) The development of efficient vector code (for the Cyber 205) for an adiabatic NLNMI process for the full GLAS GCM.

2) The use of the linear normal mode projectors to examine the feasibility of normal mode filtering of high latitude gravity waves to ensure model linear stability. A scalar version is used with a shallow water model on the Amdahl V6. A vector version is being developed for use with the full GLAS GCM on the Cyber 205.

FUTURE PLANS:

Once the adiabatic version of the NLNMI has been fully implemented on the Cyber 205, the following projects can be started:

1) Development of a diabatic NLNMI. In addition, various approaches to the entire initialization process will be tested.

2) Development of a coupled analysis/initialization scheme. In this procedure, an optimum interpolation analysis will be combined with an NLNMI in an iterative manner to try to obtain a more accurate set of initial fields.

3) Use of a coupled analysis/initialization scheme to investigate the influence of analysis as well as NLNMI on the nature of the short-term (1-3 days) systematic forecast error in the GLAS GCM.

TECHNICAL PUBLICATIONS:

Bloom, S. C., 1983: Normal Modes of the GLAS 4th Order Model. Research Review 1982, NASA Tech. Memo 84983, 99-103.

Bloom, S. C., 1984: Design of a Linear Projector for use with the Normal Modes of the GLAS 4th Order GCM. Research Review 1983, NASA Tech. Memo. 86053, 101-115.

Navon, I. M., S. C. Bloom, and L. Takacs, 1984: Computational Aspects of the Non-Linear Normal Mode Initializaiton of the Grid Model of GLAS. Research Review 1983, NASA Tech. Memo. 86053, 106-112.

FORECAST IMPACT OF COMPONENTS OF THE FGGE OBSERVING SYSTEM

(E. Kalnay, R. Atlas, W. Baker and J. Susskind-GSFC)

RESEARCH OBJECTIVES:

To assess the prognostic impact of the complete FGGE Special Observing System as well as its individual components.

CURRENT RESEARCH:

We have recently conducted experiments to assess the summer and winter forecast impact of the FGGE system, and of its main observing components: temperature sounding data derived from the TIROS-N polar orbiting satellite, cloud track winds determined from geostationary satellite observations and drifting buoy data which were collected by satellite during FGGE. The Analysis/Forecast System used has a number of improvements upon the system utilized by Halem et al. (1982) for the FGGE Special Observing Period-1 (SOP-1). Several modifications were made in the analysis scheme, the most important being the interpolation of the analysis minus 6 h forecast deviations rather than of the analyzed fields themselves. The analysis scheme with the present modifications is described in detail in Baker (1983). The forecast model is still the 4° lat, 5° lon and 9 vertical levels GLAS Fourth Order GCM with several minor corrections implemented in the physics and numerics.

The improved vertical interpolation in the analysis resulted in better assimilation of rawinsonde data, which has more vertical structure than satellite data. As a result, there was an improvement of the forecasts derived from conventional data only, and, consequently, a small reduction of the positive impact of satellite data from that obtained by Halem et al. (1982).

SIGNIFICANT RESULTS:

Although the experiments are not yet completed, the following preliminary figures summarize the number of cases of positive and negative forecast impacts verified so far separately over two regions in the Northern Hemisphere (covering approximately North America and Europe) and the Southern Hemisphere (Australia and South America). Two forecasts are considered to be different if their S_1 skill scores, verified with the ECMWF analysis differ by more than 2 points. Only those forecasts for which at least one of the forecasts retains useful skill (defined as S1 $\leq$ 80 for sea level pressure and $\leq$ 60 for 500 mb heights) are counted.

a) Comparison of SOP-1 and SOP-2 Forecast Impacts

Figs. 1 and 2 present the results corresponding for SOP-1 and SOP-2. In the Northern Hemisphere the forecast impact of the FGGE Special Observing System is positive, and somewhat larger in winter than in summer. In the Southern Hemisphere the impact is much larger both in the winter and in the summer seasons.

b) Forecast Impact of Drifting Buoys

Two recent papers (Bourke et al., 1982, Kalnay et al., 1983) have presented results of studies of the impact of the FGGE observing system in the Southern Hemisphere. While both papers concluded that the TIROS-N satellite temperature soundings had a large positive impact, the conclusions were significantly different with respect to the impact of the drifting buoys.

The Bourke et al. (1982) study was based on the comparison of assimilation cycles covering the period 17 May to 26 May 1979 using the ANMRC analysis/forecast system. Three assimilation cycles were performed: a control assimilation cycle including all FGGE data, a cycle without using buoys (NB), and a cycle without using satellite temperature soundings (NT). Only three forecasts from 20 May, 22 May and 24 May 1979 were performed from each cycle. The results indicated that over the Australian region, the buoys had a significant positive impact. In hemispheric verifications the impact of the buoys was much smaller than that of satellite soundings, except on 12 h sea level pressure forecasts.

Kalnay et al. (1983) performed a study covering the FGGE SOP-1 period (5 January to 5 March 1979). Four assimilation cycles were conducted: a "FGGE" cycle which used all FGGE data, a "NOSAT" cycle which used only conventional data (surface observations by land stations and ships, rawinsondes and aircraft reports), a "NOSAT plus BUOYS" in which the buoy data was added to the conventional data base and a "FGGE minus BUOYS" cycle in which drifting buoys were subtracted from the FGGE data. About 14 forecasts from initial conditions every four days in the cycle were performed for each cycle. The results verified over the South American region indicated that the buoys had a substantial positive impact when added to the NOSAT system, but on the average a negligible impact when deleted from the full FGGE four-dimensional assimilation.

There are several possible causes for these different results: a) The two studies used different seasons: Southern Hemisphere summer in the Kalnay et al. paper, and early winter in the Bourke et al. paper. This introduces significant differences in the atmospheric circulation, and hence, possible data impact differences. b) The number of buoys, which started to be deployed during the early FGGE period, increased considerably during the SOP-2. c) There is a possible sampling problem in comparing about a dozen forecasts covering two months with 3 forecasts corresponding to one week. d) The results were verified in different regions, and the data impact may depend on this factor. e) The two analysis/forecast systems may show different sensitivity to the data.

It is of great practical importance to determine the factors that may have influenced these results. For this purpose Kalnay et al. (1984) extended the study to FGGE SOP-2 (May and June 1979), and performed similar buoy data impact studies. This study included the 3 forecast cases previously performed by Bourke et al., and verifications over the same regional areas.

The results of Kalnay et al. (1984) are summarized as follows: As indicated in Fig. 3 and Fig. 4, the addition of buoys had little effect in the Northern Hemisphere both in winter and in summer. In the Southern Hemisphere, the addition of buoy data to the conventional observing system has a clear positive impact, especially in the sea level pressure forecast in both seasons.

The result of deleting the buoy data from the complete FGGE system is shown in Figs. 5 and 6. In agreement with Kalnay et al. (1983) the impact of the buoys' loss is negligible during SOP-1 both in the Southern and Northern Hemispheres. During SOP-2 the impact is somewhat larger especially during the first two days of the Southern Hemisphere forecasts. The buoy information is therefore less redundant during SOP-2 than SOP-1, which helps to explain the difference in the results obtained by Kalnay et al. (1983) and Bourke et al. (1982).

c) Impact of GLAS Temperature Soundings and Cloud Tracked Winds

Susskind et al. (1984) have developed a temperature retrieval system based on the inversion of the physical radiative transfer equation using simultaneously infrared and microwave channels. As a result, the system not only produces atmospheric temperature soundings (GLAS retrievals) but also a number of important climate and weather parameters (ice and snow cover, cloud heights and amounts, day and night, land and sea surface temperatures, and others, which are discussed elsewhere in this volume).

In Fig. 7 we present a preliminary comparison of the forecast skill using the FGGE system, in one case with the GLAS temperature retrievals, and in the other the NESS retrievals operational during FGGE SOP-1. In the Northern Hemisphere, the use of the GLAS soundings produces a significant improvement in the sea level pressure forecasts. Most of the improvements are as large as 5 S_1 points or more, and almost all take place over North America, virtually eliminating the cases of negative impacts when compared with NOSAT forecasts. This suggests that the GLAS retrievals are superior to the FGGE operational retrievals in the Pacific Ocean. This may be partly due to the data gap present in the operational retrievals off the west coast of North America at 00 GMT (see Fig. 1a of Halem et al., 1982). Furthermore, the accuracy of the GLAS retrievals is much less affected by cloudiness than that of the operational retrievals (Susskind et al., 1984), which may have been an advantage in generating temperature soundings in the Pacific storm track region. In the Southern Hemisphere, on the other hand, the use of the GLAS retrievals produces, for the first two days, slightly worse forecasts than the operational retrievals, although both systems are vastly superior to the NOSAT forecasts.

In Fig. 8 we make a preliminary comparison of the forecasts using conventional data with GLAS soundings, and the full FGGE system, also with GLAS soundings. It is clear that the additional components of the FGGE system (and in particular cloud tracked winds which constitute the largest component) have made a very significant contribution to the forecast skill in the Southern Hemisphere. Even in the Northern Hemisphere their contribution is important, especially in the 3 day forecast.

d) Hemispheric Verification

In the previous comparisons, verifications were limited to land areas where there are enough conventional observations, avoiding a possible bias towards satellite data that constitute most of the oceanic observations. In Figs. 9 and 10 we now present the ensemble of about 8-10 hemispheric verifi-

cations against the ECMWF analysis for SOP-2. Fig. 9a shows that the FGGE satellite data improved the forecast in the Northern Hemisphere by about 6 hours, indicated schematically by the dotted lines. In the Southern Hemisphere the improvement is much larger, about 48 to 60 hours.

Fig. 10a indicates that the buoys added to the sparse conventional (NOSAT) system in the Southern Hemisphere improves the forecast skill by about 24 hours. In the presence of the satellite observing system, however, they contribute only about 12 hours (Fig. 10b). Fig. 10c demonstrates that the rest of the satellite temperature retrievals and cloud tracked winds added to the NOSAT system contribute 24 to 36 hours more forecast skill than the buoys.

FUTURE PLANS·

We plan to: a) study the impact of GLAS integrated retrievals both in winter and in summer; b) study the impact of cloud tracked winds; c) utilize, for the first time, water vapor winds in the analysis cycle, which should provide a useful spacial complement to the coverage of cloud tracked winds.

REFERENCES

Baker, W. E., 1983: Objective analysis and assimilation of observational data from FGGE. Mon. Wea. Rev., 111, 328-342.

Baker, W. E., R. Atlas, M. Halem, and J. Susskind, 1984: A case study of forecast sensitivity to data and data analysis techniques. Mon. Wea. Rev., 112, in press.

Bourke, K. Puri, and R. Seaman, 1982: Numerical weather studies from the FGGE Southern Hemisphere data base. Mon. Wea. Rev., 110, 1787-1800.

Halem, M., E. Kalnay, W. E. Baker, and R. Atlas, 1982: An assessment of the FGGE satellite observing system during SOP-1. Bull. Amer. Meteor. Soc., 63, 407-426.

Kalnay, E., R. Atlas, W. Baker, and M. Halem, 1983: FGGE forecast impact studies in the Southern Hemisphere. Proceedings of the First International Conference on Southern Hemisphere Meteorology, July 31-August 6, pp. 180-183.

Kalnay, E., R. Atlas, and M. Halem, 1984: Forecast skill of drifting buoys in the Southern Hemisphere. Proceedings of Tenth Conference on Weather Forecasting and Analysis, June 25-29, Clearwater Beach, Florida.

Kalnay-Rivas, E., A. Bayliss, and J. Storch, 1977: The 4th Order GISS Model of the global atmosphere. Beitr. Phys. Atmos., 50, 299-311.

Kalnay-Rivas, E., and D. Hoitsma, 1979: The effect of accuracy, conservation, and filtering on numerical weather forecasting. Preprints, Fourth Conference on Numerical Weather Prediction (Silver Spring), AMS, Boston, pp. 302-312.

Susskind, J., J. Rosenfield, D. Reuter, and M. T. Chahine, 1984: Remote sensing of weather and climate parameters from HIRS2/MSU on TIROS-N. J. Geophys. Res., in press.

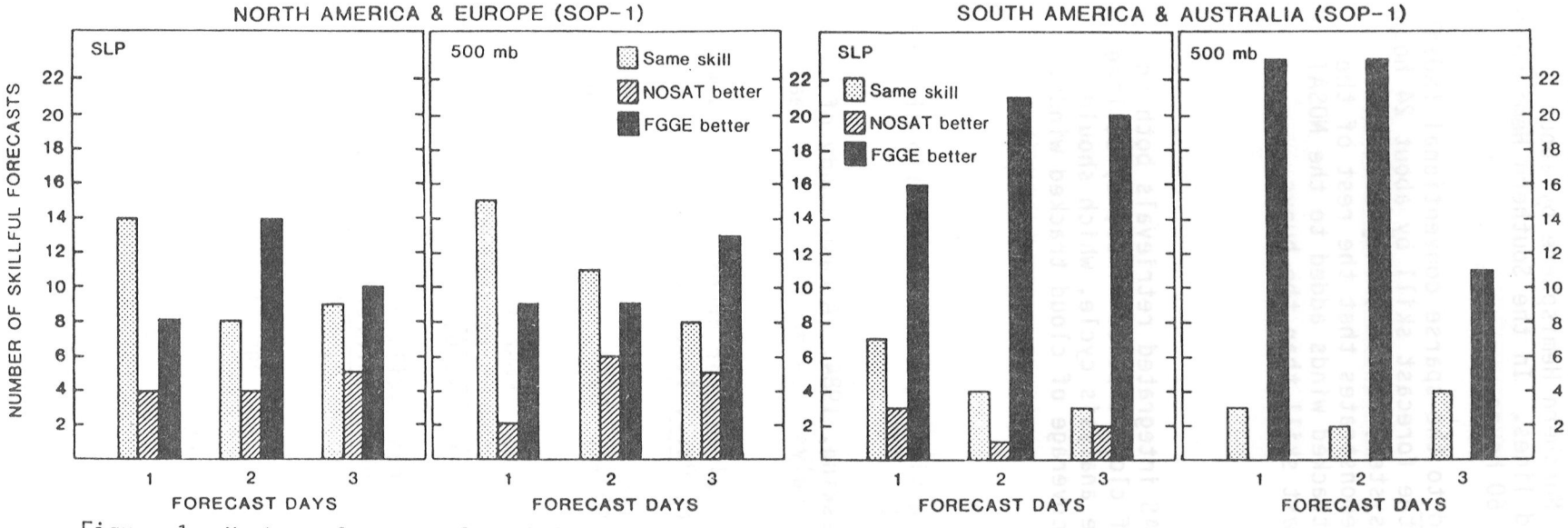

Figure 1. Number of cases of positive and negative forecast impacts from the FGGE Special Observing System during SOP-1.

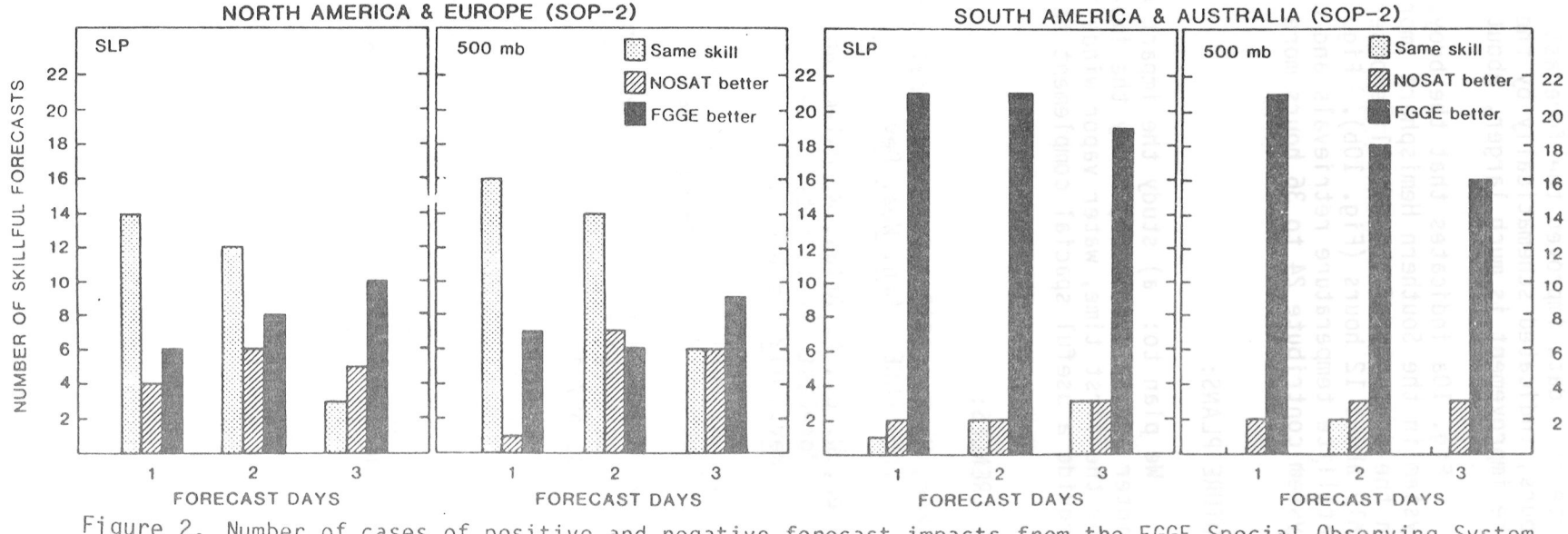

Figure 2. Number of cases of positive and negative forecast impacts from the FGGE Special Observing System during SOP-2.

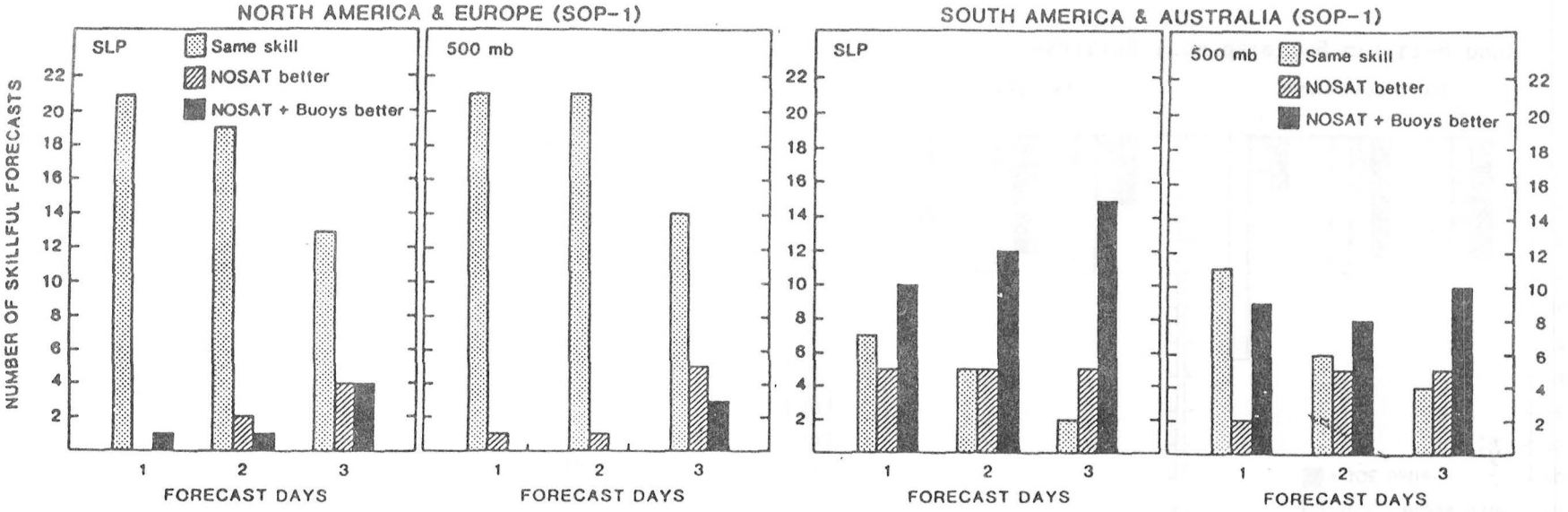

Figure 3. Number of cases of positive and negative forecast impacts resulting from adding drifting buoy data to the NOSAT system during SOP-1.

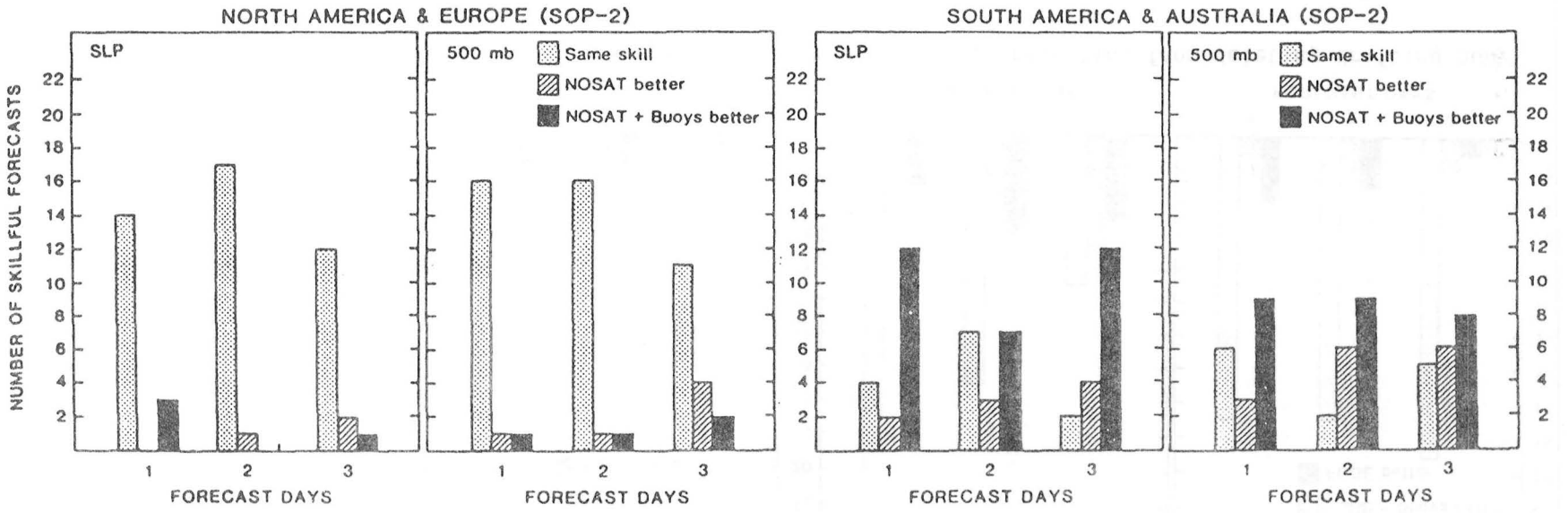

Figure 4. Number of cases of positive and negative forecast impacts resulting from adding drifting buoy data to the NOSAT system during SOP-2.

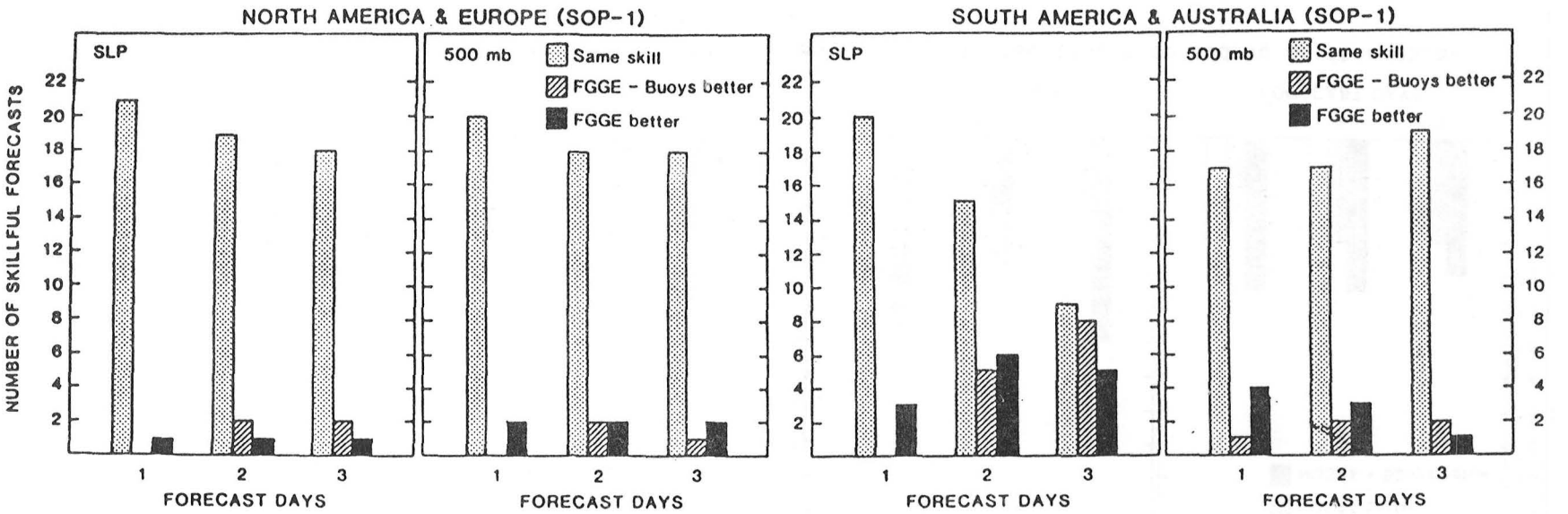

Figure 5. Number of cases of positive and negative forecast impacts resulting from deleting drifting buoy data from the FGGE system during SOP-1.

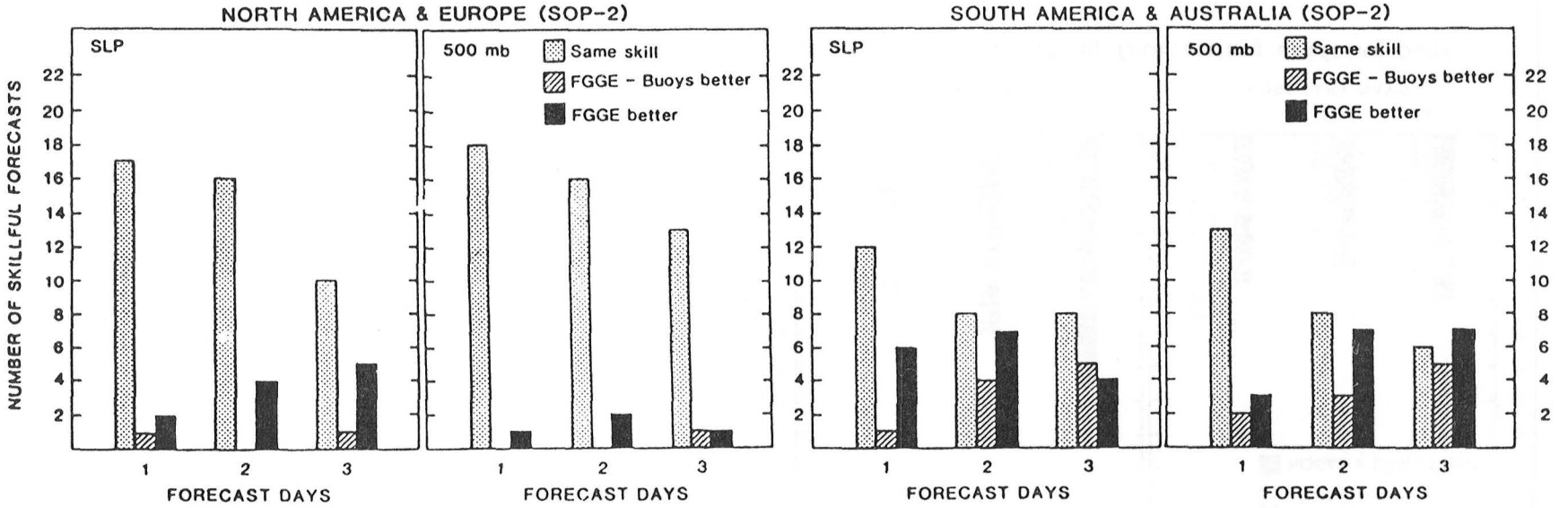

Figure 6. Number of cases of positive and negative forecast impacts resulting from deleting drifting buoy data from the FGGE system during SOP-2.

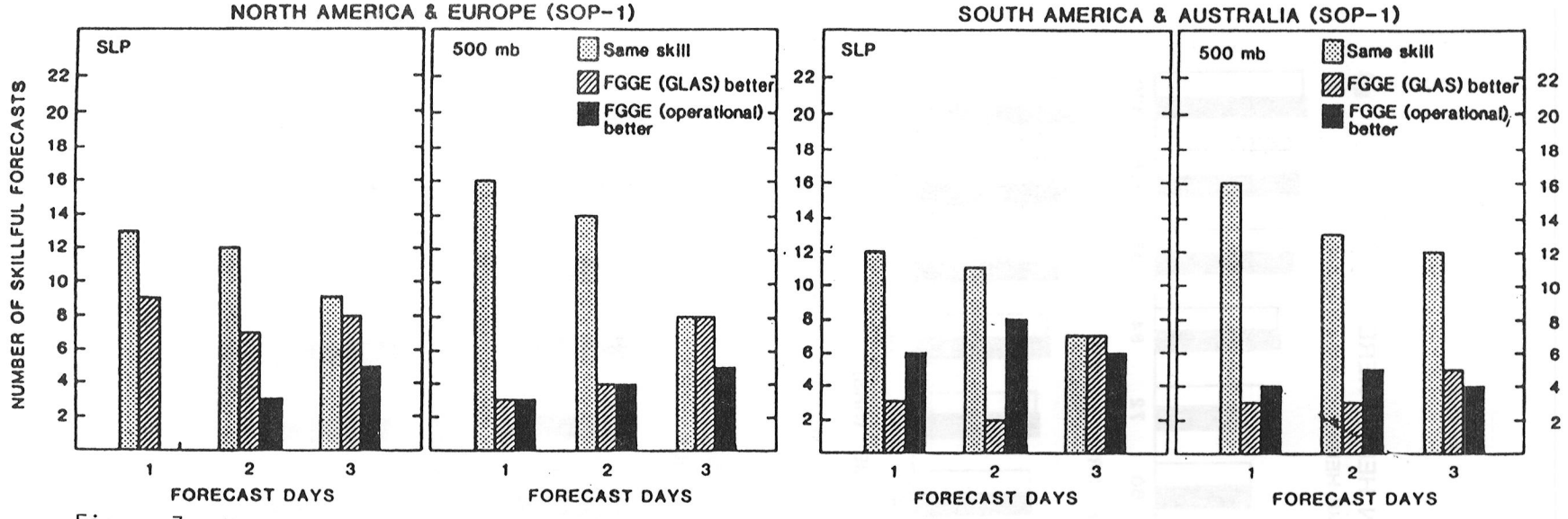

Figure 7. Number of cases of positive and negative forecast impacts from replacing the operational TIROS-N soundings with GLAS temperature soundings during SOP-1.

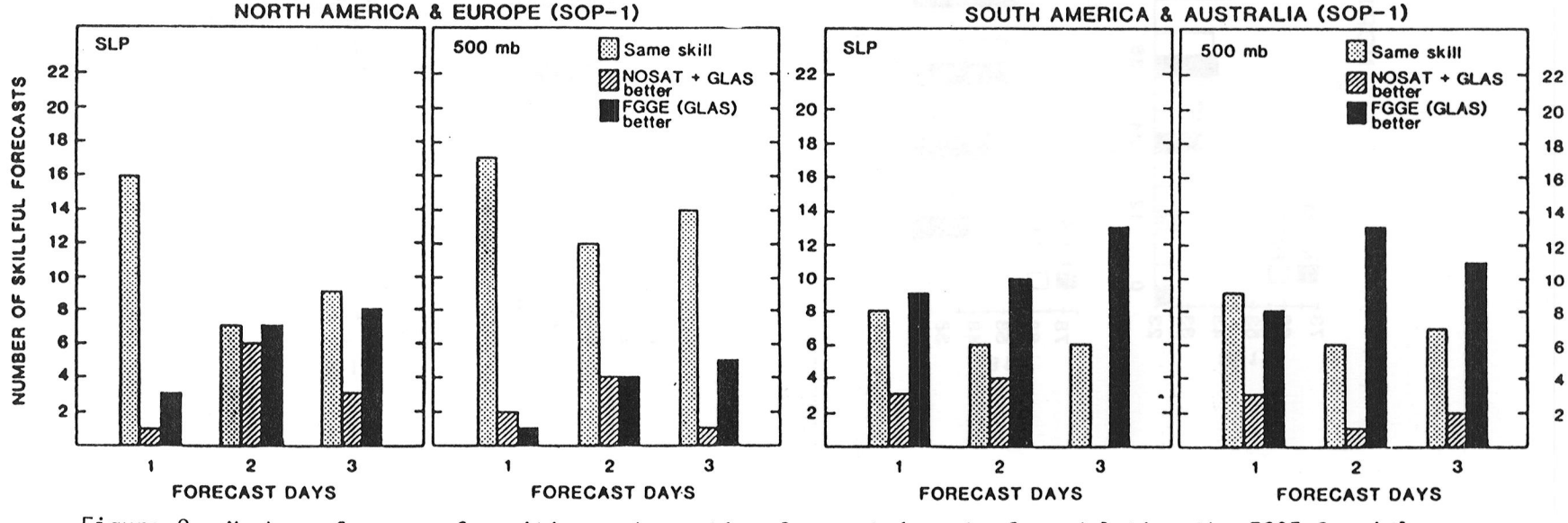

Figure 8. Number of cases of positive and negative forecast impacts from deleting the FGGE Special Observing System except for the GLAS temperature soundings (SOP-1).

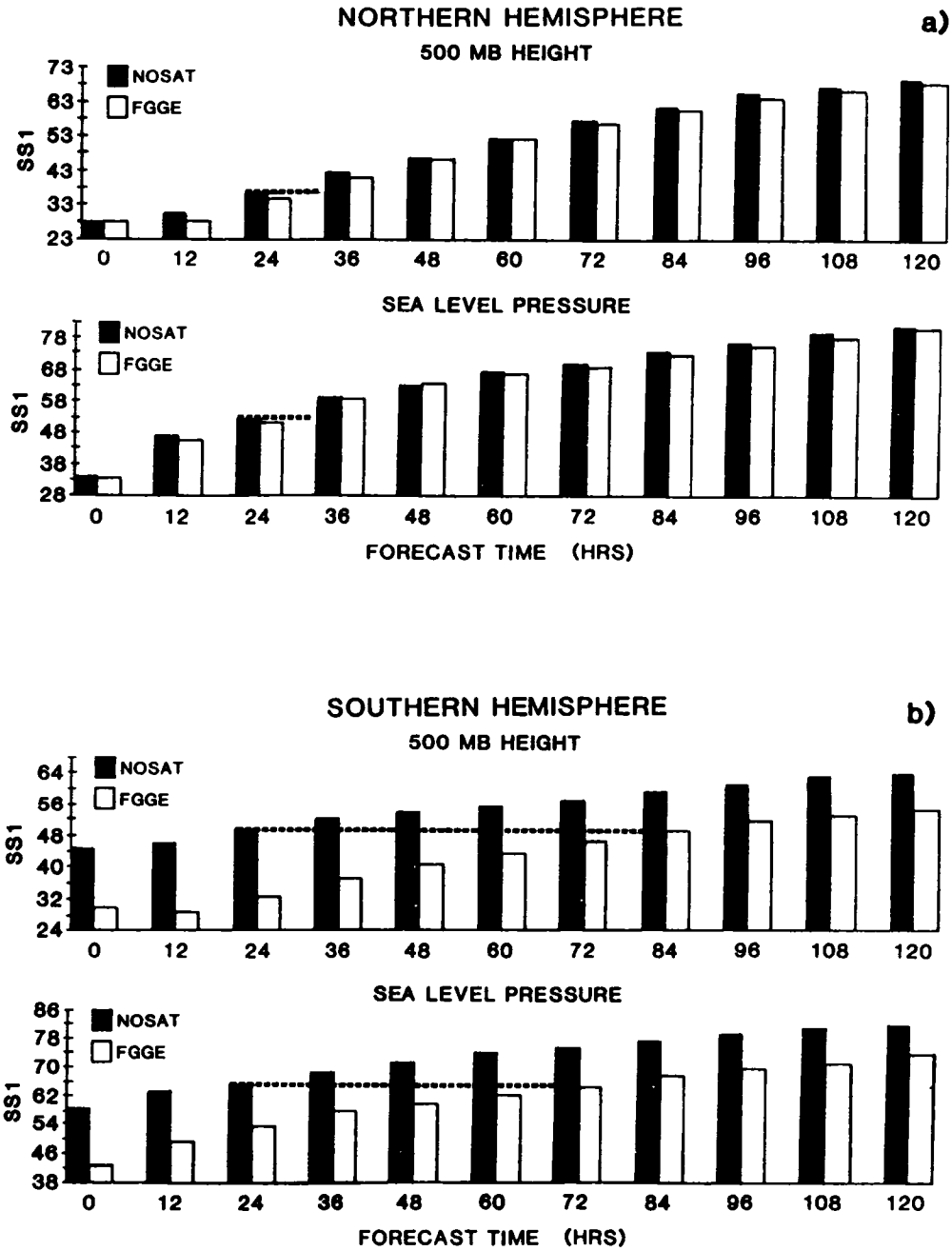
NORTHERN HEMISPHERE
a)
500 MB HEIGHT
NOSAT
FGGE
SS1
73
63
53
43
33
23
0 12 24 36 48 60 72 84 96 108 120
SEA LEVEL PRESSURE
NOSAT
FGGE
SS1
78
68
58
48
38
28
0 12 24 36 48 60 72 84 96 108 120
FORECAST TIME (HRS)
SOUTHERN HEMISPHERE
b)
500 MB HEIGHT
NOSAT
FGGE
SS1
64
56
48
40
32
24
0 12 24 36 48 60 72 84 96 108 120
SEA LEVEL PRESSURE
NOSAT
FGGE
SS1
86
78
70
62
54
46
38
0 12 24 36 48 60 72 84 96 108 120
FORECAST TIME (HRS)

Figure 9.

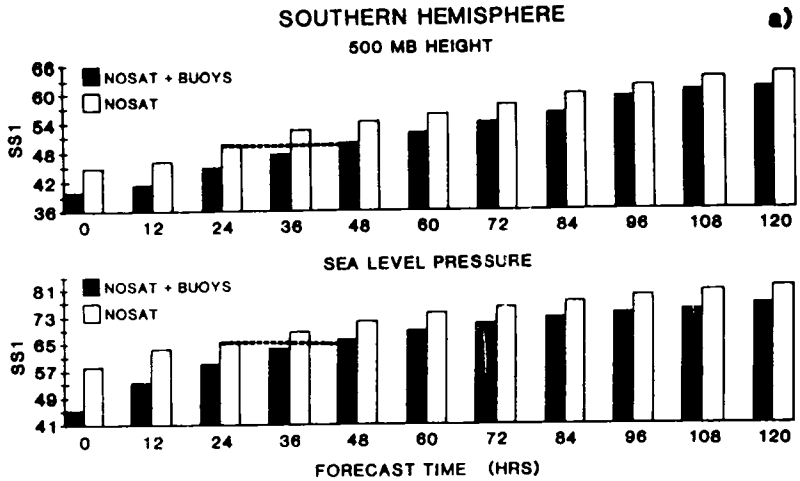
SOUTHERN HEMISPHERE
a)
500 MB HEIGHT
NOSAT + BUOYS
NOSAT
SS1
66
60
54
48
42
36
0 12 24 36 48 60 72 84 96 108 120
SEA LEVEL PRESSURE
NOSAT + BUOYS
NOSAT
SS1
81
73
65
57
49
41
0 12 24 36 48 60 72 84 96 108 120
FORECAST TIME (HRS)

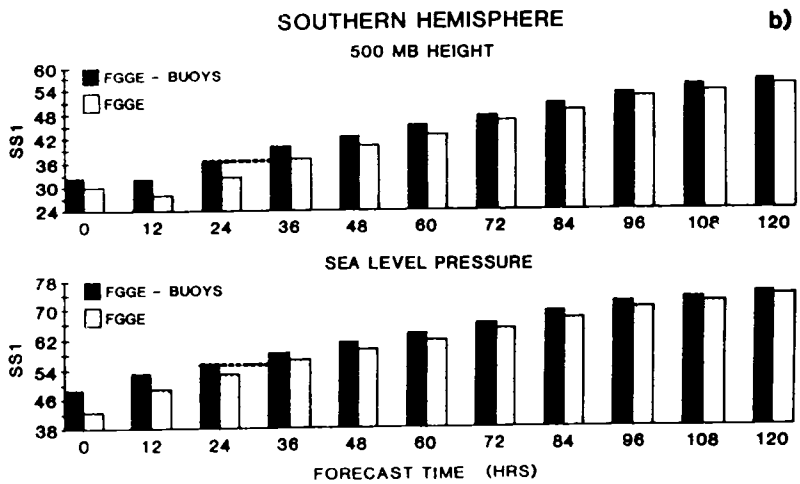
SOUTHERN HEMISPHERE
b)
500 MB HEIGHT
FGGE - BUOYS
FGGE
SS1
60
54
48
42
36
30
24
0 12 24 36 48 60 72 84 96 108 120
SEA LEVEL PRESSURE
FGGE - BUOYS
FGGE
SS1
78
70
62
54
46
38
0 12 24 36 48 60 72 84 96 108 120
FORECAST TIME (HRS)

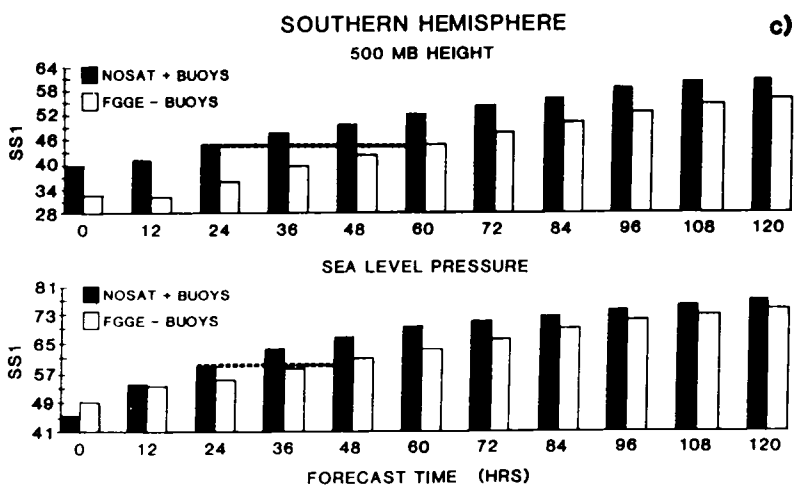
SOUTHERN HEMISPHERE
c)
500 MB HEIGHT
NOSAT + BUOYS
FGGE - BUOYS
SS1
64
58
52
46
40
34
28
0 12 24 36 48 60 72 84 96 108 120
SEA LEVEL PRESSURE
NOSAT + BUOYS
FGGE - BUOYS
SS1
81
73
65
57
49
41
0 12 24 36 48 60 72 84 96 108 120
FORECAST TIME (HRS)

Figure 10.

APPLICATIONS OF SEQUENTIAL ESTIMATION TO NUMERICAL WEATHER PREDICTION

(M. Ghil-Courant Institute of Mathematical Sciences, New York University)

RESEARCH OBJECTIVE:

The main objective of the author's cooperative research with NASA's Goddard Laboratory for Atmospheric Sciences (GLAS) is to use information about the atmosphere acquired from new types of observations, especially from satellites, in order to deepen our understanding of its behavior on time scales from hours to years. This is achieved by: 1) improving the methods for processing point observations into complete fields in space and time, using sequential estimation theory; and 2) analyzing low-frequency atmospheric variability by the methods of dynamical system theory, suitably modified to enhance practical predictability. The purpose of this extended abstract is to report on those activities which pertain to applications of sequential estimation to data assimilation and initialization (item 1 above).

SIGNIFICANT ACCOMPLISHMENTS:

Sequential estimation theory deals with methods for estimating the state of a physical system evolving in time, such as the atmosphere, using imperfect dynamical models, such as current numerical weather prediction (NWP) models, on the one hand, and observations which are imperfect, incomplete and irregularly distributed in space and time, on the other. Such observations are currently provided in great numbers, and with various error characteristics, by ground-based and space borne meteorological observing systems (Bengtsson et al., 1981, preface).

Given random model errors and observing errors, the optimal estimate of the state of the system is provided by the Kalman filter. This result is known from the engineering and mathematical literature, but has had no applications to systems of considerable size, like NWP models. We have undertaken to modify and simplify the Kalman filter (Ghil et al., 1981), so as to make it useful for meteorological data assimilation on the next generation of vector-processing computers, which will become available in 1986.

Large-scale atmospheric motions contain slow Rossby waves, as well as faster, enertia-gravity waves, both of which are present in current, primitive-equation (PE) NWP models. The Rossby waves are responsible for most meteorological phenomena on planetary and synoptic scales, while the faster waves are mostly important on smaller scales. In the process of data assimilation with large-scale models, the faster waves can lead to spurious rejection of significant data, due to insufficiently sophisticated quality control procedures. It is often deemed necessary therefore to eliminate the faster waves, in a process called initialization.

The first modification of the Kalman filter necessitated by its planned application to operational NWP was therefore to obtain an optimal estimate of large-scale atmospheric states, subject to the constraint of belonging to the slow invariant manifold of the model equations. This modification was developed and tested in Cohn (1982) and Ghil et al. (1981, 1982).

The next modification has to do with the fact that the standard Kalman filter assumes that statistics of the system noise, i.e., the difference between the model tendencies and the true atmospheric tendencies, as well as statistics of the observational noise, are known. Adaptive filters, which determine the covariances of these noises in the process of data assimilation, are computationally much more expensive than the basic filter. In Dee (1983) and Dee et al. (1984), we have developed an adaptive filter which has the same computational complexity as the standard filter.

Finally, we have attacked the problem of the computational expense of the standard filter itself. The most important way in which the Kalman filter differs from current NWP practice is that it computes the forecast error covariance matrix P_f exactly, while so-called "optimal interpolation" (OI) schemes use ad-hoc procedures for approximating P_f. A naive Kalman filter algorithm is equivalent therefore to N forecasts, where N is the total number of model variables, with $N = O(10^5\text{-}10^6)$ in current NWP models.

Using the sparseness of model matrices and the rapid decay in space of forecast error correlations, it is possible to compute P_f in $O(N \log N)$, rather than $O(N^2)$ operations (Ghil et al., 1981, 1983; Cohn, 1982). This permits the implementation of a Kalman filtering code for a barotropic PE model in two space dimensions (2D), i.e., the shallow-water equations on the sphere, with a resolution of 1° latitude x 2° longitude, on a current vector machine like the Cyber 205 (Cohn et al., 1984). It should permit the implementation of such a code for a baroclinic PE model in three dimensions (3D), with 10 levels in the vertical, on the next generation of vector machines. These machines, such as the CDC-Eta, will be O(10) times faster than the current generation, have a memory $O(10^2)$ larger, and become available at the end of 1986.

A by-product of this research is the evaluation and improvement of suboptimal filters in current use. The performance of OI schemes can be evaluated exactly by sequential estimation theory (Cohn et al., 1981; Ghil et al., 1982), and the deleterious effect of various approximations in P_f compared and removed in order of importance. Balgovind et al. (1983) have evaluated the effect of the Gaussian model of geopotential forecast error correlations and geostrophically-derived wind error correlations, using a semi-operational baroclinic PE model, the GLAS second-order model, and real atmospheric observations from the DST-6 data set. They have proposed an improved Bessel-function model for the geopotential correlations. Likewise, Cohn and Morone (1984) have evaluated the effect of spatial invariance of forecast error correlations and introduced the slow change of these correlations with geographic position into a scheme currently being tested for operational use at the National Meteorological Center.

CURRENT RESEARCH AND FUTURE PLANS:

Much of the author's theoretical research outlined above was motivated by his strong involvement in NASA's application program of meteorological satellite data, and his close collaboration with the research staff at GLAS in the time-continuous assimilation of these data (Ghil et al., 1979; Atlas et al., 1981, 1982). This collaboration is continuing in the application of the theoretical results to the development of the GLAS data assimilation system.

Dr. Amnon Dalcher of GLAS and the author are working on modifying and implementing the forecast error correlation functions recommended by Balgovind et al., 1983) to the GLAS fourth-order NWP model (Kalnay et al., 1983) using FGGE data and results from the European Center for Medium Range Weather Forecasts (ECMWF). The final model correlations thus determined should be especially useful in the assimilation of scatterometer wind data for the improvement of lower-tropospheric and surface flux analyses over ocean areas (Baker et al., 1984; Ghil et al., 1983).

Dr. Stephen Bloom of GLAS and the author are also working on determining the exact amount of energy in fast, as opposed to slow modes, present in GLAS and ECMWF analyses and forecasts. Such a separation was until recently impossible, due to the insufficient accuracy of observations and forecasts. An exact determination of their energy should help remove the deleterious effect of the fast waves on data assimilation (see Significant Accomplishments), without prohibiting these from carrying out their important role in energy exchanges between synoptic scales and meso-scales.

The major thrust of future work will be to continue the computational design of Kalman filters for 2D and 3D NWP models (Ghil, 1984). This work will severely tax the computational resources currently available to the Goddard Space Flight Center, and help justify the acquisition of vector machines of the next generation. Such an acquisition appears essential for GLAS and the Center to keep their position in the forefront of space applications and of the atmospheric sciences.

BIBLIOGRAPHY:

The references given here are restricted by the format imposed for the Science Review of the Global Scale Atmospheric Processes Program to reflect mainly the author's work over the last three years, in the area of activity indicated by the title of this abstract. The items which refer specifically to work by the author and co-workers over this period, acknowledging the support of NASA in the area of data assimilation and initialization, are indicated by an asterisk.

*Atlas, R., M. Ghil and M. Halem, 1981: Reply to comments by L. Druyan on Ghil et al. (1979). Mon. Wea. Rev., 109, 201-204.

*_____, _____ and _____, 1982: The effects of model resolution and satellite sounding data on GLAS model forecasts. Mon. Wea. Rev., 110, 662-682.

Baker, W. E., R. Atlas, E. Kalnay, M. Halem, P. M. Woiceshyn and D. Edelmann, 1984: Large-scale analysis and forecast experiments with wind data from the Seasat-A scatterometer. J. Geophys. Res., in press.

Balgovind, R., A. Dalcher, M. Ghil and E. Kalnay, 1983: A stochastic-dynamic model for the spatial structure of forecast error statistics. Mon. Wea. Rev., 111, 701-722.

Bengtsson, L., M. Ghil and E. Källén (eds.), 1981: Dynamic Meteorology: Data Assimilation Methods, Springer-Verlag, New York/Heidelberg/Berline, 330 pp.

Cohn, S. E., 1982: Methods of sequential estimation for determining initial data in numerical weather prediction. Ph.D. Thesis (advisors M. Ghil and E. Isaacson), published as Report CI-6-82, Courant Institute, NYU, 183 pp.

_____, and L. Morone, 1984: The dependence of OI forecast error correlations on horizontal derivatives of forecast error variances. In preparation.

*_____, M. Ghil and E. Isaacson, 1981: Optimal interpolation and the Kalman filter. Proc. 5th Conf. Numer. Weather Pred., American Meteorological Society, Boston, pp. 36-42.

_____, L. Morone and D. Parrish, 1984: A Kalman filter algorithm for a two-dimensional barotropic model. In preparation.

*Dee, D. P., 1983: Computational aspects of adaptive filtering and applications to numerical weather prediction. Ph. D. thesis (advisor M. Ghil), published as CI-6-83, Courant Institute, NYU, 150 pp.

*_____, S. E. Cohn and M. Ghil, 1984: An efficient algorithm for estimating noise covariances in distributed systems. IEEE Trans. Automatic Control, submitted.

*Ghil, M., 1984: Future possibilities in objective analysis and data assimilation for atmospheric dynamics. Proc. Natl. Res. Council Workshop on Results of the Global Weather Experiment, Natl. Acad. Sci. Study Center, Woods Hole, Mass., July 1984.

_____, M. Halem and R. Atlas, 1979: Time-continuous assimilation of remote-sounding data and its effect on weather forecasting. Mon. Wea. Rev., 107, 140-171.

*_____, S. Cohn, J. Tavantzis, K. Bube and E. Isaacson, 1981. Applications of estimation theory to numerical weather prediction. In Bengtsson et al. (1981). pp 139-224.

*_____, S. E. Cohn and A. Dalcher, 1982: Sequential estimation, data assimilation and initialization. In The Interaction between Objective Analysis and Initialization, D. Williamson (ed.), Publ. Meteorol 127 (Proc. 14th Stanstead Seminar), McGill Univ., Montreal, pp. 83-97.

*_____, _____ and _____, 1983: Applications of sequential estimation to data assimilation. In Large-Scale Oceanographic Experiment in the World Climate Research Programme, WCRP Publ. Series, No. 1, Vol. II, WMO/ICSU, Geneva, Switzerland, pp. 341-356.

Kalnay, E., R. Balgovind, W. Chao, D. Edelmann, J. Pfaendtner, L. Takacs, and K. Takano, 1983: Documentation of the GLAS fourth order general circulation model, Vol. I: Model documentation. NASA Tech. Memo. 86064, Goddard Space Flight Center, Greenbelt, MD 20771.

SOME NEW MATHEMATICAL METHODS FOR VARIATIONAL OBJECTIVE ANALYSIS

(G. Wahba and D. R. Johnson-University of Wisconsin-Madison)

RESEARCH OBJECTIVES:

To develop new and/or improved variational methods for simultaneously combining forecast, heterogeneous observational data, a priori climatology, and physics to obtain improved estimates of the initial state of the atmosphere for the purpose of numerical weather prediction. To apply cross validated spline methods to atmospheric data for the purpose of improved description and analysis of atmospheric phenomena such as the tropopause and frontal boundary surfaces.

SIGNIFICANT ACCOMPLISHMENTS: (Numbers in [ ] refer to references)

i) Development of theoretical foundations for combining forecast, observational data, and a priori climatology into a single variational problem [9, 15].

ii) Development of vector splines on the sphere, for the global analysis of wind fields and the dynamic allocation of energy between the divergent and non-divergent wind field by cross validation methods [2, 16].

iii) Development and application of three dimensional thin plate splines [3] to estimate height and horizontal wind fields, divergence, and vorticity. These methods may be used, for example, to obtain cross-sectional contour plots of divergence and vorticity as a function of longitude and pressure at a fixed latitude, or as a function of latitude and pressure at a fixed longitude [18]. Some examples are given in Figure 1.

iv) Development of adaptive methods for estimating the relative weight to be given to observational data and forecast, from the data and forecast [17].

v) Development of nonlinear cross validated regularization methods for the recovery of atmospheric temperature distributions from satellite observed radiances [1, 6, 13].

vi) Development of variational methods for simultaneously combining forecast, observational data, and climatology; and performing nonlinear normal mode initialization (preliminary results, [11].

vii) Development of new design criteria for satellite computed tomography [8].

viii) Development of some numerical methods useful in analyzing large data sets simultaneously by cross validated spline methods [4, 5]. Although not specifically developed for meteorological applications, these methods have potential applicability to the efficient simultaneous three dimensional analysis of data sets of the order of many hundreds or even thousands.

ix) Development of cross validated constrained spline methods for low pass filtering with linear inequality constraints. Although not developed specifically for meteorological applications, these methods also have potential application in objective analysis [7, 14].

CURRENT RESEARCH:

i) Completion of work listed under "Significant Accomplishments:" i), ii), iii), iv) and v).

ii) Continuation of "Significant Accomplishments:" vi), including the development of appropriate numerical methods for the large nonquadratic variational problems that will result.

FUTURE PLANS:

Immediate plans are to complete work listed under "Current Research." Four major tasks have been identified in our proposal which are described below. Work on tasks three and four has already begun with "Significant Accomplishments:" iv) and vi). The first (development) task emphasized techniques for merging satellite radiance data with other information, in particular radiosonde data and tropopause and frontal height information to obtain an enhanced two or three dimensional thermal wind or temperature analysis. The second (applications) task is to apply cross-validated thin plate spline analysis techniques and computer programs developed under an earlier contract to an empirical study of the relationship between certain surfaces of constant potential temperature and frontal boundary surfaces. The third (development) task concerns techniques for the dynamic estimation of the relative accuracy of forecast and observational data for use in optimum weighting when these two sources of information are merged. In addition, the development of hypothesis tests for the consistency of forecast with observational data is proposed. If time and resources permit, a fourth task, a study of the merging of the functions of variational objective analysis and nonlinear normal mode analysis into a single variational problem, is proposed.

JOURNAL PUBLICATIONS:

Wahba, G., 1984: Cross validated spline methods for the estimation of multivariate functions from data on functions. In Statistics, and Appraisal, H. A. David and H. T. David, eds. The Iowa State University Press, pp. 205-235.

Wahba, G., 1982: Vector splines on the sphere, with application to the estimation of vorticity and divergence from discrete, noisy data. In Multivariate Approximation Theory, Vol. 2, W. Schemmpp and K. Zeller, eds., Birkhauser-Verlag, Basel-Boston-Stuttgart.

Wahba, G. and J. Wendelberger, 1980. Some new mathematical methods for variational objective analysis using splines and cross validation. Mon. Wea. Rev., 108, 1122-1143.

Wahba, G., 1980: Spline bases, regularization, and generalized cross validation for solving approximation problems with large quantities of noisy data. In Approximation Theory III, ed. W. Cheney, Academic Press, pp. 905-912.

TECHNICAL PUBLICATIONS.

Bates, D. and G. Wahba, 1983: A truncated singular value decomposition and other methods for generalized cross-validation. University of Wisconsin-Madison, Statistics Dept., TR 715, submitted.

O'Sullivan, F., 1983: The analysis of some penalised likelihood estimation schemes. Ph.D. Thesis, University of Wisconsin-Madison, Statistics Dept. TR 726.

Villalobos, M., 1983: Estimation of posterior probabilities using multivariate smoothing splines and generalized cross-validation. Ph. D. Thesis, University of Wisconsin-Madison, Statistics Dept. TR725, to be submitted.

Wahba, G., 1983. Design criteria and eigensequence plots for satellite computed tomography. University of Wisconsin-Madison, Statistics Dept. TR 732, submitted.

CONFERENCE PUBLICATIONS:

Wahba, G., 1982: Variational methods in simultaneous optimum interpolation and initialization. In The Interaction Between Objective Analysis and Initialization, Publication in Meteorology 127, Dept. of Meteorology, McGill University and Atmospheric Analysis and Prediction Division, NCAR, D. Williamson, Ed.

Wahba, G.,1981: Some new techniques for variational objective analysis on the sphere using splines, Hough functions, and sample spectral data. Preprints, Seventh Conference on Probability and Statistics in Atmospheric Sciences, Monterey, CA, Nov. 1981.

PRESENTATIONS:

"Cross validation in variational methods for objective analysis and nonlinear initialization." Talk given by G. Wahba at NCAR, February 7, 1984.

"Vector splines on the sphere, with application to the estimation of vorticity and divergence from discrete, noisy data." Talk given by G. Wahba at Australian Numerical Meteorological Research Centre, Melbourne, Australia, May 14, 1984.

IN PREPARATION

O'Sullivan, F. and G. Wahba, 1984. Remote sensing of temperature profiles in the atmosphere, in preparation.

Villalobos, M. and G. Wahba, 1984: Inequality constrained multivariate smoothing splines, in preparation.

Wahba, G., 1984: Bayes theorem and the optimal merging of forecast, data, and climatology, in preparation.

Wahba, G., D. R. Johnson, and D. S. Kim, 1984: Optimal adaptive merging of forecast and observations, in preparation.

Wendelberger, J., D. R. Johnson, G. Wahba, and D. S. Kim, 1984: Two and three-dimensional thin plate spline estimation of meteorological fields, in preparation.

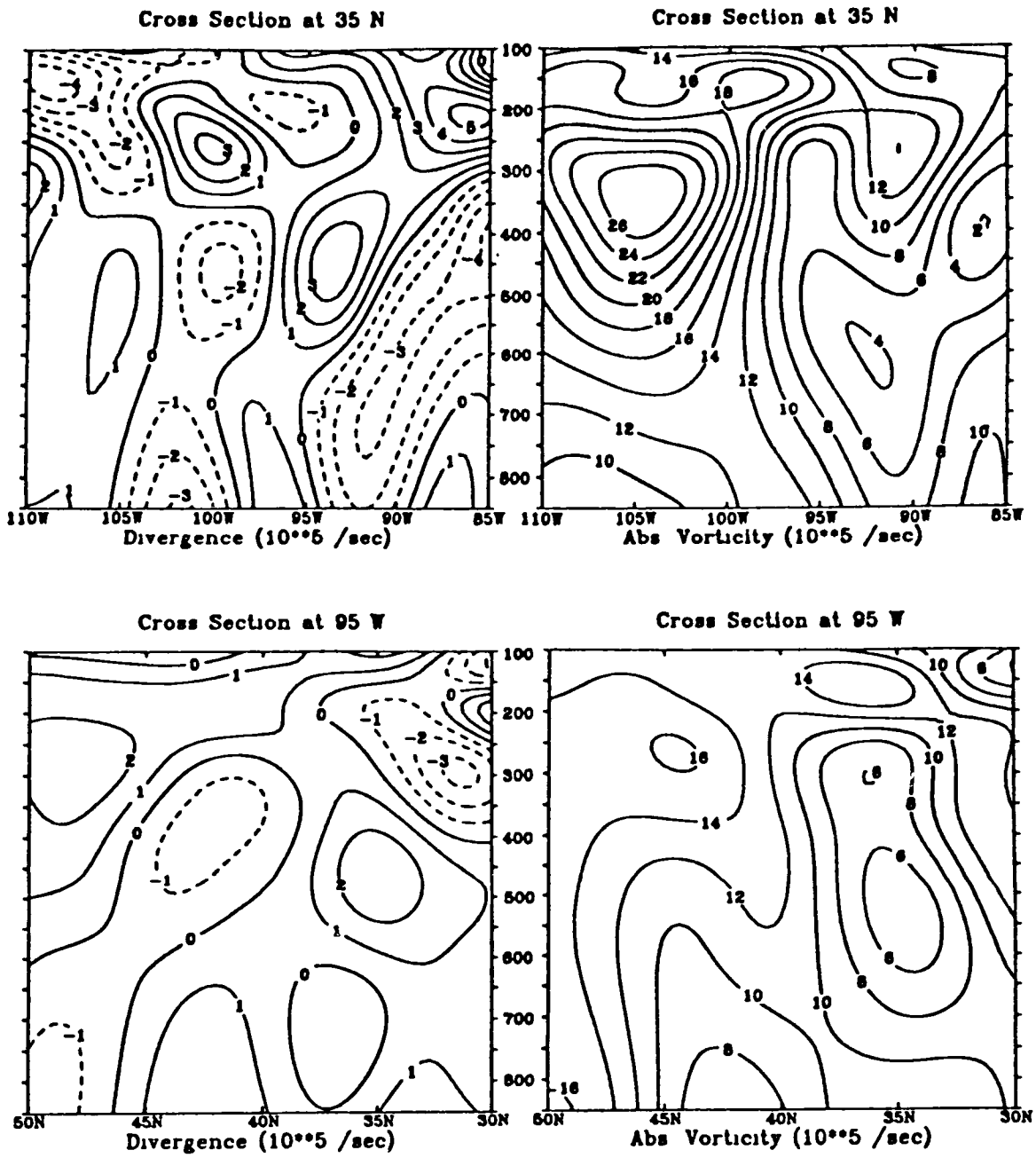

Fig. 1. Vertical cross sections of divergence and absolute vorticity, based on a three dimensional scaled cross validated spline analysis of observations from 46 North American stations at nine levels. 00Z Jan 25, 1978.

EXTENDED RANGE FORECASTING
(E. Kalnay-GSFC, A. Dalcher-Sigma Data and Y. Sud-GSFC)

RESEARCH OBJECTIVES·

Explore atmospheric predictability between a week and a month by means of the use of comprehensive atmospheric models, and with emphasis on *a priori* estimations of forecast skill.

CURRENT RESEARCH.

We have two main research projects as part of our role in the Experimental Climate Forecast Center established at GLAS by the National Climate Office:

1) Systematically explore the existence, if any, of predictability of monthly mean anomalies associated with initial conditions and with anomalies in the boundary forcing. This will be done by means of numerical integrations of the GLAS Fourth Order GCM, using real initial conditions corresponding to different years, and boundary conditions corresponding both to climatology and to observed anomalies at different years. A first result of this program is presented in Fig. 5 of Kalnay (1984 this volume). It indicates that the model has captured the most important monthly anomaly of July 1979 when started from 15 June 1979 initial conditions. The complete plan is described in a proposal recently submitted to NASA Headquarters.

2) Application of the Lagged Average Forecasting Method

Hoffman and Kalnay (1983, denoted HK from here on, and 1984) formulated the lagged averaged forecast (LAF) method, which has all the advantages of Monte Carlo forecasting and can be attained at virtually no cost. It makes use of not only the latest operational forecast, but also of forecasts for the same verification time started one or more days earlier than the latest one. The LAF method, in which the forecasts are weighted by a simple regression scheme based on a parameterization of the forecast error growth, was tested using low order "nature" and "forecast" models. The most important result of this study was that the spread of members of the ensemble forecast was a good *a priori* estimator of the skill of the ensemble forecast (see Fig. 8 from HK).

The LAF method seems particularly appropriate for long range forecasting, in combination with a comprehensive GCM and with observed boundary conditions. In this context, the longer predictability expected for time averages will naturally give rise to regression weights different from zero for periods beyond the limit of deterministic predictability. The LAF method should provide more accurate forecasts than a single dynamical forecast because the unpredictable components will be filtered out by the ensemble averaging, and it may also generate meaningful estimates of the confidence limits for individual anomaly forecasts.

We are presently applying for the first time, the LAF technique to the 100-day samples of 10-day forecasts (500 mb geopotential height data only) which were originally prepared for the study by Lorenz (1982) and also used by Wallace *et al.* (1983).

The purpose of this study is to improve the medium and long range forecast by reducing the error variance, and at the same time to produce an a priori estimate of the forecast skill. In order to develop and test the methodology, we first concentrate on preparing a LAF forecast for the 5-day forecast (Fig. 1). This provides us with an ensemble of six elements, which as shown by HK is probably sufficient, and the forecast is long enough that the ordinary dynamic forecast may be improved upon (see also HK). The 5-day LAF, y_5, is given by

$$y_5 = \sum_{i=0}^{5} \alpha_i \, x_{5+i}$$

where α_i are regression coefficients and x_{5+i} forecasts started i days ago, valid five days from today if $\bar{y}$ is the verification. The forecast squared error can be expressed as

$$\langle (x - \bar{y})^2 \rangle = \langle x - \bar{y} \rangle^2 + \langle (x' - \bar{y}')^2 \rangle$$

i.e., the mean square error is equal to the systematic error squared plus the error variance. In the implementation of LAF, the systematic error is automatically corrected (we will assume for this project that 100 days is a large enough sample to determine the systematic error). We note in passing that the systematic error growth in the winter 100 days is greatly dominated by the components with total wavenumber n=0 (global average) and n=6, and m=0 to 3, and n=3, m=0 to a lesser extent (Fig. 2). The summer systematic error (not shown) is more uniformly spread among several more spherical components.

The regression coefficients, x_i, must satisfy

$$\langle \bar{y}_5 \, x_{5+j} \rangle = \sum_{i=0}^{5} \alpha_i \, \langle x_{5+i} \, x_{5+j} \rangle \, , \quad j=0, \ldots, 5$$

so that we must be able to provide stable estimates of the covariances $\langle \bar{y}_5 \, x_{5+j} \rangle$, $\langle x_{5+i} \, x_{5+j} \rangle$, or equivalently, of the forecast error growth, since, for example,

$$\langle (x_i - x_j)^2 \rangle = 2 \langle x_i^2 \rangle \left[1 - \frac{\langle x_i \, x_j \rangle}{\sqrt{\langle x_i^2 \rangle \langle x_j^2 \rangle}} \right]$$

i.e., the error variance between two forecasts verifying on the same day is equal to twice the variance times one minus their correlation.

SIGNIFICANT ACCOMPLISHMENTS:

An analysis of the ECMWF data has allowed us to make simplifying assumptions that ensure that we have both stable statistics and a good representation of the error growth. We have also modified the parameterization of forecast error growth by Lorenz (1982, Fig. 8) in two ways: Computing error variance rather

than rms error, and including an external source of error to represent model deficiencies. Like Lorenz (1982), we allow for saturation at large error levels.

$$\frac{dV}{dt} = \alpha (V + S) (V^{\infty} - V)$$

Fig. 3 which shows the contribution to analysis and forecast variance for total wavenumbers $n \leq 5$, $n \leq 10$, and $n \leq 15$. It indicates that, to a good approximation, we can assume the analysis and forecast variances to be the same. (This is less true in the summer 100 days). Fig. 4 shows the contributions to forecast error variance, and indicates that the forecast error variance due to low wavenumbers increases with the length of the forecast. Moreover, if we consider only the lowest 15 total wavenumbers, we include more than 90% of the forecast error variance. Fig. 5 presents the error growth of each total wavenumber n for n=0 to n=19. Several observations stand out: a) the forecast error variance grows with wavenumber from n=0 to n=7, where it acquires its maximum amplitude. From n=8 to n=15 it decreases monotonically, and beyond n=16, it is quite small; b) forecast error saturation, when no further error growth is observed, is reached at longer times for longer wavelengths. Waves with $n<5$ have error variances which are only starting to grow within the 10-day forecast period, waves with $n<10$ start to reach saturation at about or after 10 days, and saturation is reached at earlier times for larger n's. Beyond n=15, wave error reaches saturation within the first five days, and no further predictability can be expected.

Fig. 9 shows that this parameterization works remarkably well when all scales are combined together. Furthermore, the shape of the individual error growths for each total wavenumber suggests that the same parameterization can be applied to each total wavenumber. The results (not shown) are also excellent, except for n=0, and n=1 which have only a few components, and therefore are more sensitive to sampling fluctuations but which have, in any case, very small amplitude errors (see Fig. 2.5).

FUTURE PLANS:

From this study, and since we have obtained excellent results so far in our modeling of error growth, we expect to improve significantly the ECMWF 5-day forecast. This result would be better than in our original study (HK) where the LAF forecast was not much better than an ordinary dynamical forecast, probably because we were less successful in the modeling of forecast error.

We also expect to be able to estimate forecast breakdown time for each wavenumber n. From this it will be possible to produce, for the first time, a priori maps of expected forecast skill.

PUBLICATIONS:

Kalnay, E., and R. Livezey, 1983: Weather Predictability Beyond a Week: An Introductory Review. Turbulence and Predictability in Geophysical Fluid Dynamics and Climate Dynamics. (M. Ghil, R. Benzi and G. Parisi, eds.), North Holland, in press.

Kalnay, E., R. Balgovind, W. Chao, D. Edelmann, J. Pfaendtner, L. Takacs and K. Takano, 1983: Documentation of the GLAS Fourth order General Circulation Model. NASA Tech. Memo. 86064.

Hoffman, R. N. and E. Kalnay, 1984: Lagged Average Forecasting, Some Operational Considerations. Predictability of Fluid Motions, G. Holloway and B. J. West, eds. American Institute of Physics.

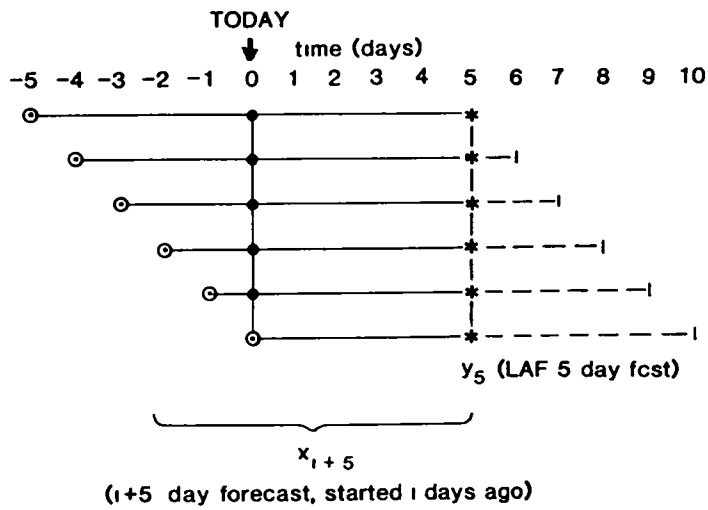

Figure 1

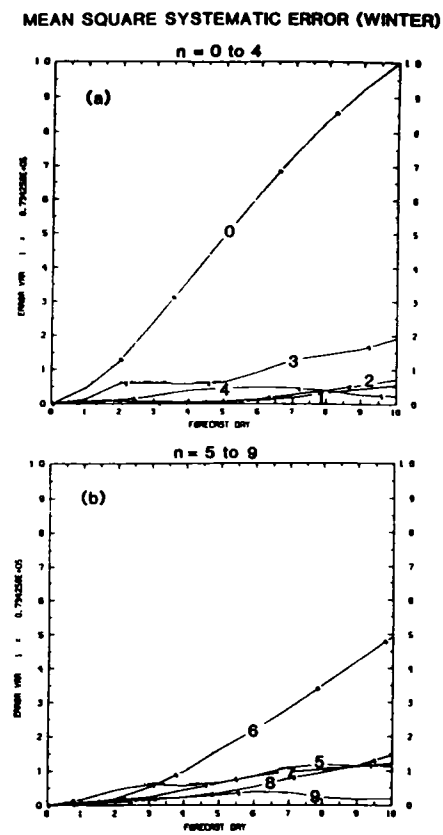

Figure 2

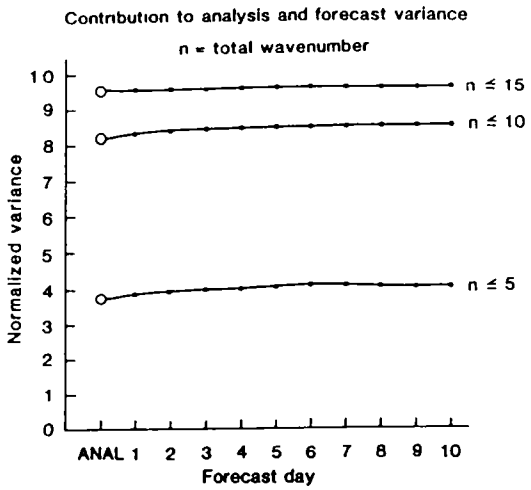

Figure 3

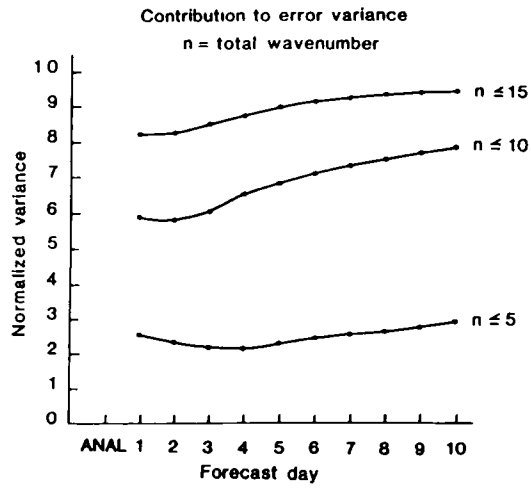

Figure 4

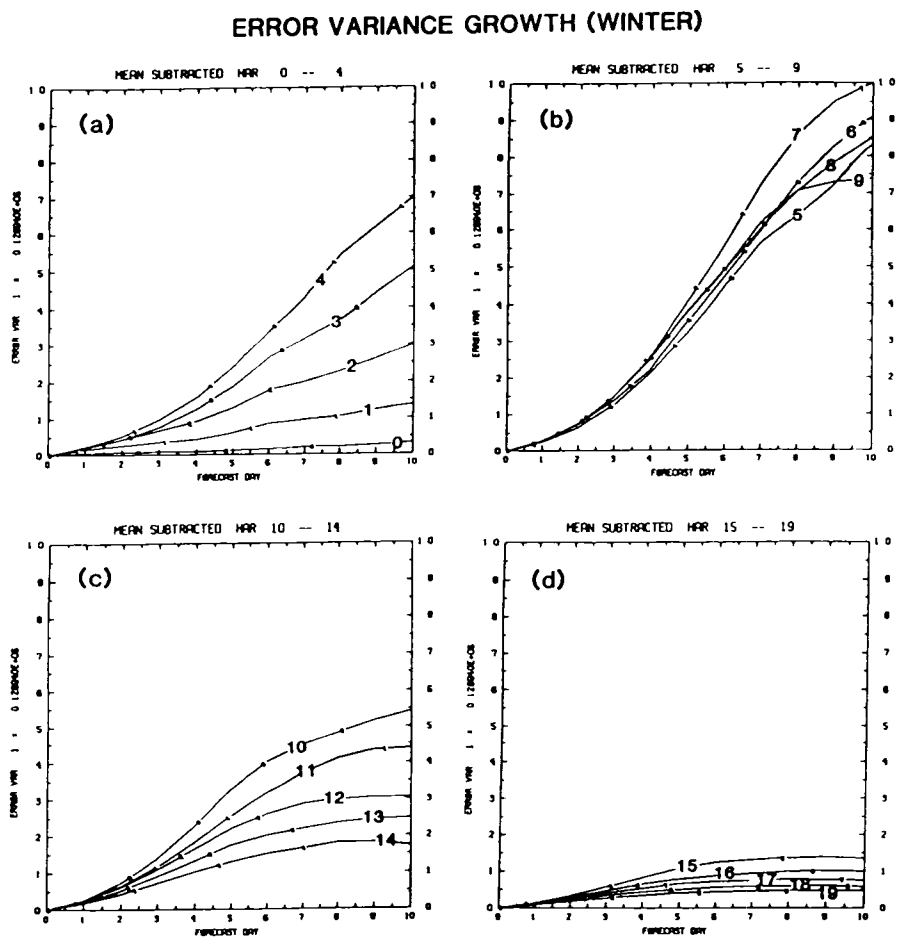

Figure 5

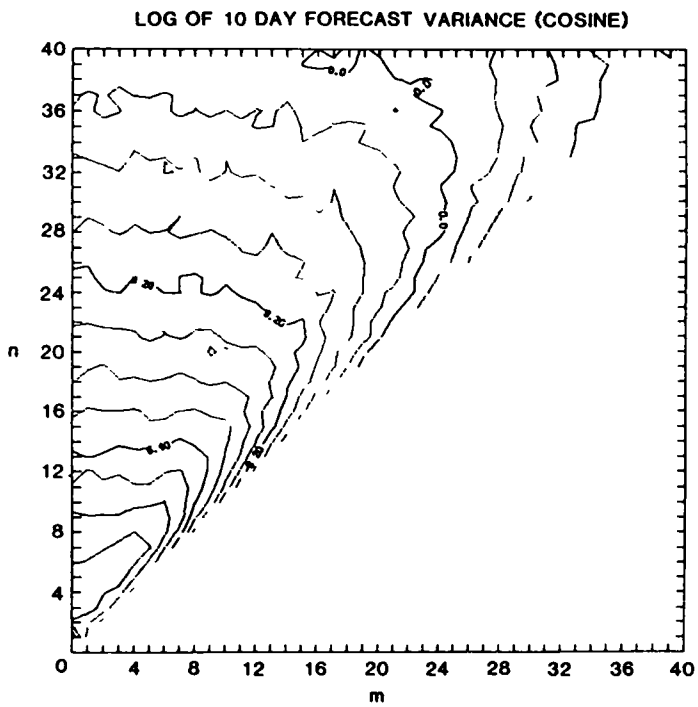

Figure 6

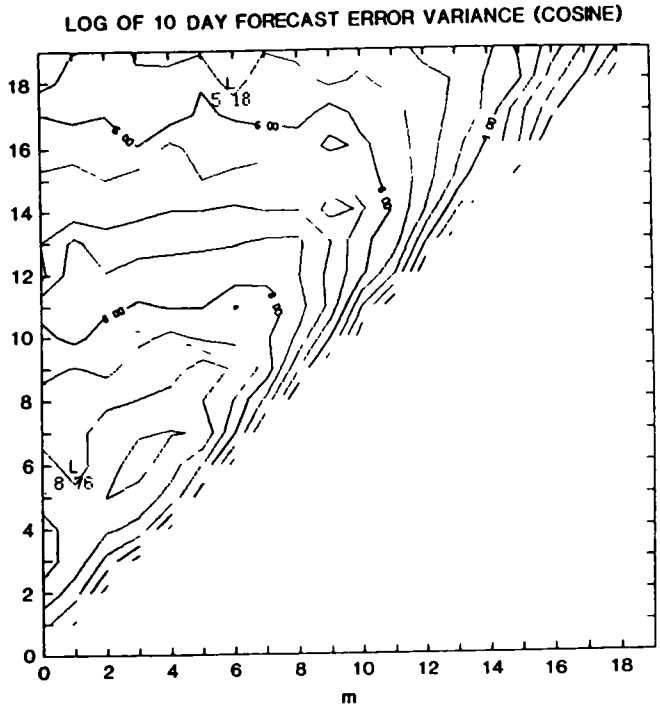

Figure 7

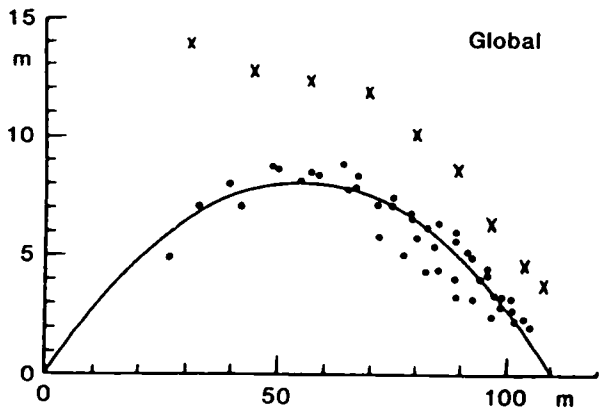

Figure 8

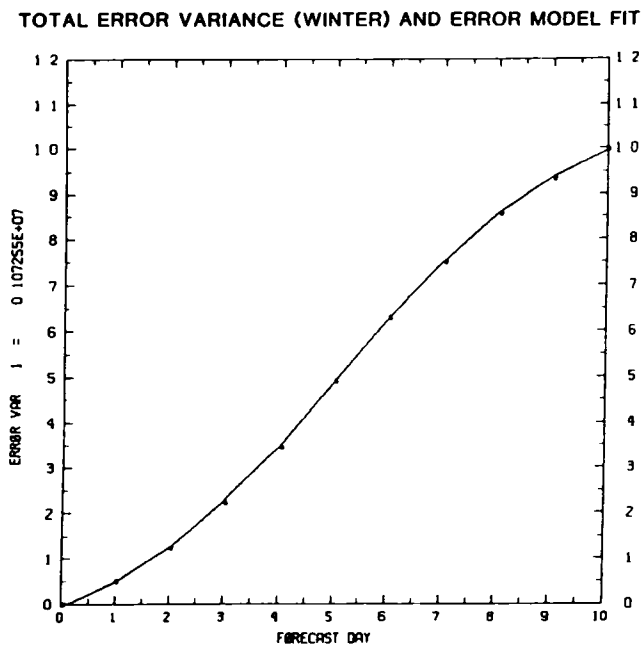

Figure 9

III. SATELLITE RETRIEVAL METHODS

Page intentionally left blank

WEATHER AND CLIMATE PARAMETERS FROM TIROS-N
(J. Susskind-GSFC, D. Reuter-GSFC/USRA)

RESEARCH OBJECTIVE:

The objective of the research is to develop a processing system for analysis of HIRS2/MSU data on the TIROS/NOAA meteorological satellites to be used both to improve forecasting skill and to develop climatological data for at least a five year period. Research involves both the development of improved techniques and validation studies of the retrieved products.

SIGNIFICANT ACCOMPLISHMENTS:

Details of the Baseline I processing system, and results for January 1979, are described in Susskind et al., 1984. Since then, an improved Baseline 1.5 system has been developed and implemented. Global retrievals (50000 retrievals per day) have been run at 125 km resolution for January and July 1979 and March and July 1982. Complete processing of 1 day's retrievals takes about 50 minutes wall clock time on the CYBER 205. In addition to producing atmospheric temperature profiles, which are significant for initialization of general circulation models to improve numerical weather prediction, the system also provides the following parameters: sea/land surface temperature and their day night differences which, over land, is related to soil moisture; fractional cloud cover, cloud top pressure, and cloud top temperature, and their day night differences; and ice and snow cover, which is derived from combined use of the retrieved surface emissivity at 50.3 GHz and the ground temperature. Research with the fields have shown the following:

1) Forecast assimilation cycles for SOP-1, substituting GLAS-retrieved HIRS2/MSU temperature profiles for operational retrievals, resulted in significant improvement in satellite forecast impact over North America and Europe.

2) Monthly mean sea surface temperature fields derived by GLAS from HIRS2/MSU data were compared with those derived from ships, AVHRR, and SMMR in a NASA sea surface temperature intercomparison workshop. The results showed HIRS/MSU to be the most accurate, both in RMS error and anomaly patterns.

3) Monthly mean day-night ground temperatures difference fields were computed from the GLAS HIRS2/MSU retrievals for a number of months, from which monthly mean soil moisture and evapotranspiration fields were derived. These fields were consistent both with climatological values of soil moisture and with the cloud fields derived from HIRS2/MSU data.

4) Global monthly mean fields of cloud fraction (high/middle/low) and their day-night differences were generated from HIRS2/MSU data. The results were consistent with climatology as well as model-generated rainfall. Cloudiness in highly convective regions was found to be more prevalent at night over land and during the day over ocean. Low clouds showed the reverse behavior in both cases.

5) Monthly mean ice and snow fields were derived from HIRS2/MSU data for a number of months. Weekly fields showed reasonable consistency and variations.

CURRENT RESEARCH AND FUTURE PLANS:

Current research involves implementation of a humidity solution algorithm, which has been tested in simulation, and the restructuring and full vectorization of the retrieval program so as to be able to produce retrievals at 60 km resolution in 5-10 minutes a day wall clock time on the CYBER 205. Our immediate plans are to run retrievals for SOP-1 and SOP-2 of FGGE using the new system in a completely interactive forecast-retrieval-analysis mode, in which a 6 hour forecast will be used as a first guess for the retrievals. The retrievals will then be used, together with other measurements such as ship and radiosondes, to generate the global analysis used to produce the next 6 hour forecast, etc. Previous experience (Baker et al., 1984) has indicated that such a cycle is capable of further significant improvement in forecast skill.

REFERENCES:

Baker, W. E., R. Atlas, M. Halem and J. Susskind, 1984: A case study of forecast sensitivity to data and data analysis techniques. Mon. Wea. Rev., 112, in press.

Susskind, J., J. Rosenfield, D. Reuter and M. T. Chahine, 1984: Remote sensing of weather and climate parameters from HIRS2/MSU on TIROS-N. J. Geophys. Res., 89D, 4677-4697.

WATER VAPOR PROFILE RETRIEVALS FROM THE HIRS/MSU SATELLITE SOUNDER

(D. Reuter-GSFC/USRA and J. Susskind-GSFC)

RESEARCH OBJECTIVE:

The objective of this research is to develop a method for the retrieval of atmospheric water vapor profiles within the context of the GLAS physically based retrieval scheme. The GLAS retrieval method is currently capable of producing accurate atmospheric temperature retrievals as well as cloud fields and retrieved surface properties such as temperature and microwave emissivity (Susskind et al., 1984). In the GLAS retrieval scheme, the water vapor field used in the computation of the atmospheric transmittance functions is obtained from a 6 hour forecast and is not modified in the retrieval process. Improved estimates of the water vapor field, in addition to being in themselves variables of meteorological interest, may, therefore, result in improved estimates of the other retrieved parameters obtained from the system.

For a particular atmospheric water vapor and temperature profile (including surface temperature), an estimate of the upwelling thermal radiation which would be observed in a certain channel of a satellite borne sensor may be calculated given an algorithm for the computation of channel averaged atmospheric transmittances as a function of atmospheric conditions and satellite viewing angle. Differences between the actual observed radiances and the calculated radiances are then due to differences between the actual temperatures and water vapor amounts and the prescribed temperatures and water vapor amounts, errors in the transmittance algorithm, and the estimated effects of clouds if they are present. The currently operational GLAS retrieval scheme uses a combination of microwave and infrared observations and an initial guess to obtain first estimates of the reconstructed clear column brightness temperatures (i.e. the brightness temperatures which would be observed in the absence of clouds (Smith 1968, Chahine 1974)). These estimates of the clear column brightness temperatures are then used to adjust the atmospheric and surface temperatures which are used to obtain new estimates of the reconstructed clear column brightness temperatures in an iterative fashion, until the calculated clear column brightness temperatures agree with the reconstructed clear column brightness temperatures to within a specified amount. These retrievals use theoretical relationships between changes in atmospheric and surface temperature and changes in channel brightness temperatures.

In the water vapor retrieval procedure, the retrieved atmospheric temperature profile and ground temperature are used, along with a first guess water vapor profile, to compute estimated clear column brightness temperatures for those channels most sensitive to water vapor (channels 8, 10, 11, 12 for the HIRS instrument). As in the case of the temperature sounding channels, the differences between the computed and observed brightness temperatures (or reconstructed brightness temperatures in the case of cloud contamination) are functions of numerous parameters. However, since the temperature profiles used in the calculation of the computed clear column brightness temperatures are the retrieved atmospheric temperature profiles, the differences between observed and computed brightness temperatures are attributed to errors in the prescribed first guess water vapor profile. Because these differences are roughly linear with small errors in water vapor profile estimates, a regression relationship may be found which relates known differences between the true water vapor profiles and the first guess profiles to the differences between the observed and computed clear

column brightness temperatures. Note that the satellite observations are at a zenith angle θ. To first order this has the effect of multiplying the water vapor column densities by a factor of sec θ. Thus the actual water vapor column density differences are scaled by sec θ in finding the regression relationship.

The entire regression and verification process may be summarized in the following steps:

1) The retrieved temperatures and a first guess water vapor profile q(FG) are used to estimate clear column brightness temperatures (Θ (CALC) for those channels which are to be used in the water vapor retrieval scheme.

2) Regression expressions are found which relate the difference between the true and first guess water vapor profiles, (Δq), to the difference between the observed (or reconstructed) clear column brightness temperatures, $\Delta\Theta$.

An attempt was made to take into account the fact that the height of the water vapor sensitivity function is a function of the total amount of water vapor in the column. Specifically, as the water vapor column density increases, the sensitivity function tends to peak higher in the atmosphere and vice-versa. In this case the regression relationship becomes

$$\Delta_{qI} = (A + C(W_I - \overline{W}_I))\Delta\Theta + B \qquad (1)$$

where W_I is the total integrated first guess water vapor column density from the bottom of pressure layer I to the top of the atmosphere, and W_I is the same quantity for the average water vapor column density profile in the set. Here for pressure layer I and satellite zenith angle θ, $\Delta_{qI} = (q(\text{true})_I - q\ (FG)_I)\ \sec\theta$, $q(--)_I$ is the integrated water vapor column density in pressure layer I, and $\Delta\Theta = \Theta$ (clear) - Θ (calc). A, B, and C are the regression coefficients to be determined.

3) The regression relationships generated are used to obtain retrieved water vapor column densities from an independent set of radiances. The calculated clear column radiances for the channels to be used in the water vapor retrievals use retrieved temperatures and a first guess water vapor profile as in step 1 above.

SIGNIFICANT ACCOMPLISHMENTS:

In the first phase of this research simulation studies were undertaken in which the atmospheric and surface properties were known exactly. Clear radiances were simulated using an atmospheric transmittance model developed at GLAS (Susskind et al., 1983) and a selected set of radiosondes from January and June of 1979. The true ground temperatures were specified so as to be meteorologically reasonable. Cloudy radiances were simulated using the same method except that two layers of broken opaque clouds between 700 and 300 mb were allowed to contaminate the radiances. Details of the clear and cloud simulations may be found in Susskind et al., 1982 and Reuter et al., 1982.

Some results of the cloud contaminated simulation studies are given in Figures 1 and 2. In Figure 1 is plotted the RMS column density error (in g/cm^2) from pressure P to the top of the atmosphere for the first guess and the retrieval.

These results are for radiances simulated from 200 ocean and 200 land radiosondes ranging from 60°N to 30°S from June 1979. The water vapor column density first guess profiles are calculated from climatological relative humidity profiles and the retrieved temperatures. As may be seen from this figure the retrieved water vapor column densities are 30% to 50% better then the first guess throughout the atmosphere.

Figure 2 is a plot for the same data set of the percent error of the column density from pressure P to the top of the atmosphere. The percent error is defined as the RMS error divided by the average column density. This figure indicates that the retrievals are accurate to about 20% to 30% throughout the atmosphere.

The second phase of the research is being carried out using actual satellite observations. In this case there is a difficulty in determining the true water vapor profiles because radiosonde relative humidity measurements have larger errors than radiosonde temperature measurements. Furthermore, since humidity varies much more rapidly spatially than temperature, collocation errors are larger for water vapor than for temperature. Bearing both these factors in mind, the water vapor retrievals will still be verified against collocated radiosondes.

Figure 3 is a plot of the RMS total column density errors from pressure P to the top of the atmosphere for the retrievals and the first guess, for a global set of January ocean radiosondes. In this case the first guess is a 6 hr forecast. From this figure it is seen that the retrieved humidity is an improvement upon the forecast first guess.

From an operational standpoint it may be convenient to use a system which does not depend upon the availability of radiosondes or an analysis to determine a regression matrix. In order to test a system of this sort an experiment was performed in which the forecast was taken to be the true water vapor profile and a fixed relative humidity profile was used as the first guess to find the regression matrix. This matrix was then used on the set of colocated January ocean radiosondes described earlier in which now the forecast was taken to be the first guess in the calculation of the clear column brightness temperatures. The results of this experiment are shown in Figure 4 in which are plotted the RMS column density errors for both the retrieval and the forecast first guess. It should be stressed that these are errors with respect to the radiosonde measurements.

As expected the results shown in Figure 4 are degraded somewhat with respect to the results shown in Figure 3, however Figure 4 still shows an improvement of the retrievals with respect to the forecast first guess. This is especially gratifying since the fixed relative humidity profile used as a first guess in obtaining the regression matrix used in generating the results shown in Figure 4 was very unlike the true mean atmospheric relative humidity.

FUTURE PLANS.

It must be stressed that the real data results presented here are quite preliminary and that much work remains to be done. Specifically we are now in the process of implementing the water vapor retrievals on the operational retrieval system in order that we may obtain larger data sets to investigate.

We are also in the process of modifying the McIDAS retrieval system in order that we may use the capabilities of this system for investigating fields of retrieved water vapor profiles on a finer scale than the current operational system.

REFERENCES:

Chahine, M. T., 1974: Remote soundings of cloudy atmospheres. I. The single cloud layer. J. Atmos. Sci., 31, 233-243.

Reuter, D., J. Susskind, and A. Dalcher, 1982: Simulation studies of the HIRS2/MSU and AMTS/MSU satellite sounding units: Cloudy conditions. NASA Tech. Memo 84983, pp 68-76.

Smith, W. L., 1968: An improved method for calculating tropospheric temperatures and moisture from satellite radiometer measurements. Mon. Wea. Rev., 96, 387-396.

Susskind, J., D. Reuter, and A. Dalcher, 1982: Simulation comparison study of the AMTS and HIRS2 sounders. NASA Tech. Memo. 84983, pp 59-67.

Susskind, J., J. Rosenfield and D. Reuter, 1983: An accurate radiative transfer model for use in the direct physical inversion of HIRS2 and MSU temperature sounding data. J. Geophys. Res., 88C, 8550-8568.

Susskind, J., J. Rosenfield, D. Reuter, and M. T. Chahine, 1984: Remote sensing of weather and climate parameters from HIRS2/MSU on TIROS-N. J. Geophys. Res., 89D, 4677-4697.

TECHNICAL PUBLICATION:

Reuter, D. and J. Susskind, 1983: Water Vapor Profile Retrieval Simulation Studies for the HIRS/MSU and AMTS/MSU Sounders. NASA Tech. Memo 86053.

CONFERENCE PUBLICATION:

Reuter, D. and J. Susskind, 1983: Water Vapor Profile Retrievals from the HIRS/MSU Sounder. Fifth Conference on Atmospheric Radiation, Baltimore, MD, Oct. 31-Nov. 4, 1983, pp 62-64.

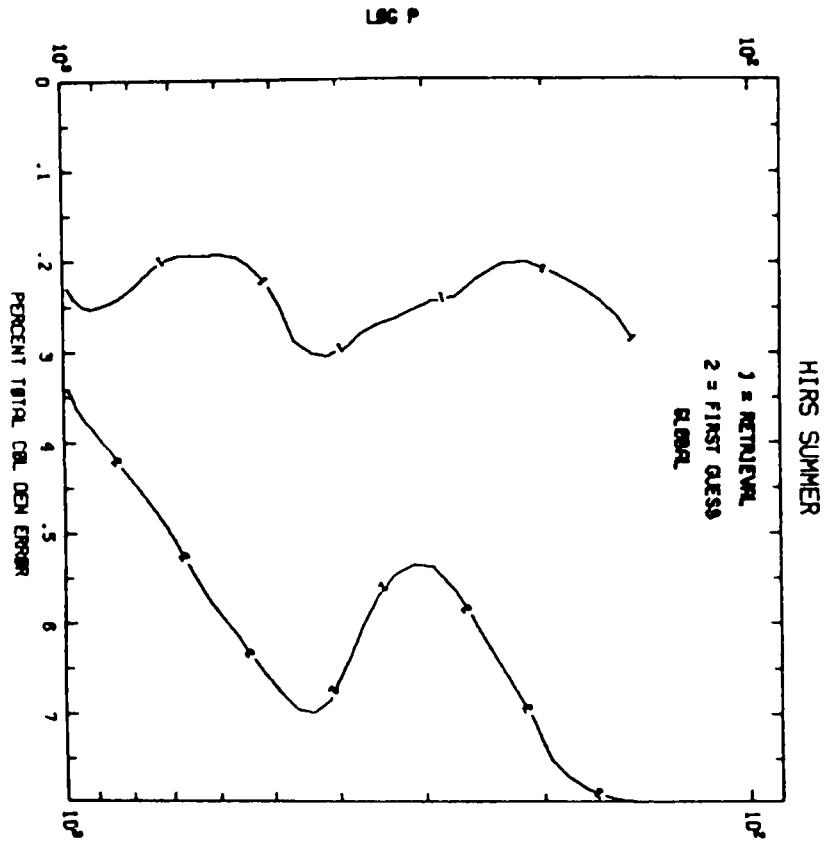

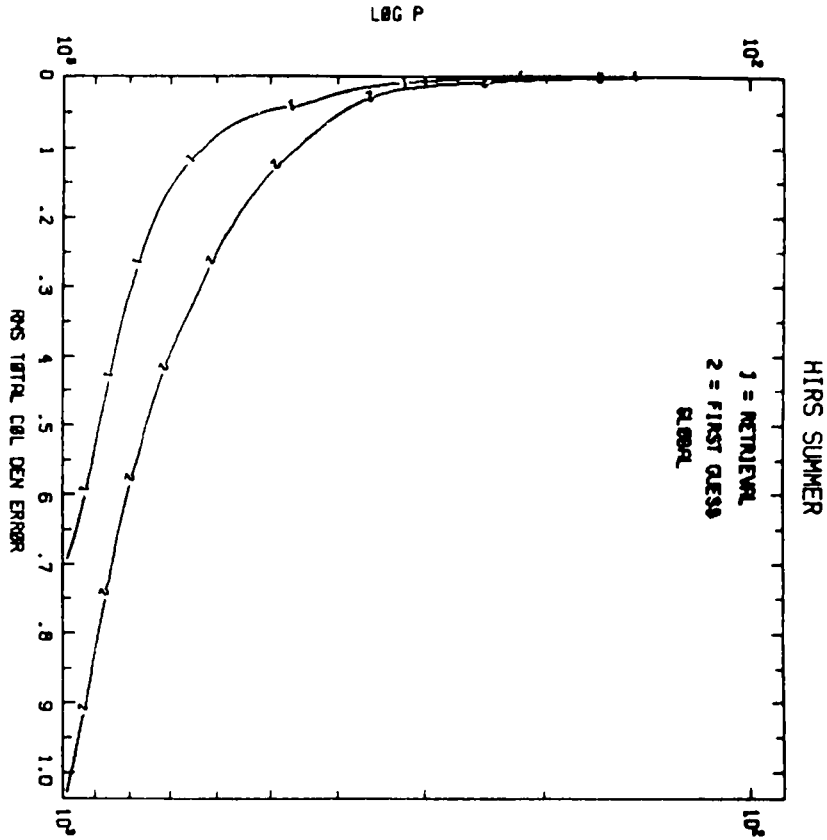

Fig. 1. RMS column density errors from pressure P to the top of the atmosphere as a function of P. Simulation study performed on a set of 200 land and 200 ocean radiosondes from June 1979. 60°N to 30°S.

Fig. 2. Fractional column density errors as a function of P. Same data set as in Fig. 1. Simulation study.

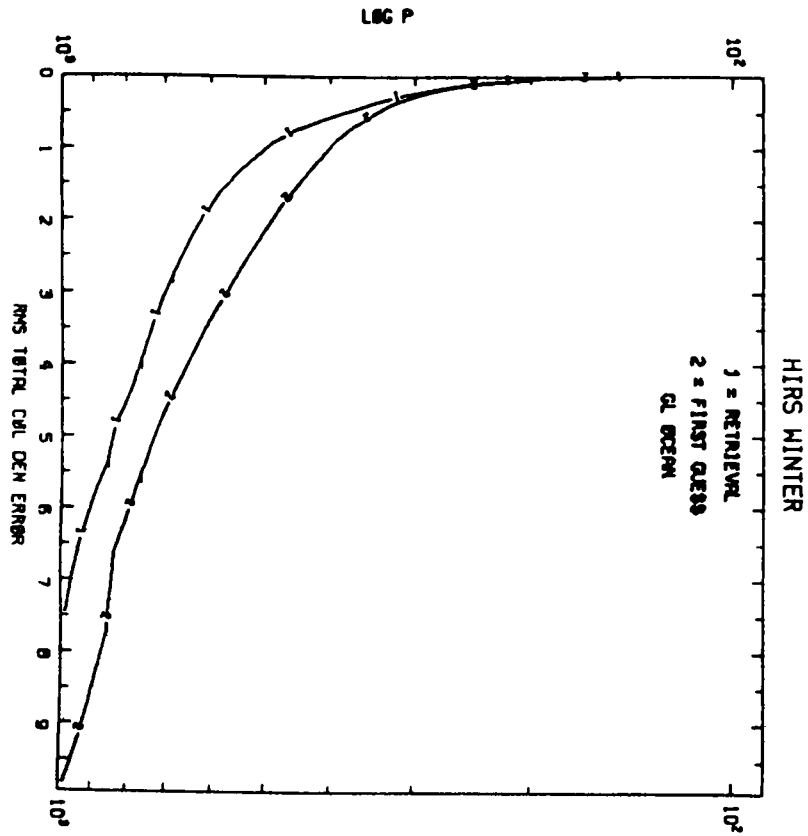

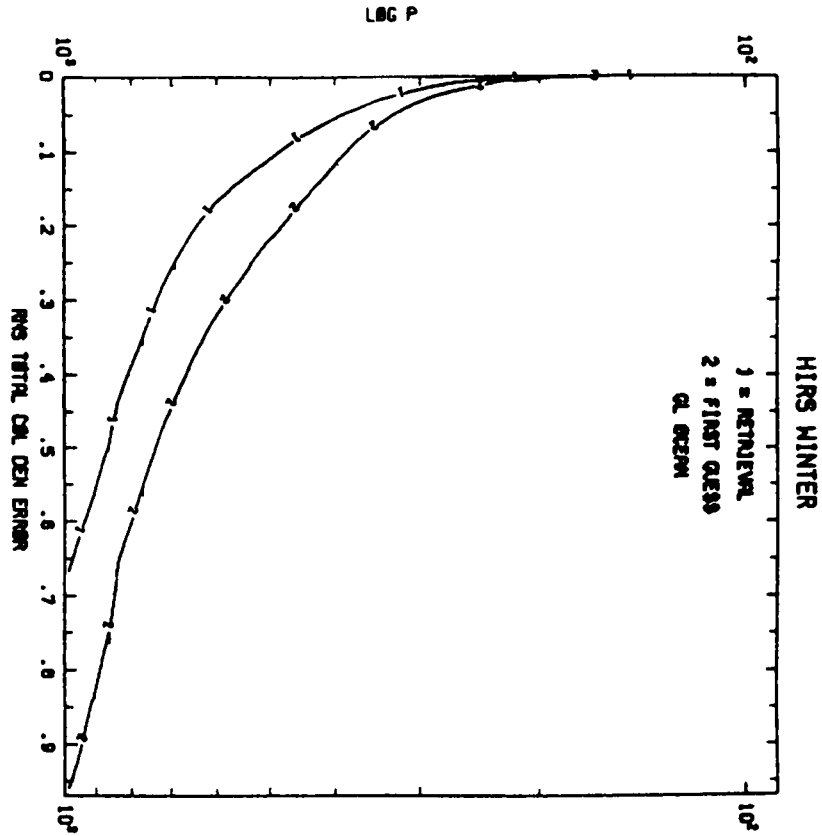

Fig. 3. RMS column density errors from pressure P to the top of the atmosphere as a function of P. Real data results using a regression matrix obtained from a forecast first guess January 1979 global ocean data set.

Fig. 4. RMS column density errors as a function of P. Real data results using a regression matrix obtained from a fixed relative humidity first guess profile forecast first guess taken as truth in obtaining regression matrix (see text for details). Same data set as in Fig. 3.

APPLICATIONS OF TOMS OZONE DATA AND CLUSTERING TECHNIQUES IN SATELLITE SOUNDINGS
(M.-J. Munteanu)

RESEARCH OBJECTIVES:

Two primary areas are being pursued: i) Applications of TOMS total ozone data to estimate the tropopause height and consequently to improve the temperature retrievals from satellite measurements. The strategy is to either use regression retrievals stratified by tropopause or to use the tropopause information as a constraint on the solution of the physical retrieval method; ii) Applications of cluster analysis to satellite soundings.

SIGNIFICANT ACCOMPLISHMENTS:

A. APPLICATIONS OF TOMS TOTAL OZONE DATA TO SATELLITE RETRIEVALS

This year we analyzed two case studies over Europe in which we have collocated NIMBUS-7 TOMS data and radiosondes and simulated the corresponding MSU brightness temperatures. Important improvements in retrieval accuracy have been obtained using the TOMS prediction of the tropopause height to stratify regression retrievals.

The use of TOMS total ozone globally over oceans and especially in the data sparse regions of cloudy cases could potentially be powerful.

With this purpose in mind research has been concentrated in the following areas:

I. Determination of the tropopause using TOMS data.

II. Impact of tropopause errors in microwave MSU retrievals.

III. Impact of tropopause errors in future AMSU retrievals.

IV. Use of air-mass to stratify regression retrievals.

V. Use of total ozone measurements to estimate tropopause height and the impact of stratified by tropopause temperature retrievals.

Major findings of these investigations in these areas are:

I. Determination of the Tropopause Using TOMS

1. The sample corrections were found to be 0.94 and 0.96. As a result of this high correlation the r.m.s error in the prediction of the tropopause height from total ozone was found to be at most around 20 mb.

2. Correlation between tropopause height and total ozone is the highest among all the other correlations with variables such as: brightness temperatures from microwave channels, ratios and differences of these quantities, latitude, mean layer temperatures, surface temperatures or surface pressure.

3. Experiments correlating tropopause data with mean layer temperatures derived directly from radiosonde data showed that even if we measured these quantities exactly the prediction of the tropopause was inferior to that with the total ozone. Specifically, the highest sample correlation coefficient was 0.86 instead of the 0.96 obtained using total ozone.

4. The folding of the tropopause should be taken into account because it is associated with the highest gradient in the ozone field.

II. Impact of Tropopause Errors in Microwave MSU Retrievals

Tables with r.m.s. at mandatory levels for the whole sample of profiles for April 15 and April 25 are shown in Table 1. The conclusions may be stated as follows for the second part:

1. In the low tropopause cases there is a large bias and large residual error.

2. The low tropopause cases produced very poor temperature retrievals. The overall r.m.s. is large in the region of the tropopause.

3. The tropopause is mislocated by 100-150 mb in the operational microwave retrievals in the extreme cases.

4. It is observed that the MSU regression temperature retrieval damps almost entirely the trough in the two dimensional field of the tropopause height for April 15 and in general does not contain all of the highs and lows for April 25 (see Fig. 2).

III. Impact of Tropopause Errors in Future AMSU Retrievals (see Fig. 1)

1. The location of the tropopause is not improved with respect to the MSU in the low tropopause cases.

2. The retrievals based on the 5 AMSU channels generally perform better in the average tropopause height cases.

3. The general conclusion of these experiments may be described by saying that the resolution in the region of the tropopause is not improved by the additional AMSU channels, especially in the cases of low tropopause.

IV. Use of Air-Mass To Stratify Regression Retrievals

Experiments using stratified-by-air mass regression formulas indicate that they perform better in the region of the tropopause (see Fig. 1).

V. Use of Total Ozone Measurements To Estimate Tropopause Height and the Impact of Stratified-by-Tropopause Temperature Retrievals

This part contains the main results of this study. In the first stage we take the tropopause height prediction from the first part and apply stratified by tropopause regression retrievals.

As a measure of improvement in retrieval accuracy obtained from supplementary ozone information we compare the fields of tropopause pressures derived from RAOB's with the fields derived from ozone prediction, from local or global MSU regression retrieval and finally from stratified-by-tropopause regression retrievals. The tropopause fields derived from local or global regression retrieval are smooth and bear little resemblance to true tropopause fields. In contrast, the fields derived from radiometric data supplemented with the total ozone information closely resemble the original fields (see Fig. 2).

Finally, the r.m.s. errors of the stratified-by-tropopause retrievals are presented in Table 1. (The prediction of the tropopause height from TOMS total ozone is performed in the sample regression or cross validation manner). Note, in particular, the important improvement of these retrievals over the local or global retrieval in the vicinity of the tropopause. However, the improvement generally extends over a broad range, typically from 500 mb to 100 mb. A few individual average profiles and the low tropopause profiles and their improved stratified-by-tropopause regression are displayed in Fig. 3.

The results presented here in Sec. V strongly suggest that a substantial improvement in MSU thermal retrieval accuracy can be obtained by using TOMS measurements of total ozone content and its relationship to tropopause pressure.

B. APPLICATIONS OF CLUSTERING TECHNIQUES TO SATELLITE SOUNDINGS

We have completed a limited feasibility study of the use of clustering techniques in temperature retrievals from simulated satellite measurements. The results of this study were extremely encouraging and showed substantial improvement over regression retrievals stratified by latitude season, land and ocean rather than cluster.

In our preliminary work we investigated the usefulness of clustering analysis in various ways in order to achieve improved satellite temperature retrievals on N. Phillips' data set. Clustering divides the whole data set into groups, alias clusters, or very similar vectors or profiles.

As a first conclusion of these studies we can state that clusters of temperature profiles (weighted and unweighted) are very promising in generating a first guess regression retrieval if one applies it in conjunction with discriminatory analysis in order to locate the correct cluster from satellite measurements.

Specifically, we obtained as a final result, improved stratified regression schemes in comparison with currently used retrieval schemes based on categorizing satellite soundings according to latitude, season, and land vs. ocean (see Table 2). The use of clustering methods based on the quasi-multinormal distribution of atmospheric temperature soundings characteristic of different types of air masses resulted in a natural division into groups of characteristic patterns.

Another important conclusion from our preliminary studies is that clusters of brightness temperatures could provide basic information about the shape of the temperature profiles, specifically, tropopause height. The results of the first stage of the experiment can be expressed in terms of the overall r.m.s. for the tropopause prediction, viz., 16 mb for the summer and 23 mb for the winter. These extremely encouraging tropopause prediction results can be used

in a variety of ways. In the second stage of this experiment we chose to use the excellent tropopause prediction generated in the first stage in order to use regression retrievals stratified by tropopause involving the 3 MSU and 5 IR channels. The regression retrievals stratified by tropopause are obtained from the same data sample for each 30 mb layer of tropopause pressures, separately for winter and summer. We compared the results against the same control experiment described previously.

As can be seen in our tables with r.m.s., the performance of the regression retrievals stratified by tropopause for the summer as well as for the winter is excellent (see Table 3).

FUTURE PLANS:

I plan to extend my earlier work in the estimation of the tropopause height from total ozone and using this to improve temperature retrievals from satellite measurements. I plan to derive extensive statistics about the correlation between tropopause height and total ozone data from Dynamics Explorer 1 satellite. Another objective of this proposal is to explore new ways to maximize the use of tropopause information in the temperature retrievals.

I also plan to continue my earlier work on temperature retrievals from brightness temperatures through the use of clustering techniques and discriminatory analysis, and especially, develop a new technique named "fuzzy" clustering which greatly improves standard clustering by being able to handle the imprecise boundaries between clusters. Fuzzy set theory provides the framework for the formulation of an objective criterion as well as the optimization algorithm for constructing the optimal solution. This represents a step toward an artificial intelligence approach in analyzing meteorological satellite data.

I also plan to implement clustering techniques including new channels with simulated HIRS/MSU data and to incorporate the method into analysis of real data.

TECHNICAL PUBLICATIONS:

Munteanu, M.-J., E. R. Westwater and N. C. Grody, 1984: Improvements of MSU temperature retrievals by use of tropopause height derived from TOMS ozone measurements. Submitted for publication.

Munteanu, M.-J., 1984: Study of tropopause height estimate from TOMS total ozone data from NIMBUS-7 and from the microwave regression temperature retrieval of simulated brightness temperatures. To be submitted for publication.

Munteanu, M.-J., P. Piraino and E. Kalnay, 1983: Regional correlation between TOMS total ozone from NIMBUS-7 satellite and geopotential height from GLAS analysis. 1983 Research Review, Global Modeling and Simulation Branch, Goddard Space Flight Center.

Munteanu, M.-J., O. Jakubowicz, E. Kalnay and P. Piraino, 1983: Applications of cluster analysis to satellite soundings. 1983 Research Review, Global Modeling and Simulation Branch, Goddard Space Flight Center.

Susskind, J., M.-J. Munteanu and P. Piraino, 1983: Improved HIRS2/MSU soundings using tropopause information. 1983 Research Review, Global Modeling and Simulation Branch, Goddard Space Flight Center.

RMS by Levels

	April 15, 1979			April 25, 1979	
Pressure in mb	Local Clim	Strat Trop		Global Clim	Strat Trop
1000	-	-		5.889	-
850	-	-		2.276	-
700	4.321	4.311		2.721	3.324
500	4.035	2.514		3.278	1.885
400	2.900	2.797		3.809	2.060
300	4.543	1.828		2.096	1.880
250	3.475	2.213		2.418	1.823
200	3.539	2.453		4.064	1.979
150	2.361	2.570		2.687	2.112
100	1.687	1.760		2.753	1.840
70	2.118	2.090		1.061	1.742
50	1.867	1.844		2.086	2.014

Table 1

Comparison of RMS Temperature Retrievals (Summer) 5IR & 3 MSU

Pressure	Control Experiment	Clusters of Weighted Temperatures	Clusters of Temperature (Nonweighted)	Clusters of 5IR & 3 MSU
30 mb	2.00	1.94	1.92	2.02
50 mb	1.88	1.76	1.76	1.90
70 mb	1.69	1.56	1.59	1.70
100 mb	1.66	1.54	1.52	1.63
150 mb	1.93	1.59	1.69	1.94
200 mb	2.51	1.78	1.87	2.40
250 mb	2.36	1.62	1.80	2.20
300 mb	2.03	1.55	1.59	1.98
400 mb	1.80	1.51	1.37	1.77
500 mb	1.63	1.35	1.28	1.57
700 mb	1.84	1.59	1.51	1.84
850 mb	2.29	2.03	1.86	2.04
1000 mb	2.29	2.16	2.16	2.28

Table 2

Pressure	Stratified by Tropopause (Total RMS	Control Experiment	Stratified by Tropopause (Total RMS	Control Experiment
30 mb			2.02	4.71
50 mb	1.56	1.88	1.81	2.88
70 mb	1.29	1.69	2.33	1.89
100 mb	1.37	1.66	2.20	2.31
150 mb	1.62	1.93	1.97	2.15
200 mb	1.46	2.51	1.69	2.36
250 mb	1.51	2.36	1.82	2.42
300 mb	1.70	2.03	1.90	2.53
400 mb	1.72	1.80	2.22	2.40
500 mb	1.61	1.63	2.27	2.62
700 mb	1.82	1.89	2.10	2.57
850 mb	2.03	2.29	2.57	2.75
1000 mb	2.39	2.29	2.62	2.72

Table 3

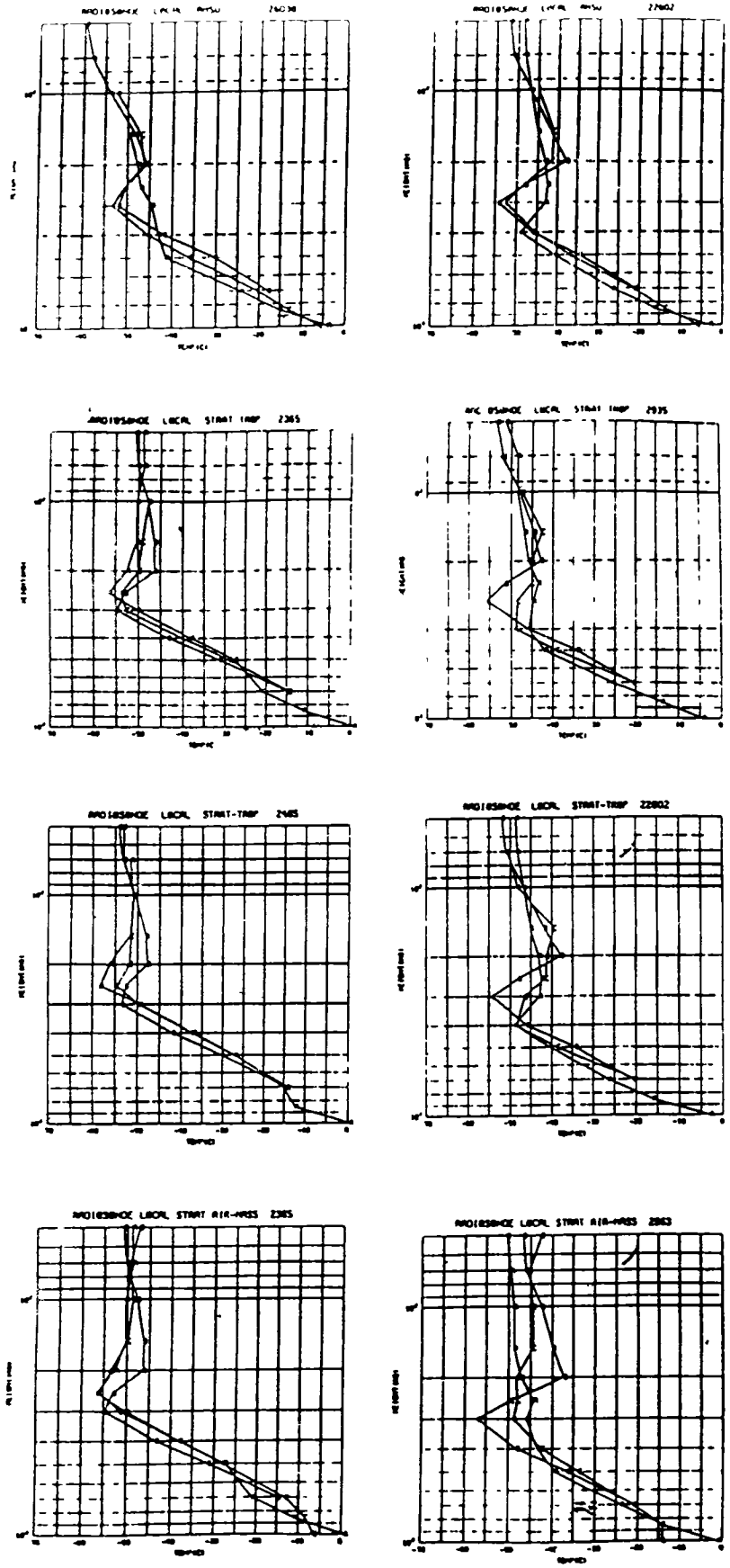

Figure 1

April 15

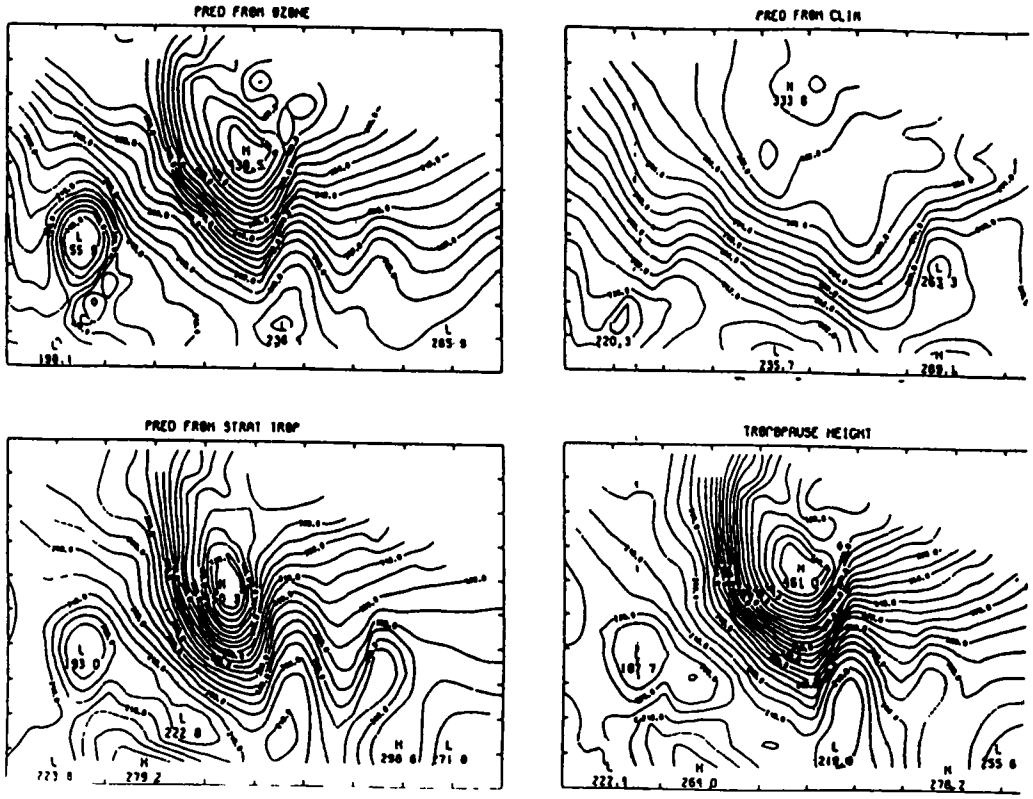

Figure 2

April 25

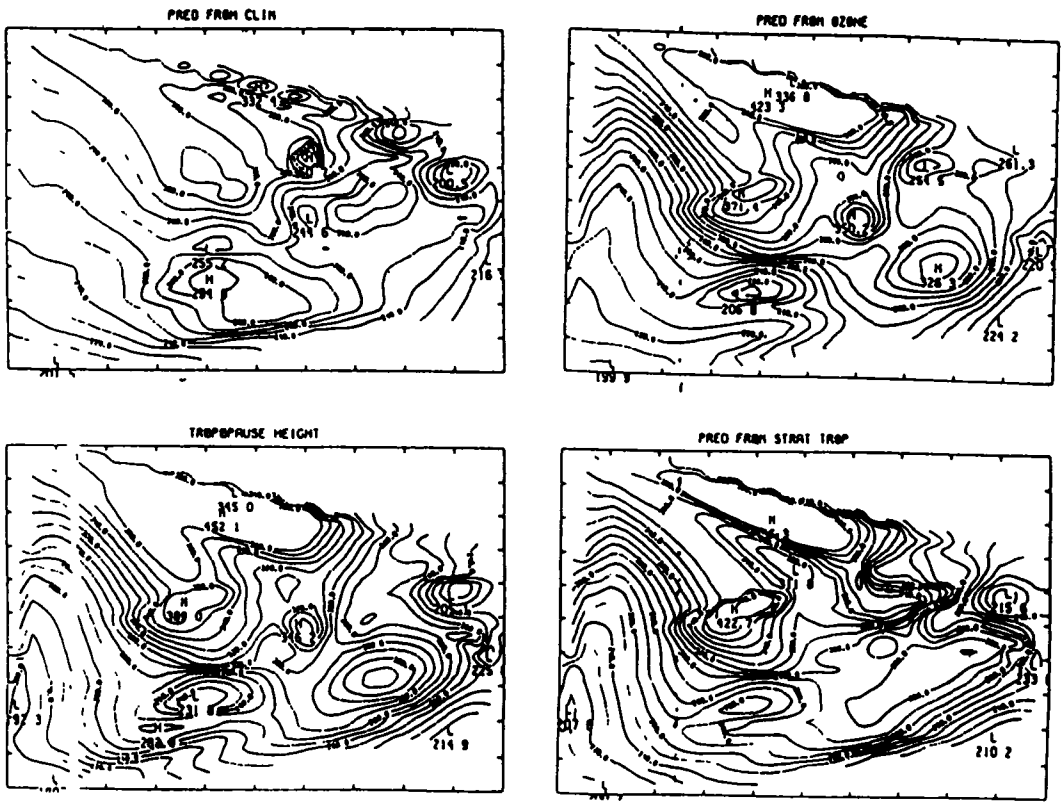

RESEARCH RELATIVE TO HIGH SPATIAL RESOLUTION PASSIVE MICROWAVE SOUNDING SYSTEMS
(D. H. Staelin and P. W. Rosenkranz-MIT)

RESEARCH OBJECTIVES:

The objectives of this research are improved understanding of methods for obtaining high-resolution passive microwave weather observations, and improved understanding of their probable impact on numerical weather prediction accuracy. The study of observation methods has focused first on development of synthetic aperture concepts for geosynchronous passive microwave sounders. Subsequently it will focus more on the effects of clouds, precipitation, surface phenomena, and atmospheric thermal fine structure on a scale of several kilometers. The latter study will also include flights on a NASA Convair 990 aircraft and an associated theoretical effort.

High-resolution passive microwave sounders (e.g. AMSU) with an increased number of channels will eventually produce initialization data for numerical weather prediction (NWP) models with both increased spatial resolution and coverage. The full consequences of these improvements are not quantitatively well understood. For example, the relative impacts of initialization error fields of different spatial scales upon the evolution of forecast error spectra have not been carefully studied. One objective of this theoretical study is development of statistical models for error growth in high resolution primitive equation NWP models; such a development would permit the consequences of various observing system alternatives, including sensors and assimilation times and procedures, to be better understood quantitatively without requiring in each specific case large NWP experiments, which typically are enormously expensive and time consuming.

The approach being taken is an extension of the formulation of Lorenz (1969), who considered two-dimensional incompressible flow in an infinite plane. He found that error growth could be modeled in a relatively simple way. This study uses a high-resolution three-dimensional primitive equation NWP model to determine parameters in an error-growth model similar to that formulated by Lorenz, but with more degrees of freedom.

SIGNIFICANT ACCOMPLISHMENTS:

The major accomplishment of the study of high resolution passive microwave observation techniques is the development of a system concept appropriate for high-resolution temperature and humidity profile sensors operating in geosynchronous orbit. In particular, the 118-GHz band of oxygen was studied, and a system achieving a nominal resolution of 35 km at 45 degrees latitude was designed and evaluated. The assumed dimensions of the slowly rotating antenna were 35 x 335 cm, and it would map an ellipse of ~ 330 km mean diameter at 45° latitude on a time scale of minutes with an rms sensitivity of ~ 0.2-0.3 K for each of ~ 10 channels. The required electronics would be somewhat less complex than that in the proposed AMSU microwave sounder.

In Figure 1 are illustrated representative antenna patterns for the synthesized beam. The sidelobes for the better designs appear to be acceptably low. This design should be substantially less expensive than the lower resolu-

tion filled-aperture 4-m reflector designs considered previously. Thus the aperture synthesis concept appears worthy of further pursuit and should become a strong candidate for inclusion on future geosynchronous operational meteorological platforms.

Significant progress has also been made in the development of models for error growth in large NWP models. This work, principally by P. W. Rosenkranz, has begun with emphasis on developing methods for perturbing the initial states of NWP models with pure spectral impulses without introducing deleterious gravity waves. In addition several initial experiments testing the linearity of NWP models have been successfully performed, as discussed later.

The experiments were performed using the University of Wisconsin (Madison) adaptation of the Australian Region primitive equation model of Gauntlett et al. (1978). This adaptation has 10 levels, from σ = 0.05 to 0.95, and covers the contiguous United States with either 67.6 or 135.2 km horizontal resolution. Our experiments have used 135.2 km resolution and 15-minute time steps; the grid is a polar stereographic projection with 24 x 29 elements.

Vertical basis functions for the perturbations have been chosen and perform satisfactorily. Baseline states of the NWP model have been established for three days: July 20, 1981, March 6, 1982, and April 26, 1982.

The most important experiments have concerned superposition of perturbations. The two test functions were balanced sinusoidal waves of 2.34 and 1.25 cycles per 1000 km; these had x-y wave numbers of 1.32-1.93 and 0.79-0.96 cycles per 1000 km, respectively. The amplitudes of each corresponded roughly to $\pm$ 1.5 ms^{-1} for the second vertical basis function. In Figure 2 are shown the results of one such experiment where the two-dimensional spectra of the wind perturbations after 9 hours are plotted for each of the two perturbations and for the superposition experiment. The axes of the figure are 1 cycle/270 km; the origin is at the left center of each at 9 hours and the sum of the two separate perturbation energies at 9 hours is approximately 0.7 percent of the total perturbation energy for wind, and 11 percent of the total perturbation "energy" for temperature. Thus superposition appears to apply reasonably well under these circumstances.

CURRENT AND FUTURE RESEARCH:

Current efforts in modeling error growth in NWP models continue to focus on the linearity and superposition issue, and experiments have begun to determine the sensitivity of the error-growth results to the model's initial state. If these results continue to confirm the validity of the general Lorenz formulation, then these results will be used to construct an extended C-matrix model for error growth that will be tested for various meteorological cases. Such a validated model for error growth can then be used to evaluate a wide variety of alternative remote sensing or data reduction and assimilation methods, and to provide better and faster insights into the consequences of various operational observing strategies.

The work on aperture-synthesis techniques for geosynchronous sounders is now being documented for publication. Significant further work in this area will await a better understanding of mission opportunities and likely mission constraints.

The work on high-resolution retrieval techniques is awaiting the flight in 1985 of the imaging 7-channel 118-GHz spectrometer now being prepared for the NASA Convair-990 aircraft. It will provide the first high-spatial-resolution images of the three-dimensional thermal structure of frontal systems and other storms in the presence of cirrus or other IR-obscuring clouds. This retrieval work will also draw upon the rapid progress being made in our parallel video-image-processing group, which is addressing similar problems in a different context.

JOURNAL PUBLICATIONS:

Two journal papers are in rough draft form; one described the work on the application of aperture synthesis techniques to passive microwave sounders in geosynchronous orbit, and the other presents the results of the initial error-growth and perturbation-superposition experiments performed with a high-resolution primitive equation NWP model.

CONFERENCE PUBLICATIONS:

An abstract of the paper "Synthetic Aperture Imaging of the Earth from Synchronous Orbit," by A. C. Briancon and D. H. Staelin, appears on page 184 of the record of the 1984 United States Spring Meeting of U.R.S.I. held June 25-29 in Boston, Massachusetts.

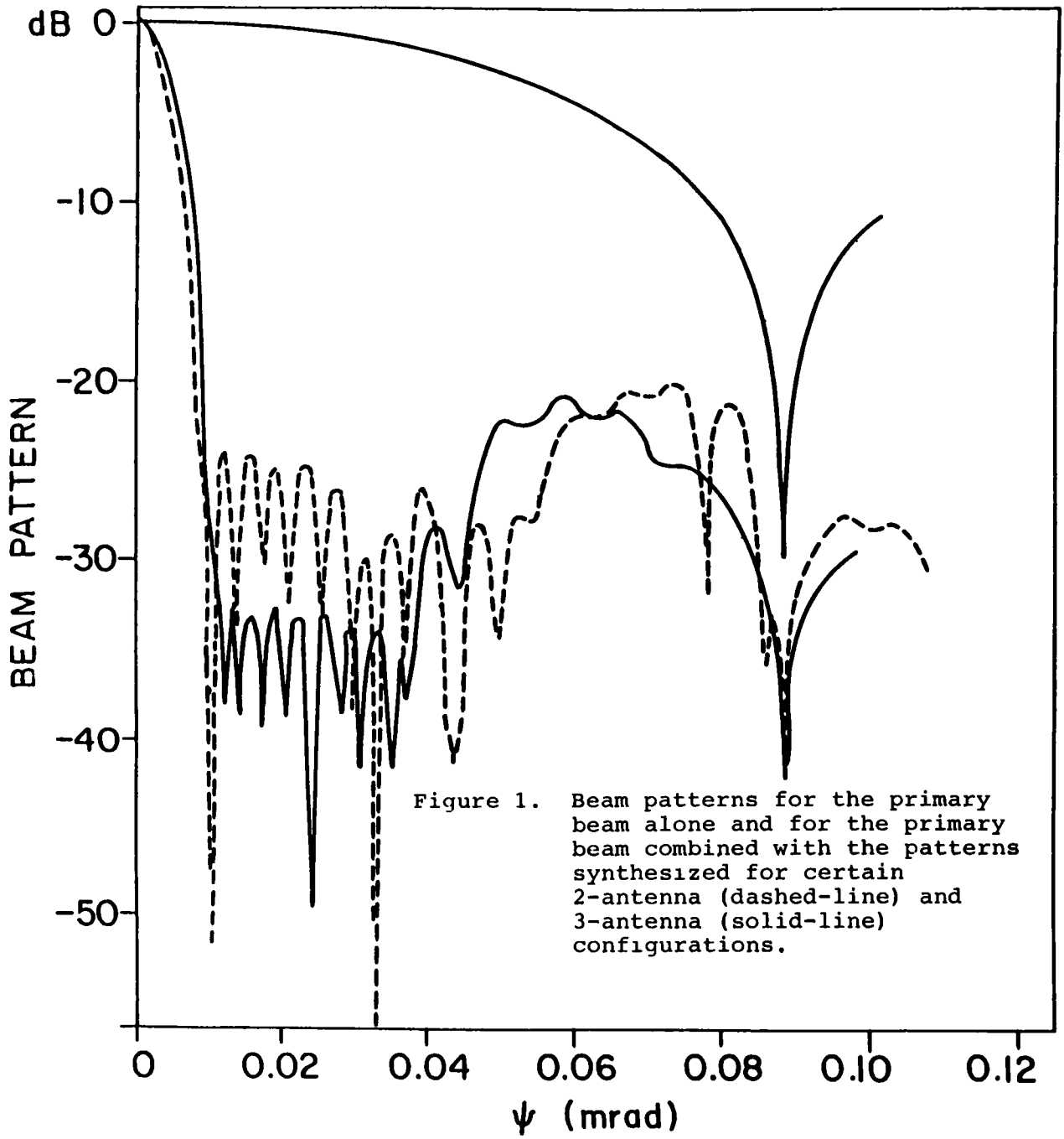

Figure 1. Beam patterns for the primary beam alone and for the primary beam combined with the patterns synthesized for certain 2-antenna (dashed-line) and 3-antenna (solid-line) configurations.

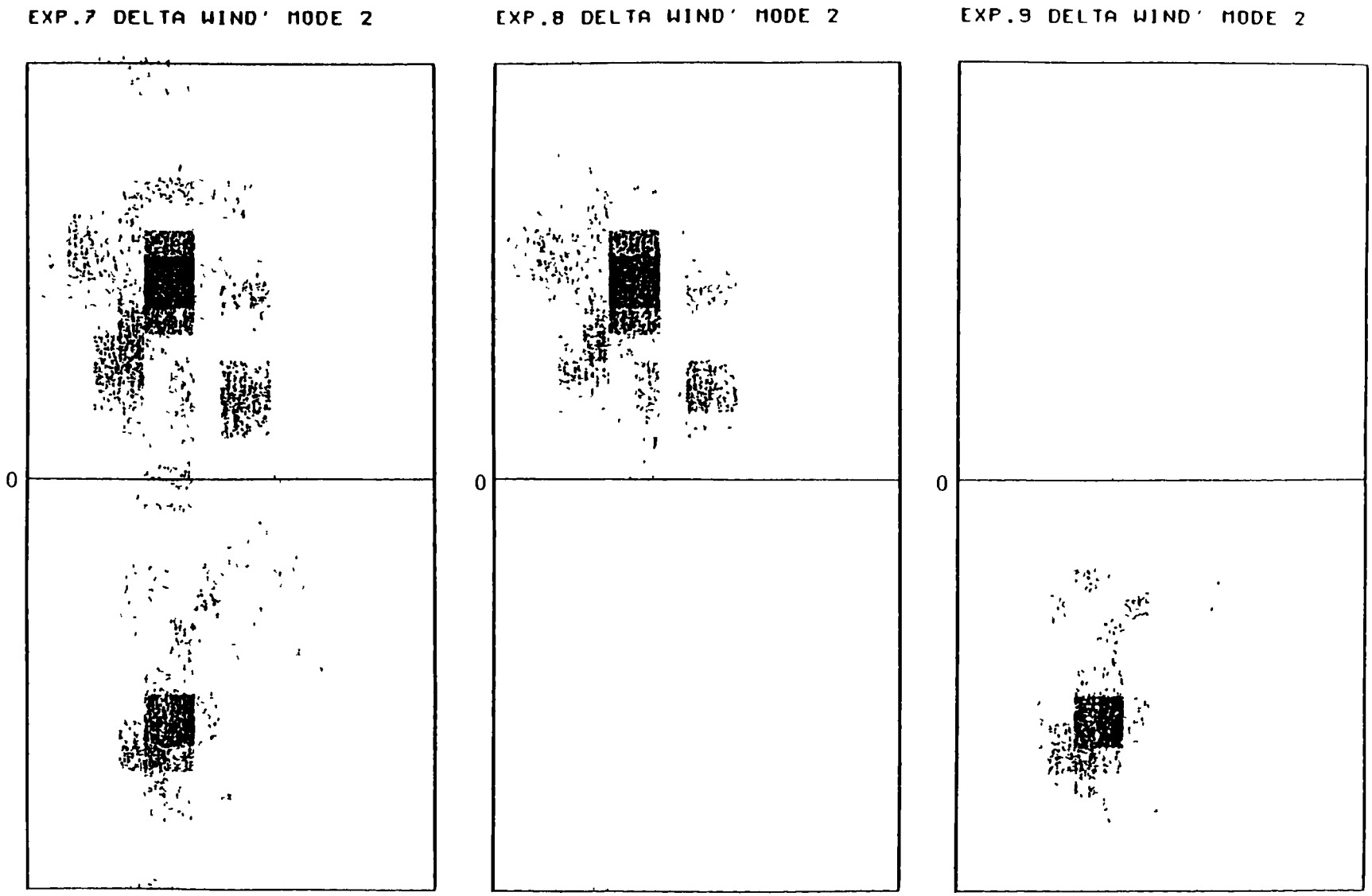

Figure 2. Representative result of perturbation superposition experiment. Exps. 8 and 9 are spectral energy distributions for the wind perturbation 9 hours after initialization; Exp. 7 is the 9-hour result when the stimulae were superimposed at initialization. The axes are longitudinal and latitudinal wave numbers ranging linearly from zero to 1 cycle/270 km.

INVESTIGATION OF SATELLITE MEASUREMENTS IN THE PRESENCE OF CLOUDS, FORCING INFLUENCES ON CLOUDS AND FEEDBACK TO THE LARGE SCALE FOLLOWING CONVECTION

(C. Warner-Dept. of Environmental Sciences, University of Virginia)

RESEARCH OBJECTIVES:

1) Did any marked thermal feature aloft pass near the northern Bay of Bengal at the time of formation of the July 1979 monsoon depression?

2) How are regions of dense high overcast clouds to be recognized in satellite radiances?

3) How did the observed monsoon cloud systems evolve? What factors controlled the clouds, and what effects did the clouds have on thermodynamic and wind structures?

4) What improvements can be made in numerical models?

SIGNIFICANT ACCOMPLISHMENTS:

Relating to the above questions,

1) No, not as discerned using Channel 3 of the Microwave Sounding Unit aboard TIROS-N. The instrument had a footprint size on the order of 50000 km^2. A thermal anomaly of magnitude 2 K at this size would have been discernible in the time series of data mapped at 12 h intervals.

Coherent structural features in the monsoon depression have been discerned in the lower troposphere but not the upper troposphere. It appears that primarily, the monsoon depression involves a strong low-level current that arises in response to an externally forced meridional pressure gradient. The current is so strong that barotropic instability becomes a factor. The current impinges on the Arakan mountains of Burma. There is static instability. Under these conditions line formations of cumulus congestus and cumulonimbus follow. If the external forcing is sustained, the lines of clouds and areas of compensating subsidence form a depression.

Diurnal variations in brightness temperatures were found in Channels MSU 3 and MSU 2. These were consistent with strong topographic forcing, and the presence of deep convection.

2) Microwave radiometry seems important in treating dense high overcast clouds. It seems to be nearly the only possibility in remote sensing from space for differentiating between anvil cirrus with clear air beneath, as opposed to anvil cirrus topping large amounts of active cumulus. The latter regime often occurs along one side of an anvil, with much clear air beneath an extensive plume.

Detailed radiative transfer calculations, which have matched up well with observations, have shown that an ice anvil makes little difference to brightness temperatures in MSU Channels 1 and 2 if the air below is clear. If cloudy, the brightness temperature is much changed, and an ice anvil can make a great difference.

A microwave radiometer with a number of channels in the frequency range $\leq$ 50 to 58 GHz, in equatorial orbit for a period of a few hours, would be very valuable for monitoring tropical weather systems.

3) Mesoscale assemblies of cumulus clouds dominated the structure of the depression. Commonly, lines of cumulus were oriented across the flow at low levels. Across these lines, abrupt changes occurred in wind and thermodynamic fields. The cyclonic streamlines of the depression vortex showed abrupt changes of direction at such features. Here were concentrated vertical motion, and matching horizontal convergence at low levels and divergence aloft. Subsidence occurred in adjacent clear areas.

The cloud lines sometimes alleviated conditions of barotropic instability: meridional gradients of westerly winds were concentrated at cloud lines. Instead of having a uniform gradient of westerly wind over about 5° of latitude (barotropically unstable), it was found that to the south of a cloud line there were strong winds with little gradient, that the westerlies diminished abruptly through the line, and that winds were light to the north, again with small meridional gradient.

It appears that the depression consisted essentially of a series of mesoscale cloud features, each generally lasting a few hours and being succeeded by other like features. The configuration showed diurnal variations. It is inferred that a monsoon depression requires sustained large-scale forcing to maintain the meridional pressure gradient which drives low-level westerly winds across the Bay of Bengal: The sustained forcing is met by a continuous series of cloud formations.

The thermodynamic and wind structures in the depression were integral with the cloud formations, the structures could be perceived as responses of forcing in terms of static instability, topography and barotropic instability. By producing anvil cirrus aloft, and low fragmentary stratus, it appears that cumulus do alter large-scale radiative forcing. This appears to be an important aspect of cumulus heating. Release of latent heat and consequent alterations of flow and warming by subsidence, all appear to be parts of an integrated response to forcing. Production of sheets of high-level stratus, following ascent of cumulonimbus in small areas, appears to be important in altering the forcing. The feedback of cumulus to the large scale seems to be of two kinds: first, alleviation of instablility; second, alteration of radiative forcing, chiefly stratus layers.

4) In GATE, in Winter MONEX and in Summer MONEX, it has been found always in the low troposphere over the tropical oceans that ascent occurs in cumulus clouds. Any upward motion at levels below about 400 mb means cumulus convection. No instance has been found of 'stable ascent' except at mountains. Upward motion in the low troposphere is integral with cumulus convection. Following cumulonimbus convection, mesoscale ascent in anvil clouds in the high troposphere has been bound.

If substantial low-level convergence occurs in the course of numerical modeling, this means that cumulus convection is also occurring. The arrangement of this vertical motion is such as to alleviate instabilities. It seems that a proper approach to the parameterization of cumulus convection should involve inquiry as to prevailing instabilities. 'Cumulus parameterization' implies

simultaneously 'vertical motion parameterization' and 'low-level convergence parameterization'.

Cumulus convection generally leads to stratus. It is found that the area coverage of substantial ascent in cumulus is generally accompanied by an area coverage roughly 20 times greater of thin fragmentary stratus. This might be parameterized by introduction of a thin layer of stratus at the level of greatest horizontal divergence. Radiative forcing then changes: upward motion always leads to changes in external forcing.

The 'cloudy virtual potential temperature' should be given due attention in modeling. Where ascent occurs in the tropical oceanic lower troposphere, the atmospheric stratification tends toward constant cloudy virtual potential temperature. This has been explained by Alan K. Betts. It refers to conditions which are just saturated, with density the same at any level as that of air ascended adiabatically from cloud base, bearing condensate. The corresponding lapse rate is slightly steeper than the moist adiabat.

JOURNAL PUBLICATIONS:

Warner, C., 1984: Core structure of a Bay of Bengal monsoon depression. Mon. Wea. Rev., 112, 137-152.

Warner, C., and R. H. Grumm, 1984: Cloud distributions in a Bay of Bengal monsoon depression. Mon. Wea. Rev., 112, 153-172.

Warner, C., and D. P. McMamara, 1984: Aircraft measurements of convective draft cores in MONEX. J. Atmos. Sci., 41, 430-438.

Warner, C., 1984: Stereo-pair photographs of monsoon clouds. Bull. Amer. Meteor. Soc., 65, 344-347.

TECHNICAL PUBLICATION:

Warner, C., 1984: Satellite observations of a monsoon depression. Final Report to NASA Under Grant NAG 5-297. University of Virginia, Charlottesville. 54 pp, 10 tables, 40 figs.

CONFERENCE PUBLICATION:

Warner, C., 1984: Satellite observations of a monsoon depression. Postprints, 15th Conf. on Hurricanes and Tropical Meteor., Jan 9-13, Miami, FL., Amer. Meteor. Soc., Boston. 386-393.

STUDIES OF ATMOSPHERIC WATER IN STORMS WITH THE NIMBUS 7 SCANNING MULTICHANNEL MICROWAVE RADIOMETER

(K. B. Katsaros-Univ. of Washington)

RESEARCH OBJECTIVES:

To make full use of the new tools for studying mid-latitude cyclones provided by the atmospheric water channels of the Scanning Multichannel Microwave Radiometer (SMMR) on Nimbus 7.

SIGNIFICANT ACCOMPLISHMENTS.

Employing data on integrated atmospheric water vapor, total cloud liquid water and rain rate obtainable from the Nimbus 7 Scanning Multichannel Microwave Radiometer (SMMR), we have studied the frontal structure of several mid-latitude cyclones over the North Pacific Ocean as they approached the West Coast of North America in the winter of 1979. The fronts, analyzed with all available independent data, are consistently located at the leading edge of the strongest gradient in integrated water vapor (Fig. 1). The cloud liquid water content, which unfortunately has received very little in situ verification, has patterns which are consistent with the structure seen in visible and infrared imagery (Fig. 2). The rain distribution is also a good indicator of frontal location, and rain amounts are generally within a factor or two of what is observed with rain gauges on the coast. Furthermore, the onset of rain on the coast can often be accurately forecast by simple advection of the SMMR observed rain areas.

CURRENT RESEARCH:

We have recently compared radar images obtained on the west coast of Washington during the Cycles project (Hobbs and Persson, 1982) with simultaneous SMMR rain rate patterns. Fig. 3 shows how frontal rainbands identified by the radar are reflected in the isohyeths from SMMR.

The winter MONEX (Monsoon Experiment) provided another opportunity to compare radar and SMMR imagery, and again certain mesoscale features can be identified in both types of data. (This work is done in cooperation with Robert Houze of my department). We are also currently analyzing a SMMR underflight by the National Center for Atmospheric Research Electra aircraft which I was able to do on March 25, 1979 off the west coast of Washington. Of particular interest is comparison between the boundary layer winds obtained on the Electra and the winds produced by the recent wind algorithm of the Nimbus 7 SMMR project (Fu, 1983).

FUTURE PLANS.

During November and December 1980 the Storm Transfer and Response Experiment (STREX) was carried out in the North Pacific. It was a comprehensive atmospheric and oceanographic field experiment centered on weathership Papa at 50°N, 145°W, with a second research vessel, the Oceanographer, located at 50°N, 140°W. The experiment and the measurements are described by Fleagle et al. (1982). In this data set are aircraft measurements of cloud parameters and atmospheric profiles,

on a few occasions coincident with SMMR overpasses. Radiosonde ascents were frequent from the two ships and dropsonde surveys of the atmospheric structure were made from high flying aircraft. Several buoys were operated in the research area. The most valuable source of surface data for SMMR is, however, likely to be the radar data obtained by a high resolution radar on the weathership Vancouver at station Papa. The radar has 2 km resolution and a range of 100 km. When the "third year" of Nimbus 7 SMMR data becomes available we will: a) use the STREX data to examine the equality of SMMR sea surface temperature, wind speed, water vapor, cloud liquid water and rain rate, and b) use SMMR data to meet the objectives of STREX, namely to produce a composite picture of the structure of the various portions of an oceanic cyclone at various stages in its development while far from continental influences.

REFERENCES:

Fleagle, R. G., M. Miyake, J. F. Garrett and G. A. McBean, 1982: Storm transfer and response experiment. Bull. Amer. Meteor. Soc., 63, 6-14.

Fu, C. C., 1983: Analysis of SMMR Retrieval Wind Speed. Technical Report, Systems and Applied Sciences Corporation, Riverdale, MD, 35 pp.

Hobbs, P. V. and P. O. G. Persson, 1982: The mesoscale and microscale structure and organization of clouds and precipitation in midlatitude cyclones. Part V: The substructure of narrow cold-frontal rainbands. J. Atmos. Sci., 39, 280-296.

JOURNAL PUBLICATIONS:

We have contributed our rain rate results to the SMMR team paper:

Gloersen, P., D. J. Cavalieri, A. T. C. Chang, T. T. Wilheit, W. J. Campbell, O. M. Johannessen, K. B. Katsaros, K. F. Kunzi, D. B. Ross, D. Staelin, E. P. L. Windsor, F. T. Barath, P. Gudmandsen, E. Langham and R. O. Ramseier, 1984: A summary of results from the first Nimbus 7 SMMR observations. J. Geophys. Res., 89, 5335-5344.

We are also preparing an article for the Journal of Geophysical Research - Oceans Special Collection from the International Union of Radio Science Meeting in Israel, May 14-23, 1984.

TECHNICAL PUBLICATIONS:

Katsaros, K. B. and R. M. Lewis, 1984: Integrated Water Vapor, Liquid Water and Rain Areas Observed with the Scanning Multichannel Microwave Radiometer on Nimbus 7. Technical Report, NASA Contract NAG 5-354, Dept. of Atmospheric Sciences, Contribution Number 717, University of Washington, Seattle.

A technical report on our mid-latitude cyclone work will appear in September 1984.

CONFERENCE PUBLICATIONS:

Katsaros, K. B. and R. M. Lewis, 1984: Observing Atmospheric Water in Storms with the Nimbus 7 Scanning Multichannel Microwave Radiometer. Preprint Volume, International Union of Radio Science Meeting, Israel, May 14-23, 1984.

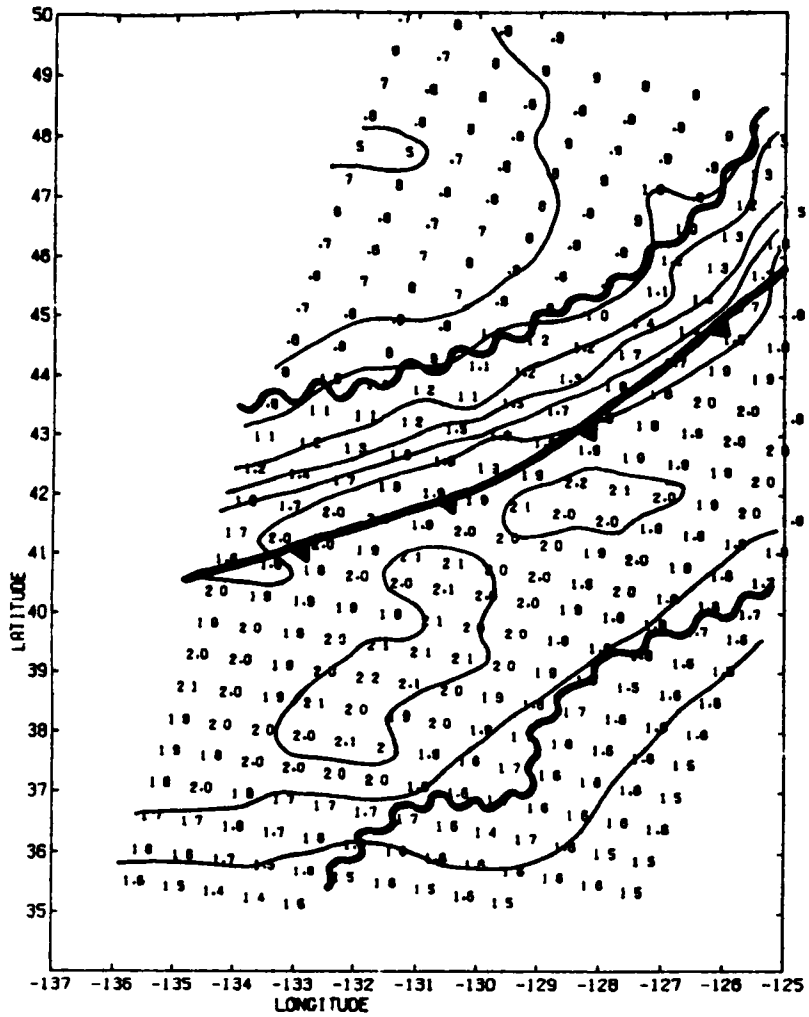

Figure 1. SMMR values of integrated water vapor from a portion of orbit 1743, valid at 0059 PST 27 February, 1979. Units are 10 km m^{-2}. The thin lines are contours at intervals of 0.2. The thick wavy lines depict the northern and southern boundaries of the frontal cloud band revealed by IR imagery (Fig. A.2.2). Also shown is the location of the cold front as determined from independent data.

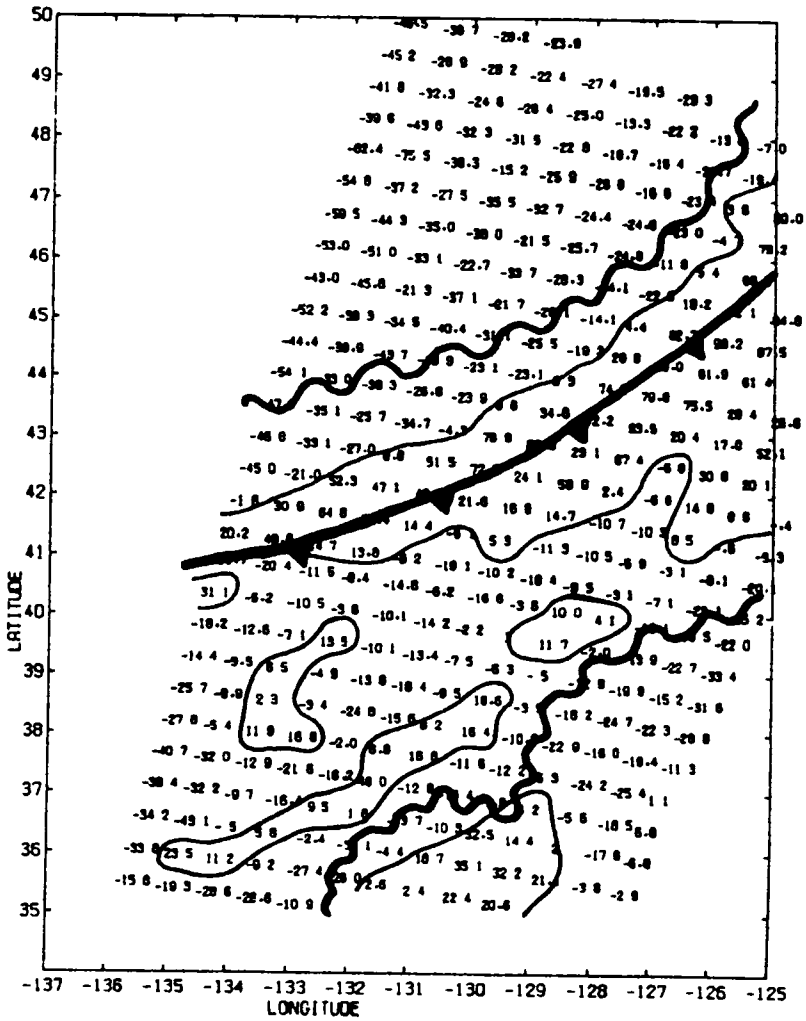

Figure 2. SMMR values of integrated liquid water content from a portion of orbit 1743. Units are 10^{-3} kg m^{-2} but an unknown problem which may be due to a constant bias effect has resulted in some negative numbers. The thin solid lines denote the zero contour. All else as in Fig. B.2.1.

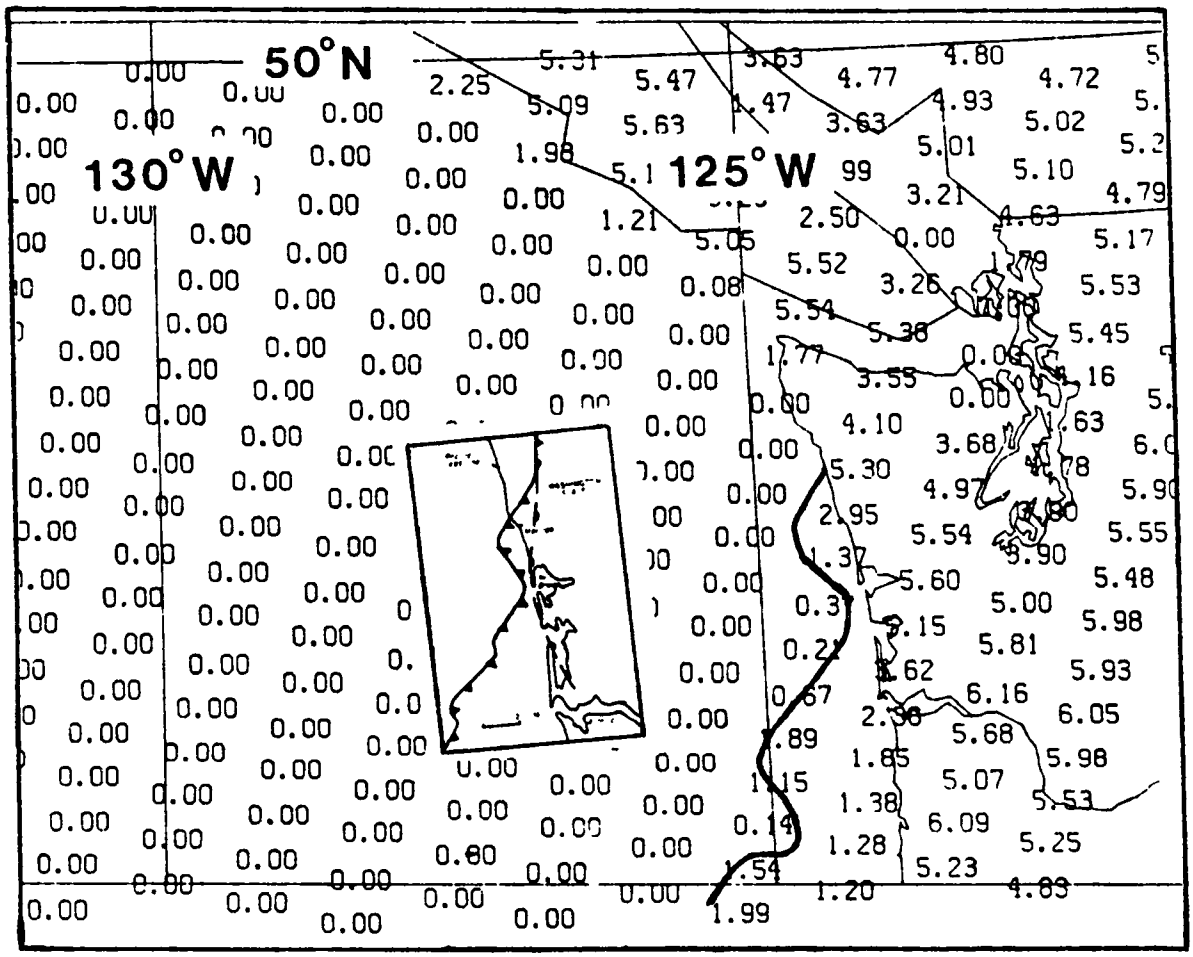

Figure 3. SMMR-derived rainrates from part of orbit 1743 (mm/h). All the scans are plotted but only every other pixel in the cross-track direction is shown. The 1 mm/h contour has been drawn using all of the data. And shown both oriented and to scale is a reproduction on Fig. 9 of Hobbs and Persson (1982) depicting their analysis of the surface cold front location near the coast (see insert).

FIDELITY OF SATELLITE SOUNDINGS
(O. Thompson-University of Maryland)

RESEARCH OBJECTIVES

Two pattern recognition procedures are developed to provide improvements to first guess fields for satellite temperature retrievals. The first is a technique whereby a radiometer measurement may be used to select one or more historical radiosonde temperature profiles as analog estimates of ambient thermal structure. The vertical scales of the analogs are those of radiosondes - the vertical resolving power of the satellite radiometer being relevant only to a decision process. The analog selection process is shown to be much more effective if implemented in an orthogonalized space of measurement information. The second procedure is one which partitions a priori dependent data into shape-coherent pattern libraries using structure information inherent in the data itself. This is an alternative to traditional partitioning schemes whereby proxy classifiers such as season, location and surface type are used.

SIGNIFICANT ACCOMPLISHMENTS.

These pattern recognition techniques are shown to be able to reduce first guess profile errors by nearly 50%, in an independent test of about 800 diverse retrievals. The impact of pattern recognition on temperature retrieval error is assessed using regression and physical-iterative retrieval algorithms. The influence of improved first guess fields is markedly different on these two types of algorithm. Pattern recognition is shown to have a strong, positive impact on the physical-iterative method but little significant impact on regression when evaluated in an overall batch sense. A case study suggests that a small number of very poor retrievals may particularly mash the potential benefits of pattern recognition on both methods.

Page intentionally left blank

IV. SIMULATION OF FUTURE OBSERVING SYSTEMS

Page intentionally left blank

NOAA/NASA JOINT SIMULATION OF AMTS AND HIRS
(J. Susskind-GSFC and D. Reuter-GSFC/USRA)

RESEARCH OBJECTIVE:

The joint NASA/NOAA AMTS/HIRS2 sounding simulation test was designed to compare the relative accuracies of atmospheric temperature profiles retrieved from HIRS2, the current operational infra-red temperature sounder, and AMTS, a proposed advanced high-spectral resolution infra-red sounder. The test compared retrievals generated by GLAS, using their physical retrieval algorithm, and NESDIS, using their operational statistical regression algorithm, for both instruments under clear and cloudy conditions. In the cloudy portion of the test, MSU data, corresponding to the microwave component of the current operational sounding system, was used in conjunction with both instruments to aid in cloud filtering. The test has been completed.

SIGNIFICANT ACCOMPLISHMENTS:

The details of the test and the methods used by GLAS to analyze the clear and cloudy data are given in Susskind et al. (1983) and Reuter et al. (1983). The methods are quite similar to those used by GLAS in analysis of HIRS2/MSU TIROS-N data (Susskind et al., 1984). The results of the clear test, containing 400 simulated global soundings based on radiosonde reports from the SOP-1 (winter) and SOP-2 (summer) period of FGGE, are shown in Fig. 1. RMS errors of layer mean atmospheric temperatures are shown for 18 tropospheric layers and 4 stratospheric layers whose midpoints are indicated in the chart. In addition, RMS errors of surface skin temperature are plotted at 1000 mb.

The primary reason for doing retrievals for both instruments using both techniques was to determine the degree to which the relative improvement of one instrument over another was method dependent. In addition, the test can be used to compare two methods, though the true test of method, at least for HIRS2, is with real data. It is apparent from Fig. 1 that AMTS retrievals above 300 mb tend to be about 1°C more accurate than HIRS retrievals, relatively independent of method, the physical retrievals being about .3° better than the statistical retrievals for AMTS, but showing less improvement for the HIRS. From 300-600 mb, the average improvement of AMTS over HIRS is about .3°C, again roughly independent of method, with physical retrievals about .2°C better for each instrument. Beneath 600 mb, the improvement of AMTS over HIRS is about 50% larger using the physical retrieval scheme (.3°C) compared to the statistical scheme (.2°C) and the difference in accuracy for retrieval type is bigger than for instrument type. A similar result holds for the surface skin (ground) temperatures.

The results from the cloudy portion of the test, containing 40 land mid-latitude winter cases, are shown in Fig. 2. The same general trends hold for the cloudy case except that the improvement of AMTS over HIRS, especially in the lower troposphere, and of the physical retrieval method over statistical method, are considerably enhanced in the cloudy cases. It should be noted that in the cloudy portion of the test, with cloud fraction ranging from 65% to 95%, GLAS performed retrievals in all 40 test cases, while NESDIS performed retrievals in only 36 cases out of 40, considering 4 cases to be too cloudy to

do retrievals. The results of the test are summarized in Table 1 showing RMS temperature errors for 18 tropospheric layers, 4 stratospheric layers, and surface skin temperature.

The results of the test are consistent with our findings with real HIRS2/MSU data (Susskind et al., 1982) which indicates that the GLAS retrievals are more accurate than the operational NESDIS retrievals, especially with increasing cloud cover. As a result of this test, NOAA has decided that physically based retrievals are indeed superior to statistically based retrievals and are beginning to develop a physically based system for operational use. In addition, NASA is considering development of AMTS for a research satellite mission.

TABLE 1

NASA/NOAA COMPARISON TEST

Clear-Column Case (400 Cases)

Sounder-Retrieval	ΔT°C Troposphere	ΔT°C Stratosphere	ΔT°C SST
AMTS - Physical Relaxation	1.39	1.58	0.28
AMTS - Statistical Regression	1.62	1.69	1.05
HIRS - Physical Relaxation	2.00	2.49	0.72
HIRS - Statistical Regression	2.14	2.46	1.01

Cloudy Case (40 Cases)

Sounder-Retrieval	ΔT°C Troposphere	ΔT°C Stratosphere	ΔT°C SST
AMTS - Physical Relaxation	1.72	1.82	0.73
AMTS - Statistical Regression*	1.97	1.95	1.82
HIRS - Physical Relaxation	2.36	3.03	1.06
HIRS - Statistical Regression*	2.80	3.24	1.76

*36 Cases

CURRENT RESEARCH AND FUTURE PLANS:

Current research involves the simulation of global radiances for both HIRS2 and AMTS, using realistic surface, atmospheric, and cloud conditions to be used

to generate global retrievals which will be used in a simulation forecast impact test. The objective is to determine the extent the improved retrievals of AMTS will improve forecasting skill. Results are expected in FY85.

REFERENCES

Reuter, D., J. Susskind, and A. Dalcher, 1982: Simulation studies of the HIRS/MSU and AMTS/MSU satellite sounding units: Cloudy conditions. NASA Tech. Memo. 84983, pp. 58-73.

Susskind, J., D. Reuter, and A. Dalcher, 1983: Simulation comparison study of the AMTS and HIRS2 sounders. NASA Tech. Memo. 84983, pp. 59-67.

Susskind, J., J. Rosenfield, D. Reuter and M. T. Chahine, 1984: Remote sensing of weather and climate parameters from HIRS2/MSU on TIROS-N. J. Geophys. Res., 89D, 4677-4697.

Fig. 1

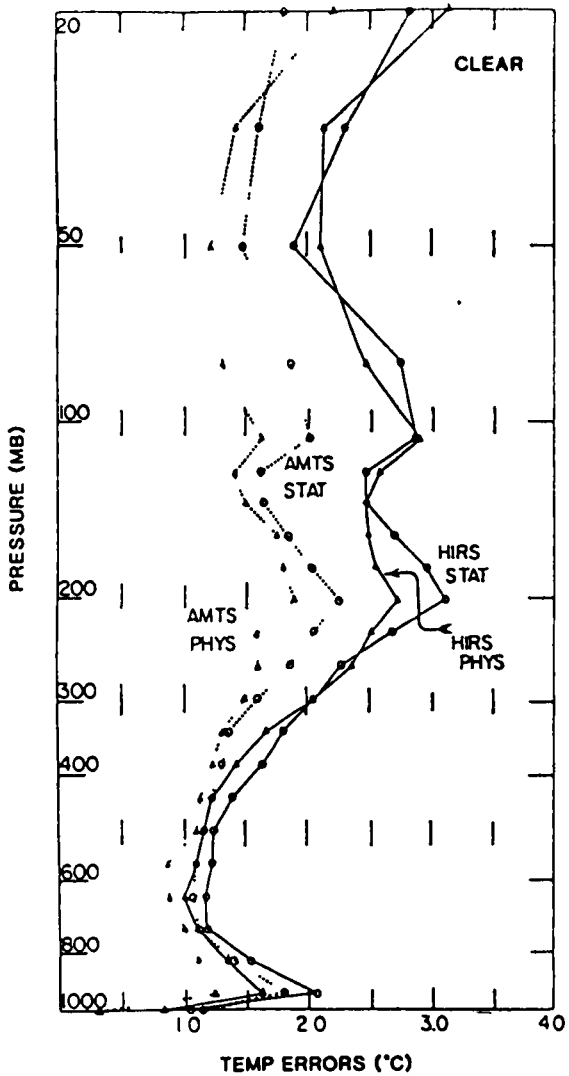

Fig. 2

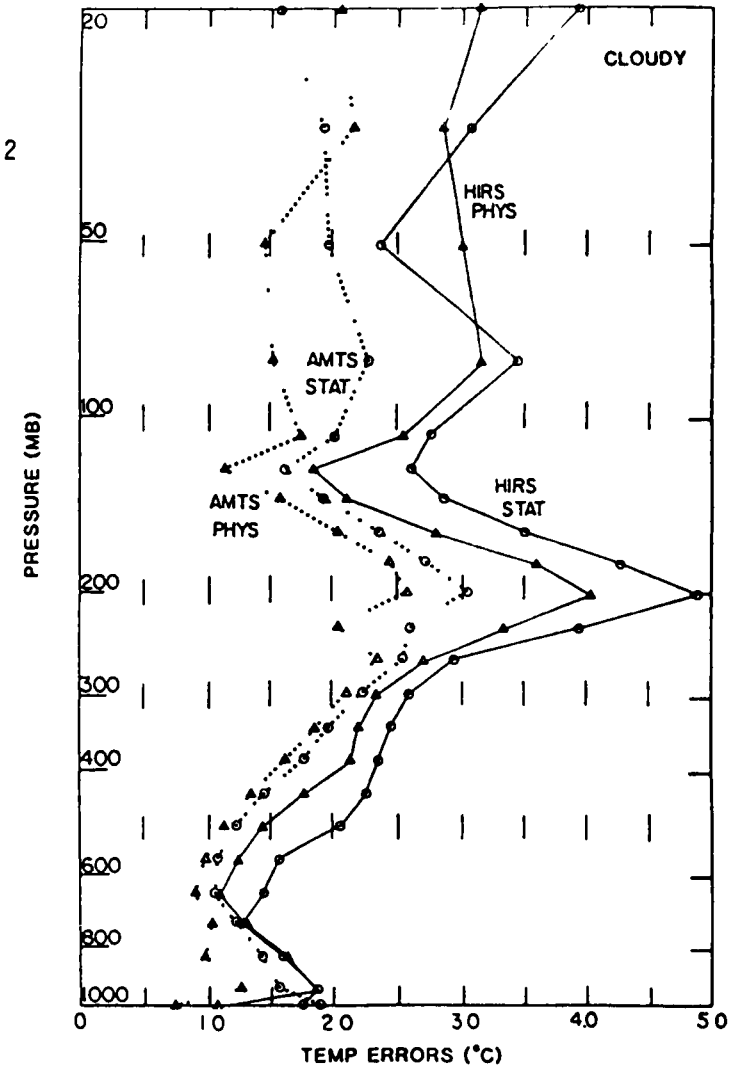

Fig. 1. Vertical distribution of rms retrieval error for 400 clear soundings averaged over all latitudes and both seasons. Values are plotted at the mean log p for each layer.

Fig. 2. Vertical distribution of rms retrieval error averaged over forty mid-latitude cloud scenes for HIRS PHYS and 36 cloud scenes for HIRS STAT. Values are plotted at the mean log p for each layer.

ECMWF/NMC/GLAS JOINT SIMULATION STUDY
(R. Atlas-GSFC)

RESEARCH OBJECTIVE

A series of simulation experiments is being conducted as a cooperative effort between the European Centre for Medium Range Weather Forecasts (ECMWF), the National Meteorological Center (NMC), and the Goddard Laboratory for Atmospheric Sciences (GLAS), to provide a quantitative assessment of the potential impact of proposed observing systems on large scale numerical weather prediction. Instruments to be simulated include current conventional and satellite observing systems, advanced passive sounders such as the AMTS and AMSU, and active LIDAR systems for the measurement of wind, temperature and humidity profiles. In addition to determining the potential impact of individual observing systems, the effect of coverage, resolution, accuracy and assimilation methodology will be studied.

SIGNIFICANT ACCOMPLISHMENTS

An analysis/forecast simulation system has been developed which provides for a more realistic assessment of the potential impact of proposed observing systems than was possible in earlier studies. This simulation system consists of four elements: 1) An atmospheric model integration to provide a complete record of the "true" state of the atmosphere (called nature). This record is then used to fabricate observational reports and to evaluate analyses and forecasts. 2) A conventional data assimilation cycle that is used as the "control experiment." The control experiment is like an operational forecast-analysis cycle based on conventional observations, except that it makes use of fabricated conventional data obtained from the nature run to produce the analyzed fields. 3) A satellite data assimilation that differs from the control in also including fabricated satellite data incorporated in an intermittent or time-continuous manner, in the forecast-analysis cycle. 4) Forecasts produced from both control and satellite initial conditions. Comparison of these forecasts with nature provides an assessment of the impact of the satellite data.

Previous simulation studies have been characterized by the use of the same model to simulate "nature" and to produce forecasts. This "idential twin" problem can distort the conclusions derived from such studies. In the present study we attempt to minimize this and other difficulties of earlier studies. To avoid the identical twin character of previous experiments, the high resolution (1.875° x 1.875° x 15 level) ECMWF model has been used to generate the nature run while the 4° x 5° x 9 level GLAS model is being used for assimilation and forecasting. In addition, the simulation experiments are calibrated against a real data experiment.

A real data experiment, assessing the impact of the FGGE satellite observing systems on analysis and forecasts from November 10-30, 1979 has been completed. For the same period simulation experiments assessing the impact of simulated TIROS-N data, and LIDAR wind profiles of 1-3 m sec^{-1} accuracies were performed. Preliminary results from these experiments indicate that wind profile data is more effective in controlling analysis errors than temperature data and that if proposed accuracies and coverage for a LIDAR wind profiler can be achieved, then

Southern Hemisphere analyses and forecasts should become about as accurate as those for the Northern Hemisphere.

CURRENT RESEARCH:

Simulation experiments to assess the impact cloud-track winds and drifting buoys alone and in combination with advanced passive temperature and humidity sounders are being conducted. The GLAS physical retrieval system is being used to realistically simulate passive retrievals. Other methods for more realistically simulating the errors associated with conventional observations are being explored.

FUTURE PLANS:

Different observing system configurations and alternative coverages and accuracies for proposed observing systems will be studied.

JOURNAL PUBLICATION:

Atlas, R., E. Kalnay, and M. Halem, 1984: The impact of satellite temperature sounding and wind data on numerical weather prediction. Accepted for publication by Optical Engineering.

CONFERENCE PUBLICATION:

Atlas, R., E. Kalnay, J. Susskind, W. E. Baker, and M. Halem 1984: Simulation studies of the impact of advanced observing systems on numerical weather prediction. Proceedings of Conference on Satellite Meteorology/Remote Sensing Applications. June 25-29, Clearwater Beach, Fla.

SIMULATION EXPERIMENTS ON THE RELATIVE ACCURACY OF INFERRED ATMOSPHERIC STATES FROM IDEALIZED WIND AND TEMPERATURE PROFILING SYSTEMS

(M. Halem-GSFC and R. Dlouhy-Sigma Data)

INTRODUCTION:

The First GARP Global Experiment (FGGE) led to the planning, design and implementation of a global observing system that became the prototype for the systems employed operationally in the eighties. This observing system was mainly an outgrowth of technologies and data analysis requirements developed in the early to mid-seventies. In recent years, new technology such as coherent CO_2 LIDAR systems and highly sensitive IR detectors have appeared which offer the potential of more accurate global space-borne observing systems. At the same time, the advent of super computers opened the door to higher resolution general circulation modeling and more sophisticated data analysis schemes. This combination of developments suggests the consideration of advanced space-borne systems better suited to meet the new emerging requirements. The Global Weather Experiment provides us with a new baseline for assessing data accuracy and forecasting capabilities which we can now use to study the incremental performance afforded by such future systems.

RESEARCH OBJECTIVES:

We present, in this review, a series of highly idealized simulation experiments to determine the relative accuracy of inferred atmospheric states from a possible LIDAR wind profiling system compared with similarly idealized temperature and pressure sounding systems. The experiments are carried out for three distinct representations of the 'true' atmosphere to assess the validity of the interpretation of the results. Three fields used in this study are obtained respectively from: (i) a long, general circulation integration of the GLAS 4th Order Model (4° x 5° lon x 9 levels); (ii) a continuous sequence of real NMC operational analysis and; (iii) a simulated long integration from the ECMWF high resolution (1.875° lat x 1.875° lon x 15 layers) operational forecast model. These fields are interpolated to the grid resolution of the GLAS model and used to simulate the observed global analyzed fields of winds, temperature, moisture and surface pressure. The same interpolated fields are also used for verification of forecast impact.

The experiments compare first, the inferred 12 h forecast fields made from an assimilation of complete, instantaneous, global fields of the primary variables, i.e., wind, temperature, and surface pressure, respectively. A subsequent series of experiments compares composite systems of the above basic variables, i.e., wind and surface pressure, temperature and surface pressure.

SIGNIFICANT ACCOMPLISHMENTS:

Results show that the LIDAR wind fields can infer most meteorological fields in the extratropics significantly more accurately than can be inferred from temperature or pressure observing systems. The results obtained are consistent for all three 'nature' fields. The 12 h forecast errors in the extratropics from wind data alone are almost as accurate as that obtained from

the complete specification of all initial conditions. In tropical latitudes, only the LIDAR wind system showed the capability of inferring useful 12 h forecast winds. The experiments indicate that the accuracy of inferred states from temperature data are greatly enhanced by the addition of surface pressure data more so than are the wind data fields. The derived fields for temperature and surface pressure are still consistently less accurate than those of an idealized LIDAR wind system alone. A by-product of these simulation studies is a measure of sensitivity to the 'nature' assumption. The identical twin experiments using the GLAS model and the GLAS 'nature' provide the most optimistic performance estimates, while the results from real NMC data and ECMWF model integration 'natures' are much more similar to each other than to the identical twin.

Three major potential sources of errors that influence the performance of the proposed LIDAR wind profiling systems are distributions and concentrations of aerosols, available power for pulsing the LIDAR and the effects of clouds and large-scale precipitations. Idealized simulation studies are also performed to study their sensitivity. Two experiments are performed in which we assign random error levels of 3 m/s and 6 m/s to simulate the potential effects of errors corresponding to 2 pulses or 10 pulses per grid area. These results are then compared with the idealized LIDAR wind profile accuracies. Results of experiments introducing wind profiles only down to cloud top are also presented. Finally, an experiment assuming global aerosol concentrations only in the lower troposphere shows the resultant impact on forecast accuracy.

V. MODEL AND OBSERVED ENERGETICS

Page intentionally left blank

THE USE OF AVAILABLE POTENTIAL ENERGY TO EVALUATE TWO GLAS FGGE DATA SETS

(L. H. Horn and T. L. Kohler-Dept. of Meteorology, University of Wisconsin-Madison)

RESEARCH OBJECTIVE:

Meteorological data derived from satellites provided an essential component of the FGGE data sets, especially in data sparse regions of the globe. Many ongoing studies are investigating the impact of satellite-derived observations on objective analyses and numerical model predictions. Our project focuses on how well the FGGE data sets and resulting numerical forecasts are able to define the available potential energy of the atmosphere, and its relationship to synoptic scale features such as extratropical cyclones.

CURRENT RESEARCH:

Research during the first year of this grant involves computing the APE in its zonal and eddy components in the FGGE and NOSAT analysis fields during SOP-1. The APE computations are being performed for three domains: the entire globe, and separately for both the Northern and Southern Hemisphere. The APE variations will also be related to extratropical cyclone activity during the period. Some comparisons between the exact and approximate forms will also be made.

FUTURE PLANS:

While the first year research involves analysis fields, work in the second year will include the APE computation for the FGGE and NOSAT forecast fields, and an assessment of the difference between the two sets of forecasts. Another important aspect of the forecast evaluations will be the determination of extratropical cyclone tracks from the SOP-1 forecast data, and comparing them against their observed counterparts. These studies should aid in defining the ability of FGGE satellite data to improve numerical weather prediction forecasts.

GENERATION OF AVAILABLE POTENTIAL ENERGY AND OTHER DIAGNOSTIC STUDIES DURING FGGE

(D. A. Salstein and R. D. Rosen-Atmospheric and Environmental Research, Inc.)

RESEARCH OBJECTIVES:

Utilizing gridded analyses of the state of the atmosphere produced by a special objective analysis system (Baker, 1983) and the GLAS Fourth Order General Circulation Model (Kalnay et al., 1983), we are currently examining the energy cycle of the atmosphere. These analyses of a one month period during the First Special Observing Period of FGGE are now being produced at GLAS. Central to their production is the great care being undertaken to archive the various diabatic heating fields necessary for direct computation of the generation of available potential energy (P).

The generation, G, of P due to total diabatic heating and due to the individual components of diabatic heating will be computed. We will also divide each of these G terms into their zonal mean (M), transient eddy (TE) and standing eddy (SE) components in the framework of Peixoto and Oort (1974):

$$G(P_M) = \int \gamma \, [\overline{T}]'' \, [\overline{Q}]'' \, dm \quad \text{where} \quad [\overline{T}]'' = [\overline{T}] - \int [\overline{T}] \cos\phi \, d\phi$$

$$G(P_{TE}) = \int \gamma \, [\overline{Q'T'}] \, dm$$

$$G(P_{SE}) = \int \gamma \, [\overline{Q^*T^*}] \, dm$$

(T = temperature, dm = element of mass, ϕ = latitude, γ = static stability,

$\overline{\ }$ = monthly mean, [ ] = zonal mean, ' = departure from monthly mean,

* = departure from zonal mean)

Compilation of the above terms will fill in gaps in the atmospheric energy cycle which, in the past, had only been estimated as residuals.

SIGNIFICANT ACCOMPLISHMENTS:

As a prelude to examining the generation of P, we have been using the GLAS analyses during the same FGGE period to study the relative impact due to the satellite-based and other special observing systems then in use. As part of this assessment, we computed the three components of the kinetic energy (K) and of the potential energy in addition to the conversion (C) between various energy forms. The aforementioned computations were performed for (i) the GLAS analysis incorporating all available data (denoted FGGE), (ii) a parallel analysis from which satellite-derived and special data were omitted (NOSAT) and (iii) a separate type of analysis based on rawinsonde stations alone (STATIONS). Hemispheric values of these quantities are given in Table 1, and more details can be found in Salstein and Rosen (1982). Lorenc and Swinbank (1984) have compared values in Salstein and Rosen with other FGGE analyses.

We examined the basic fields produced by the FGGE and NOSAT analyses, from which the integrated quantities in Table 1 were divided. It was apparent that

by and large, the two sets of fields were quite close over much of the globe, although locally the satellite systems led to distinctions, particularly over the Southern Hemisphere oceans. As one example, we show in Figure 1 the temperature field at 850 mb from (a) FGGE, (b) NOSAT, and (c) the difference FGGE - NOSAT.

Upon examining the differences between the FGGE and NOSAT cases, the question arose concerning whether the GLAS model itself was playing a large role in producing features in the analysis fields, independent of the assimilated input data. To answer that question, the GLAS model was run in a CLIMATE mode, into which no observations were entered.

The results of this CLIMATE run are somewhat inconclusive. In many cases the CLIMATE values are rather different from the FGGE and NOSAT values, which are themselves quite close; this indicates that the model climate does not dominate. Such a feature can be observed, for example in the u field at 200 mb, for example (Figure 2), south of Australia. However, some unexpected influences of the model climate were encountered, such as in the strong center in the $\overline{u'v'}$ field at 200 mb in the Pacific off the coast of North America, apparent in the FGGE and NOSAT cases, but totally absent in the STATION analysis (Figure 3).

We are making use of the full FGGE fields mentioned above in conjunction with the diabatic heating and vertical motion fields produced by the GLAS model to complete the analysis of the atmospheric energy cycle.

REFERENCES:

Baker, W. E., 1983: Objective analysis and assimilation of observational data from FGGE. Mon. Wea. Rev., 111, 328-342.

Kalnay, E., R. Balgovind, W. Chao, D. Edelmann, J. Pfaendtner, L. Takacs, and K. Takano, 1983: Documentation of the GLAS fourth-order general circulation model. NASA Tech. Memo. 86064.

Lorenc, A. C. and R. Swinbank, 1984: On the accuracy of general circulation statistics calculated from FGGE data - a comparison of results from two sets of analyses. Quart. J. Roy. Met. Soc., in press.

Peixoto, J. P. and A. H. Oort, 1974: The annual distribution of atmospheric energy on a planetary scale. J. Geophys. Res., 79, 2149-2159.

Salstein, D. A. and R. D. Rosen, 1982: Impact of satellite data on large-scale circulation statistics as determined from GLAS analyses during FGGE SOP-I. Final report, NASA Contract NAS5-26515.

Table 1. Energy terms (in units of 10^5 J m^{-2}) and energy conversion terms (in units on W m^{-2}) between 1000 and 100 mb. SH quantities restricted to north of 68°S.

	Northern Hemisphere			Southern Hemisphere	
	NOSAT	FGGE	STATION	NOSAT	FGGE
K_M	9.22	8.78	8.12	5.22	5.10
K_{TE}	8.16	8.00	7.49	4.79	4.75
K_{SE}	2.49	2.36	2.16	1.25	1.25
$C(K_{TE},K_M)$	.23	.21	.22	.48	.46
$C(K_{SE},K_M)$	.20	.22	.08	.08	.07
P_M	55.30	52.56	56.67	22.22	19.88
P_{TE}	5.81	5.11	6.40	2.41	2.05
P_{SE}	4.90	4.59	7.57	1.09	.79
$C(P_M,P_{TE})$	2.04	1.84	1.39	1.21	.70
$C(P_M,P_{SE})$	1.05	.99	1.07	.05	.11
$C(P_M,K_M)$	.38	.87	1.15	-.73	-.21

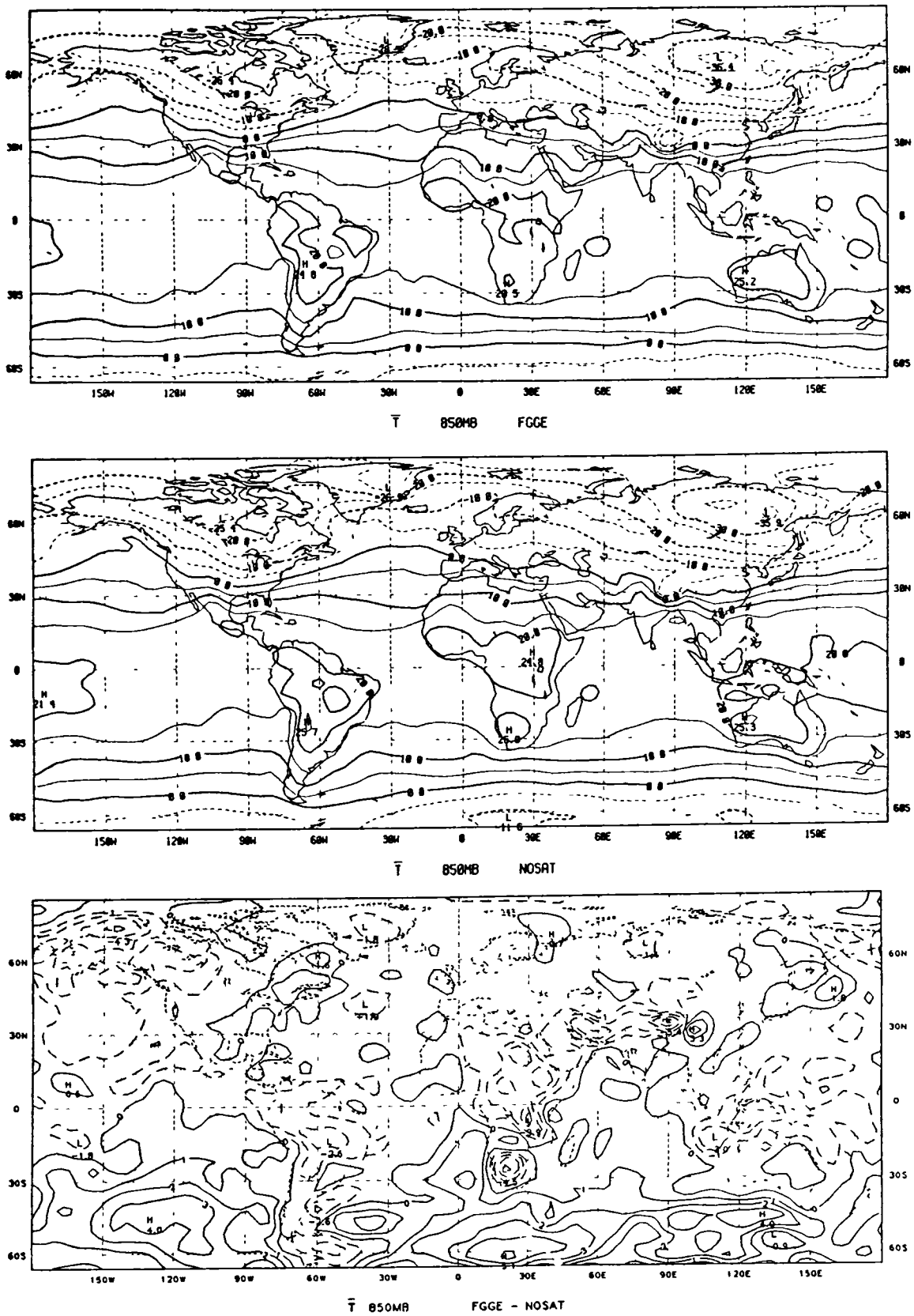

Figure 1. Temperature in °C at 850 mb for the FGGE and NOSAT analyses and their difference (FGGE - NOSAT).

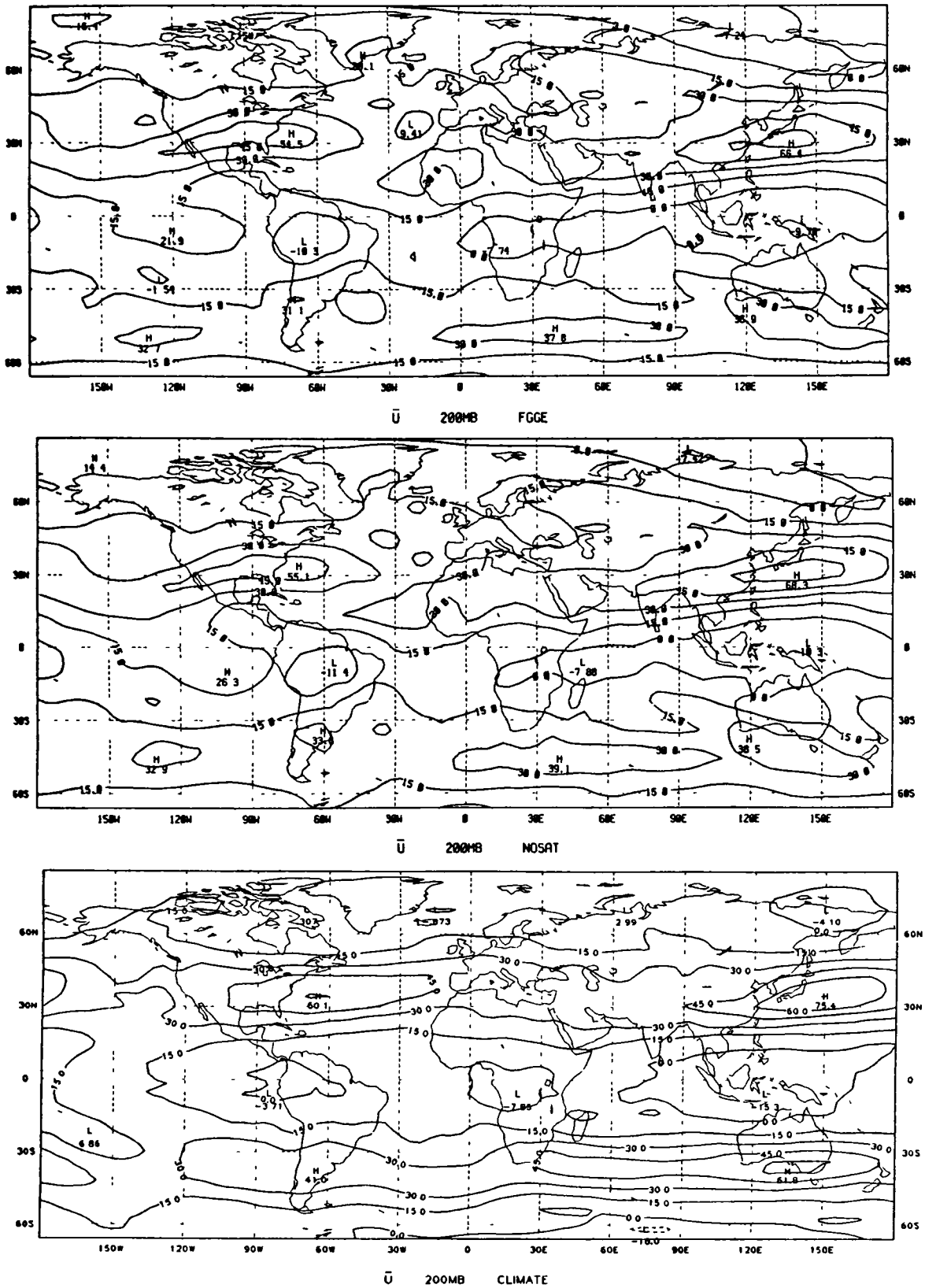

Figure 2. Zonal wind in m s^{-1} at 200 mb for the FGGE and NOSAT analyses, and for the CLIMATE run.

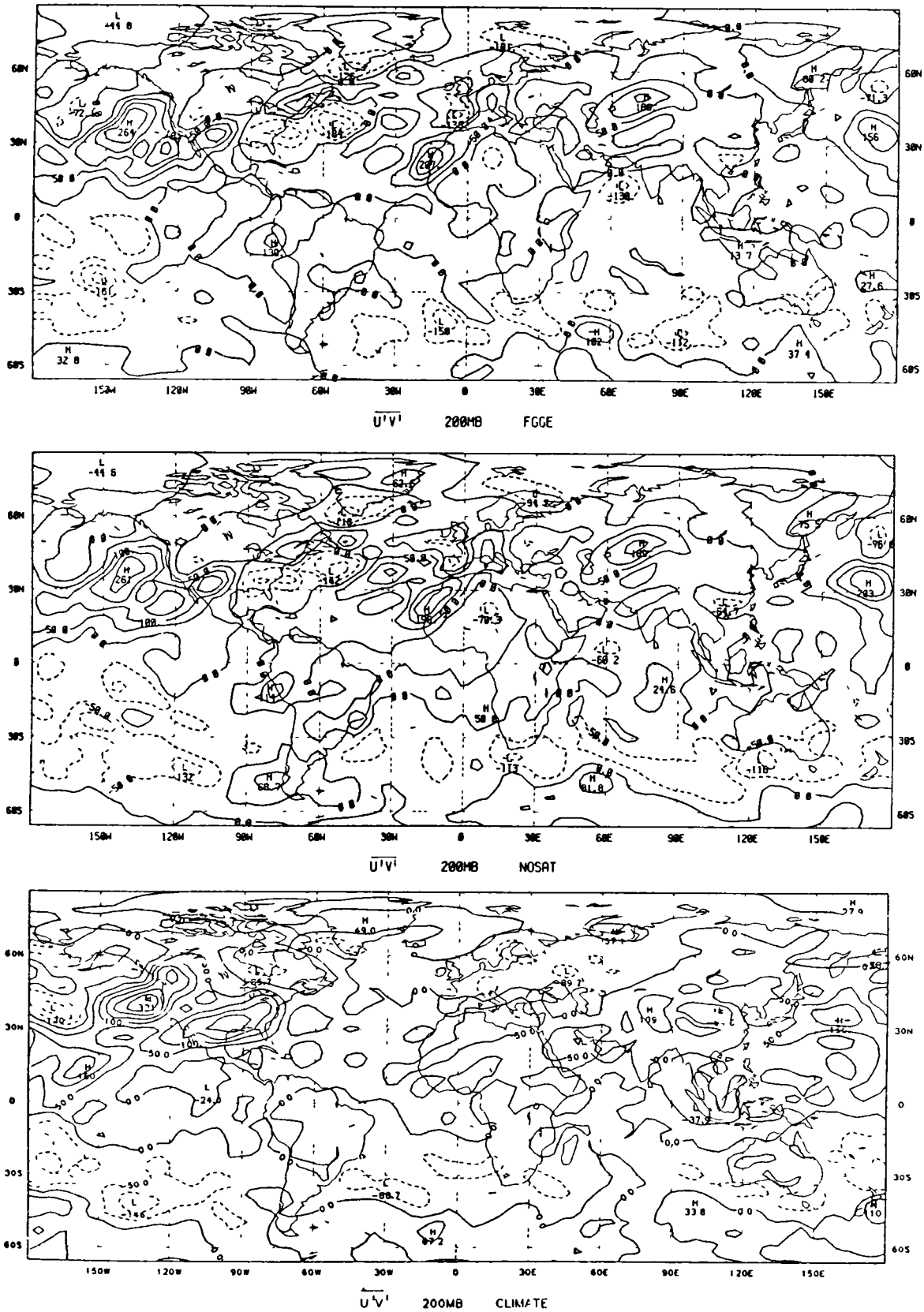

Figure 3. $\overline{u'v'}$ in m^2s^{-2} at 200 mb for the FGGE and NOSAT analyses, and for the CLIMATE run.

COMPARISON OF FORECAST AND OBSERVED ENERGETICS
(W. E. Baker-GSFC, Y. Brin-Sigma Data)

RESEARCH OBJECTIVES:

The objective of this investigation is to perform diagnostic studies aimed at furthering the understanding of the atmospheric general circulation and providing important insight into the NASA/Goddard analysis/forecast system as it continues to evolve.

SIGNIFICANT ACCOMPLISHMENTS:

An energetics analysis scheme has been developed to compare the observed kinetic energy balance over North America with that derived from forecast fields of the GLAS fourth order model for the 13-15 January 1979 cyclone case. The major findings of that investigation are:

1) The observed and predicted kinetic energy and eddy conversion are in good qualitative agreement, although the model eddy conversion tends to be 2 to 3 times stronger than the observed values (see Figs. 1 and 2). The eddy conversion being stronger in the 12 h forecast than in observations may be due to a number of factors (e.g. an imbalance from the initial data, overestimation of the release of available potential energy from the physical parameterizations, etc.) which we plan to investigate.

2) In agreement with previous studies of cyclonic disturbances (see Fig. 3) vertical profiles of kinetic energy generation and dissipation exhibit lower and upper tropospheric maxima in both the forecast and observations.

3) An interesting time lag is noted in the observational analysis with the maximum in the observed kinetic energy occurring at 0000 GMT 14 January over the same region as the maximum eddy conversion 12 h earlier (compare Fig. 1a with Fig. 2a).

FUTURE PLANS:

Future work includes the examination of the forecast error over North America in terms of the energetics utilizing the limited-area, analysis scheme previously developed. The observed energetics will be compared with those from model forecasts in which the resolution, physics, or initial data have been modified.

JOURNAL PUBLICATIONS:

Baker, W. E., and Y. Brin, 1984: A comparison of observed and forecast energetics over North America. Submitted to Quart. J. R. Meteor. Soc.

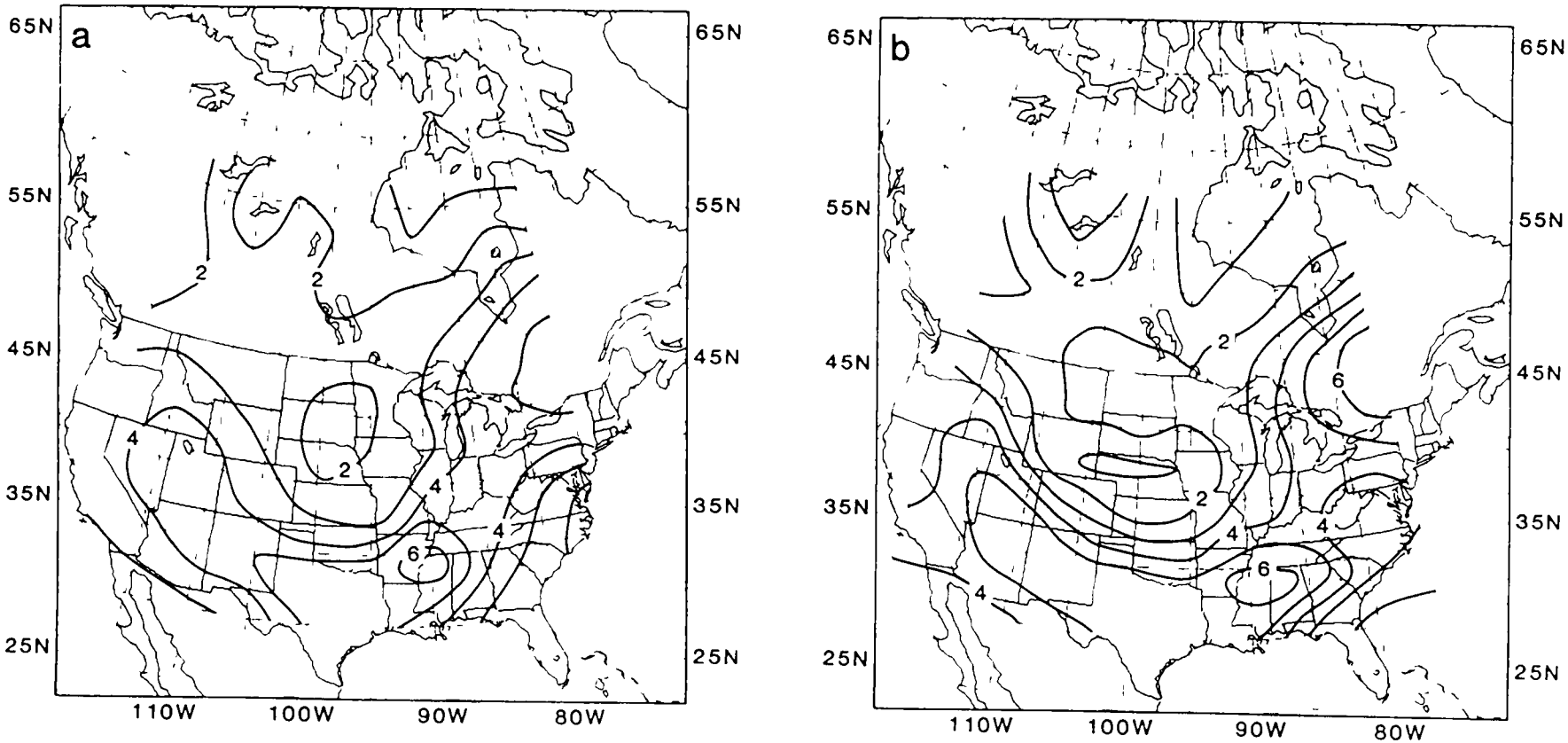

Fig. 1. Vertically integrated (surface to 100 mb) kinetic energy in $10^6 Jm^{-2}$ for 0000 GMT 14 January 1979.
a. Observations (station analysis).
b. 24h forecast.

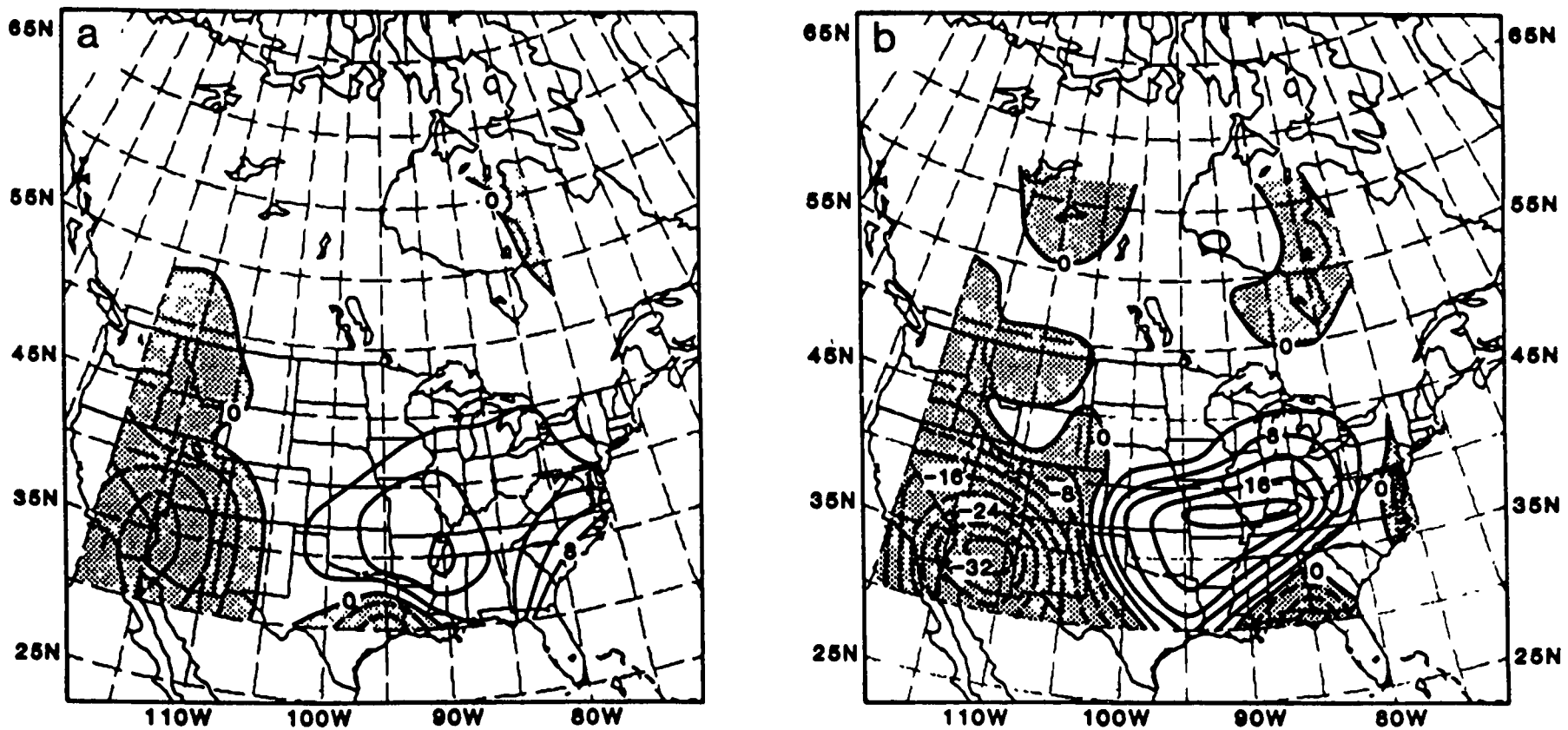

Fig. 2. Vertically integrated (surface to 100 mb) eddy conversion in 10 wm^{-2} for 1200 GMT 13 January 1979. Stippling indicates areas of negative conversion.
a. Observations (station analysis).
b. 12h forecast.

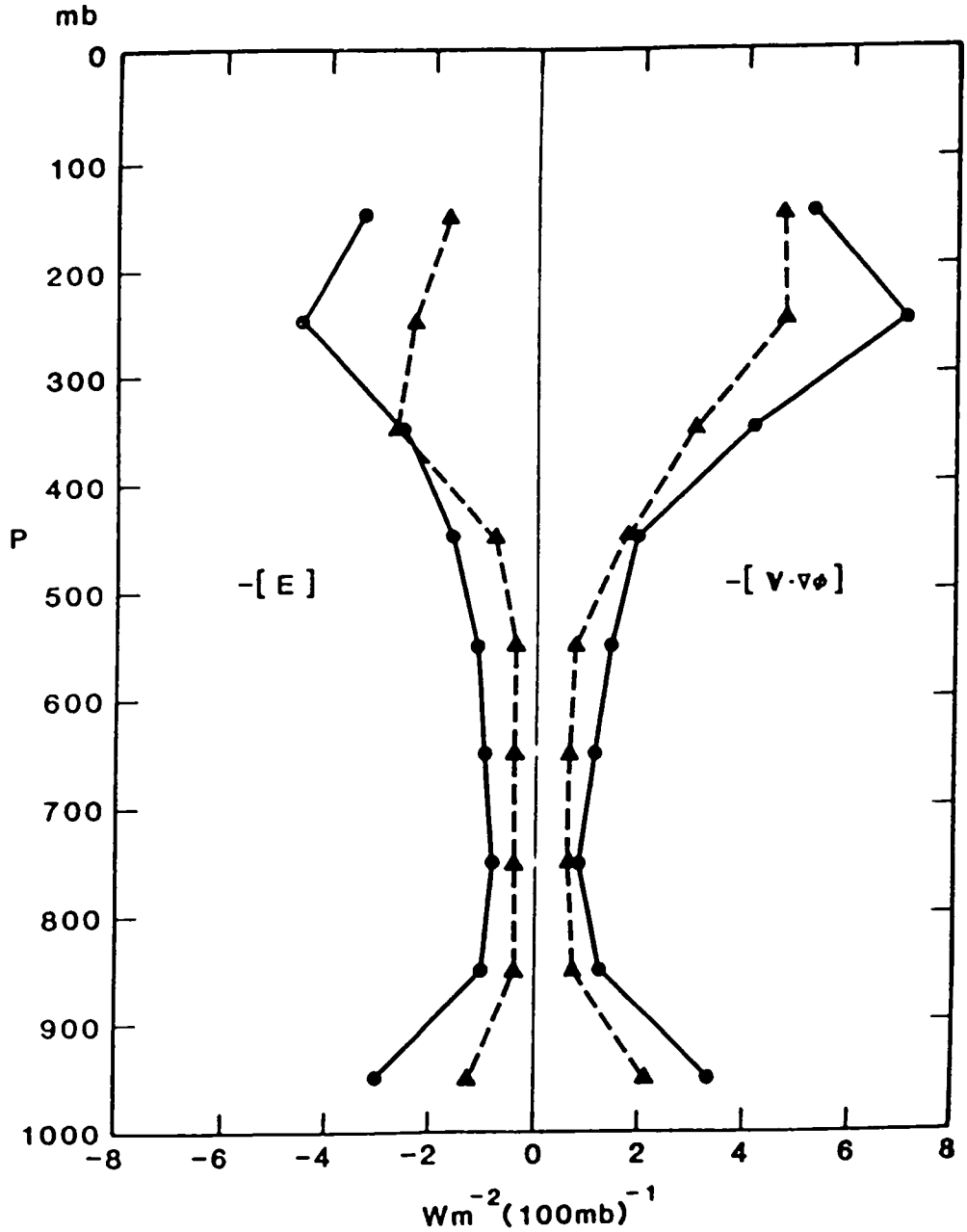

Fig. 3. Vertical profiles of area-averaged kinetic energy generation and dissipation for 1200 GMT 13 January 1979. The station values are denoted by a solid line and the 12h forecast by a dashed line.

ENERGY DIAGNOSTICS AND IMPACT STUDIES OF FGGE GLOBAL DATA SETS AND GLAS GCM SIMULATIONS

(D. R. Johnson-Univ. of Wisconsin-Madison)

RESEARCH OBJECTIVES:

1. To study the physical and dynamical structure of observed and GLAS GCM simulated atmospheres.

2. To assess the accuracy of analyses and predictions and ascertain the utility of observational systems implemented for FGGE.

3. To transfer software for both quasi-Lagrangian and Eulerian diagnostic techniques to the NASA/GSFC computer for the diagnosis of atmospheric circulation and further develop these methods.

4. To study the exchange of mass, momentum, and energy within the planetary and secondary scales of atmospheric circulation during FGGE.

SIGNIFICANT ACCOMPLISHMENTS: (Numbers in [ ] refer to references)

1. Completion of an analysis and publication of a case study of favorable impact of satellite data assimilation on model cyclone prediction [1].

2. Isolation of systematic biases in the vertical structure of SAT temperatures which in all probability negatively impact the prediction of ocean cyclones during periods of rapid baroclinic amplification [2].

3. Access to CYBER 205 and transfer of software for Eulerian and quasi-Lagrangian diagnostic studies of atmospheric circulation.

CURRENT RESEARCH:

A primary focus of our current research is the study of FGGE satellite data on GLAS analyses of oceanic cyclones over data sparse oceans. The objective is to ascertain whether the use of satellite data in data sparse regions improves analyses of the thermal and boundary layer structure of oceanic cyclones and whether more accurate analyses results in improved numerical weather prediction. In the current FGGE research, two oceanic cyclones which developed in the western Pacific and Atlantic oceans during January 1979 are analyzed. The analyses describe satellite data impact on temperature and static stability, available potential energy, and the development of the cyclones. Results show sizable temperature impacts of satellite data throughout the troposphere. Characteristic features of the satellite temperature impact within amplifying oceanic cyclones include the following: 1) NOSAT thermal troughs and ridges of the surface to 500 mb thickness are decreased in amplitude through warm SAT temperature impacts within NOSAT thermal troughs and cold impacts within thermal ridges; 2) differences in magnitude or sign of the temperature impact occur between the upper troposphere and lower troposphere; 3) the amplitude of the cold SAT temperature impact within the storm follows the amplitude of the low tropospheric thermal ridge close to the cyclone center. The SAT temperature impact also produces a sizable increase in tropospheric static stability in the

central storm area and a noticeable decreased stability in the cold troughs both to the rear and ahead of the cyclone.

Although the net effect of area averaged satellite temperature impact for the storms is small, the association of the warm and cold impact on thermal trough and ridge structures reduces the areal temperature and static stability variance within the storm areas. For the Pacific storm these impact statistics imply a nearly 10% reduction of storm available potential energy, a significant reduction in vertical phase tilt of the baroclinic waves, and a potentially greater than 10-20% reduction of the baroclinic growth rate of cyclone waves. The decreased baroclinic amplification is inferred from a stabilization of the highest lapse rates and a reduction of the largest vertical thermal wind shears in the low troposphere of the storm area. Overall the results stress the need to identify features of satellite impact on analyses that have the potential to negatively affect the numerical weather prediction of cyclone development.

In a study of the planetary scale distribution of vertical mass flux, adiabatic and diabatic components of ω are being compared. The study is being conducted to determine changes in the planetary scale circulation that occur during the Asiatic monsoon during the FGGE year. Results show that for periods of several days the timed average diabatic component of ω is generally comparable in magnitude with its adiabatic counterpart at the planetary scale. The aim of this research is to ascertain the relation between diabatic processes and energy transport at the planetary scale and to assess the importance of diabatic forcing in the initialization of numerical prediction experiments. Another study is focused towards the application of available potential energy theory to planetary circulation processes and to study the atmospheric diagnostics. The results emphasize that a variable static stability factor is important in minimizing errors used to approximate available energy both for theoretical, diagnostic and numerical work. In calculations of available energy with mountains, the form of topography and numerical methods used to evaluate the available energy of the actual and reference state atmosphere are important factors to consider.

In this first year, a part of our effort is devoted to the transfer of software to the NASA/GSFC computer and activation and checking of the software. Software used in analyses of planetary and secondary scale circulations have been developed at the University of Wisconsin through support of the National Science Foundation. This software is to be used for analyses of the observed and GLAS GCM simulated atmospheres during the FGGE year.

FUTURE PLANS.

With the completion of the transfer of software for Eulerian and quasi-Lagrangian diagnostics and access to the NASA CYBER computer, detailed studies of the mass, momentum, and energy transport from GLAS FGGE analyses and numerical predictions will be initiated. In conjunction with such analyses, the impact of FGGE SAT information on energy transport within cyclone waves will be assessed.

JOURNAL PUBLICATIONS:

[1] Vergin, J. M., D. R. Johnson, and R. Atlas, 1984: A quasi-Lagrangian diagnostic case study of the effect of satellite sounding data assimilation on model cyclone prediction. Mon. Wea. Rev., 112, 725-739.

[2] Gallimore, R. G. and D. R. Johnson, 1984: A case study of satellite data impact on GLAS assimilation analyses of ocean storm baroclinic structure during FGGE. In preparation.

SPECTRAL ENERGETICS DIAGNOSES FOR FGGE SPECIAL OBSERVING PERIODS AND ENERGETICS ANALYSES OF FORECAST EXPERIMENTS WITH GLAS GCM

(E. C. Kung-ECK Research Consulting, Inc., Columbia, Missouri)

RESEARCH OBJECTIVES:

This research aims at comprehensive energetics diagnoses in the spectral domain with FGGE GLAS analysis and simulation data sets. Specifically, the following three areas are identified as the areas of attention in this study:

1. Energetics characteristics of GLAS GCM as they are reflected on the FGGE analysis data set.

2. Energetics description of GLAS GCM forecast experiments.

3. Energetics response of GLAS GCM climatic simulation experiments.

These three are not isolated problems, but mutually related, interwoven subjects of complexity. A systematic investigation in these areas is being attempted to provide useful information for the study of long-range predictability and further, for the study of long-range prediction.

SIGNIFICANT ACCOMPLISHMENTS:

Since this research project has just begun, research is necessarily in the initial computational phase. However, the results from the initial analysis are encouraging. To date, the spectral energetics have been computed with the SOP-1 Level IIIb GLAS analysis data set and the 40-day climatic simulation data set initialized at December 15, 1978.

The energetics computed with the analysis data for the period 1/5/79 - 3/5/79 are taken as those of FGGE SOP-1 GLAS version Level IIIb data, to be compared with SOP-1 energetics by other versions of FGGE Level IIIb data. The energetics computed with the simulation data for the partial period 1/5/79 - 2/4/79 are taken to indicate the model simulation energetics, whereas the energetics of the whole simulation period 12/15/78 - 2/4/78 are utilized to study the forecast experiment.

Initial diagnosis of the computed energetics and associated fields of motion indicate the following:

1. There are important differences in the field of motion, as exemplified in the vertical field of motion, among different versions of FGGE analysis data sets.

2. There are significant differences in the spectral energetics among different FGGE analysis data sets as contrasted between GLAS and GFDL versions in the SOP-1 energy flow diagram (Fig. 1).

3. The difference in spectral energetics of the real atmosphere and simulation experiment is also very significant, as illustrated in the energy flow diagram of Fig. 2.

4. The development of synoptic patterns during SOP-1 in the Northern Hemisphere are marked by a series of blockings. There are definitive roles of specific planetary scale wave numbers in heat transport through the period. The blocking-like patterns also developed in the simulation run, but they are quite different in location, extent, strength and in their general behavior (Fig. 3).

CURRENT RESEARCH:

The spectral energetics differences between FGGE GLAS SOP-1 analysis data and other versions of analysis data are cross examined in proper context of the models and data assimilation procedures. The difference between GLAS SOP-1 analysis data and GLAS simulation data is also under systematic investigation to evaluate energetics of model behavior in long range prediction. The energetics responses of the model to initialization are studied as part of this broad problem. Energetics functions of specific planetary scale waves in the formation, maintenance and recess of blockings are studied in the synoptic-time series of energetics details for the real atmosphere vs. simulated atmosphere.

FUTURE PLANS:

Study will be extended to SOP-2 with SOP-2 analysis and simulation data sets. Because of the basic difference of patterns in the general circulation during SOP-1 and SOP-2, the ongoing SOP-1 study will have to be complemented with the SOP-2 study.

Data from a series of forecast-simulation experiments with the GLAS GCM will be examined in a systematic energetics diagnosis. Such forecast-simulation experiments are expected to be for the same SOP-1 and SOP-2 periods initialized by different sets of sea surface temperature.

REFERENCES:

Kung, E. C., S. E. Masters and J. A. M. Corte-Real, 1983: Large-scale energy transformations in high latitudes of the Northern Hemisphere. J. Atmos. Sci., 40, 1061-1072.

Masters, S. E., and E. C. Kung, 1983: Energetics of the Aleutian Low area. J. Meteor. Soc. Japan, 61, 51-59.

Kung, E. C., and H. Tanaka, 1983: Energetics analysis of the global circulation during the special observation periods of FGGE. J. Atmos Sci., 40, 2575-2592.

Kung, E. C., and H. Tanaka, 1984: Spectral characteristics and meridional variations of energy transformations during the first and second special observation periods of FGGE. J. Atmos. Sci., 41, (in press).

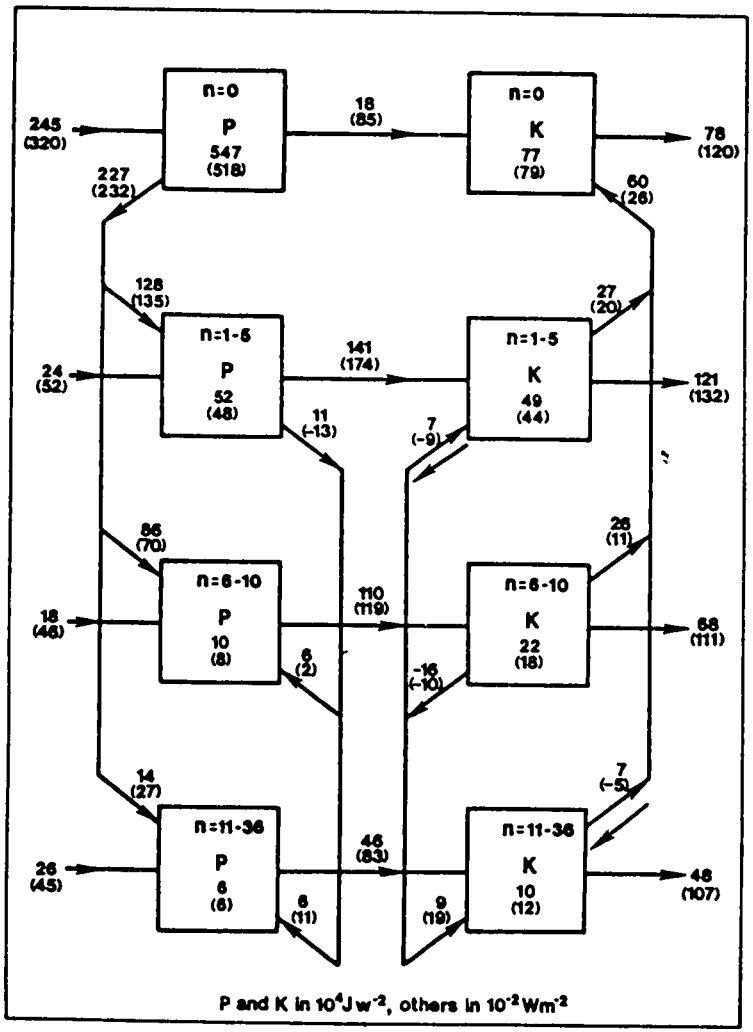

Fig. 1 Energy flow diagram of GLAS and GFDL analysis data sets during SOP-1.

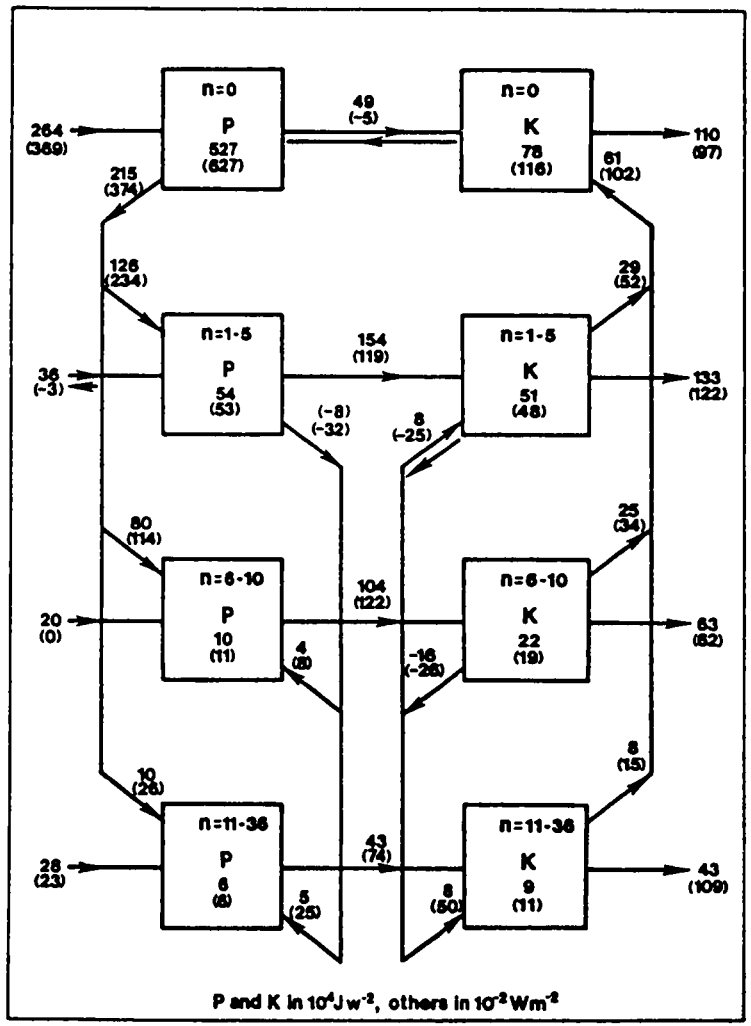

Fig. 2 Energy flow diagram of GLAS analysis data and simulation experiment. Both for the period from 1/5/79 to 2/4/79.

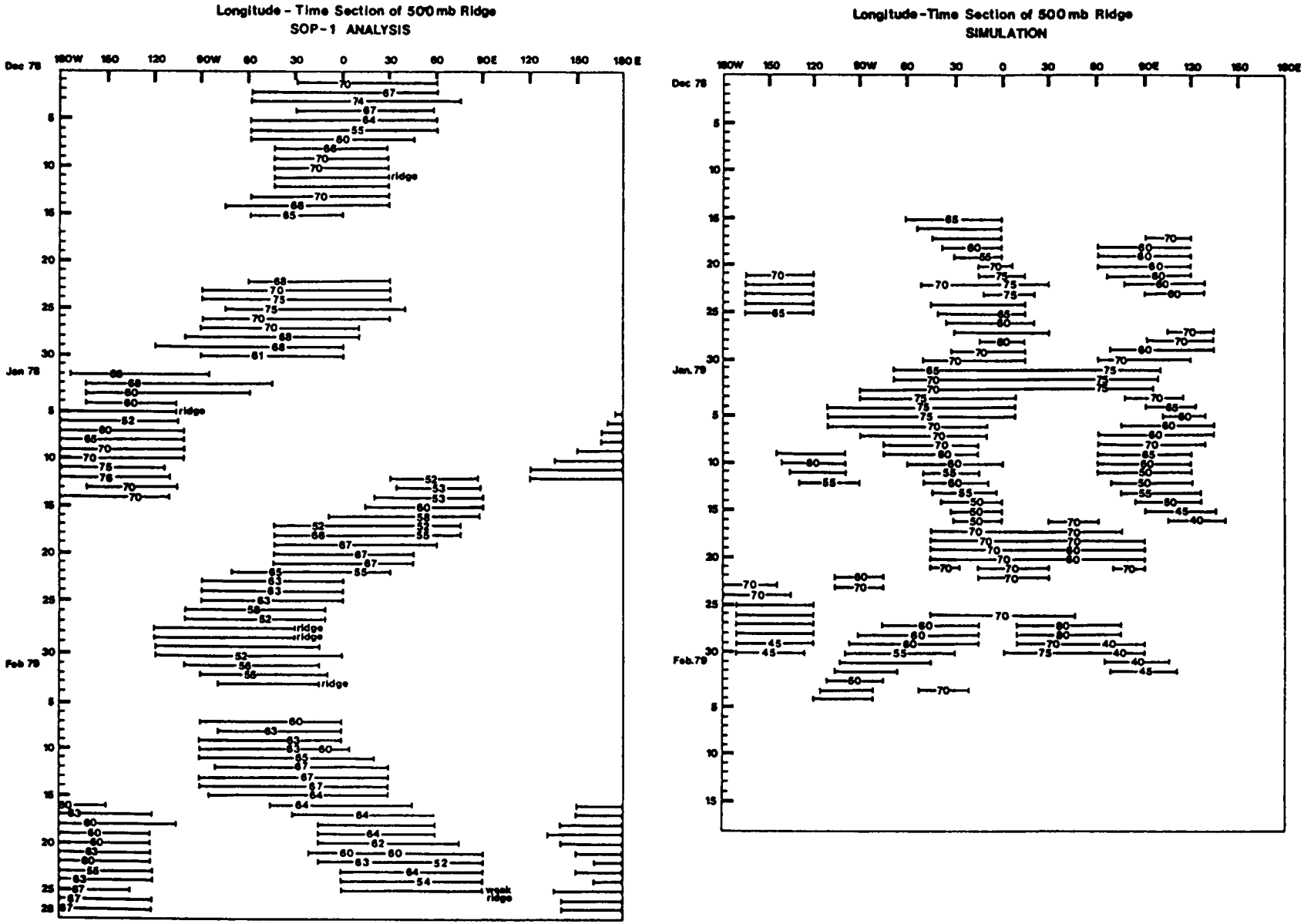

Fig. 3 Comparison of blocking high development in the observed atmosphere and simulated atmosphere. The strip expresses the longitudinal extent of 500 mb ridge; and the number inside the strip, the latitude of the ridge. The simulation is from 1/5/79 to 2/4/79.

JET STREAM ERRORS AND TROPOSPHERIC-STRATOSPHERIC INTERACTIONS IN THE GLAS GENERAL CIRCULATION MODEL

(J. Tenenbaum-SUNY Purchase)

RESEARCH OBJECTIVES:

This project used the GLAS general circulation model (GCM) to explore the causes of erroneously weak shears above the subtropical jet in GCMs. This problem has been seen over the past 15 years of general circulation modeling both as a weak vertical shear and as a cold polar stratosphere. Although recent models now have closed zonal wind contours in their monthly Northern Hemisphere winter climatologies (Fig. 1), the weak shears are still present in both winter, summer, Northern, and Southern hemispheres. Numerous hypotheses have been advanced to explain this failure including the rigid top, poor vertical resolution, incorrect modeling of radiative processes, and incorrect model generation of tropospheric waves. Although the NCAR Community Climate Model, illustrated in Fig. 1, has attempted to deal with many of these causes, especially radiative processes, the problem is still present.

SIGNIFICANT ACCOMPLISHMENTS:

Our major recent accomplishment has been to document the widespread nature of the problem (Tenenbaum, 1982) and to show that the initial failures occur in a characteristic time of 4 days starting above strong initial state jets (Tenenbaum, 1982 and 1983). This failure mode occurs almost always above the East Asian jet and in about one out of five cases off North America. The association with jet streams is further illuminated by the striking alternation of error maxima with jet streaks shown in Fig. 2. Finally, in terms of forecasting abilities, we have shown that the cases conducive to excess stratospheric winds at day 5 of the forecast have a characteristic large scale anticyclonic flow at day 0, and that the same anticyclonic flow is also associated with poor day 5 forecast skill scores over Europe.

CURRENT RESEARCH:

Our specific tasks are threefold. First, we are extending the results of Tenenbaum 1982 and 1983 to more statistically independent cases. One of the main limitations on our prior results is that they deal with 27 cases starting at two day intervals during the FGGE winter (January - March, 1979). We are currently running the model for 15 additional cases, using 3 cases from each of the past 5 winters. Second, we are exploring the Southern Hemisphere and summer seasonal results. One of the suggested causes for weak shears, internal gravity waves, are likely to show differing effects due to the substantially different distributions of orography and continentality in the Southern Hemisphere.

Third, we are exploring other mechanisms which could be producing the weak shears. Although previous work in this area has been expressed in terms of energetics, most recent work has been done in terms of wave-mean flow interactions. One approach to the weak shear problem is to argue that the model forecasts contain excessive wave-mean flow accelerations. Our current work explores these interactions as given by the Eliassen-Palm fluxes (Edmon et al., 1980), their longitudinally dependent form (Plumb, 1984), and ωu, ωv, $\overline{\omega T}$, and ωKE.

Our primary goal here is to determine whether the Eliassen-Palm type fluxes, which have been successfully applied to transient and stationary means, can also be applied as a diagnostic of short, 5 day forecast runs. As shown in Geller et al., (1983), the atmosphere has limited Eliassen-Palm flux divergence near the tropospheric jets. We will study the corresponding values for the model. As a baseline, we will examine the fluxes of the model's monthly mean climatology using an approach similar to that of Andrews et al. (1983). Determining the validity of the modeled cross-tropopause fluxes should indicate whether the weak shear problem is best approached by studying the model's wave-mean flow accelerations or stratospheric energy dissipations.

JOURNAL PUBLICATIONS:

Tenenbaum, J., 1982: Integrated and spectral energetics studies of the GLAS general circulation model. Mon. Wea. Rev., 110, 962-980.

Tenenbaum, J., 1983: Stratospheric wind errors, initial states and forecast skill in the GLAS general circulation model. Mon. Wea. Rev., 111, 1736-1745.

REFERENCES:

Andrews, D. G., J. D. Mahlman and R. W. Sinclair, 1983: Eliassen-Palm diagnostics of wave-mean flow interaction in the GFDL "SKYHI" general circulation model. J. Atmos. Sci., 40, 2768-2784.

Edmon, Jr., H. J., B. J. Hoskins and M. E. McIntyre, 1980: Eliassen-Palm cross sections for the troposphere. J. Atmos. Sci., 37, 2600-2616.

Geller, M. A., M.-F. Wu and M. E. Gelman, 1983: Troposphere-stratosphere (surface-55 km) monthly winter circulation statistics for the Northern Hemisphere-Four year averages. J. Atmos. Sci., 40, 1134-1352.

Pitcher, E. J., R. C. Malone, V. Ramanathan, M. L. Blackmon, K. Puri and W. Bourke, 1983: January and July simulations with a spectral general circulation model. J. Atmos. Sci., 40, 580-604.

Plumb, R. A., 1984: On the three-dimensional propagation of stationary waves. [Submitted to J. Atmos. Sci.].

Tenenbaum, J., 1982: Integrated and spectral energetics studies of the GLAS general circulation model. Mon. Wea. Rev., 110, 962-980.

Tenenbaum, J., 1983: Stratospheric wind errors, initial states and forecast skill in the GLAS general circulation model. Mon. Wea. Rev., 111, 1736-1745.

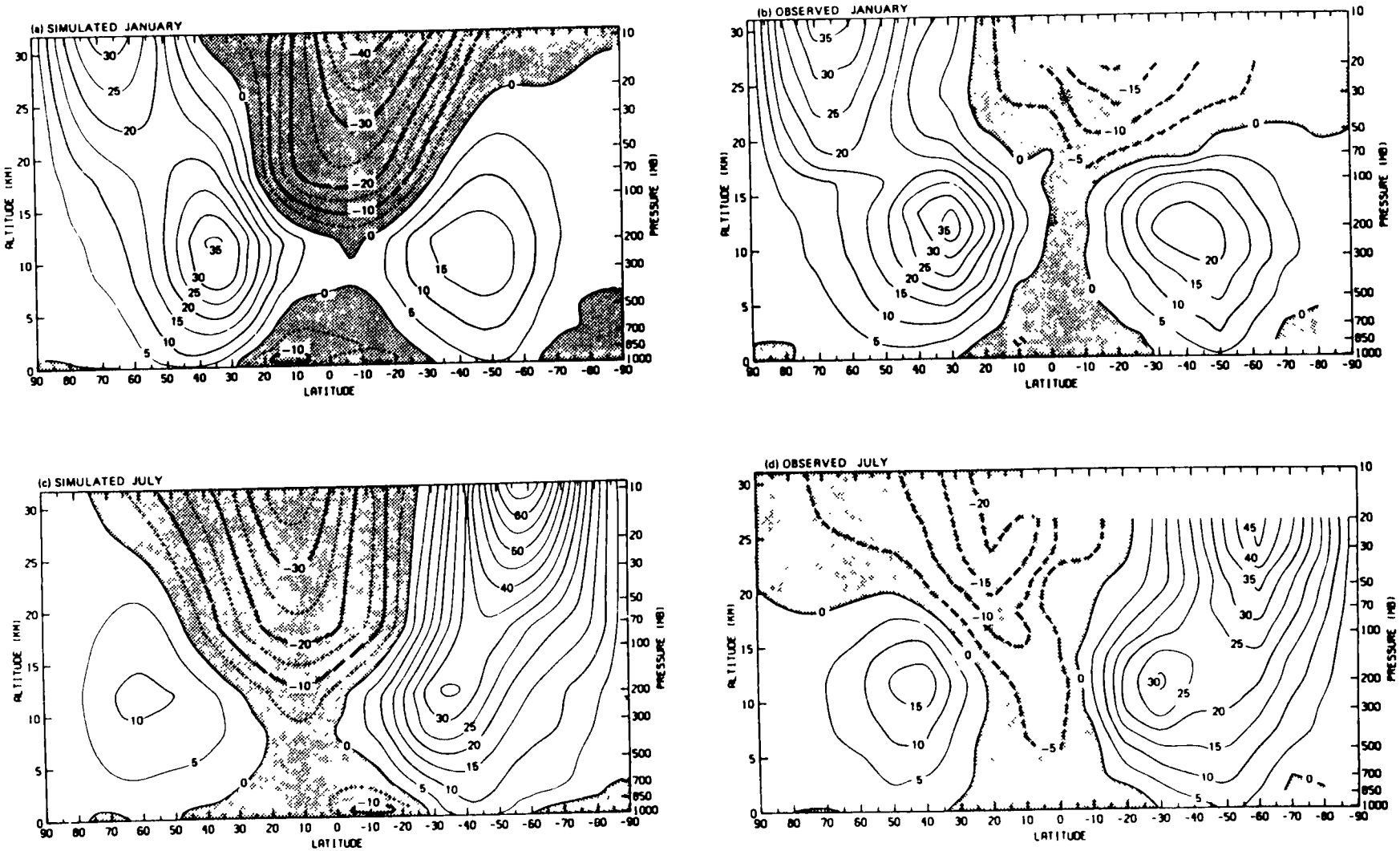

Fig. 1. Meridional cross-sections of the zonal wind (m/s) for the NCAR Community Climate Model. The subtropical jets are all qualitatively well modelled and yet all have weak shears upward and poleward of the core. Taken from Pitcher et al. (1983).

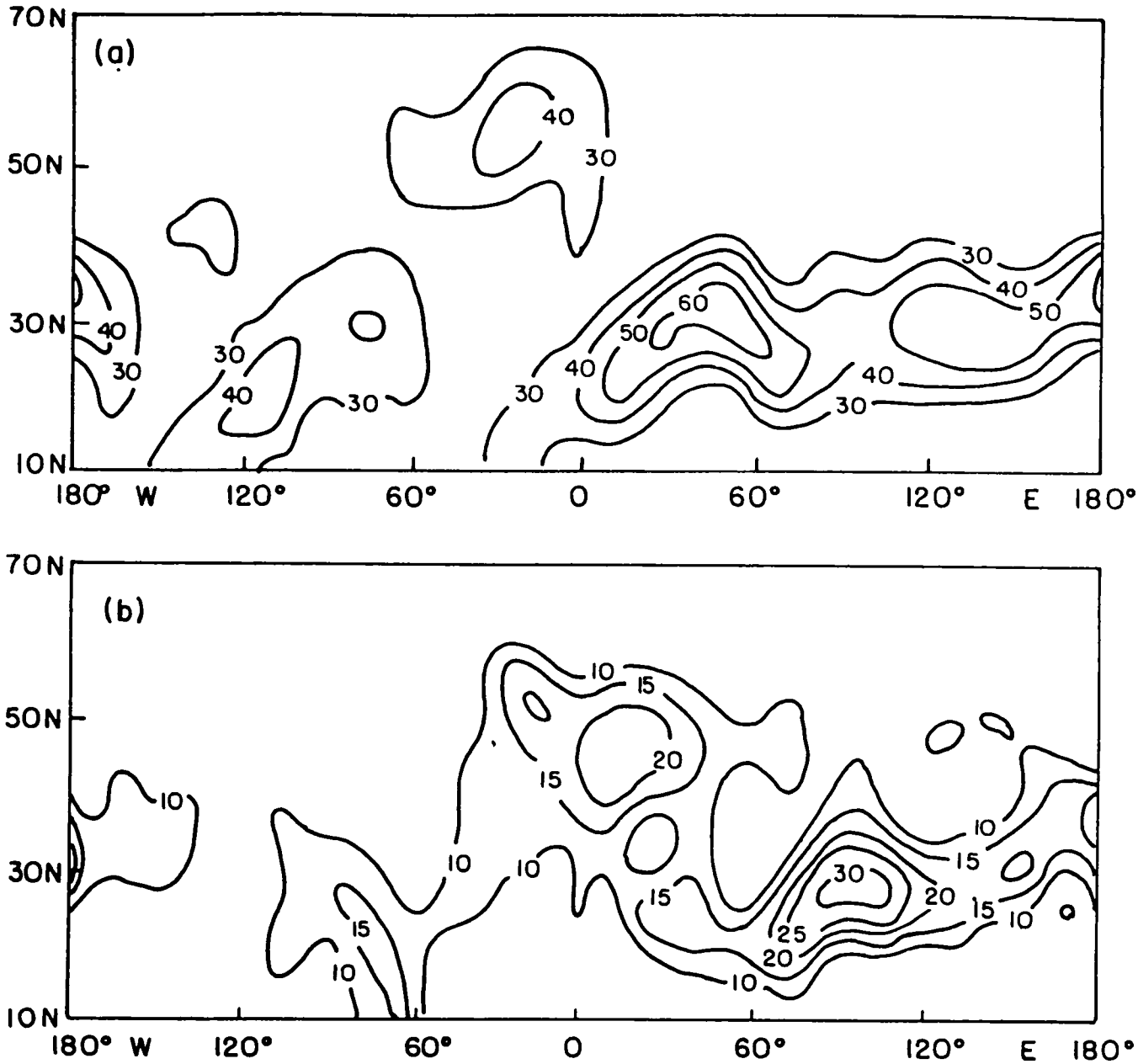

Fig. 2. Ensemble average over the 27 cases of the initial state jet (a), 230-120 mb, and the day 5 forecast wind speed error (b), 120-10 mb. Units: m/s.

ANALYSIS OF DIABATIC HEATING DURING FGGE

(T.-C. Chen-Iowa State University)

RESEARCH OBJECTIVE:

The objective of this project is to examine: a) the maintenance of momentum and thermal fields in the Southern Hemisphere, and b) the diabatic heating and generation of available potential energy of the entire global atmosphere. The data generated by the GLAS FGGE III-b analyses for SOP1 and SOP2 are used for this effort.

SIGNIFICANT ACCOMPLISHMENTS:

It is observed that the atmospheric circulation of the Southern Hemisphere exhibits a double jet structure (subtropical jet and polar jet) in winter and a single jet in summer during the FGGE year. The geographic distribution of standard deviation of the height field at 500 mb indicates that the major eddy activities occur in the downstream side of the polar jet and poleward side of the subtropic jet in winter. However, the major eddy activities go hand-in-hand with the jet stream in summer. The momentum transport is essentially carried out by the transient eddies in both seasons.

The distribution of the temperature field is more axisymmetric in the Southern Hemisphere than in the Northern Hemisphere. The sensible heat is mainly transported poleward by transient eddies along the strong baroclinic zone where the jet streams are located. In other seasons, it is shown from the geographic distribution of the divergence of transient eddy sensible heat flux that the Antarctic continent acts as a heat sink to consume the sensible heat converged toward the polar area from the middle and low latitudes.

CURRENT RESEARCH:

We are currently examining the diabatic heating over the entire globe during the FGGE SOP1 and SOP2 using the residual method. The generated diabatic heating will be used to evaluate the generation of available potential energy. The computations and analyses of primary results are under way. In addition, we are also examining the generation of available potential energy in wavenumber domain in such a way that we can understand the contribution from various sides of atmospheric motion.

FUTURE PLANS:

Three tasks are planned in our next research proposal. They are as follows. 1) to examine the horizontal structure of low-frequency (> 10-day period) and high-frequency (< 10-day period) disturbances in the Southern Hemisphere using the data of the GLAS FGGE III-b analyses, Australian analyses, and the IGY; 2) to examine diagnostically the meridional transport of energy and enstrophy in the spectral domain from the tropics to midlatitudes in various forecast experiments in such a way that we can understand better how the initial data in the tropics affect the forecast of ultralong waves in midlatitudes; 3) to examine the forecastability and predictability of barotropic and baroclinic flows of the atmosphere.

JOURNAL PUBLICATIONS:

Chen, T.-C. and A. J. G. Kpaeyeh, 1984: On the moisture transport over Africa with the FGGE III-b data of various analyses. (To be submitted to J. Appl. Meteor. and Climatology).

Chen, T.-C., L. E. Buja and W. E. Baker, 1984: The maintenance of momentum and thermal fields of the Southern Hemisphere during FGGE. (In preparation).

CONFERENCE PUBLICATION:

Chen, T.-C. and Y.-H. Lee, 1984: A comparison study of spectral energetics analysis using various FGGE III-b data. To be presented at the FGGE Workshop, Woods Hole, MA, July 9-20, 1984.

VI. DYNAMICS OF PLANETARY WAVES

Page intentionally left blank

GLOBAL SCALE DIAGNOSIS OF FGGE DATA

(J. Paegle-Univ. of Utah)

RESEARCH OBJECTIVES:

Our research objective has been to perform descriptive global-scale diagnoses of the GLAS FGGE SOP-1 analyses and to compare these diagnoses against controlled, real-data integrations of the GLAS GCM as well as other data sets. Specifically, we are:

1) Studying the effects of critical latitudes;

2) Diagnosing the influence of tropical wind data and latent heating upon the GLAS GCM;

3) Investigating planetary wave structure on various time scales from the diurnal to the monthly;

4) Comparing the GLAS analyses with other analyses.

SIGNIFICANT ACCOMPLISHMENTS·

Our prior SOP-1 diagnoses (Paegle and Baker, 1982a, 1982b) suggest the following conclusions regarding global-scale waves:

1) Because the divergent component of the meridional flow is not much smaller than the rotational component, the global scale structures resemble forced rather than free modes of linear theory.

2) The vertically reversing structure indicates that longitudinal heating gradients are probably important components of the forcing.

Short-term controlled GLAS GCM integrations (Baker and Paegle, 1983) have shown that:

3) The inclusion of tropical wind data in real data integrations of the GLAS GCM has an important influence in the mid-latitude prediction in both hemispheres.

4) The tropical divergent wind reacts almost immediately to alteration of the tropical latent heating, while the rotational wind reaction requires several days. Furthermore, the presence or absence of zonally averaged easterlies depends strongly upon the presence of tropical latent heating.

CURRENT RESEARCH:

The above results have provided direction for our current research. In particular, in order to advance our understanding of how much of the long-wave structure is a consequence of tropical latent heating, it is necessary to describe the full latent heating fields in some detail. Fortunately, the GLAS SOP-1 analyses contain estimates of the heating. As a preliminary check of the

reliability of these fields in the tropics (where latent heating may account for the strongest heating rates) we are comparing GLAS heating analyses with independent precipitation observations.

Precipitation

The tropics are characterized by local areas of heavy rain embedded within large regions without condensation.

Extreme precipitation rates computed from precipitation data integrated over successive periods of SOP-1 exceed 6 cm/day in the tropical South Pacific Ocean during the first 14 days. This maximum value results from the time average of three distinct observation points lying within one grid square. Peak rates exceed 7 cm/day on the northeast coast of Australia during the second periods. The latent heating associated with this precipitation rate is sufficient to warm the tropospheric column from 850 mb to 20 mb by about 20°C/day.

Heating

Heating rates are analyzed for the same periods as shown in the precipitation data. These heating rates are obtained from the objective analysis of the FGGE data on a 4° x 5° latitude-longitude grid by GLAS. The peak rates vary from 10°C/day in the first periods to as much as 20°C/day in the second period. The former region is coincident with the tropical precipitation maximum of the first period but the second is over the Indian Ocean in a region lacking rainfall observations.

Detailed comparisons with the averaged outgoing long wave radiation derived by NESS from the polar-orbiter satellites show little agreement between the high heating rates in the Indian Ocean and the outgoing long wave radiation. It is to be noted that several days of data are missing from the satellites. Therefore, we are now retrieving the cloud track-winds of the level II-b data sets resident at GLAS to check this feature against other independent observations.

Detailed agreement between the condensation heating implied by the precipitation rates and the GLAS estimates of the heating may not be expected because of the lack of precipitation data over the oceans, representativeness problems of station precipitation data and the presence of other sources of heating. Nevertheless, the precipitation data does support latent heating rates that may locally exceed 20°C/day.

These extreme heating rates should produce vertical velocities on the order of 10 cm/s (i.e. vertical motions of approximately 300 mb/day) according to scaling arguments applied to the thermodynamic equation. The vertical motions we have computed from the horizontal divergence fields associated with the first period are this strong.

Divergent and Rotational Winds

Strongly divergent, upper tropospheric outflow is observed at the perimeter of highly precipitating regions of the tropics. This outflow should connect smoothly to surrounding regions of relatively weak divergence, and the result is a superposition of rotational and divergent wind having rather differing origins.

It is of obvious interest to describe this superposition. One method of quantifying this mixture is to describe the relative magnitude of the divergent and rotational components of the total wind field that projects upon the long waves. We have such an analysis for 15 January 1979, a time when the South Pacific convergence zone is particularly active. This analysis contains the zonal mean and longitudinal Fourier modes 1-4.

We display three different analyses (ECMWF, GLAS, GFDL) of the data to emphasize that the strongest divergent wind regions are resolved in different objective analyses of the raw data. The weaker divergent winds of the ECMWF analyses probably reflect the first guess initialization procedure that is based upon an adiabatic formulation. The GFDL initialization uses a diabatic formulation at this stage of the analysis and the GLAS analysis does not incorporate any explicit initialization balances. It is interesting to note that the rotational wind field is less sensitive to the initialization procedure.

The variation of the meridional divergent wind from 20°S to 20°N is about as great as is the variation of the rotational meridional wind in this tropical belt. The amplitude of each is about 10 m/s to this truncation. This is quite different than in the mid-latitudes where the divergent wind is only a few m/s and the rotational wind may be much larger than 10 m/s. We conclude that although the regions of pronounced divergence are rather restricted, their influence projects strongly upon the global scale wind pattern of the tropics. Furthermore, since the rotational and divergence wind components of the large scale waves are of similar amplitude, they are both approximately equally observable in the tropics, at least for the long wave components. This is distinct from the mid-latitudes where the divergent wind field is generally weak enough to be obscured by observational error.

Controlled integrations of the GLAS GCM (Paegle and Baker, 1983) from this initial state confirm the fact that the tropical divergent wind field is sustained almost totally by latent heating. This experiment also shows that the adjustment of the tropical divergent wind to the heating requires less than one day, while the rotational wind requires several days, suggesting a more rapid adjustment mechanism and more rapidly propagating modes associated with the former.

One possibility is that gravity waves may dominate the adjustment of the divergent wind. To the extent that this is correct, and to the extent that the divergent wind contributes to the total tropical wave field, it may be inappropriate to study latitudinal wave connections through the tropics purely in terms of quasi-rotational wave theory. Silva Dias and Paegle (1984) have shown that gravity and Kelvin modes are the main contributors to the tropical divergence field in 3 week averages of ECMWF level III-b data sets.

Tropical Data Impact

One of the fundamental questions is whether tropical critical latitudes may trap tropical waves or merely be a response to the tropical wave sources. Our observational and modeling studies (Paegle and Baker, 1982b, 1983) suggest that tropical waves and the zonally averaged westerly flow increase and decrease simultaneously, making it difficult to assess cause-effect. To the extent that tropical easterlies do inhibit meridional wave propagation, we may expect less impact for mid-latitudes out of regions of tropical easterly winds than from regions of tropical westerly winds. With this motivation, Dr. Wayman Baker

has performed a series of assimilation experiments during February 1979 that are initialized when critical latitudes for stationary Rossby waves were more commonly found than during January. In the first experiment all available tropical wind data were used between 20°S and 20°N. In the second experiment, the tropical wind data were retained in regions of westerlies and suppressed in regions of easterlies. In a third experiment, tropical wind data were retained in regions of easterlies and suppressed in regions of westerlies. Finally, all tropical wind data were withheld in a fourth experiment.

We have begun to analyze the results of these forecasts. An example of the initial long wave and zonal flow rotational wind difference between assimilations that retain all available tropical wind data and those that neglect all or part of the tropical wind data is analyzed. It appears that the inclusion of tropical easterly winds only in the assimilation is more effective in simulating the initial state than is the inclusion of only tropical westerlies.

The larger tropical differences at 72 h for the westerly data retention case with respect to the easterly data retention case reflect the larger initial differences for this case. However, near the perimeter of the significant Northern Hemisphere influence (at about 44°N), the influence of tropical easterlies is about as great as is the influence of tropical westerlies.

These experiments do not support a major role for critical latitude trapping with respect to meridional propagations in this GCM. We now conjecture that the observed association of equatorial westerlies with enhanced tropical divergent flow is either coincidental or that the enhanced tropical wave sources produce the zonally averaged tropical westerlies. This question and the explanation of the modes of tropical-extra-tropical wave interaction remain to be clarified, and provide focus for our future research plans.

FUTURE PLANS:

Our immediate plans include:

1) Completion of the study of the tropical data impact on the GLAS GCM.

2) Description of the heating fields.

3) Projection of the FGGE data upon the normal modes of the primitive equations.

4) Comparison of the GLAS analyses with those of other data sets.

Some progress in steps one and two has been reported here. The computer code for the normal mode decomposition has also been developed and is necessary to describe the relative gravity wave and Rossby wave projection upon the full field. The gravity wave projection is particularly influenced by analysis of the divergence, that shows fairly substantial differences between different analyses.

JOURNAL PUBLICATIONS:

Baker, W. E. and J. Paegle, 1983: The influence of tropics on the prediction of ultra-long waves. Part I: Tropical wind field. Mon. Wea. Rev., 111, 1341-1355.

Paegle, J. and W. E. Baker, 1982a: Planetary-scale characteristics of the atmospheric circulation during January and February 1979. J. Atmos. Sci., 39, 2521-2538.

Paegle, J. and W. E. Baker, 1982b: Global-scale weekly and monthly energetics during January and February 1979. J. Atmos. Sci., 39, 2750-2759.

Paegle, J. and W. E. Baker, 1983: The influence of the tropics on the prediction of ultra-long waves. Part II: Latent heating. Mon. Wea. Rev., 111, 1356-1371.

Paegle, J., J. N. Paegle and Y. Hong, 1983: The role of barotropic oscillations within atmospheres of highly variable refractive index. J. Atmos. Sci., 40, 2251-2265.

Paegle, J., J. N. Paegle and F. P. Lewis, 1984: Large-scale motions of the tropics in observations and theory. Pure and Applied Geophysics, in press.

TECHNICAL PUBLICATIONS:

Paegle, J. N. and J. Paegle, 1984: Selected comparisons of FGGE level III-b winds. FGGE Newsletter, #3, USC-GARP, NAS.

Paegle, J. and J. N. Paegle, 1984: GLAS heating rate estimates for SOP-1. FGGE Newsletter, #3, USC-GARP, NAS.

Paegle, J. and G. W. Sampson, 1984: Estimates of the weekly evolution of heating fields and available potential energy during SOP-1. FGGE Newsletter, #4, USC-GARP, NAS.

CONFERENCE PUBLICATIONS:

Paegle, J., 1983: Longitudinally Asymmetric Heating and Ultra-long Waves. Proceedings of the IAMAP-WMO Symposium on Maintenance of the Quasi-Stationary Components of the Flow in the Atmosphere and in Atmospheric Models, 1983.

Paegle, J. N., F. P. Lewis and J. Paegle, 1983: Observed and Modelled Long Wave Patterns of the Southern Hemisphere. Proceedings of the First International Conference on Southern Hemisphere Meteorology, 1983.

Kalnay, E. and J. Paegle, 1983: Large Amplitude Stationary Waves in the Southern Hemisphere: Observations and Theory. Proceedings of the First International Conference on Southern Hemisphere Meteorology, 1983.

Baker, W. E. and J. Paegle, 1983: The Influence of the Tropics Upon the Prediction of the Southern Hemisphere Circulation within the GLAS GCM. Proceedings of the First International Conference on Southern Hemisphere Meteorology, 1983.

Paegle, J. and J. N. Paegle, 1983: Modes of Inter-Hemispheric Wave Propagation. Proceedings of the First International Conference on Southern Hemisphere Meteorology, 1983.

Paegle, J. N. and J.-D. Gu, 1984: Interaction of orography and heating for planetary scales. Proceedings of the International Symposium on Plateau and Mountain Meteorology, Beijing, China, March 1984.

Paegle, J. N., Z. Zhao, Y. Hong and J. Paegle, 1984: Sources of flow variability in barotropic primitive equation models. Proceedings of the International Symposium on Plateau and Mountain Meteorology, Beijing, China, March 1984.

Silva-Dias, P. L. and J. N. Paegle, 1984: The partition of energy associated with tropical heat sources. FGGE Workshop, Woods Hole, July 9-22, 1984.

THEORETICAL MODELING FOR NUMERICAL WEATHER PREDICTION

(R. C. J. Somerville-Scripps Institution of Oceanography,
Univ. of California at San Diego)

RESEARCH OBJECTIVE:

The goal of this research is to utilize predictability theory and numerical experimentation to identify and understand some of the dynamical processes which must be modeled more realistically if large-scale numerical weather predictions are to be improved. The emphasis in this research is on the use of relatively simple models to explore the properties of physically comprehensive general circulation models (GCM's). The simple models lack the detailed realism of GCM's, but may for many purposes capture the essential dynamics economically and intelligibly. The role of the simple models is not to replace the GCM but to complement it and to help improve it. The primary GCM employed in this work is that of the NASA Goddard Laboratory for Atmospheric Sciences (GLAS).

A principal theme of this work is the use of predictability theory to evaluate the current skill of numerical weather prediction models and to suggest means of improving it. Despite recent advances, the skill of even the best current models in forecasting planetary waves at short and medium ranges is still far short of the limit set by predictability theory. Relative to theoretical expectations, the major errors of large-scale forecasts still occur preferentially in the ultralong waves and occur on shorter time scales than anticipated theoretically (Somerville, 1980). This research is motivated by the need to understand the causes of these errors and to find means of alleviating them through model improvements and through better specification of initial conditions.

SIGNIFICANT ACCOMPLISHMENTS:

This research has been carried out since May, 1982 with support from NASA Grant NAG5-236. In early work, a global linear quasi-geostrophic model and the GLAS GCM were used to investigate several mechanisms which are responsible for the decay of large-scale forecast skill in mid-latitude numerical weather predictions. Five-day forecasts for an ensemble of cases were made using FGGE data. We found that forecast skill depends crucially on the specification of the stationary forcing. A lack of stationary forcing leads to spurious westward propagation of the ultralong waves. Forecasts made with stationary forcings derived from climatological data are superior to those using forcings inferred from observations immediately preceding the forecast period. Interhemispheric forecast differences were analyzed, and the model errors were compared to errors of a simple persistence-damped-to-climatology scheme and to errors of the GLAS GCM (Roads and Somerville, 1984).

CURRENT RESEARCH:

In more recent work supported by Grant NAG5-236, not yet published, we have compared simple statistical models and no-skill controls (such as persistence and climatology) with GLAS forecasts and an ensemble of 100 forecasts from the GCM of the European Centre for Medium Range Weather Forecasts (ECMWF). We found that the error spectra of the primitive-equation ECMWF and GLAS models were

similiar, except for some systematic errors, to the spectra of the statistical models. The performance of the dynamical models was clearly superior at short range, while a combination of statistical and dynamical forecasts was best at longer range. Post-processing a dynamical forecast by a linear regression procedure analogous to the operational Model Output Statistics algorithm of Glahn and Lowry (1972) can remove some systematic error at sufficiently long range, principally by damping the GCM results toward an appropriate climatology. A criticism of such an approach is that the forecast maps tend to lose spatial detail and to resemble smooth climatological maps rather than instantaneous weather. Of course, this spectral evolution simply reflects the result of predictability theory that details are unpredictable at long range.

FUTURE PLANS:

We propose to develop a spherical, spectral, two-layer, quasi-geostrophic model, coded efficiently for the Floating Point Systems FPS 100E array processor and VAX 11/750 host super-mini computer of the Scripps Climate Computing Facility.

We intend to apply this model to the problem of incorporating non-linearities efficiently in a statistical methodology for large-scale numerical forecasting. Lorenz (1977) used real-data forecasts with the barotropic vorticity equation to test the effects of incorporating non-linearity in a regression scheme. A great deal remains to be done to determine both the potential benefits and the optimal means of including nonlinear processes in a statistical approach.

The spectral quasigeostrophic model can be used in conjunction with GCM experiments to refine estimates of the "error budgets" of present-day numerical weather predictions, i.e., the sensitivity of forecasts to each of the many possible defects in both the forecast models and the specification of initial states. It is often not clear just which aspects of "improved" model physics contribute to a given increment in forecast skill (Hollingsworth, et al., 1980). By simulating potential forcings due to parameterized physics, we can estimate their effect on forecasts (Roads and Somerville, 1984). In addition, cloud radiation feedback parameterizations which are under development in the Scripps Climate Research Group and which are being verified with satellite data, will be tested in the GLAS GCM.

In connection with this work, we plan to compare results of predictability studies with the quasi-geostrophic model to those with GCM's. By introducing simulated errors of prescribed spectral and regional distribution, we can address the question of the extent to which GCM forecast errors are in fact due to uncertainties in small spatial scales in the initial state, as envisioned in classical predictability theory. A topic closely related to the previous one is the possibility that the effects of systematic model errors can be mitigated not only by statistical post-processing of model output, but by empirically correcting the model during the course of the integration.

CONFERENCE PUBLICATIONS:

Roads, J. O. and R. C. J. Somerville, 1983: Predictability of planetary waves: Interhemispheric differences and the effects of stationary forcing. (Preprint) First International Conference on Southern Hemisphere Meteorology. Amer. Meteor. Soc., 93-99.

Somerville, R. C. J. and J. O. Roads, 1983: Linear predictability: The effects of stationary forcing. IAMAP-WMO Symposium - Paris 1983 - Extended Abstracts, 201-203.

TECHNICAL PUBLICATION:

Roads, J. O. and R. C. J. Somerville, 1983: Linear predictability: The effects of stationary forcing. Research Activities in Atmospheric and Oceanic Modelling, No. 5, World Climate Research Program, WMO, 3.1-3.3.

JOURNAL PUBLICATIONS:

Roads, J. O. and T. P. Barnett, 1984: Forecasts of the 500 mb height using a dynamically oriented statistical model. Mon. Wea. Rev., in press.

Roads, J. O. and G. K. Vallis, 1984: Linear and turbulent flow over topography, I. Time-averaged solutions. (Submitted for publication).

BOOK PUBLICATION:

Roads, J. O. and R. C. J. Somerville, 1984: Linear predictability: Effects of stationary forcing. Predictability of Fluid Motions, G. Holloway and B. J. West., eds., American Institute of Physics, 557-570.

REFERENCES:

Glahn, H. R. and D. A. Lowry, 1972: The use of model output statistics (MOS) in objective weather forecasting. J. Appl. Meteor., 11, 1203-1211.

Hollingsworth, A., K. Arpe, M. Tiedtke, M. Capaldo and H. Savijarvi, 1980: The performance of a medium-range forecast model in winter - impact of physical parameterizations. Mon. Wea. Rev., 108, 1736-1773.

Lorenz, E. N., 1977· An experiment in nonlinear statistical weather forecasting. Mon. Wea. Rev., 105, 590-602.

Roads, J. O. and R. C. J. Somerville, 1984: Linear predictability: Effects of stationary forcing. Predictability of Fluid Motions, G. Holloway and B. J. West, eds., American Institute of Physics, 557-570.

Somerville, R. C. J., 1980: Tropical influences on the predictability of ultralong waves. J. Atmos. Sci., 37, 1141-1156.

LARGE SCALE ROSSBY WAVES DURING FGGE

(R. S. Lindzen-MIT, D. M. Straus-GSFC, and B. Katz-Univ. of MD.)

RESEARCH OBJECTIVE:

The purpose of this research is to explore the behavior and significance of global-scale rotational normal modes (free Rossby waves) in the atmosphere. Although these modes have received a great deal of attention in the past (Rossby et al., 1939; Madden, 1978; Kasahara, 1980; Salby, 1981a, 1981b; Ahlquist, 1982), the lack of accurate global data has severely hampered efforts at estimating the amplitudes and time dependence of these waves in the real atmosphere. With FGGE, the availability of accurate data that is truly global in coverage presents an important opportunity for a better understanding of the role of Rossby waves in the atmosphere.

SIGNIFICANT ACCOMPLISHMENTS:

In the results to be presented, emphasis is placed on the temporal evolution of the amplitude and phase of the Rossby waves, rather than on characteristics of the time spectra of these waves. On the basis of previous work (Madden, 1978; Kasahara, 1980; Salby, 1981a, 1981b; Ahlquist, 1982), we felt it would be adequate to consider the 500 mb level in isolation from the others, and that the Hough functions (which are vector functions of the horizontal wind components and the height field) were good approximations to the "true" eigenfunctions (normal modes). Thus, the first steps of the analysis consisted of projecting the 500 mb height and wind data (obtained from the ECMWF analyses) onto Hough functions for each synoptic time. The seasonal cycle and time mean were removed separately for each season, and all remaining eastward propagating components removed on a seasonal basis; all remaining westward propagating components were retained.

A sample of the results is given in Fig. 1, which shows the evolution of the amplitude and phase of the (1,4) mode (zonal wavenumber 1, meridional index 3; i.e., second symmetric mode for wavenumber 1) as a function of time for the winter season. The amplitude scale gives the value of the geopotential height at 66°N, the latitude where the (1,4) Hough mode is strongest. (The phase is plotted only when the amplitude is above 20% of its maximum value). This mode exhibits several features which all the modes have in common. The amplitude evolution takes the form of a series of pulses of duration 5-20 days, indicating that the waves have an episodic nature, growing and decaying on time scales not longer than a few wave periods, at most. The phase progresses westward with a phase speed remarkably close to that predicted by Kasahara (1980), given by the dotted line.

This type of analysis was carried out for the following modes for all four seasons: (1,2), (1,3), (1,4), (2,3), (2,4), (2,5), (3,4), (3,5), (3,6). On the whole, the slope of the phase history lines agrees with the theoretical predictions of Kasahara (1980). However, this agreement does not always hold; in fact, some disagreement is to be expected based on the discrepancies between the variable, latitude-height profile of the zonal wind occurring in nature and the climatological barotropic zonal wind assumed by Kasahara. However, in a

given set of modes for the same zonal wavenumber (e.g. (1,2), (1,3) and (1,4)), the phase speed of each mode, variable as it is, is still noticeably different from the phase speed of the neighboring mode.

As the meridional index of the mode increases, the amplitudes become larger, and the time scale for their change generally increases. While episodes of well defined wave propagation generally last for at least one-half of a wave period, they rarely, if ever, endure for more than three wave periods.

It is of some interest to determine whether the behavior of these global waves exhibits a large seasonal dependence. Examination of all nine modes across the four seasons indicates a remarkable statistical homogeneity with respect to the time of year.

The total Rossby wave field consisting of the sum of the westard propagating components of all nine Hough modes can be fairly large. Figure 2 shows the geopotential height of the Rossby wave field at 500 mb for 12Z on 12 January, 1979. The maximum amplitude of 131 m is large enough to cause serious errors in analyzed or forecast fields if these waves are not correctly handled by a model. The high center of 131 meters at 65°N, 85°E can be followed as far back in time as 0Z on 9 January, when it was at 65°N, 125°E with an amplitude of 78 m, and as far forward as 12Z of 19 January, at 65°N, 30°E with amplitude 120 m. The total time span for which the height field remains above 100 m at 65°N, 85°E is about 3-1/2 days. Although this is not long enough to meet the usual criteria for persistent anomalies (Dole and Gordon, 1983), it suggests that Rossby waves can contribute to such anomalies.

The evolution of Rossby waves as portrayed from the ECMWF analyses were compared to equivalent results obtained from data produced by the GLAS analysis scheme (Baker et al., 1981) for the three months of May-July, 1979. The correspondence between the evolution of both amplitude and phase is generally very good, confirming that the picture presented of the evolution of global scale Rossby waves is not an artifact of the analysis scheme.

CURRENT RESEARCH:

Currently, we are studying the vertical structure of the Rossby waves, as well as documenting the variances (both in space and time) involved with the total Rossby wave field. We find that modes are well defined up to at least 100 mb, and that the vertical structure is (as expected) barotropic, at least in the sense that the wave phases slope very little with altitude. The amplitudes generally increase strongly with altitude, but in a manner somewhat more complex than suggested by the simple (no mean wind) theory. The variances of the Rossby wave field tend to be a much more significant fraction of the observed variances in the Southern Hemisphere than they are in the Northern Hemisphere during the December 1978-February 1979 season. The geographical pattern of time variance of the Rossby wave field shows very little longitudinal structure, indicating essentially no geographical preference for the growth of these waves.

FUTURE PLANS:

In the future, we plan to examine the role of global scale Rossby waves in the problem of numerical weather prediction. Are the Rossby waves which occur

in nature properly maintained by the numerical model? Do models tend to generate their own, spurious waves due to imbalances between the naturally occurring and modeled stationary wave distribution? Finally, how much of the root mean-squared forecast error can be explained by failure to accurately predict the Rossby wave field? These questions will be studied by analyzing a number of forecasts carried out with the GLAS 4th order GCM, forecasts whose initial conditions will be chosen to sample the range of Rossby wave amplitudes present in nature.

JOURNAL PUBLICATION:

Lindzen, R. S., D. M. Straus and B. Katz, 1984: An observational study of large-scale atmospheric Rossby waves during FGGE. J. Atmos. Sci., 41, to be published.

TECHNICAL PUBLICATION:

Lindzen, R. S., D. M. Straus and B. Katz, 1984: The growth, propagation and decay of global scale Rossby waves during FGGE. NASA Tech. Memo. 86053, 175-179.

REFERENCES

Ahlquist, J. E., 1982: Normal-mode global Rossby waves: Theory and observations. J. Atmos. Sci., 39, 193-202.

Baker, W., D. Edelmann, M. Iredell, D. Han, and S. Jakkempudi, 1981: Objective analysis of observational data from the FGGE Observing Systems. NASA Tech. Memo. 82062.

Dole, R. M., and N. D. Gordon, 1983: Persistent anomalies of the extratropical Northern Hemisphere wintertime circulation: Geographical distribution and regional persistence characteristics. Mon. Wea. Rev., 111, 1567-1586.

Kasahara, A., 1980: Effect of zonal flows on the free oscillations of a barotropic atmosphere. J. Atmos. Sci., 37, 917-929.

Madden, R. A., 1978: Further evidence of traveling planetary waves. J. Atmos. Sci., 35, 1605-1618.

Rossby, C.-G. et al., 1939: Relations between variations in the intensity of the zonal circulation of the atmosphere and the displacements of the semi-permanent centers of actions. J. Mar. Res., 2, 38-55.

Salby, M. L., 1981a: Rossby normal modes in nonuniform background configurations. Part I: Simple fields. J. Atmos. Sci., 38, 1803-1826.

Salby, M. L., 1981b: Rossby normal modes in nonuniform background configurations. Part II: Equinox and solstice conditions. J. Atmos. Sci., 38, 1827-1840.

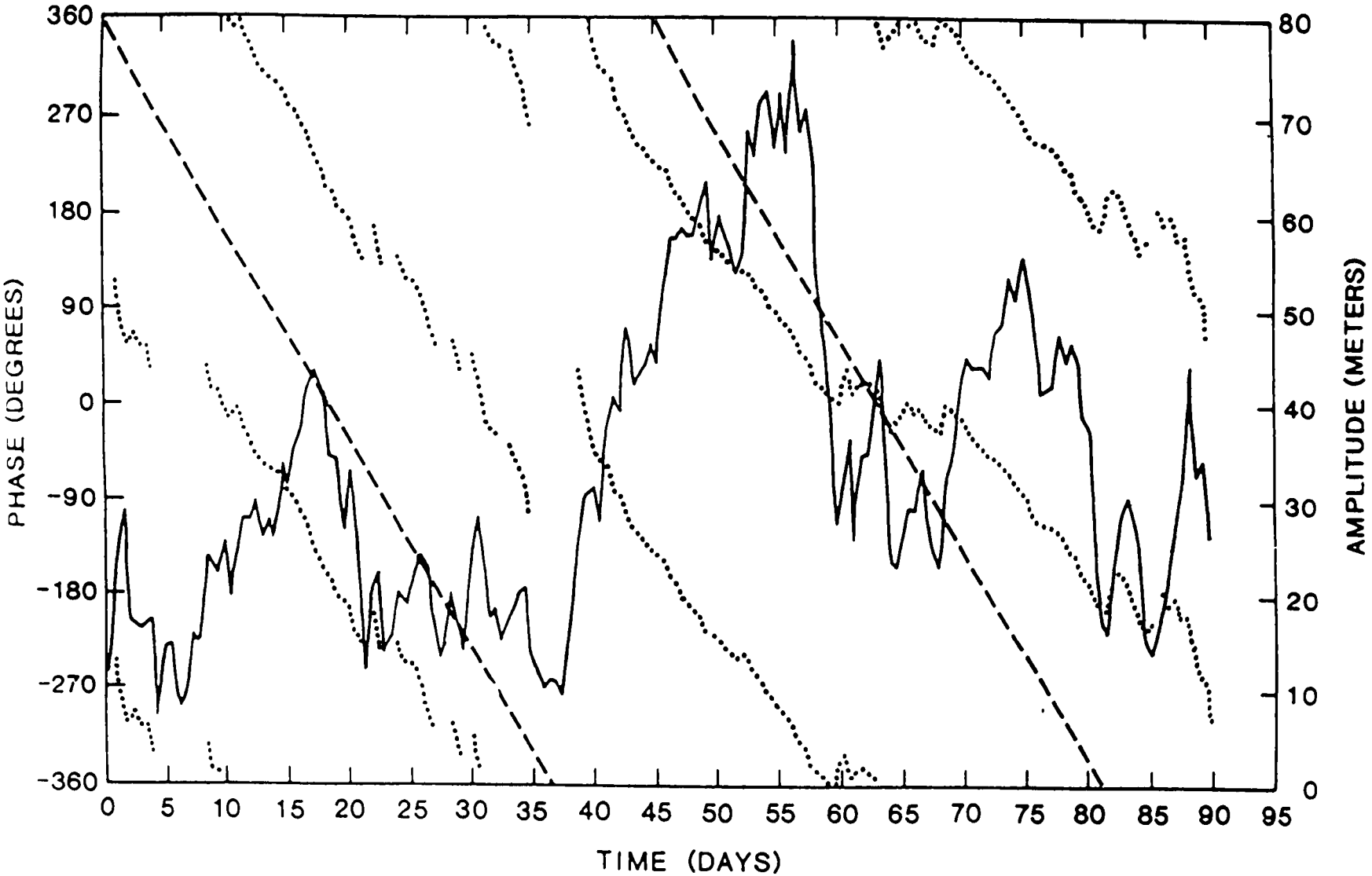

Figure 1. Amplitude and phase of (1,4) Hough mode during winter. The amplitude is given by the solid line, with the corresponding scale on the right, while the phase is given by the dotted line, with the corresponding scale on the left. Two cycles of the phase are plotted. The dashed line corresponds to the phase evolution that would occur were the Hough function to propagate uniformly westward with the period given by Kasahara (1980). The phase is omitted whenever the amplitude falls below 20% of its maximum value.

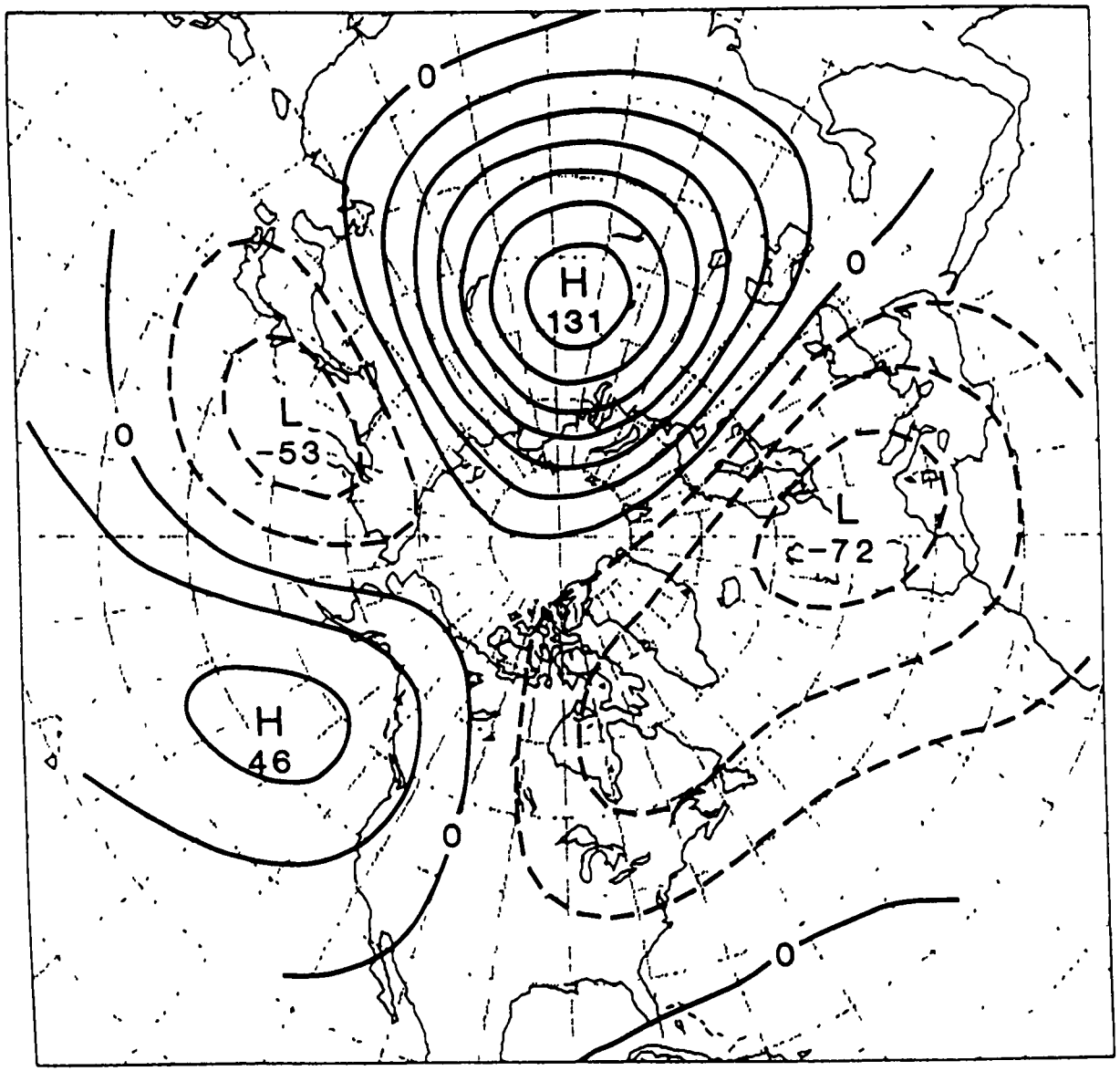

Figure 2. Geopotential height field consisting of the sum of all nine westward propagating Hough modes at 500 mb for 12Z of 12 January, 1979. Contour interval of 20 m.

PLANETARY SCALE INTERACTIONS
(W. K.-M. Lau-GSFC)

RESEARCH OBJECTIVE:

To study atmospheric teleconnections in the medium to long (10-90 days) time scales focusing on the interactions between extratropical circulation and tropical convection.

SIGNIFICANT ACCOMPLISHMENTS:

In a continuing effort to study short-term climate variability and atmospheric teleconnection as inferred from satellite observed outgoing longwave radiation, we have examined the low frequency variability (LFV) of tropical and extratropical cloud fluctuation over the Pacific. We found that during the Northern winter, the LFV of tropical cloud fluctuation is dominated by a 40-50 day dipole-like oscillation linking convection over Indonesia and the equatorial central Pacific. Eastward propagating signals appearing as outbursts of convective cloud clusters originating from the Indian Ocean appear to periodically feed energy into this dipole oscillation.

Also found are cloud features appearing over East Asia and subsequently over the eastern North Pacific which vary coherently with the tropical dipole anomaly. Based on our analysis and an a priori phenomenological model (Lau et al., 1983), we believe that the cloud fluctuations are associated with two space/time extended normal modes of tropical-extratropical interactions over the Pacific involving a coupling between the tropical dipole convective heating anomaly with cold surges over East Asia, and blocking over the eastern North Pacific respectively. A typical sequence of tropical-extratropical interaction can be described by a combination of the spatial and temporal variation associated with these two normal modes. We tentatively hypothesize that the tropics and extratropics may both play an important role in the make-up of the 40-50 day oscillation over the Pacific. In the tropics, this oscillation is manifested as fluctuations in convective heating, and in the midlatitudes, most likely in the form of two-dimensional dispersive Rossby waves.

In conjunction with the above satellite data analysis, we found further supporting evidences of the above hypothesis using conventional data. Specifically, we have established a connection between extratropical 500 and 200 mb geopotential height field and the Pacific dipole-like convective heating anomaly studies. Two specific observations should be highlighted. First, an upstream wavetrain over Eurasia is found to precede convection over Indonesia. The orientation and evolution of this wavetrain indicated a predominantly midlatitude-to-tropics energy propagation. Subsequently, wavetrain signals indicating both poleward and equatorward energy propagation are found downstream over the Pacific-North America region. Second, convection over the equatorial central Pacific is preceded by a blocking-like, large geopotential height anomaly over the eastern North Pacific and is simultaneously correlated with a downstream wavetrain over the Pacific-North America sector where a poleward energy propagation is indicated. Hence, an extratropical anomaly appears to be precursor to convection at both poles of the dipole heating pattern, suggesting that in the medium range time scale, these convections

are at least partially forced by midlatitude systems. Yet, the tropics is by no means a passive partner in the above process. The poleward energy flux from the tropical central Pacific is an indication of a feedback from the tropics. The morphology of the interaction over a complete oscillation cycle reveals a coupling between tropical convection over the Pacific and a possibly global circulation mode covering the entire northern Midlatitudes. These results are also consistent with recent theories of atmospheric teleconnections.

FUTURE PLANS:

We plan to extend the studies described above to cover a longer (> 7 years) data period and to study possible midlatitude-tropical interactions in general as a coupling between global normal modes and tropical convection.

JOURNAL PUBLICATIONS:

Lau, K. M., C. P. Chang and P. H Chan, 1983: Short-term planetary scale interaction over the tropics and midlatitudes. Part II: Winter-MONEX period. Mon. Wea. Rev., 111, 1372-1388.

Lau, K. M., and P. H. Chan, 1983: Climate variability and atmospheric teleconnections from satellite-observed outgoing longwave radiation. Part I: Simultaneous relationships. J. Atmos. Sci., 40, 2735-2750.

Lau, K. M., and P. H. Chan, 1983: Climate variability and atmospheric teleconnections from satellite-observed outgoing longwave radiation. Part II: Lagged correlations. J. Atmos. Sci., 40, 2751-2767.

Lau, K. M. and P. H. Chan, 1984: Climate variability and atmospheric teleconnections from satellite-observed outgoing longwave radiation. Part III: Association with the 40-50 Day Oscillations. J. Atmos. Sci., 41, (submitted).

Lau, K. M. and H. Lim, 1984: On the dynamics of equatorial forcing of climate teleconnections. J. Atmos. Sci., 41, 161-176.

Lau, K. M. and M. T. Li, 1984: The monsoon of East Asia and its global associations - A Survey. Bull. Amer. Meteor. Soc., 65, 114-125.

Lau, K. M. and T. J. Phillips, 1984: Extratropical geopotential height fluctuation associated with tropical convection. J. Atmos. Sci., (submitted).

Lau, N. C. and K. M. Lau, 1984: The structure and energetics of midlatitude disturbances accompanying cold-air outbreak over East Asia. Mon. Wea. Rev., 112, (in press).

TECHNICAL AND CONFERENCE PUBLICATIONS:

A diagnostic study of the large scale aspects of northeasterly cold surges over East Asia. Proceedings of the 14th Conference on Hurricane and Tropical Meteorology, 1982.

Low-frequency variability of the large-scale tropical circulation as inferred from satellite outgoing longwave radiation. Proceedings of the NMD Regional Conference on Tropical Meteorology, Tsukuba, Japan, 1983.

Climate variability and atmospheric teleconnection from satellite-observed cloud fluctuations. Proceedings of the 5th Conference on Atmospheric Radiation, Baltimore, Maryland, 1983.

Diabatic heating and large scale circulation during the 1976-77 and the 1982-83 ENSO's. Tropical Ocean Atmosphere Newsletter, March 1983.

Tropical anomalies asociated with ENSO: A comparison between the 1976-77 and the 1982-83 events. Proceedings of the Eighth Annual Climate Diagnostic Workshop, Downsville, Ontario, Canada, 1983.

Bimodal Climate State, Atmospheric Teleconnection and the ENSO. Proceedings of the Fifth Conference on Ocean-Atmosphere Interaction, Miami, Florida, 1984.

Cloudiness fluctuation associated with midlatitude-tropical interactions. Proceedings of the 15th Conference on Tropical Meteorology and Hurricanes, Miami, Florida, 1984.

Extratropical geopotential height fluctuation associated with tropical convection. Proceedings of the 15th Conference on Tropical Meteorology and Hurricanes, Miami, Florida, 1984.

A STUDY OF THE ADEQUACY OF QUASI-GEOSTROPHIC DYNAMICS FOR MODELING THE EFFECT OF FRONTAL CYCLONES ON THE LARGER SCALE FLOW

(S. Mudrick-Dept. of Atmospheric Science, University of Missouri-Columbia)

RESEARCH OBJECTIVES:

The major objectives of this study are summarized as follows: 1) To test the validity of quasi-geostrophic (QG) dynamics, compared to primitive equation (PE) dynamics, for modeling the effect of cyclone waves on the larger scale flow, and 2) To study the formation of frontal cyclones and the dynamics of occluded frontogenesis.

SIGNIFICANT ACCOMPLISHMENTS:

In order to extend the realism of the initial conditions over those used in earlier work of this nature (see Mudrick, 1982, hereafter called M), in particular, in order to include strong surface frontal zones in the initial conditions, a horizontal resolution on the order of 100 km between gridpoints is needed. (A discussion of the finite-difference, dry, mid-latitude beta plane models used appears in M). In order to allow for integrations of up to two weeks simulated time and to keep the logistics and cost of the runs feasible, the horizontal domain of the models must be reduced compared to those used in M.

Based on work concerning "polar lows" (see Mullen, 1982), the tropospheric static stability was reduced and was also allowed to vary in different tropospheric layers. The previous work, described in M, has used a "standard atmosphere" temperature lapse rate. Stratospheric stability remains unchanged.

The use of one of these "reduced stability" cases, with no surface frontal zone present and with a similar zonal flow to those described in M, resulted in the discovery of "normal mode" perturbations that possess the following characteristics:

1) Their horizontal wavelength is smaller than those previously used, one being 1800 km compared with the 3600 and 4800 km wavelength perturbations used in M. (The smaller horizontal scale seems more realistic, compared to typical atmospheric cyclones, as well as allowing for the reduced horizontal domain mentioned above).

2) The maximum disturbance amplitude for the reduced stability perturbations is in the upper troposphere whereas short wavelength perturbations possessing standard atmospheric stability are quite shallow. Thus the reduced stability perturbations may produce deeper, stronger frontal evolution than in M.

3) They possess growth rates several times greater than those perturbations used in M, hence they evolve and mature more quickly, also increasing realism as well as saving computational time.

Using an 1800 km wavelength perturbation combined with a basic state possessing reduced tropospheric stability, model integrations were made using the PE model, with and without surface friction, and the QG model, without friction. The channel width was taken as 2100 km, allowing a spacing of 75 km

between gridpoints to be used. There were 10 vertical levels, as in M.

With respect to the research objectives, the "reduced stability" integrations have been partially successful. The QG run appears to evolve more differently, compared to the PE run, than for any of the situations described in M. This is true with respect to the horizontal eddy heat fluxes. Unfortunately the 1200 km channel width was too narrow; after three days the QG run becomes seriously affected by the lateral walls, the QG potential vorticity no longer being conserved. The runs therefore need to be repeated with a wider channel, as discussed below.

While this was not a "frontal cyclone" since no surface frontal zone was present initially, the 75 km resolution allowed strong surface frontal zones "occluded front." Since the second research objective concerns the dynamics of occluded frontogenesis, the PE runs provided an opportunity to study the effect of surface friction upon the process. In addition, it appears that upper tropospheric frontogenesis may also be present in these runs. More about these integrations appears below.

During the period of this grant I have acquired a "Visual 50" terminal and a 1200 BAUD modem, through which I can communicate with the University of Missouri mainframe computers via a telephone line. My entire computer operation is now being converted to "no cards," running from magnetic tape and data sets stored on disk devices. None of this conversion to exclude cards nor the purchase of the terminal has included NASA grant monies but much time has been required to reprogram myself to the new mode (for me) of operation.

CURRENT RESEARCH:

Work continues on the conversion of all the programs to the "no card" mode. Plans are being made to rerun the reduced stability PE versus QG integrations using a wide channel and thus a more coarse resolution (perhaps 100 km instead of 75 km). The QG integration must complete a full "life cycle" without being affected appreciably by the channel walls.

Results from the 75 km PE runs are being analyzed with respect to the evolution of the occluded frontal regions. Programs remain to be written for this purpose. In addition, the upper tropospheric frontal development will be examined.

FUTURE PLANS:

In some ways the reduced stability integrations described above resemble the no moisture polar low development discussed by Mullen (1982). It is planned to modify the basic state so as to more resemble his case, ultimately with the presence of a surface frontal zone in the initial conditions. Strong surface fronts will be included in other initial conditions, also. Surface friction may be included in the QG model formulation.

I will spend a sabbatical year at the State University of New York at Albany from approximately September 1984 to June 1985. During this time I plan to pursue this work using the facilities there, under this grant.

There have been no journal, technical nor conference publications resulting from this grant so far.

REFERENCES:

Mullen, S. L., 1982: Cyclone development in polar air streams over the wintertime continent. Mon. Wea. Rev., 110, 1664-1676.

Mudrick, S. E., 1982: A study of the adequacy of quasi-geostrophic dynamics for modeling the effect of cyclone waves on the larger scale flow. J. Atmos. Sci., 39, 2414-2430.

VII. FGGE DIAGNOSTIC STUDIES

Page intentionally left blank

NUMERICAL PREDICTION OF THE PRESIDENT'S DAY CYCLONE
(R. Atlas-GSFC)

RESEARCH OBJECTIVE:

Numerical-diagnostic studies of major anomalous weather events are being conducted in order to investigate the relevant physical processes associated with the events and the role of satellite observing systems in the analysis and prediction of these phenomena. One component of this study has been concerned with the numerical prediction of intense coastal and oceanic cyclogenesis. The specific objectives of this research are: (1) to assess the accuracy of GLAS model predictions of cyclogenesis, (2) to determine the importance of large scale dynamical processes and diabatic heating to the prediction, and (3) to evaluate the sensitivity of the model predictions to the initial conditions.

SIGNIFICANT ACCOMPLISHMENTS:

A series of experiments related to the President's Day Cyclone of 18-19 February 1979 has been performed. This storm was significant because of the severity of the weather it produced and the failure of the operational models in use at the National Meteorological Center (NMC) to adequately predict the intensity of cyclogenesis. For example, the Limited-Area Fine Mesh (LFM-II) model's 12, 24, 35 and 48 h forecasts which verified at 1200 GMT 19 February 1979 all displayed serious errors in the prediction of this cyclone and associated heavy precipitation. The 12 h forecast predicted the low to be too weak and south of its observed position; the 24 h forecast predicted a much weaker low; and the 36 h forecast indicated only a trough with no closed cyclone center.

The GLAS model 36 h forecast from the GLAS analysis at 0000 GMT 18 February correctly predicted intense coastal cyclogenesis and heavy precipitation (Fig. 1a). When this forecast was repeated without surface heat and moisture fluxes, only an inverted trough developed along the east coast (Fig. 1b), while an experiment without surface heat and moisture fluxes failed to predict any cyclonic development (Fig. 1c). An extended-range forecast from 0000 GMT 16 February as well as forecasts from the GLAS FGGE data analysis or the NMC analysis at 0000 GMT 18 February interpolated to the GLAS grid (not shown) predicted weaker coastal low development.

Detailed examination of these forecasts showed that diabatic heating resulting from oceanic fluxes significantly contributed to the generation of low level cyclonic vorticity and the intensification and slow rate movement of an upper level ridge over the western Atlantic. As an upper level short-wave trough approached this ridge, diabatic heating associated with the release of latent heat intensified, and the gradient of vorticity, vorticity advection, upper level divergence, and upward vertical motion (Fig. 2) in advance of the trough were greatly increased, providing strong large-scale forcing for the surface cyclogenesis.

CURRENT RESEARCH:

Current research on this case is aimed at assessing the detailed effects of FGGE satellite sounding and cloud track wind data to the model predictions.

Differences between analyses with and without FGGE data as well as the prognostic evaluation of these differences are being evaluated.

JOURNAL PUBLICATIONS:

Atlas, R., 1982: The growth of prognostic differences between GLAS model forecasts from SAT and NOSAT initial conditions. Mon. Wea. Rev., 110, 887-882.

Vergin, J., D. Johnson, and R. Atlas, 1984: A quasi-lagrangian diagnostic study of the effect of satellite sounding data assimilation on model cyclone prediction. Mon. Wea. Rev.

TECHNICAL PUBLICATIONS:

Atlas, R. and R. Rosenberg, 1982: Numerical prediction of the Mid-Atlantic states cyclone of 18-19 February 1979. NASA Tech. Memo. 83992, 53 pp.

Atlas, R. 1982: A numerical investigation of intense coastal cyclogenesis. Research Activities in Atmospheric and Oceanic Modelling. 3, p. 5.44.

Atlas, R. and R. Rosenberg, 1983: Case studies of coastal cyclogenesis. NASA Tech. Memo. 84983, 13-17.

CONFERENCE PUBLICATION:

Atlas, R., 1984: The effect of physical parameterizations and initial data on the numerical prediction of the President's Day Cyclone. Proceedings of Tenth Conference on Weather Forecasting and Analysis. June 25-29, Clearwater Beach, Fla.

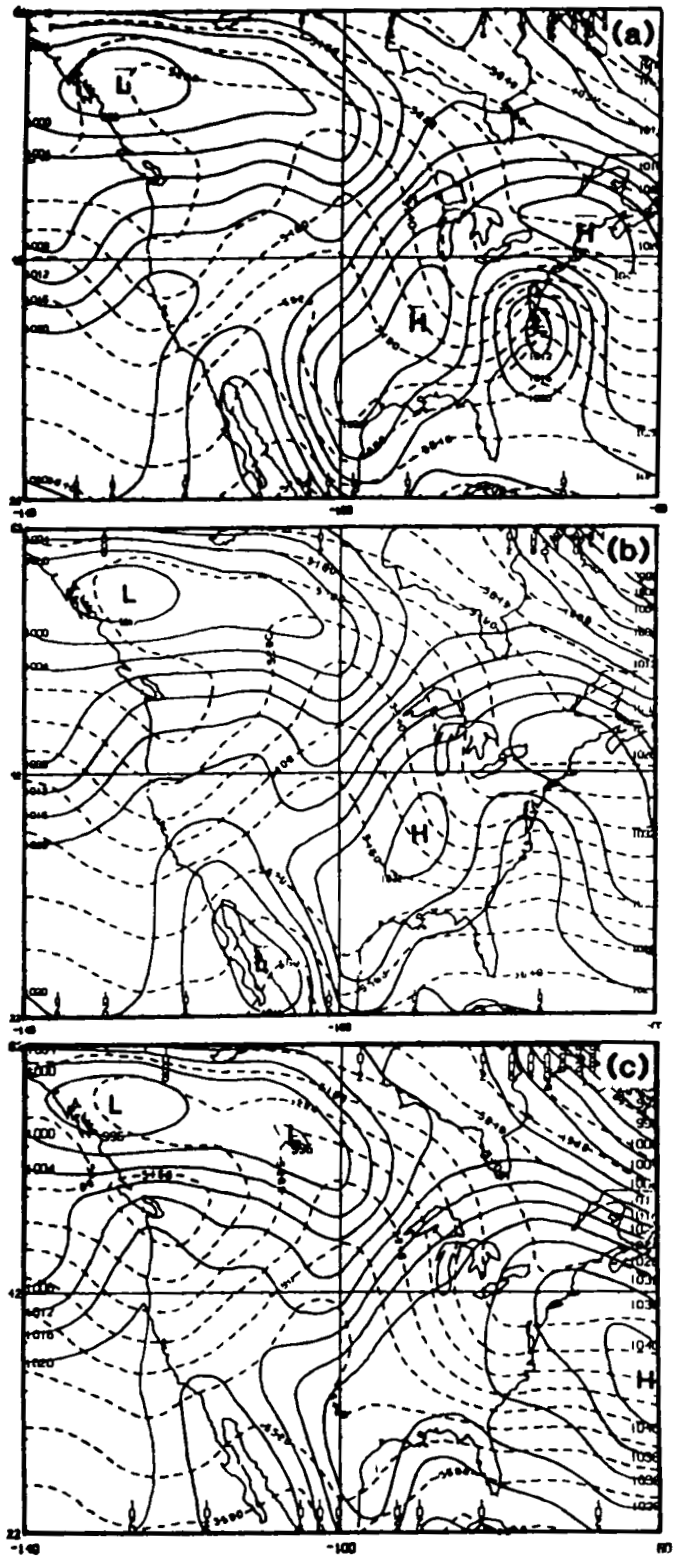

Fig. 1. GLAS model 36h sea level pressure (solid lines) and 1000-500 mb thickness (dashed lines) forecasts valid 1200 GMT 19 February 1979 with full physics (a), no surface moisture flux (b), and no surface heat or moisture fluxes (c).

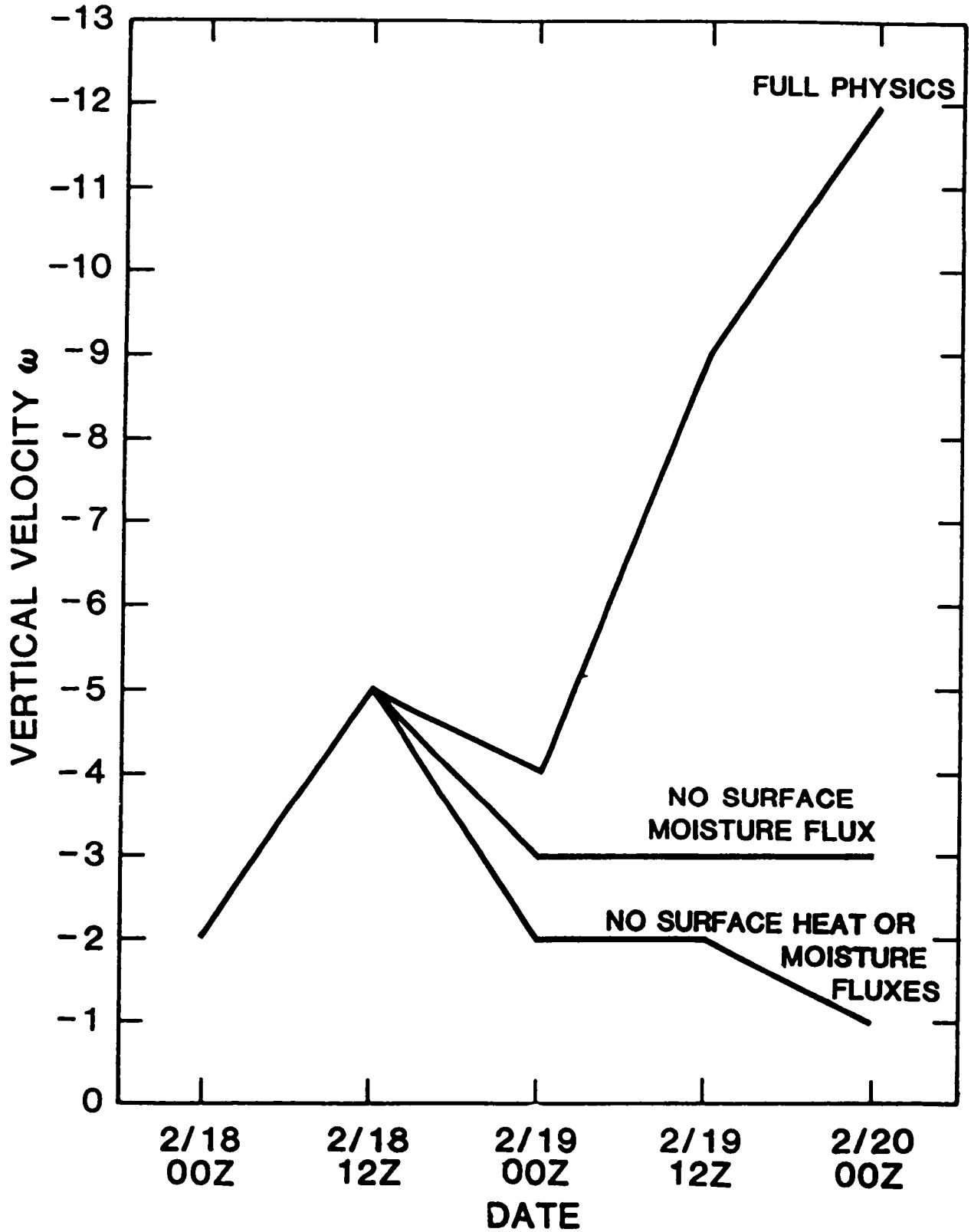

Fig. 2. Change in 500 mb vertical velocity in advance of the upper level trough.

OBSERVATIONAL-NUMERICAL STUDY OF MARITIME EXTRATROPICAL CYCLONES USING FGGE DATA

(C. H. Wash and R. L. Elsberry-Naval Postgraduate School)

RESEARCH OBJECTIVE:

The objective of this research is to better understand the development, maturation and decay of maritime extratropical cyclones using a combined observational and numerical modeling approach. The research will use FGGE Level III-b analysis for diagnostic studies and for predictions. A better understanding of maritime cyclogenesis via diagnostic studies of observed and numerical data will contribute to the GARP objectives of improving models for weather prediction and increasing predictability over oceanic regions.

SIGNIFICANT ACCOMPLISHMENTS:

Three cases of explosive cyclogenesis during the FGGE SOP-1 have been studied diagnostically using storm-following budgets derived from the ECMWF and GLAS level III-b analyses. The first case is the Presidents' Day storm of 18-20 February 1979, which was an intense subsynoptic coastal development. The second is a larger-scale system which develops over the northwestern Pacific during 12-16 January 1979. The final case is a polar-type cyclogenesis that formed south of Iceland during 25-27 January 1979. The latter two cases were selected because:

1) relatively good surface (ship) and upper level (satellite and aircraft) data coverage,

2) explosive development; and

3) straight flow aloft (500 mb), which suggests minimal upper level support for cyclogenesis as in type A category of Petterssen and Smebye (1971).

Mass, vorticity and angular momentum budgets for the moving storm environment were computed for each case. Results are contained in Naval Postgraduate School theses by Conant, Calland and Cook and in papers by Wash and Calland (1984) and Wash and Cook (1984) submitted to Monthly Weather Review. Key results from these studies include: 1) demonstration that the FGGE analyses can be used to explore oceanic circulations; 2) isolation of the role of upper level jet streaks in the initiation of the explosive period in all three cases, and 3) illustration of the lower tropospheric destabilization during each rapid deepening period, which is primarily due to sensible heating of the cold air by the warmer ocean surface.

While the budget calculations were successful with the FGGE analyses at the normal synoptic times (00 and 12 GMT) the budgets with 06 and 18 GME analysis did not succeed. The problem appears to be related to a spurious warming near the storm center in both ECMWF and GLAS analyses, and is especially pronounced in the ECMWF analyses. The GLAS analyses satisfactorily resolve the important synoptic characteristics of these cyclones even though the resolution (4° x 5°) is inferior to that of ECMWF.

The physics package of the Navy global forecast model (adopted from the UCLA GCM) was successfully utilized in a semi-prognostic mode to estimate diabatic

components of oceanic cyclone systems. Fields of sensible and latent heat fluxes, radiational heating and inferred cloud structures were computed from the ECMWF analyses and Navy operational sea surface temperatures. The west Pacific cyclone case and five cases of post-frontal convective clusters in the northeast Pacific during December 1978 and January 1979 have been studied thus far.

The diabatic estimates for the west Pacific case were included in a thermodynamic (dry static energy) budget by Bosse (1984), who computed storm-environment estimates of sensible and latent heating during the explosive deepening period. A similar budget study for one of the post-frontal convective cluster cases is nearing completion.

CURRENT RESEARCH:

Thermodynamic budgets and fields of diabatic terms are being computed for the polar low and Presidents' Day case. Results from all three cyclone cases should validate the semi-prognostic method and provide a survey of diabatic heating in polar, open-ocean and east coast situations.

Diagnostic research has moved from the ECMWF analyses to the study of GLAS model forecasts for the northwest Pacific and Atlantic polar cyclone cases. Both synoptic and diagnostic studies of the GLAS forecasts from satellite (SAT) and no satellite (NOSAT) analyses on the Pacific case are underway. Preliminary results show the NOSAT forecast is superior to that from the SAT analysis in predicting the storm positions. We are particularly interested in understanding the differences in forecast from SAT and NOSAT analyses in individual storm cases as a guide in interpreting forecast impact experiments such as Halem et al. (1982) and others.

Diagnostic studies are also being made on secondary low developments observed in numerical simulations that appear to be similar to the FGGE cases. The numerically simulated storm data provide an opportunity to close the budgets to high accuracy. The relative sizes of the various budget terms may then provide guidance for interpreting less complete budgets based on observations over relatively data-sparse oceanic regions. Where budgets based on both kinds of data agree, we have additional confidence in the physical interpretations.

FUTURE PLANS:

We are submitting a new proposal for additional oceanic cyclogenesis studies using FGGE data. Our previous work indicates the strength of the upper level forcing (from mobile short-wave troughs and jet streams) and the degree of stability in the low troposphere are critical factors in explosive cyclogenesis. We wish to generalize upon our case study results and focus specifically on these factors for a number of explosive cyclogenesis cases during SOP-1 period. Storm-environment upper level vorticity advection, or other measures of upper level forcing and stability criteria for the low troposphere will be studied for the new cases to determine indices and thresholds that suggest explosive oceanic cyclogenesis potential. FGGE forecasts of these systems will be explored to the maximum extent possible to discover the role the special observation systems play in improving forecasts of these systems. In addition, new optimal interpolation (OI) analyses

from GLAS and higher resolution model forecasts (2° x 2.5° mesh) will be compared to previous work to isolate the improvements of the new approaches.

The proposed research is directed toward the goal of achieving a better understanding of rapid oceanic cyclogenesis. We wish to produce research results which will help guide the planning and executing of future cyclone field programs such as GALE (winter, 1986) and STORM East and West (1990's).

JOURNAL PUBLICATIONS:

Uccellini, L., P. Kocin, R. Petersen, C. Wash and K. Brill, 1984: The Presidents' Day Cyclone of 18-19 February 1979: Synoptic overview and analysis of the subtropical jet streak influencing the pre-cyclogenetic period. Mon. Wea. Rev., 112, 31-55.

Uccellini, L., D. Keyser, C. Wash and K. Brill, 1984: The Presidents' Day Cyclone of 18-19 February 1979: Influence of a tropopause fold on rapid cyclogenesis. Submitted to Mon. Wea. Rev.

Wash, C. and W. Calland, 1984: Diagnostics of explosive cyclogenesis during FGGE, Part I: West Pacific cyclone of 12-16 January 1979. Submitted to Mon. Wea. Rev.

Wash, C. and W. Cook, 1984: Diagnostics of explosive cyclogenesis during FGGE, Part II: North Atlantic Case of 26-27 January 1979. Submitted to Mon. Wea. Rev.

TECHNICAL PUBLICATIONS:

Winninghoff, F. and R. Elsberry, 1983: Some Aspects of Post-Frontal Convective Areas Along the West Coast of the United States. Naval Postgraduate School Technical Report NPS63-84-005.

Conant, P., CAPT, USAF, 1982: A Study of East-Coast Cyclogenesis using Quasi-Lagrangian Diagnostics. NPS M.S. Thesis, June 1982.

Calland, W., LCDR, USN, 1983: Quasi-Lagrangian Diagnostics Applied to North Pacific Extratropical Explosive Cyclogenesis. NPS M. S. Thesis, June 1983.

Cook, W., LT, USN, 1983: A Quasi-Lagrangian Diagnostic Investigation of Rapid Cyclogenesis in Polar Air Stream. NPS M. S. Thesis, September 1983.

Bosse, T., LT, USN, 1984: Estimations of Diabatic Heating for an Explosive-Developing Maritime Cyclone. M. S. Thesis, March 1984.

Ebersole, K., LT, USN, 1984: Diagnostic Study of NASA Model Forecasts of Explosive Cyclogenesis. NPS M. S. Thesis, scheduled completion September 1984.

CONFERENCE PAPERS:

Wash, C. and W. Calland, 1984: Diagnostics of Explosive Cyclogenesis during FGGE, West Pacific Cyclone of 12-16 January 1979. Preprints for the 10th Conference on Weather Forecasting and Analysis, Clearwater Beach, Fla., pp 608-613.

Uccellini, L., D. Keyser, C. Wash and K. Brill, 1984: The Presidents' Day Cyclone of 18-19 February 1979: Influence of a Tropopause Fold on Rapid Cyclogenesis. Preprints for the 10th Conference on Weather Forecasting and Analysis, Clearwater Beach, Fla., p 614-622.

AIR-SEA INTERACTION DURING COLD AIR OUTBREAKS

(S. Chou-GSFC, Y. Yeh-GSFC/USRA, and J. Firestone-GSC)

RESEARCH OBJECTIVES:

1) To analyze the NOAA P-3 aircraft data set measured during the MASEX experiment to study the dynamics and the evolution of the Marine Atmospheric Boundary layer (MABL) during cold air outbreaks.

2) To further develop and validate Chou-Atlas (1982) remote sensing technique for ocean-air heat and moisture fluxes from the results of (1).

3) To study the climatology of cold air outbreaks along the east coast of the United States.

SIGNIFICANT ACCOMPLISHMENTS:

1) The MASEX experiment was conducted over the western Atlantic Ocean during the period 16-20 January 1983 (four flight days). The experiment was based at the Wallops Flight Facility and involved three aircraft (NOAA P-3, NASA P-3, and NASA Electra) to carry various instruments. Several computer programs for analyzing the three types of the NOAA P-3 data (1-sec, gust probe, and dropsonde data) have been developed.

2) The NOAA-7 AVHRR satellite cloud pictures including the NOAA P-3 measurement locations have been produced for the four MASEX flight days (16, 18, 19, and 20 January 1983). These pictures are to be combined with the NOAA P-3 data set to study the MABL processes.

3) The NOAA P-3 1-sec and 20 Hz gust probe data, dropsonde measurements, and lidar data (on the NASA Electra aircraft) on 20 January 1983 (Fig. 1) have been combined to study the organized convection and the effects of the coastal shape and the SST pattern on the development of the MABL during cold air outbreaks. The preliminary analysis indicated that the SST pattern and the coastal shape caused the MABL to deepen eastward and southward, which is in good agreement with the suggestion of Atlas et al. (1983). Also, good agreements were found between the lidar data and the NOAA P-3 and dropsonde date, e.g., the boundary heights, the dominant scales of motion, and the heat flux ratio between the top of MABL and the sea surface.

4) The PBL height measured by lidar was found to be in good agreement with that measured by the dropsonde temperature profile. Assuming a linear heat flux profile in the clear PBL, the heat flux ratio between the PBL top and the surface may be estimated from the ratio of the entrainment zone to the completely mixed boundary layer height. The heat flux ratio estimated by lidar measurements was found to be in good agreement with that derived from the gust probe data.

Sensible heat flux profile determined from the gust probe data appeared to be linear in the subcloud layer. The linear extrapolated heat flux at the inversion base was about 10% of that at the surface. The zero heat flux was found to be at 0.9 Z_1 (inversion base). This is in good agreement with Lenchow (1974).

CURRENT RESEARCH:

1) Currently, the work is focused on the analysis of the turbulent structure, the budgets of the turbulent kinetic energy, and the sensible and latent heat fluxes within the MABL for 20 January 1983. A power spectrum program using the correlation function and the Turkey spectral windows has been developed to analyze the gust probe data. The spectra and cospectra of wind, temperature, and water vapor density are used to study the dominant scale of motion responsible for heat and moisture transports. The physical processes in the MABL capping inversion layer, including the effects of the wind shear and the temperature lapse rate on the mixing processes are also under investigation. The results will be used to develop a new remote sensing technique for ocean-air heat and moisture fluxes.

2) Turbulent structures and budgets for 20 January 1983 are being compared with other observational studies (e.g., Willis and Deardorff 1974; Lenschow et al., 1980; Caughey and Wyngaard, 1979; Kaimal et al., 1976).

FUTURE PLANS:

1) Analysis similar to that of 20 January 1983 will be extended to the other three MASEX flight days (16, 18, and 19 January 1983). On 18 January 1983, the measurements were made across the Gulf stream. It was found that the boundary layer deepened sharply after crossing the Gulf stream. The effect of the Gulf stream on the MABL development will be studied. On 19 January 1983, the mechanism for the open cell will be studied and the results will be compared with those of AMTEX (Air Mass Transform Experiment).

2) The effect of the ocean wave on the MABL evolution will be studied from the relationship between the offshore variation in the surface heat flux and that in the ocean waves.

3) The results will be used to verify and further develop the Chou-Atlas (1982) remote sensing technique for the ocean-air heat and moisture fluxes.

4) Participation in GALE (Genesis of Atlantic Lows Experiment) to study the air-sea interaction and boundary layer processes in relation to the coastal frontogenesis and cyclogensis is planned.

CONFERENCE PRESENTATIONS:

Atlas, D., S. H. Chou, and B. Walters, 1984: Air-sea interaction during cold air outbreaks: New insights and remote sensing. 5th Conf. Ocean-Atmosphere Interaction, Amer. Meteor. Soc., Miami Beach, Fl.

Melfi, S. H., J. Spinhirne, S. H. Chou, and S. Palm, 1984: Lidar observations of organized convection over the ocean. 5th Conf. Ocean-Atmosphere Interaction, Amer. Meteor. Soc., Miami Beach, Fl.

PAPERS IN PROGRESS:

Melfi, S. H., J. Spinhirne, S. H. Chou, and S. Palm, 1984: Lidar observations of organized convection over the ocean.

Chou, S. H., D. Atlas, Y. N. Yeh, and J. Firestone, 1984: Marine atmospheric boundary layer during cold air outbreak on 20 January 1983. I: Mean Conditions.

_____, 1984: Marine atmospheric boundary layer during cold air outbreak on 20 January 1983. II: Turbulence budgets.

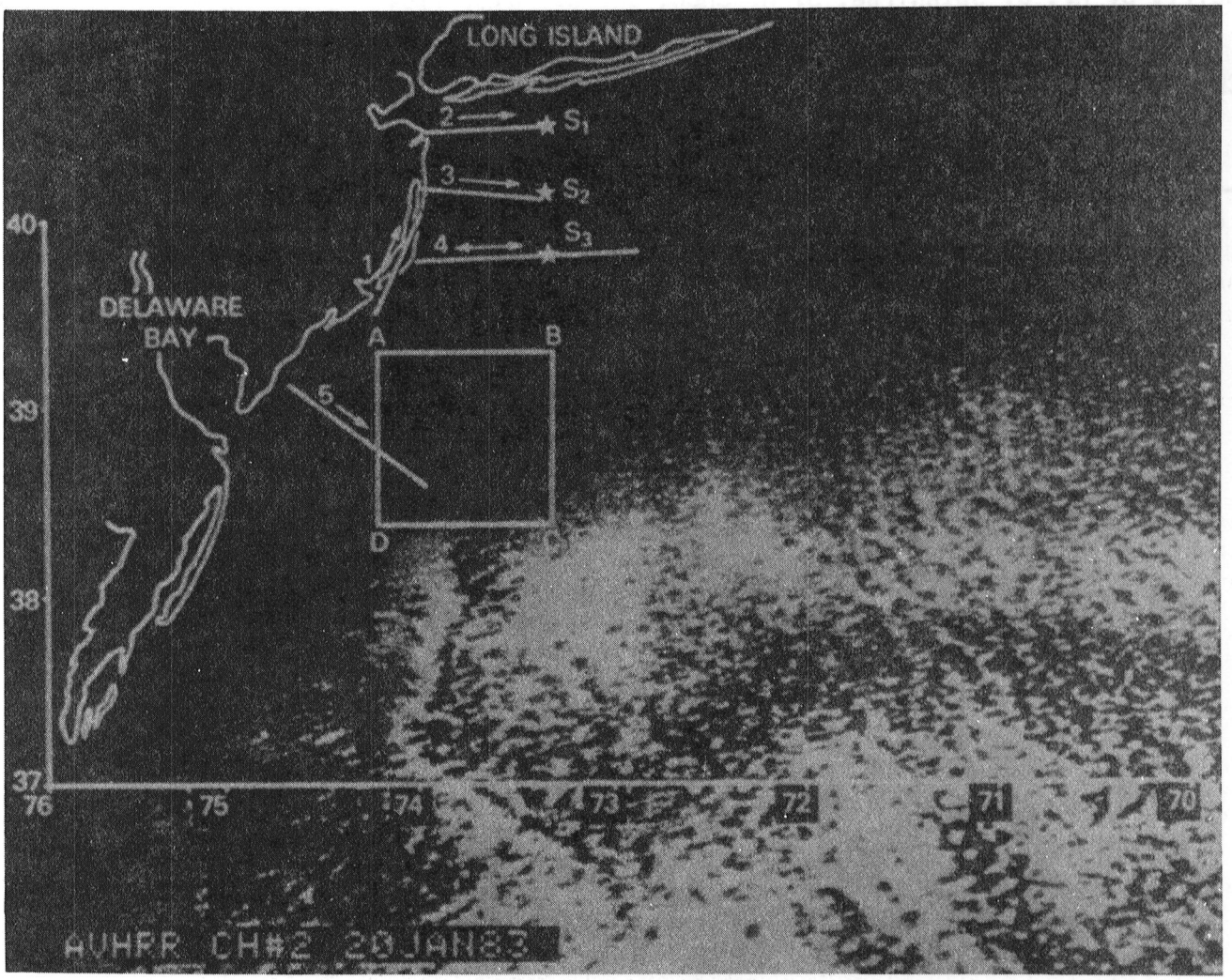

Fig. 1. The NOAA WP-3D and the NASA Electra measurement locations and the cloud picture of 20 January 1983 measured by the NOAA-7 AVHRR Ch. 2 (0.7 - 1.1 μ) at 1821 GMT. Dropsonde locations are marked by S_1, S_2, and S_3. Lidar flight tracks are marked by 1 to 5. Several flight level data are measured by the NOAA WP-3D at the box ABCD.

"CAGE" REGIONAL ENERGY BUDGETS FROM THE GLAS 4TH ORDER MODEL

(G. F. Herman, M. A. Alexander-Dept. of Meteorology, University of Wisconsin, S. D. Schubert-GSFC/RRA)

RESEARCH OBJECTIVES:

The amount of heat transferred poleward by the oceans, and the rate of energy exchange between the atmosphere and the ocean are two fundamental parameters that are required in order to understand the role of the oceans in climatic anomalies. Several methods have been employed in the past in an attempt to infer their values. These include: Direct measurements of ocean transports and surface fluxes, inferring the ocean transport by integrating observed or calculated surface fluxes; and residual methods employing the net radiation at the top of the atmosphere, and the divergence of the atmospheric energy fluxes (e.g., ICSU-WMO, 1982). This latter method was employed in the recent Northern Hemispheric heat balance of Oort and Vonder Haar (1976).

A significant limitation to the residual approach is that large gaps exist in the conventional observing system, particularly over the oceans and in high latitudes. The use of the GLAS analysis and forecast models in conjunction with satellite-derived temperature profiles provides the basis for obtaining potentially highly accurate determinations of the atmospheric divergence terms over the ocean.

This paper is a report of our preliminary attempt to use the 4th order model as a diagnostic tool for ocean energy balance studies. The work is part of a long term project to develop techniques for applying model-generated analyses, or observationally constrained diagnostics, in weather and climate studies. Our use of GLAS analyses in diagnostic studies dates to the Data Systems Test (DST) period, when the analyses were used in a study of the global heat balance (e.g., Schubert and Herman, 1981). They have also been employed to determine global cloud circulation statistics (e.g., LeMunyon, 1984), and are currently being used to drive agricultural production models.

The goal of this study is to assess the accuracy of regional energy balance calculations obtained from the 4th-order model, determine the impact of satellite data on the calculations, and determine their utility for ocean energy transport studies.

SIGNIFICANT ACCOMPLISHMENTS:

Summary of Calculations

The vertically-integrated, time and areally-averaged total energy content of a region of the atmosphere extending from the surface to the top of the atmosphere is written

$$\langle \overline{S_A} \rangle + \langle \overline{S_Q} \rangle = -\langle \overline{\mathrm{Div}\ (F_A + F_Q)} \rangle + \langle \overline{F_{LH}} \rangle + \langle \overline{F_{SH}} \rangle + \langle \overline{R_{NEA}} \rangle - \langle \overline{R_S} \rangle + \langle \overline{F} \rangle \qquad (1)$$

where the storage terms for total kinetic, potential, and internal energy (S_A) and latent energy (S_Q) are

$$\langle S_A + S_Q \rangle = \left\langle \int_{p_o}^{p^*} \frac{\partial}{\partial t} (\overline{K} + \overline{C_p T} + \overline{Lq}) \frac{dp}{g} \right\rangle \qquad (2)$$

where K is the horizontal kinetic energy, 1/2 $\underset{\sim}{v} \cdot \underset{\sim}{v}$; T, temperature, q specific humidity; C_p heat capacity at constant pressure; L, latent heat of vaporization; and $\underset{\sim}{v}$, horizontal velocity vector. The flux terms in (1) are given by

$$\langle F_A + F_Q \rangle = \int_{p_o}^{p^*} \left\langle \overline{\nabla \cdot (K + C_p T + \phi + Lq)\, \underset{\sim}{v}} \frac{dp}{g} \right\rangle \qquad (3)$$

where ϕ is the geopotential, gZ. A frictional term $F = \left\langle \int \underset{\sim}{v} \cdot \underset{\sim}{F} \frac{dp}{g} \right\rangle$, where $\underset{\sim}{F}$ is the frictional force, may also be appended to (1), but this is usually assumed to be of second order. The other terms are F_{LH} and F_{SH}, the evaporative and sensible heat fluxes at the surface; and R_{NEA} and R_S, the net radiation at the top of the atmosphere. The overbar refers to a time mean, $\frac{1}{\tau} \int (\ ) \, dt$, and the angular brackets to an areal average, $\frac{1}{A} \iint (\ ) \, a^2 \cos\phi \, d\lambda \, d\phi$, where a is the radius of the earth, ϕ latitude, and λ longitude.

In obtaining (1) the vertically-integrated condensational heating term was replaced with the water vapor equation, and the radiative flux divergence term was integrated to yield $R_{NEA} - R_S$ as the net radiative heating of the column.

Equation (1) can be used in several ways. First, if the storage term $\langle \overline{S_A} \rangle$ and $\langle \overline{S_Q} \rangle$ are known, the surface energy fluxes are obtained as residuals. Alternatively, if the model-generated values of $\langle F_{LH} \rangle$ and $\langle F_{SH} \rangle$ are provided, then comparing them with the residuals serves as a check on the validity of constructing budgets from model-generated data. Finally, we may consider the energy budget of the earth-atmosphere system,

$$\langle \overline{S_O} \rangle + \langle \overline{S_L} \rangle + \langle \overline{S_A} \rangle + \langle \overline{S_Q} \rangle = -\langle \overline{\mathrm{Div}\ (F_A + F_Q + F_O)} \rangle + \langle \overline{R_{NEA}} \rangle \qquad (4)$$

where $\langle \overline{S_O} \rangle$ and $\langle \overline{S_L} \rangle$ are the storage terms for ocean and land, respectively, and F_O is the ocean energy flux. If the storage terms can be evaluated or legitimately neglected, then knowing the net radiation and the atmospheric fluxes allows the divergence of the ocean fluxes to be inferred.

Flux Calculations

We have evaluated all of the terms in (1) using early versions of the GLAS FGGE IIIb analysis (run #1791), and analyses with satellite data deleted (#2280). We are now in the process of completing the most recent versions of the full FGGE analysis (#2760) and its NOSAT counterpart (#2739). The data were obtained from the analysis tapes at 6 hr intervals with the sampling being done just prior

to the time of the data insertion. The time period over which we average is 5 January - 5 March 1979.

The regions over which we evaluate the energy budgets are illustrated in Fig. 1. Initially we focus on selected north Atlantic and north Pacific regions, and Europe, although we ultimately intend to extend the calculation globally as shown.

Our results for these regions are shown in Table 1. Several points are apparent. The storage terms are small, although in some cases they are roughly the same magnitude as the water vapor divergence term. The budget is dominated by the surface fluxes, net radiation, and horizontal atmospheric divergence. Setting aside the issue of interannual variability, these results are consistent with the 1974-76 wintertime values of Alestalo (1981), where over Europe values of -92 Wm^{-2} were obtained for $\langle \overline{Div\ F_A} \rangle$ and $\langle \overline{Div\ F_Q} \rangle$.

Also of interest is the generally good agreement between the surface fluxes obtained by the GCM and those obtained with the residual approach. In using analyzed fields in a budget study, caution is required because conservation of heat or moisture is not imposed during the 4-dimensional assimilation procedure (e.g., Kalnay and Baker, 1983). The generally good agreement between the model generated surface fluxes and the residual fluxes indicates that excessive violation of the atmosphere's conservation conditions did not occur during the assimilation cycle.

Finally, there is clear evidence of large differences in the areal-averaged divergences that are associated with the use of the satellite temperature sounder data. Over Europe, where the conventional synoptic network is quite dense, there is generally very little difference between the two systems. However, over the data-sparse north Atlantic and North Pacific regions, the differences between the two data sets are as large as factors of 2-3. Clearly, the ocean energy fluxes computed with the SAT and NOSAT data sets likewise would be different.

CURRENT RESEARCH AND FUTURE PLANS:

The work reported here is a test of the 4th order model's usefulness for regional energy balance studies in several Northern Hemisphere regions. It is a straightforward task to extend the analysis to other regions of the global oceans. We are now carrying out these calculations for 12° latitude bands for both the winter and summer Special Observing Periods. It will also be carried out for all of 1979 when those analyses become available.

This research is part of a broader program to understand the general role of synoptic scale processes in the general circulation. Our early work focused on the diagnostics of diabatic heating and the atmospheric heat balance (Schubert and Herman, 1981, Winston, 1980) and on the structure of quasi-stationary features of the general circulation (Schubert, 1984). As a means of further illustrating the role of diabatic processes in baroclinic events we have constructed a linearized version of the 4th order model which uses a monthly averaged February climatology as its basic state. This linear model will be used in a series of process/no process experiments designed to study the role of various physical processes, including orographic interactions, in synoptic scale baroclinic development.

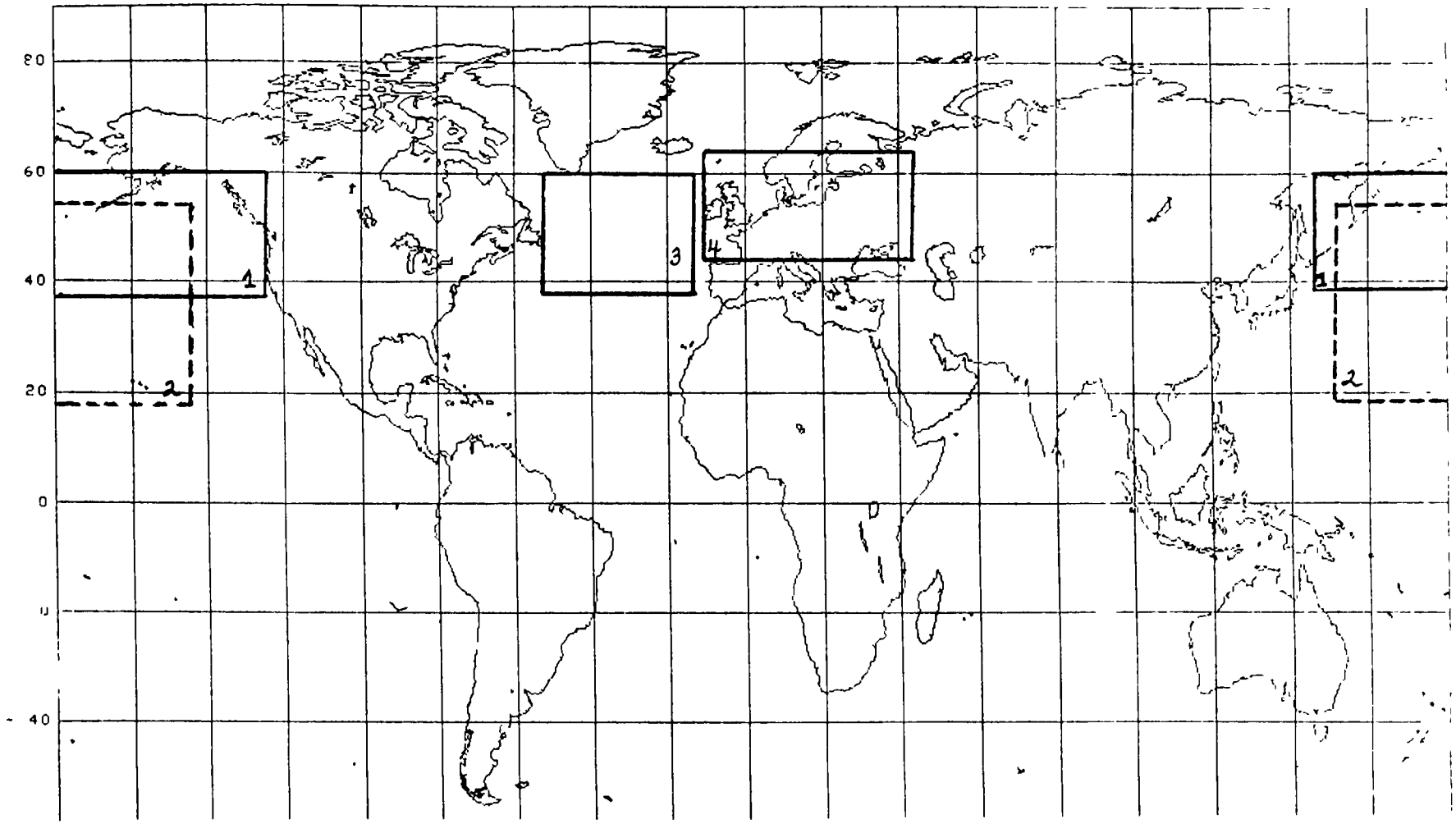

Fig. 1. Northern Hemisphere regional energy balance study areas. (1) Far North Pacific (2) Central North Pacific (3) North Atlantic (4) Europe.

A separate line of work recently initiated investigates the applicability of GLAS model diagnostics to agricultural prediction problems. In particular, we are studying the predictability of agriculturally important quantities, especially precipitation, soil moisture, surface temperature, and surface radiation. We are investigating the implications of errors in 4th order model forecasts on soil moisture, evapotranspiration, and yield prediction in several major crop producing regions.

Table 1

Terms in Regional Energy Balances (Watts m^{-2})*

Regions	$\langle S_A \rangle$	$\langle S_Q \rangle$	$\langle \text{Div } F_A \rangle$	$\langle \text{Div } F_Q \rangle$	$\langle F_{LH} \rangle + \langle F_{SH} \rangle$	Residual $\langle F_{LH} \rangle + \langle F_{SH} \rangle + \langle F \rangle$	$\langle \overline{R_{NEA}} \rangle - \langle \overline{R_S} \rangle$
1. Far North Pacific	0.6 (-0.9)	0.7 (-0.4)	26.0 (55.2)	-16.1 (-28.9)	161	137	126
2. Central and North Pacific	1.8 (-0.1)	0.1 (-2.4)	49.4 (17.1)	3.4 (14.8)	160	112	57.6
3. North Atlantic	-0.9 (-0.4)	-0.2 (-7.5)	82.5 (70.4)	4.2 (-1.0)	237	214	127
4. Europe	13.3 (12.0)	2.7 (3.0)	-71.6 (-65.2)	-23.5 (-30.6)	82.0	44.8	124

*Flux divergence terms are computed with mass balance correction included. Values obtained during the NOSAT experiment are shown in parentheses.

REFERENCES:

Alestalo, M., 1981: The energy budget of the earth-atmosphere system in Europe. Tellus, 33, 360-371.

ICSU-WMO, 1982: "Cage" Experiment: A feasibility study. (F. Dobson, ed.). 95 pp.

Kalnay, E. and W. E. Baker, 1983: Analysed and diagnosed fields in the GLAS FGGE III-b analysis.

LeMunyon, J. E., 1984: Cloud and Circulation Statistics for FGGE SOP I. MS Thesis, Univ. of Wisconsin.

Oort, A. H. and T. H. Vonder Haar, 1976: On the observed annual cycle in the ocean-atmosphere heat balance over the Northern Hemisphere. J. Phys. Ocean., 6, 781-800.

Schubert, S. D. and G. F. Herman, 1981: Heat balance statistics derived from four-dimensional assimilation with a global circulation model. J. Atmos. Sci., 38, 1891-1905.

Schubert, S. D., 1984: A statistical-dynamical study of empirically determined modes of atmospheric variability. Part I: Model analysis and interpretation. (Submitted to J. Atmos. Sci.)

Schubert, S. D., 1984: A statistical dynamical study of empirically determined modes of atmospheric variability. Part II: Model formulation and analysis. (Submitted to J. Atmos. Sci.)

Winston, H. A., 1980: A diagnostic study of potential vorticity changes in the vicinity of north Atlantic cyclones. MS thesis, Univ. of Wisconsin.

JOURNAL PUBLICATIONS:

Schubert, S. D. and G. F. Herman, 1981: Heat balance statistics derived from four-dimensional assimilations with a global circulation model. J. Atmos. Sci., 38, 1891-1905.

Schubert, S. D., 1984: A statistical-dynamical study of empirically determined modes of atmospheric variability. Part I: Model analysis and interpretation. (Submitted to J. Atmos. Sci.)

Schubert, S. D., 1984: A statistical dynamical study of empirically determined modes of atmospheric variability. Part II: Model formulation and analysis. (Submitted to J. Atmos. Sci.)

PAPERS PRESENTED:

G. F. Herman and J. E. LeMunyon: Cloud and circulation statistics for FGGE SOP I. IUGG General Assembly, Hamburg, 1983.

STRUCTURE AND ENERGETICS OF MEDIUM-SCALE ATMOSPHERIC WAVES IN THE SOUTHERN HEMISPHERE SUMMER

(W. J. Randel, J. L. Stanford-Iowa State University)

RESEARCH OBJECTIVES:

Medium-scale waves (zonal wavenumbers 4-7) frequently dominate Southern Hemisphere (SH) summer circulation patterns (Salby, 1982; Hamilton, 1983; Kalnay and Paegle, 1983, Randel and Stanford, 1983). This work is an observational study that focuses on characterizing their temporal and spatial characteristics, along with detailing forcing mechanisms responsible for their formation.

SIGNIFICANT ACCOMPLISHMENTS:

NMC analyses have been used to study medium-scale waves during three SH summers: 1978-79, 1979-80, and 1980-81. The SH summer medium-scale waves are observed to exhibit remarkably regular eastward phase progression, and wave maxima can often be traced continuously around the globe. Frequent downstream development of existing wave patterns is observed. The medium-scale waves at times appear to be longitudinally localized features; at other times they resemble truly global-scale modes. Fig. 1 shows the summer-to-summer variation in spacetime power spectra of meridional geostrophic wind at 45°S and 200 mb.

The time-mean wave structure is found to be consistent with basic-state propagation characteristics and the conservation of wave activity. There is a tendency for background wind structure to restrict wave propagation, as shown in Fig. 2. Here the seasonal mean medium-scale wave Eliassen-Palm (EP) flux vector,

$$\vec{F} = F_\theta = -(a\cos\theta\rho_s)\,\overline{u'v'}$$

$$F_z = (f R a \cos\theta\rho_s/H)\,\overline{v'T'}/N^2$$

which is proportional to the wave group velocity, is plotted along with contours of the 'refractive index'

$$Q_{k,c} = [\bar{q}_y/(\bar{u}-c) - f^2/4H^2N^2 - k^2/a^2\cos^2\theta]/\sin^2\theta \ ,$$

based on the seasonal mean zonal wind structure and typical medium-scale wave parameters. (Here all symbols have their usual meaning). Wave propagation is observed only in the regions of positive 'refractive index'; in particular, no vertical propagation is observed above 150 mb. In addition, the vectors are observed to turn equatorwards, into regions of larger refractive index.

From energetics studies it is found that wave-zonal-mean exchange is a valid concept for describing the SH summer circulation, and that the flow vacillated between periods of highly perturbed and zonally symmetric states. The medium-scale waves result from nonlinear baroclinic instabilities, and exhibit a well-defined life cycle of baroclinic growth, maturity, and barotropic decay. Fig. 3 displays the life-cycle energetics for a particular case study, while Fig. 4 shows the life-cycle averaged EP flux diagram. Both of these figures are in excellent agreement with models of global-scale baroclinic waves by Simmons and Hoskins (1978).

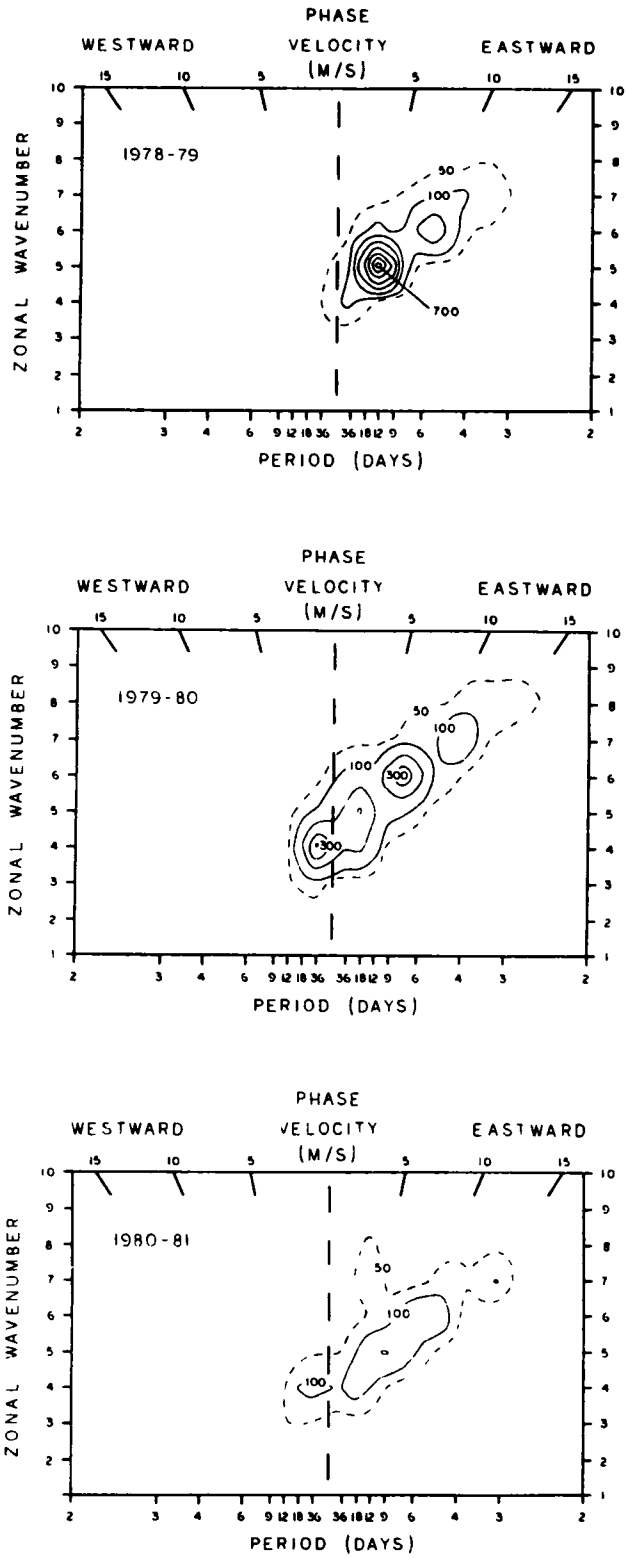

Fig. 1. Space-time spectral power density of geostrophic meridional wind at 45°S latitude and 200 mb for a) 1978-79, b) 1979-80, c) 1980-81. Power units are m^2/s^2 $1/\Delta w$, with contour intervals (solid lines) of 100 m^2/s^2 $1/\Delta w$.

Life-cycle of a baroclinic wave: This study has produced the following picture of the medium-scale wave life-cycle. A strong initial zonal mean temperature gradient is associated with a baroclinically growing wave. The wave's poleward heat flux, found initially in the lowest levels, radiates upward, reaching large values several days later in the upper levels. Reduction of the strong meridional temperature gradient in the lower troposphere is associated with smaller heat fluxes there, and baroclinic growth rate decreases.

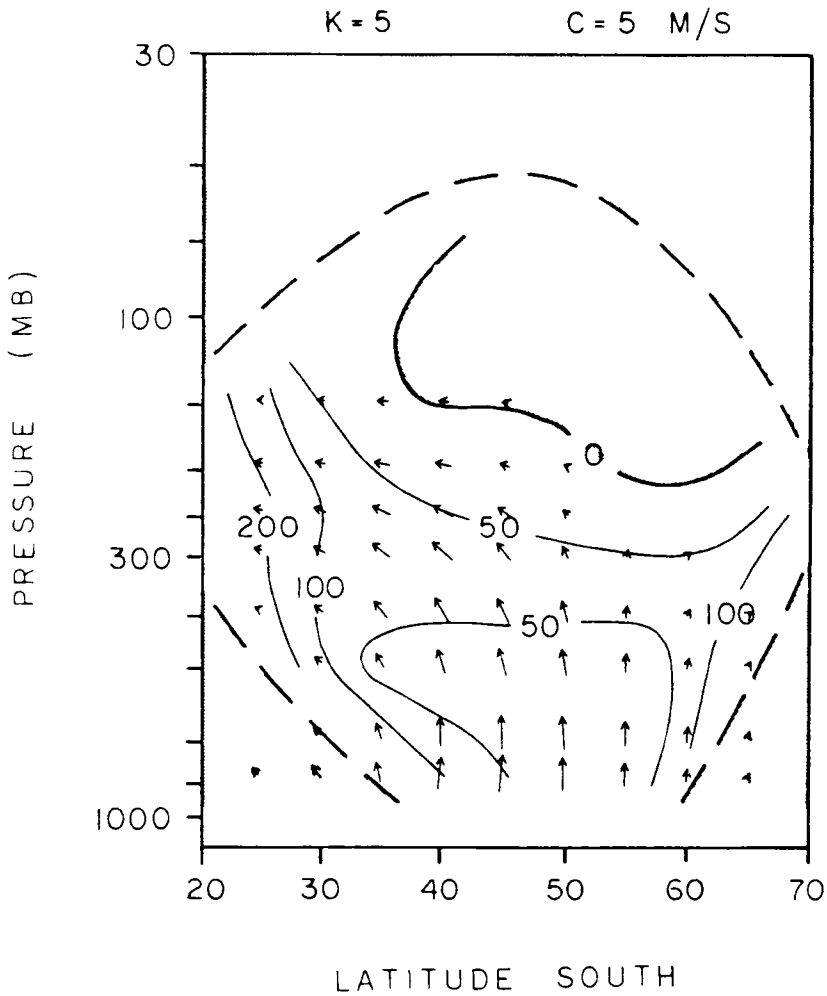

Fig. 2. Contours of the 'refractive index' Q_k (for k=5 and c=10 m/s) along with the seasonally averaged medium-scale wave EP flux vectors. Heavy dashed line is the critical line, where $\bar{u} = c$. Shading indicates regions where $Q_k < 0$. This shows the agreement between observed wave propagation characteristics and that expected due to the background wind structure.

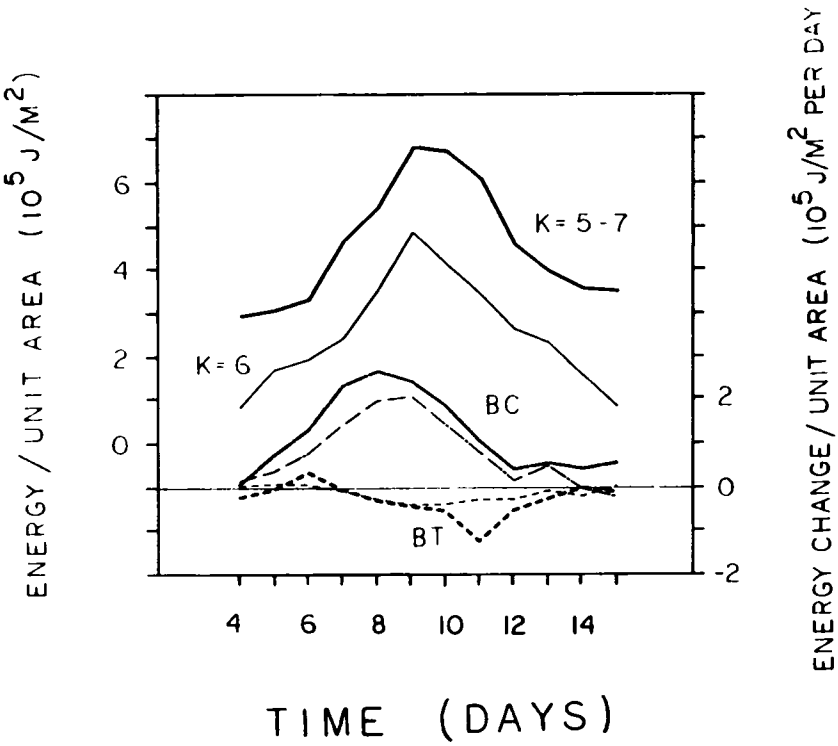

Fig. 3. Time variations in latitudinally averaged (over 25 - 65°S) and vertically integrated (over 850 - 50 mb) energetics during case study. Shown are the wave energy (solid lines), along with the baroclinic (BC) and barotropic (BT) growth terms, for both wave 6 alone (light lines) and waves 5-7 combined (heavy lines). 'Day 9' is December 13, 1979.

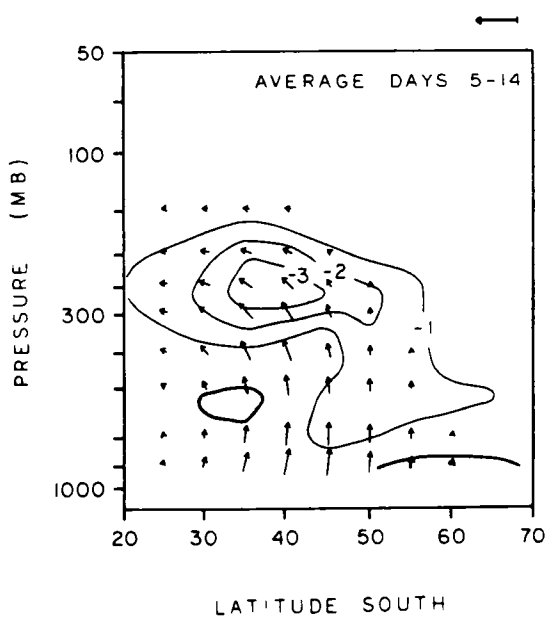

Fig. 4. Life-cycle (days 5-14) averaged EP diagram for case study. Reference arrow shows $2\pi a^2 \rho_s$ times 10 m^2/s^2 of F_θ and 0.1 m^2/s^2 of F_z. Contour interval (of $\nabla \cdot \vec{F}/a \rho_s \cos\theta$) is 1 m/s per day.

The wave reaches its largest amplitude approximately one day after its maximum baroclinic growth rate. At maturity, the heat flux is predominantly in the upper levels, and the wave begins propagating strongly equatorward. This equatorward propagation is presumably due to the latitudinal phase shift induced in the wave by latitudinal shears of the background zonal flow, as discussed by Simmons and Hoskins (1978). The barotropic decay reaches a maximum approximately two days following the wave amplitude maximum, resulting in a strengthening of the zonal mean jet. The final jet is more barotropic than that found initially.

In conclusion, the relative zonal symmetry of the SH midlatitudes provides a good laboratory for testing theoretical results. It is found that this symmetry is responsible for many of the observed medium-scale wave characteristics.

FUTURE PLANS:

The energetics of linear interference between stationary and transient medium-scale waves will be investigated more completely. In addition, because the SH circulation features frequently exhibit wave-packet-like character, it seems important, in addition to Fourier zonal analyses, to study case histories of individual vortices and their associated circulations. SH rawinsonde data will be studied in conjunction with geosynchronous and polar-orbiting satellite cloud imagery.

REFERENCES:

Hamilton, K., 1983: Aspects of wave behavior in the mid and upper troposphere of the Southern Hemisphere. Atmos.-Ocean, 21, 40-51.

Kalnay, E. and J. Paegle, 1983: Large amplitude stationary Rossby waves in the Southern Hemisphere. Observations and theory. First International Conference on Southern Hemisphere Meteorology, July 31-August 6, Sao Jose dos Compos, Brazil.

Randel, W. J. and J. L. Stanford, 1983. Structure of medium-scale atmospheric waves in the Southern Hemisphere summer. J. Atmos. Sci., 40, 2312-2318.

Salby, M. L., 1982: A ubiquitous wavenumber 5 anomaly in the Southern Hemisphere during FGGE. Mon. Wea. Rev., 110, 1712-1720.

Simmons, A. J. and B. J. Hoskins, 1978: The life cycle of some nonlinear baroclinic waves. J. Atmos Sci., 35, 414-432.

JOURNAL PUBLICATIONS:

Yu, W.-B., R. L. Martin and J. L. Stanford, 1983: Long and medium-scale waves in the lower stratosphere from satellite-derived microwave measurements. J. Geophys. Res., 88, 8505-8511.

Randel, W. J. and J. L. Stanford, 1983: Structure of medium-scale atmospheric waves in the Southern Hemisphere summer. J. Atmos. Sci., 40, 2312-2318.

Newman, P. A. and J. L. Stanford, 1983: Observational characteristics of atmospheric anomalies with short meridional and long zonal scales. J. Atmos. Sci., 40, 2547-2554.

Yu, W.-B., J. L. Stanford and R. L. Martin, 1984: Some interhemispheric comparisons of medium-scale waves in the lower stratosphere. J. Atmos. Sci., (in press).

Yu, W.-B. and J. L. Stanford, 1984: Stratospheric circulation in the southern summer/northern winter 1980-81: Behavior of zonal waves 1-10. J. Atmos. Sci., (in press).

CONFERENCE PUBLICATION:

Stanford, J. L., W. J. Randel, W.-B. Yu and R. L. Martin, 1983: Medium-scale waves in the summer southern troposphere and stratosphere. First International Conference on Southern Hemisphere Meteorology, July 31-August 6, Sao Jose dos Compos, Brazil.

INVESTIGATION OF CLOUD FEEDBACK IN THE GLAS MODEL

(W.-C. Wang-Atmospheric and Environmental Research, Inc.)

RESEARCH OBJECTIVE:

The research program is aimed at improving our understanding of the cloud-radiation interactions through the use of the GLAS GCM. We have performed two studies. The first is to conduct impact studies of the non-black cirrus cloud. Experiments were run to examine the effects on thermal radiation budget and their subsequent influences on model simulations. The second study is to examine the effect of thermal radiation parameterization on GLAS model simulations by comparing model results between the Wu-Kaplan's scheme and the Wang's scheme. The former scheme is the one currently being used in the GLAS model while the latter, which includes the multiple scattering effect due to aerosols and cirrus clouds and the temperature-dependent absorption by atmospheric water vapor, carbon dioxide and ozone, has been used in climate models (Wang et al., 1984).

SIGNIFICANT ACCOMPLISHMENTS:

A review of the theoretical and observational studies of cirrus clouds has been performed to provide information for more realistic treatments of cirrus in the general circulation models. Based on the review, one time-step (see Fig. 1) and ten-day (see Figs. 2 and 3) model simulations have been conducted to investigate the differences in the longwave radiation flux between the black and transparent cirrus treatment in the infrared. For both experiments substantial difference in the outgoing longwave flux at the top of the atmosphere is found (Wang and Kaplan, 1983). For the ten-day simulations, the differences in the convective, supersaturation and total cloudiness, temperature, and sensible and latent heat fluxes are also examined on various temporal and spatial scales. Although the cause-and-effect is difficult to identify, the results (see Fig. 4 for temperature change and Fig. 5 for changes of convective and total cloudiness during winter simulations) clearly suggest that on the time scale of a few days and longer cloud-radiation interactions play an important role.

Sensitivity study of the longwave radiation flux to different longwave radiation parameterizations has been performed by comparing the calculated fluxes between the Wu-Kaplan's scheme used in the present GLAS model and the Wang's schemes used in Wang et al. (1976, 1984) for climate studies. The two schemes differ in the methodology as well as the treatment of gaseous absorption. One-time step model calculations have been carried out and the differences in the radiation fluxes between the two schemes are found to be quite substantial, especially at the surface (see Figs. 6 and 7). However, the subsequent differences in the model responses to the different longwave radiation parameterizations remain to be investigated.

REFERENCES:

Wang, W.-C. and L. D. Kaplan, 1983: Effect of high altitude clouds on the earth's infrared radiation flux. Proceedings of the Fifth Conference on Atmospheric Radiation, Baltimore, MD, American Meteorological Society.

Wang, W.-C., G. Molnar, T. D. Mitchell and P. H. Stone, 1984: Effects of dynamical heat fluxes on model climate sensitivity. J. Geophys. Res., 89, 4099-4711.

Wang, W.-C., Y. L. Yung, A. A. Lacis, T. Mo and J. E. Hansen, 1976: Greenhouse effect due to man-made perturbations of trace gases. Science, 194, 685-690.

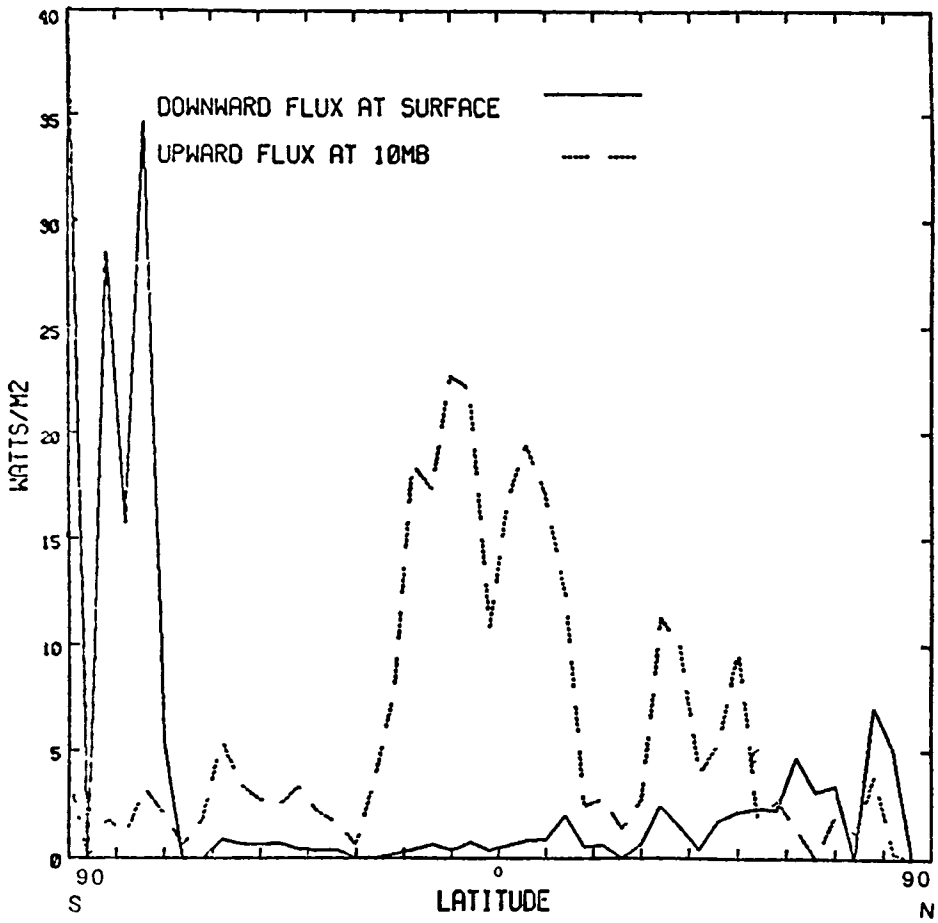

Figure 1. Change of flux due to the change of the treatments of cirrus from black to transparent in the infrared. The threshold temperature for cirrus formation is T* = -20°C. Values shown correspond to an increase for upward flux at 10 mb and a decrease for downward flux at the surface. The data of January 9, 1979 are used for the calculations.

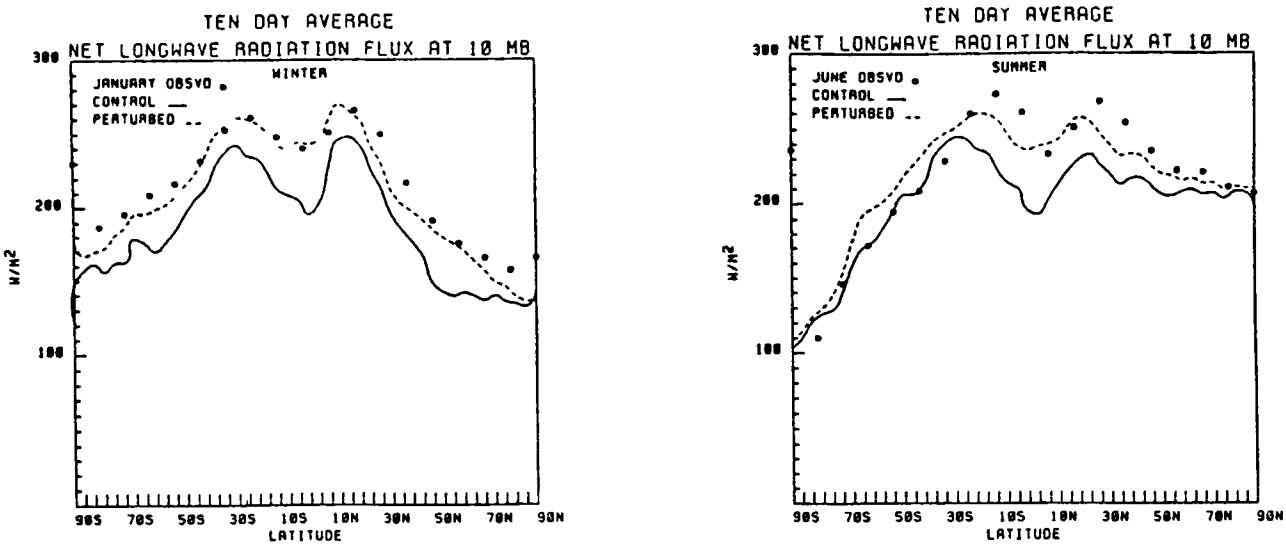

Figure 2. Zonal and ten-day averaged net longwave radiation flux at 10 mb. The observations are monthly mean at satellite levels.

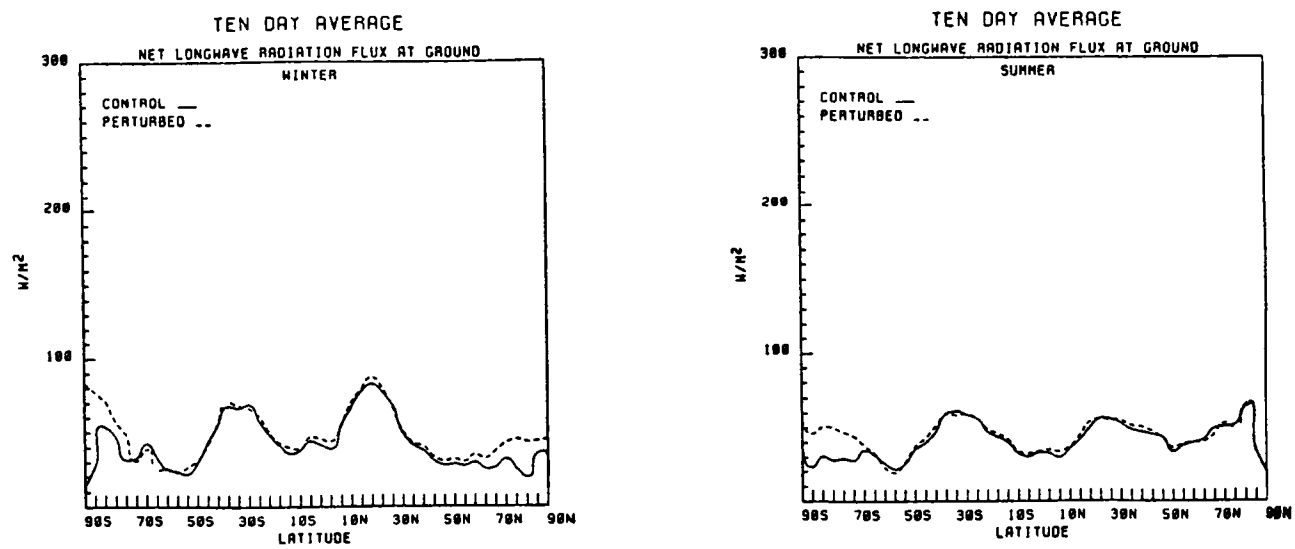

Figure 3. Same as in Fig. 2 except at ground.

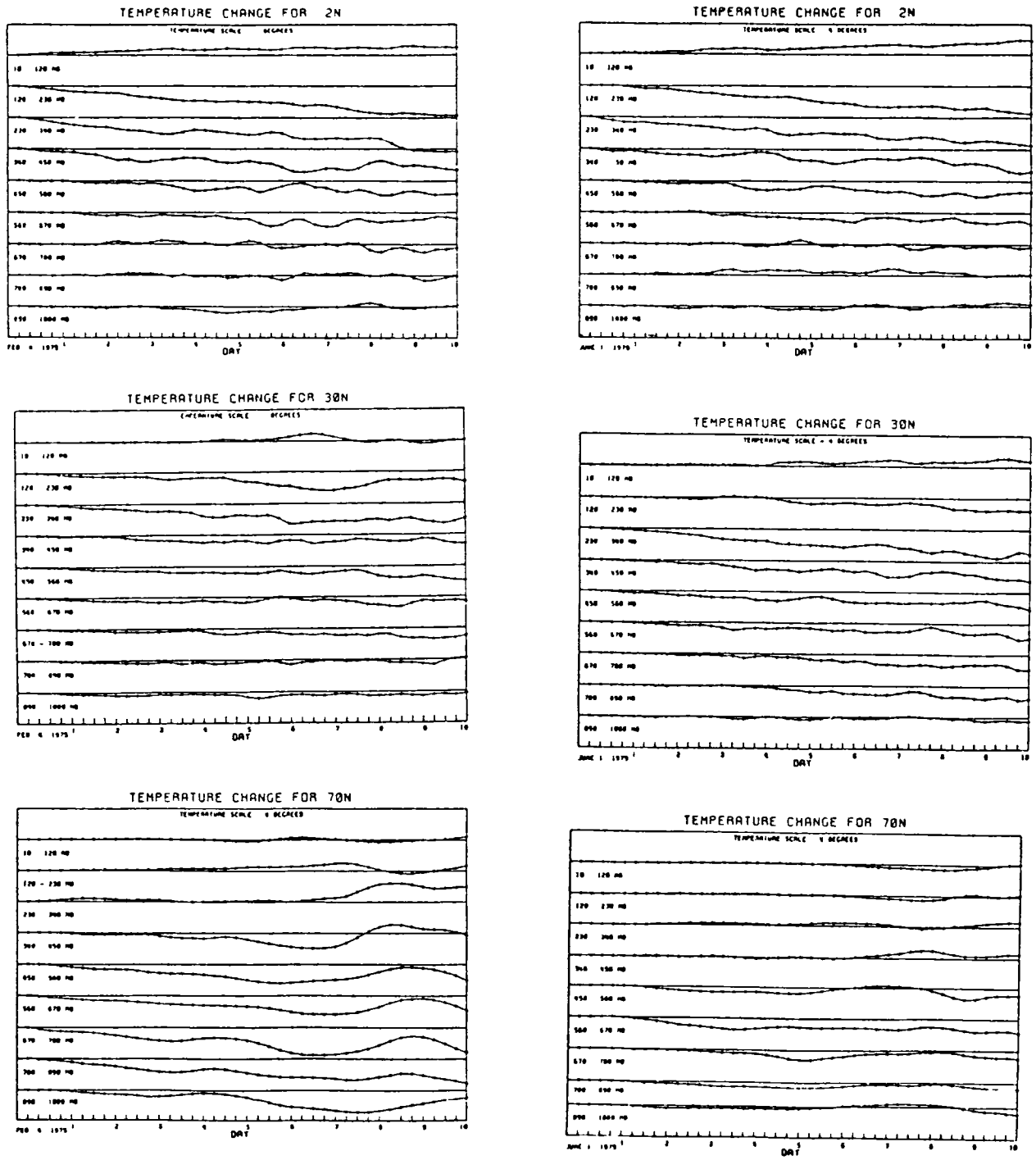

Figure 4. Time series of the temperature change at 2, 30 and 70°N.

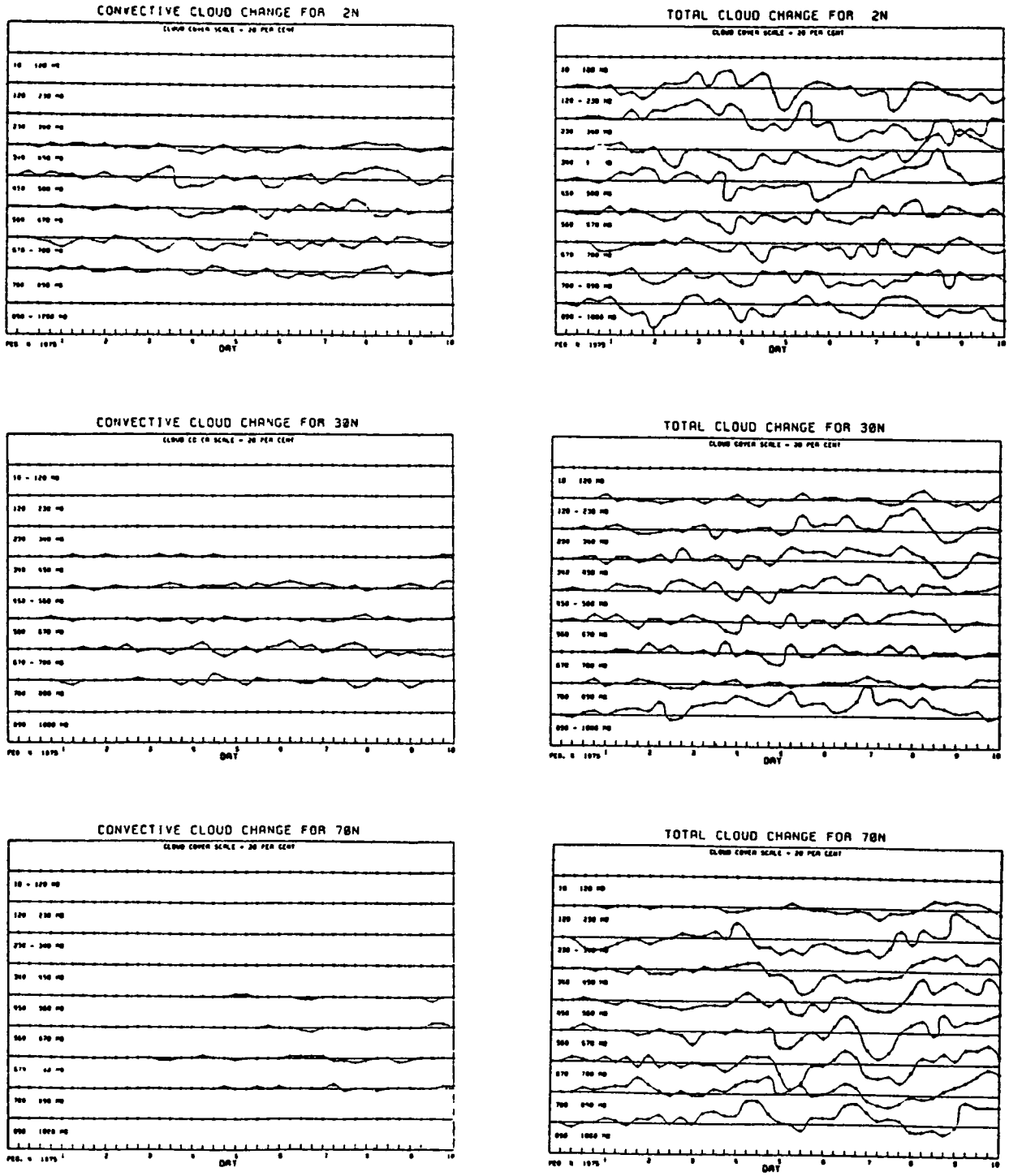

Figure 5. The changes in the convective and total cloudiness at 2, 30 and 70°N during winter simulations.

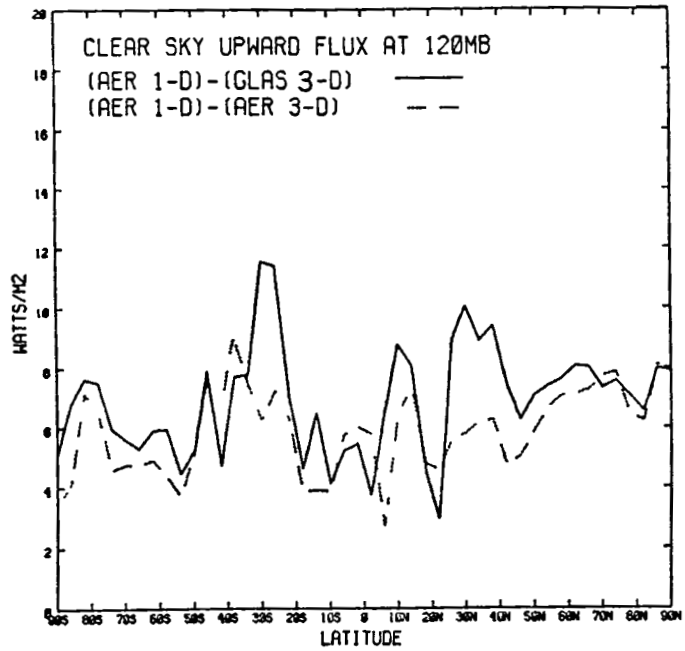

Figure 6. Difference in the clear sky upward longwave radiation flux at 120 mb between different thermal radiation schemes. AER 1-D is the radiation scheme used in Wang et al. (1976) while AER 3-D used in Wang et al. (1984)

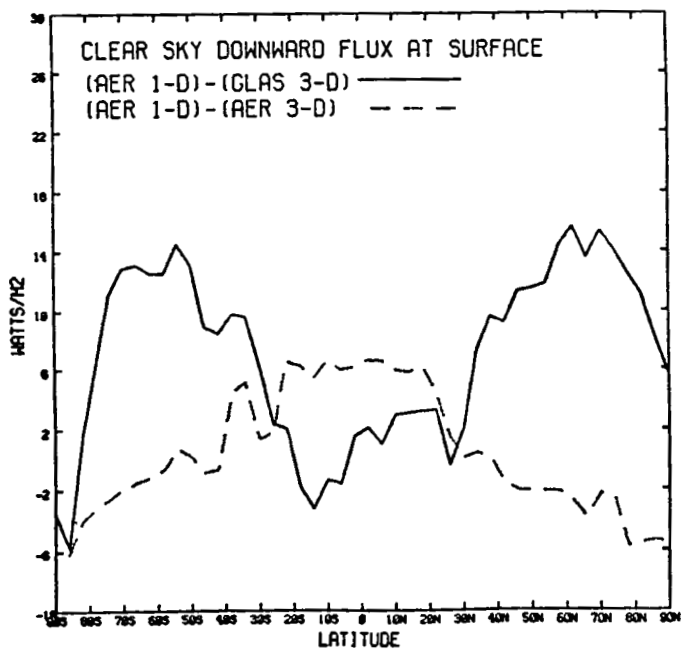

Figure 7. Same as in Fig. 6, but for downward flux at surface.

DIAGNOSTICS OF RAINFALL ANOMALIES IN THE NORDESTE DURING THE GLOBAL WEATHER EXPERIMENT

(D. N. Sikdar-Dept. of Geological/Geophysical Sciences, University of Wisconsin-Milwaukee)

INTRODUCTION:

The rainy season of Northeast Brazil (hereafter called Nordeste) is narrowly centered around March/April and is related to the southern most seasonal migration of the lower tropospheric confluence axis over the adjacent eastern tropical Atlantic.

Rainfall variations and anomalies in the Nordeste have been studied since 1950 (Namias, 1972; Ramos, 1975; Hastenrath and Heller, 1977; Kousky, 1980; Moura and Shukla, 1981; Chu, 1983). Yet, our knowledge of the influences of tropospheric circulations on drought/flood phenomena over the Nordeste is incomplete, mainly due to lack of adequate observations. This gap has been narrowed by the special observing systems - satellite, ships, buoys and aircraft - taken during the operational phase of the Global Weather Experiment which ran from December 1978 to November 1979. The data collected during this entire year, known as the FGGE year allows for extensive diagnosis of large-scale circulation features associated with rainfall variations in the Nordeste.

RESEARCH OBJECTIVES:

The general objective of this three year research program is to diagnostically investigate the behavior of the atmosphere-ocean system in the tropics in relation to extremely low rainfall events observed in Nordeste during 1979. The observational basis for this study includes the FGGE level IIIb data set, satellite images from SMS/GOES, sea surface temperature data from the FGGE level IIb and rainfall records over land.

The present study examines the relationship of the daily variability of large-scale pressure, cloudiness and upper level wind patterns over the Brazil-Atlantic sector during March/April 1979 to rainfall anomalies in northern Nordeste. The experiment divides the rainy season (March/April) of 1979 into wet and dry days, then composites bright cloudiness, sea level pressure, and upper level wind fields with respect to persistent rainfall episodes. Wet and dry anomalies are analyzed along with seasonal mean conditions.

SIGNIFICANT ACCOMPLISHMENTS:

A. Compositing Criteria

During March/April of 1979, rainfall totals for several stations in Nordeste were found to be less than 55% of the normal amounts (United States Weather Bureau, ESSA/NOAA, 1980). Northern Nordeste's 'dry region' is primarily inland from the coasts and is roughly equivalent to the region bounded by the 200 mm isoline of total precipitation for March/April 1979, excluding northeast coasts (Fig. 1). Precipitation totals for 33 stations over the Nordeste were plotted and analyzed daily for the months of March and April (61 days) using data from

the National Climatic Center in Asheville, NC. Ten stations were uniformly distributed within the dry region. Station separations average roughly 270 km. The stations are Teresina, Crateus, Quixeramobim, Floriano, Crato, Compina Grande, Guibues, Paulo Alfonso and Xique Xique. Figure 2 is an example of a histogram plot of daily rainfall at Quixeramobim (82586) for March and April. Precipitation totals for the stations were summed over the dry region and displayed in a time series histogram (Fig. 3).

Each day of the two month rainy season was tagged as either wet or dry. The definition of a wet/dry day followed two conditions, (1) more than two stations within the dry region with recorded precipitation, greater than 1 mm, (2) less than three stations with recorded precipitation, but total precipitation greater than 10 mm. If either condition (1) or (2) is met, the day is tagged as wet, otherwise the day is tagged as dry. Figure 3 shows the ten station total precipitation in the dry region (dry totals are dotted) for March and April 1979. Figures 4 and 5 are example rainfall analyses for a dry and wet day respectively. As a further specification, in order to isolate rainfall associated with large-scale systems, only days within a precipitation episode (either wet or dry) of three successive days or longer are used for compositing. Therefore, only rainfall accompanying more persistent weather systems are identified. All anomaly fields in this study are based on the above criteria.

B. Percent Bright Cloudiness

Cloud amounts were estimated in 5° latitude-longitude areas from GOES-EAST infrared full disk pictures for the region bounded by 20°N to 20°S and 20°E to 70°E. Estimates were made three times daily at 00, 12 and 18 GMT for March/April. On occasion the 00 or 12 GMT picture was missing in which case the 06 GMT picture was substituted. The procedure excluded cloudiness that appeared dull gray to the eye. The possible effect of this low brightness cutoff was to exclude cloud regions consisting primarily of stratus or small cumulus. Cloud amounts were then averaged to obtain daily means. Daily mean bright cloud amounts were averaged for a seasonal mean as well as for wet/dry anomalies.

1) Seasonal Mean

Figure 6 shows the distribution of bright cloud amount over the Brazil-Atlantic sector for March/April 1979. Maximum cloudiness (greater than 40%) occurs over the Amazon basin and between the equator and 5°N over the tropical Atlantic associated with the ITCZ. Minimum cloudiness (less than 20%) is seen over the North Atlantic Ocean north of 10°N and over eastern Nordeste extending over the South Atlantic Ocean. These minimum brightness areas are associated with the subtropical highs of both hemispheres.

2) Wet/Dry Anomalies

Figure 7a displays the cloudiness departures for the composite of dry days in the northern Nordeste. The anomaly map indicates a maximum of negative anomalies over western Nordeste. Also a small positive anomaly north of the equator centered on 30°W is noted. The negative anomalies are due to the northwestward shift of the South Atlantic High (SAH). During the wet days, cloudiness on the equatorward side of the SAH increases (Fig. 7b). Maximum positive anomalies are found over southern Nordeste and south of the equator at 30°W. Therefore, the rainy days in northern Nordeste are characterized by

positive bright cloud anomalies over southern Nordeste and over the Atlantic south of the equator. In contrast, the bright cloudiness pattern during the dry days features negative anomalies over western Nordeste and positive anomalies over the Atlantic north of the equator.

C. Sea Level Pressure (SLP)

The 00 and 12 GMT SLP were averaged for getting daily mean fields and then averaged for a seasonal mean as well as for wet/dry episodes.

1) Seasonal Mean

Figure 8 is an analysis of the seasonal mean sea level pressures over the region. Lowest pressures are found over the continents. Over Africa the minimum pressures are north of the equator and over South America they are along the equator. Over the Atlantic the equatorward extensions of both subtropical highs are evident. Over the Nordeste there is a weak north-south pressure gradient with the lower pressures in the north.

2) Wet/Dry Anomalies

Figure 9a depicts the SLP departures for composite of dry days in the northern Nordeste. The anomaly field is weak indicating only small departures from the mean. Largest positive anomalies are located over the eastern south Atlantic and over northern Africa. Largest negative anomalies are found north of the Caribbean Sea. The wet anomaly field is significantly stronger (Fig. 9b). Strong negative anomalies are located over the western south Atlantic and over northwestern Africa. According to a diagnostic study by Chu (1983), wet years were marked by negative SLP departures over the subtropical south Atlantic.

D. Upper-level Wind Fields

As with the SLP, the upper level winds were obtained from the level IIIb data set.

1) Zonal and Meridional Winds

A comparison of dry and wet composite of u-component for three tropospheric levels (200, 500 and 850 mb) shows little differences at both 200 and 500 mb. However, a significant difference is observed at 850 mb (Fig. 10a,b). During wet days at 850 mb, relatively strong easterlies are found over the subtropical south Atlantic and over the Amazon basin. This velocity pattern appears favorable for advection, a large quantity of moisture from the south Atlantic over Nordeste. In contrast during the dry days, easterlies over the western south Atlantic are relatively weak.

The meridional wind field for both dry and wet composites were computed at three tropospheric levels. Again the most noteworthy differences between wet and dry composites occur at 850 mb (Fig. 11a,b). A core of southerly winds is located over the coast of Nordeste for both composites, however, during the dry composite the speeds are stronger. The strength of the southeasterlies over northern Nordeste during dry days may inhibit the southward movement of the ITCZ.

2) Vertical p-velocity

Using the daily averaged wind components, vertical velocity has been computed using the kinematic method. Figure 12a,b shows both dry and wet composites of ω at 850 mb. At all levels and for both composites there is subsidence over the Nordeste. At 850 mb there is a southwestward shift towards the coast of the Nordeste of maximum upward motion from the dry to the wet composite. The core of maximum positive omega is associated with the ITCZ.

The analyses presented here are preliminary.

E. Temperature and Moisture Fields

At present the temperature and moisture fields at 500, 850 and 1000 mb are being processed for both seasonal mean and anomaly fields.

We have identified large-scale daily variations in both bright cloudiness and SLP over the Brazil Atlantic sector during March/April 1979. Maximum bright cloudiness associated with the ITCZ showed a southward shift during the wet composites. This southward shift of the ITCZ was also noted in the ω field. Anomalies of sea level pressures indicate a weakening in the equatorward extension of the SAH during wet days. This weakening in turn allows for a southward shift of the ITCZ over northern Brazil.

Also, the 850 mb zonal wind speed increases during the wet days which allows for an increase in moisture transport from the tropical Atlantic.

CURRENT RESEARCH.

Currently we are analyzing the position of the surface confluence axis, maximum convergence band and SST over the tropical Atlantic. Composite charts of horizontal divergence and relative vorticity are being prepared. In order to identify preferred modes of atmospheric circulation in relation to precipitation anomalies we are analyzing daily mean values of SLP and 500 mb heights over the Brazil tropical Atlantic sector. The time series of large-scale cloudiness are being analyzed using spectral techniques to isolate dominant modes of oscillation, if any, related to rainfall variations. Preliminary results will likely be communicated to a journal in early 1985.

FUTURE PLANS:

Analysis of daily charts of velocity potential, stream function and temperature will be done to depict systematically the existence of local meridional circulation over the Nordeste. By comparing the variations of velocity potential fields between wet and dry days, it may be possible to test the sensitivity of upper tropospheric outflow over the subtropics. Water vapor transports will be evaluated since the fluctuation in this flux are intimately related to problems of floods and droughts. We also propose to complete heat and moisture budgets over the Nordeste and surrounding areas during the anomalous rainfall episodes with a view towards determining quantitatively the horizontal and vertical distributions of tropospheric heat sources and sinks and towards identifying the heating mechanisms operating in the region during the 1979 rainy season.

REFERENCES:

Chu, P.-S., 1983: Diagnostic studies of rainfall anomalies in northeast Brazil. Mon. Wea. Rev., 111, 1655-1664.

Hastenrath, S. and L. Heller, 1977: Dynamics of climatic hazards in northeast Brazil. Quart. J. R. Met. Soc., 103, 77-92.

Kousky, V. E., 1979: Frontal influences on Northeast Brazil. Mon. Wea. Rev., 107, 1140-1153.

Marques, V. S., B. Rao and L. C. B. Molion, 1983: Interannual and seasonal variations in the structure and energetics of the atmosphere over NE Brazil. Tellus, 35A, 136-148.

Moura, A. D. and J. Shukla, 1981: On the dynamics of droughts in NE Brazil: Observations, theory and numerical experiments with a general circulation model. J. Atmos. Sci., 38, 2653-2675.

Namias, J., 1972: Influence of northern hemisphere general circulation on drought in Northeast Brazil. Tellus, 24, 336-343.

Ramos, R. P. L., 1975: Precipitation characteristics in Northeast Brazil dry region. J. Geophys. Res., 80, 1665-1678.

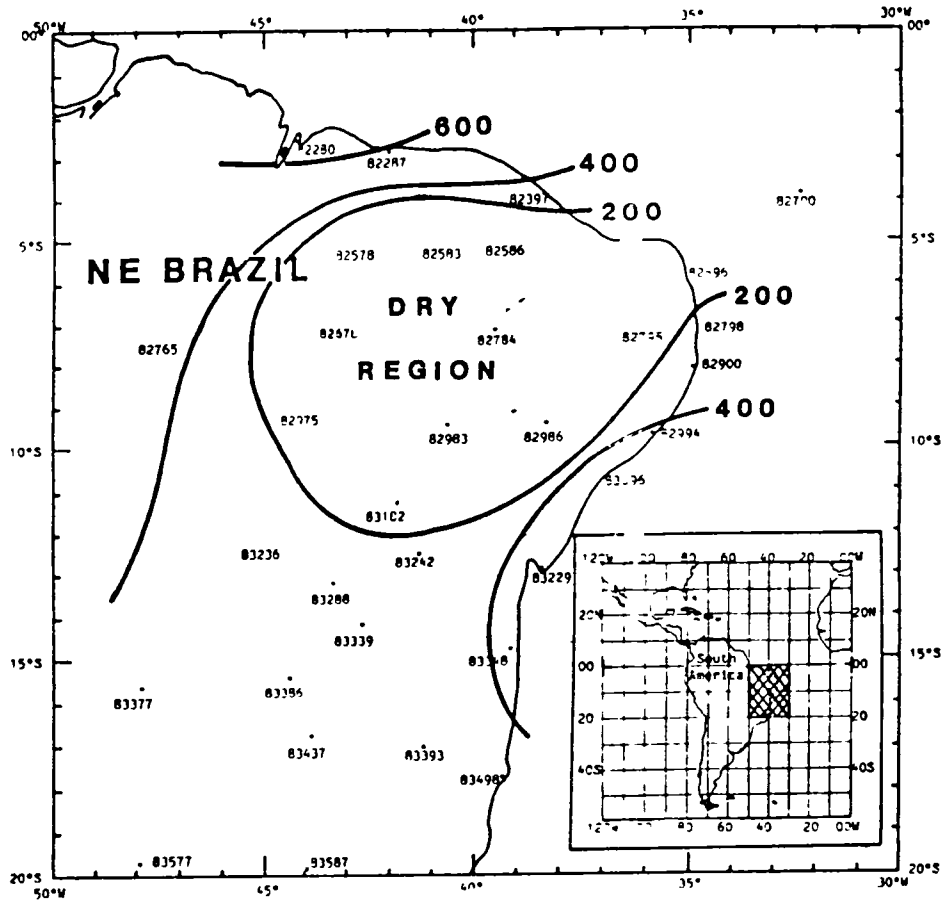

Fig. 1. Area of study and total rainfall (in mm) of March and April of 1979. (Dry region indicated total rainfall to be less than 20 mm).

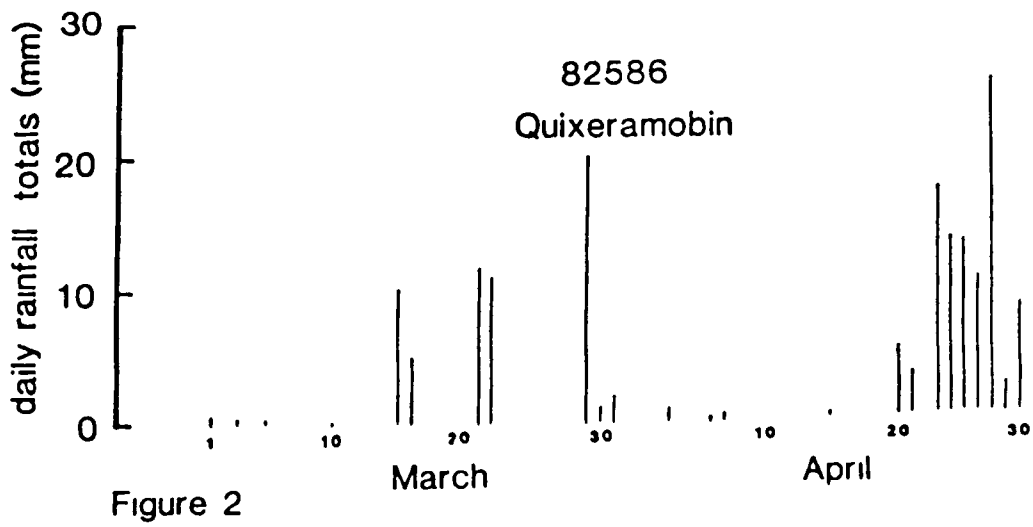

Figure 2

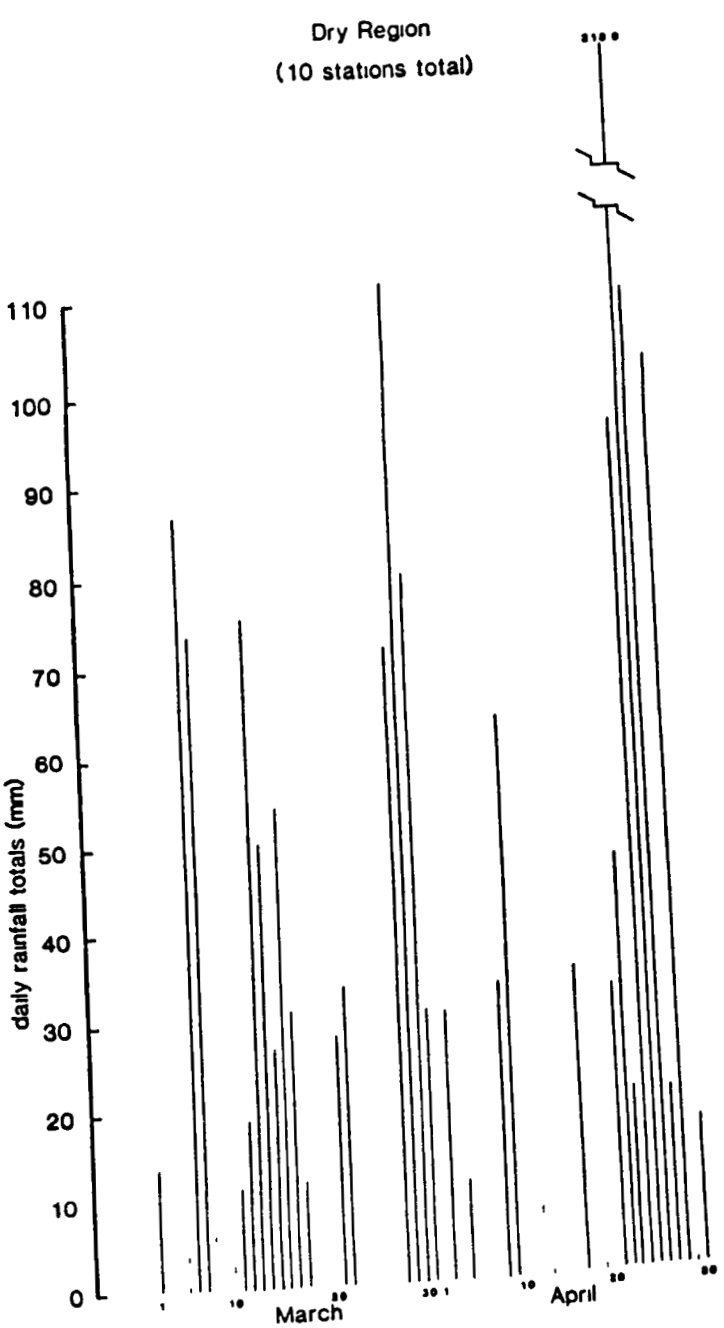

Fig. 3

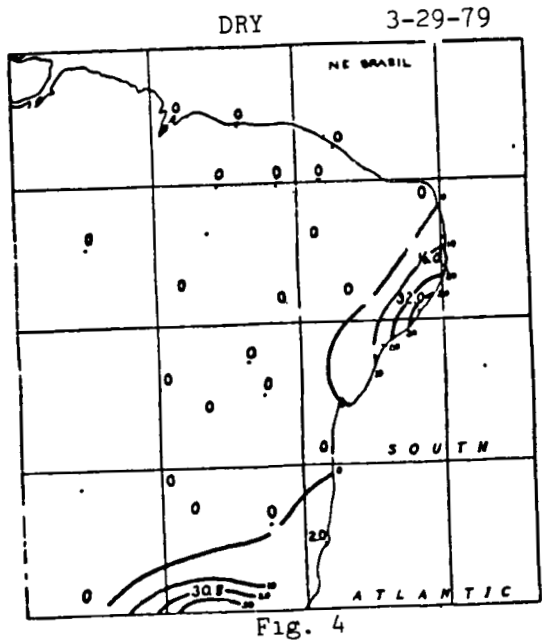

Fig. 4

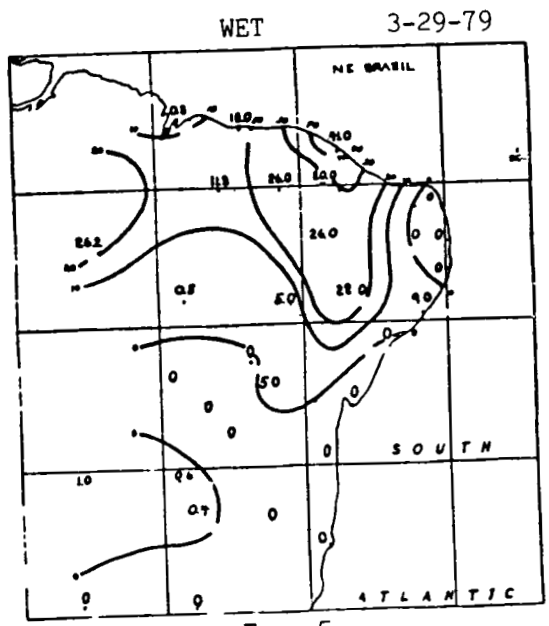

Fig. 5

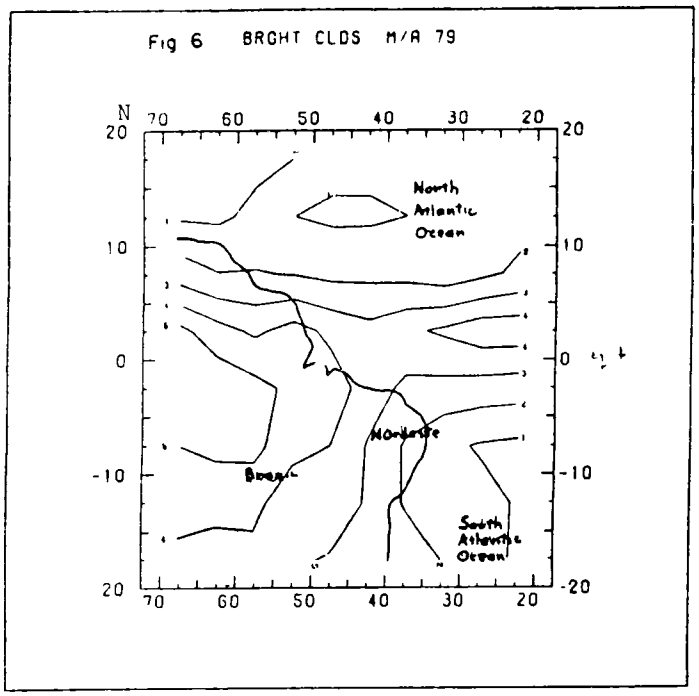
Fig 6 BRGHT CLDS M/A 79
North Atlantic Ocean
South Atlantic Ocean

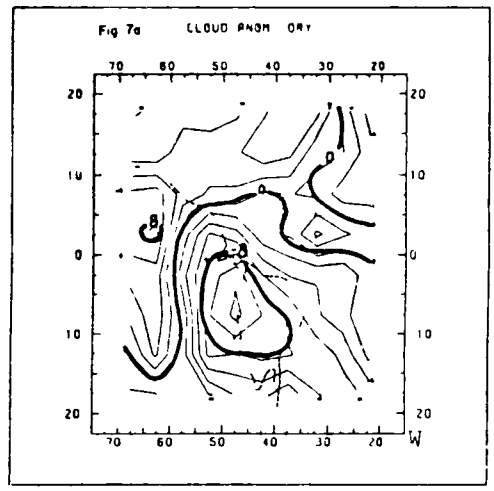
Fig 7a CLOUD ANOM ORY

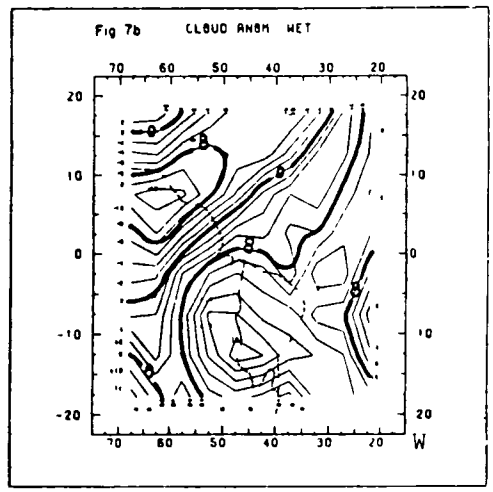
Fig 7b CLOUD ANOM WET

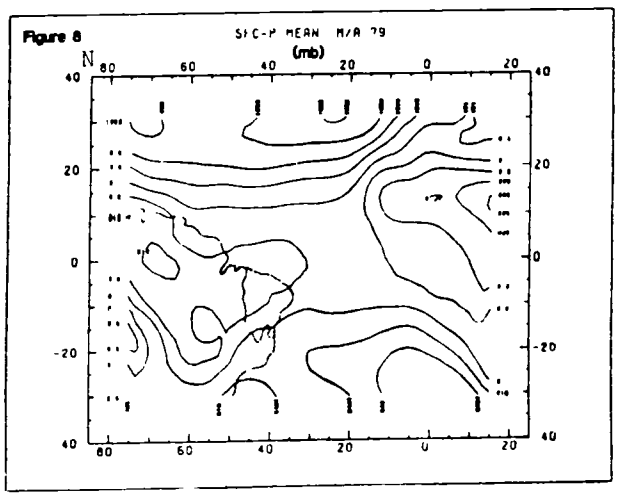
Figure 8
SFC-P MEAN M/A 79
(mb)

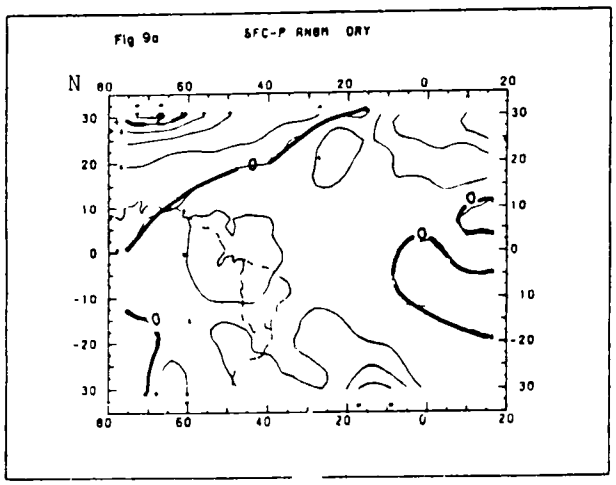
Fig 9a SFC-P ANOM ORY

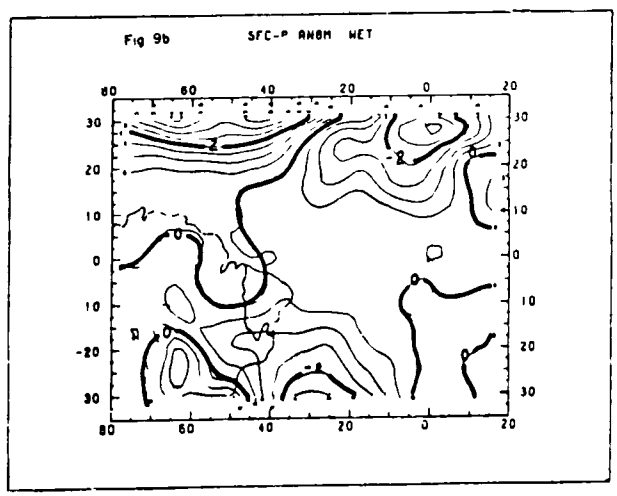
Fig 9b SFC-P ANOM WET

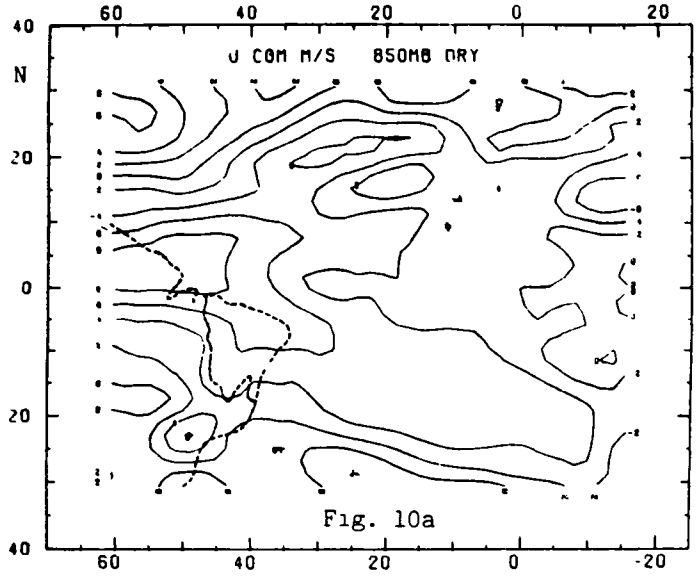

Fig. 10a

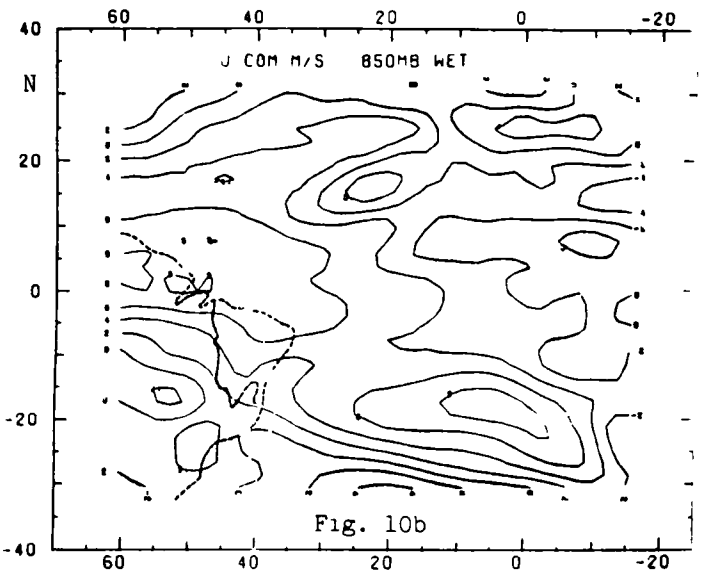

Fig. 10b

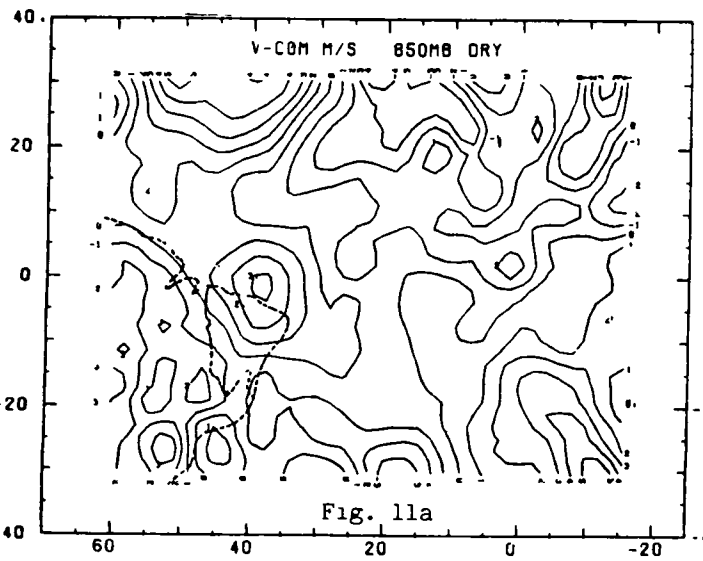

Fig. 11a

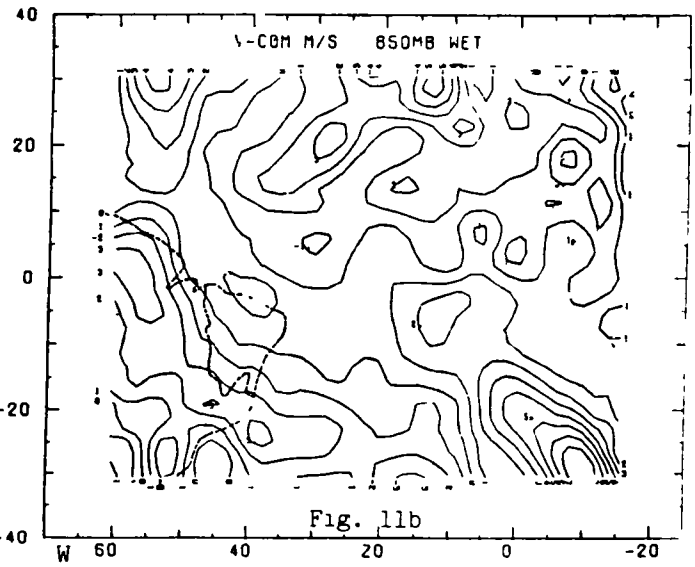

Fig. 11b

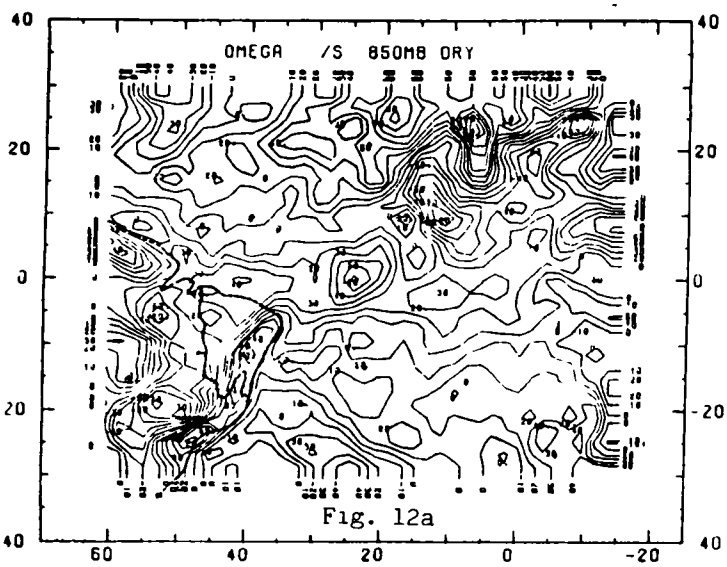

Fig. 12a

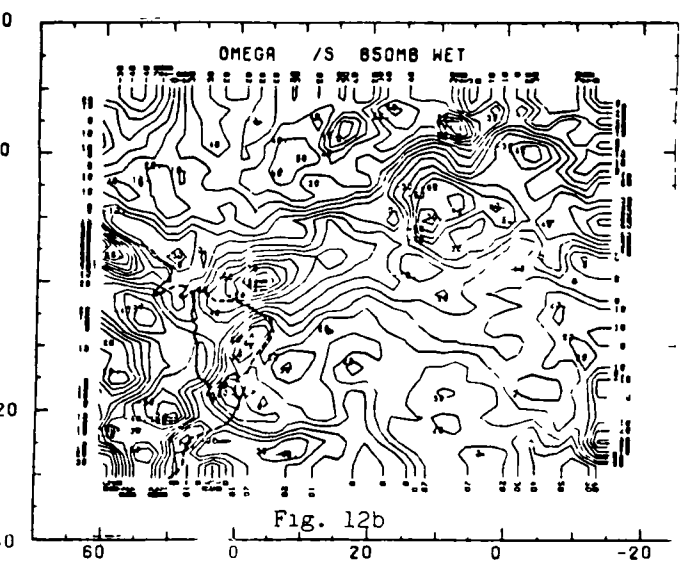

Fig. 12b

RAIN VOLUME ESTIMATION OVER AREAS USING SATELLITE AND RADAR DATA

(A. A. Doneaud, J. R. Miller, Jr., L. R. Johnson-South Dakota School of Mines and Technology, T. H. Vonder Haar and P. Laybe-Colorado State University)

RESEARCH OBJECTIVES:

The main objective of the research grant is to apply satellite data to a recently developed radar technique used to estimate convective rain volumes over areas on a dry environment (the northern Great Plains). Called the Area time integral technique, it provides a means of estimating total rain volumes over fixed and floating target areas of the order of 1,000 to 100,000 km^2 for clusters lasting >40 min (Doneaud et al., 1984a).[1] The basis of the method is the existence of a strong correlation between the area coverage (>25 dBz) integrated over the lifetime of the storm (ATI) and the rain volume.

One key element in this new simple technique is that it does not require the consideration of the structure of the radar intensities inside the area coverage (as, for instance, the Z-R technique) to generate rain volumes, but only considers the rain event per se. This fact might reduce or eliminate some sources of error in applying the technique to satellite data.

The second key element is that the ATI once determined can be converted to total rain volume by using a constant factor (average rain rate) for a given locale. This procedure has been emphasized in a recent paper (Doneaud et al., 1984b).[2] It was found that if the entire storm duration is considered, the average rain rate, in a first approximation, could be taken as independent of the rain volume or the ATI. Similarly we propose that once radiance thresholds are determined by using visible (VIS) and infrared (IR) information integrated over a storm's lifetime, the digital unit threshold should exhibit very little variation among storms if adjustments are made for regional differences.

Recently the ATI technique was examined by using Florida FACE II data (Lopez et al., 1983)[3] and the same strong correlation was found between ATI and the rain volume, thus suggesting the utility of this technique for different geographic locations.

SIGNIFICANT ACCOMPLISHMENTS:

The work started in January 1984. Some preliminary remarks are presented in the next section. No significant accomplishments could yet be reported.

CURRENT RESEARCH:

The work is based on radar data collected during the summer of 1981 in Bowman and Parshall, North Dakota, as a part of the North Dakota Cloud Modification Program (NDCMP) and on radar (Miles City) and rapid scan satellite data

[1] See publication list.
[2] See publication list.
[3] Lopez, R. E., J. Thomas, D. O. Blanchard and R. L. Holle, 1983: Estimation of rainfall over an extended region using only measurements of the area covered by radar echoes. Preprints 21st Conf. Radar Meteor., Edmonton, Canada, Amer. Meteor. Soc., 681-686.

collected during the same summer as a part of the Cooperative Convective Precipitation Experiment (CCOPE). The radar and satellite data were processed at the South Dakota School of Mines and Technology (SDSM&T) and at the Colorado State University (CSU), respectively.

Radar data were recorded whenever there was convective activity within about 150 km range, roughly every 10 min. Seven days with one to two convective clusters for which both radar and rapid scan GOES satellite data are available were selected. The selection criteria were: a) The cluster has to be individualized from other cloud systems of the time period; b) The entire cluster lifespan must be recorded in at least one of the visible and infrared rapid scan modes; c) Radar data from Miles City, Bowman, and/or Parshall are available for a similar time span. Cells bigger than a cumulus cloud but smaller than a typical mesoscale convective complex were considered "clusters."

The analysis of both radar and satellite data was performed for one of the 12 June clusters; analysis of three other clusters (12 June and 2 July 1981) is in progress. Digital printouts of the dBz-values at low tilt angles were prepared by conversion of radial to rectangular coordinate system. The rain volume for each cluster was computed using an optimized Z-R relationship, $Z = 155R^{1.88}$,[4] based on data from this region. GOES-West satellite rapid scan data were remapped from the satellite coordinate system into a Lambert conformal projection so that the radar PPI data and the satellite data are in the same perspective. Radar computed areas greater than 25 dBz have been used to delineate the areas of rainfall. The radar PPI cluster features have been used to identify a radar sector of interest (Fig. 1) upon which to "focus" using the satellite data. The computed radar data (see Table 1) were then used to determine infrared temperature and visible brightness thresholds by comparison with computed areas in the satellite data for each value of infrared temperature and visible brightness. However, since radar and VISSR data respond to different characteristics of clouds at different atmospheric levels, and because of small time differences between these data sets, a satellite sector of interest was established by applying small adjustments to the radar sector manually (to avoid cloud features suspected of not being detected by the radar). The brightness and temperature values within the satellite sector were counted and multiplied by the ground resolution pixel area (2.47 km^2) to obtain the area for each count value.

Thirteen consecutive time steps with radar and satellite data were considered during the 3-hr evolution of 12 June analyzed cluster (Table 1). Satellite times were chosen to be as close to the radar times as possible.

Using the aforementioned technique, graphs of cumulative area versus count values were obtained for every time step. From these graphs and the computed radar area, the thresholds for count values were determined by inspection. Four of the graphs, two VIS and two IR (the beginning time of the cluster and the time of the maximum echo area) are presented in Fig. 2A,B,C,D. The echo area and the respective count value threshold are also shown in these graphs. The echo areas and the corresponding threshold counts (VIS and IR) are listed in Table 1, for every time step. The step-by-step evolution of the echo areas

[4] Smith, P. L., Jr., D. E. Cain and A. S. Dennis, 1975: Derivation of a Z-R relationship by computer optimization and its use in measuring daily areal rainfall. Preprints 16th Radar Meteor. Conf., Houston, TX, Amer. Meteor. Soc., 461-466.

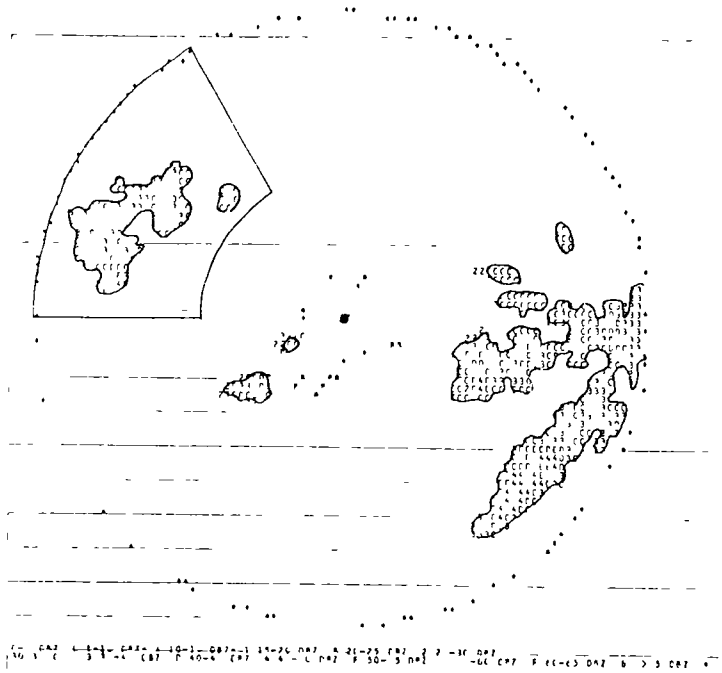

Fig. 1: Bowman radar PPI with delineated sector of interest.

threshold counts (VIS and IR) are listed in Table 1, for every time step. The step-by-step evolution of the echo areas and of the threshold count values are exhibiting similar trends, although there are time lags between radar and satellite data for most of the time steps. It is important to note that both VIS and IR threshold count values have a spectrum of variation during the storm lifetime from 50.59 to 57.46 and from -20.05°C to -40.45°C, respectively. This makes the selection of one or two thresholds to delineate the rain area for portions of the storm quite difficult.

TABLE 1

Satellite Data					12 June 1981	Bowman Radar Data						
	Maximum digital count value		Temperature of IR maximum count	Threshold count value of area which matches radar area			Area	Cum Area	Rain Vol	Cum Rain Vol	dBz	MAX*
Time GMT	Visible	Infrared	°C	Visible	Infrared/°C	Time GMT	>25 dBz km²	>25 dBz km²	mm km²	mm km²	MAX	Radar Ht km
(1)	(2)	(3)	(4)	(5)	(6)	(7)	(8)	(9)	(10)	(11)	(12)	(13)
1629	54	182	-37 2	51 16	179 60/-34 8	1627	1062	1062	692	692	47	8 3
638	55	182	-37 2	50 81	178 86/-34 06	1638	1367	2429	797	1489	47	9 4
1641	55	182	-37 2	50 59	179 17/34 37	1649	1569	3998	1007	2496	46	10 1
1702	56	183	-38 2	52 12	180 64/-35 84	1702	1820	5818	1551	4047	56	11 3
1711	55	183	-38 2	51 94	179 20/-34 40	1716	2182	8000	2116	6163	61	11 6
1732	60	182	-37 2	53 69	179 18/-34 38	1732	1789	9789	1847	8010	61	12 0
1739	60	184	-39 2	53 39	179 53/-34 73	1745	1431	11220	1178	9188	55	12 2
1759	59	186	-41 2	54 35	182 22/-37 42	1756	1097	12317	826	10014	52	10 3
1811	60	189	-44 2	54 32	163 69/-24 05	1811	985	13302	1029	11043	53	10 3
1829	61	195	-50 2	55 80	185 25/-40 45	1828	964	14266	632	11675	46	10 0
1838	61	195	-50 2	54 69	169 24/-27 82	1838	2698	16964	1637	13312	47	10 4
1841	61	194	-49 2	55 07	172 43/-29 42	1848	2002	18966	1039	14351	48	10 6
---						1859	2000	20966	1423	15774	52	11 0
----						1915	361	21327	225	15999	43	8 7
1929	62	158	-22 2	57 46	153 70/-20 05	1925	300	21627	131	16130	45	8 8

*dBz >20

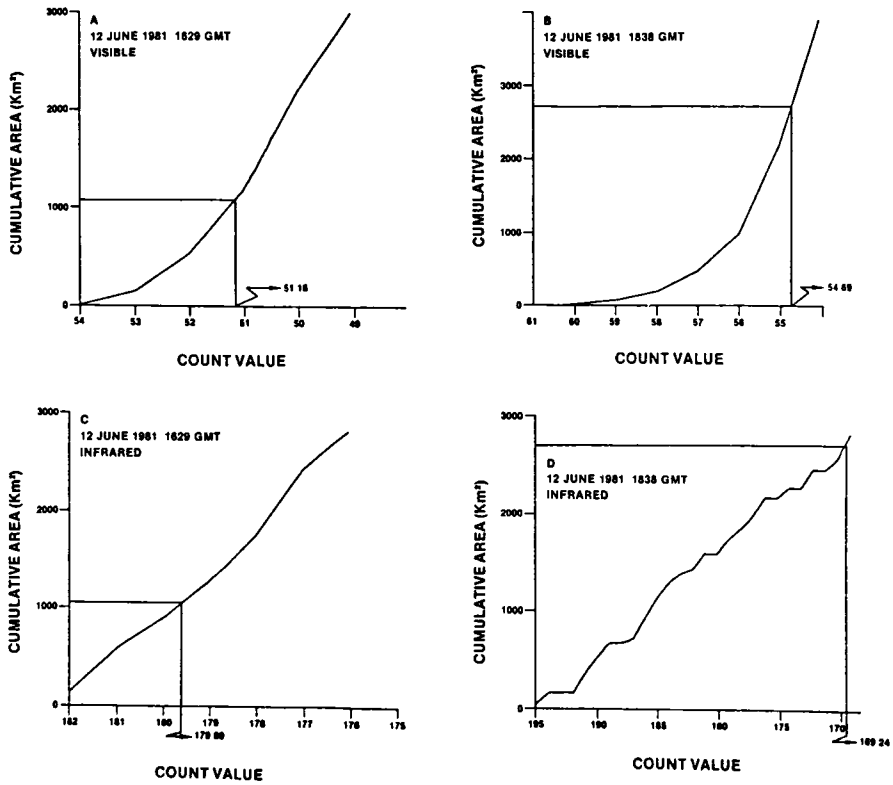

Fig. 2: Cumulative area (km^2) vs. count value.

Figure 3 exhibits the summation of the cumulative area versus count values for the 3-hr storm period. The summed cumulative areas represent the spectrum of Area Time Integral (ATI)[5] values for different count values. The thresholds 54.7 in VIS and 178.9 (≈-34.15°C) in IR representing the ATI of this cluster are within the

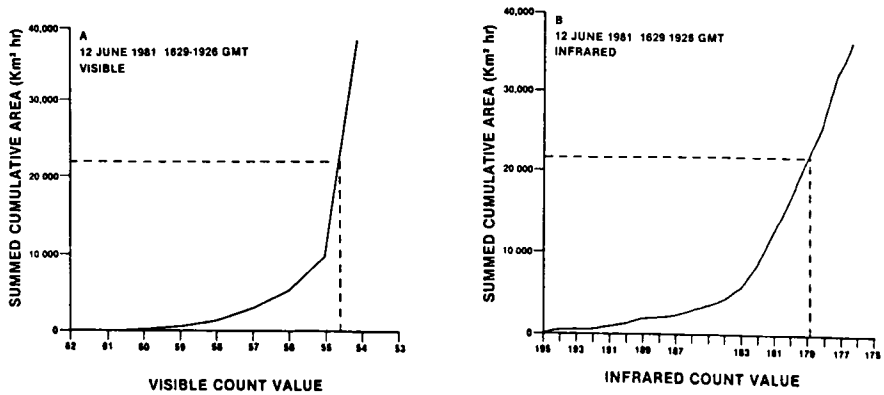

Fig. 3: Area time integral for visible (A) and infrared (B) count values.

[5]ATI: The echo area >25 dBz integrated over the storm lifetime.

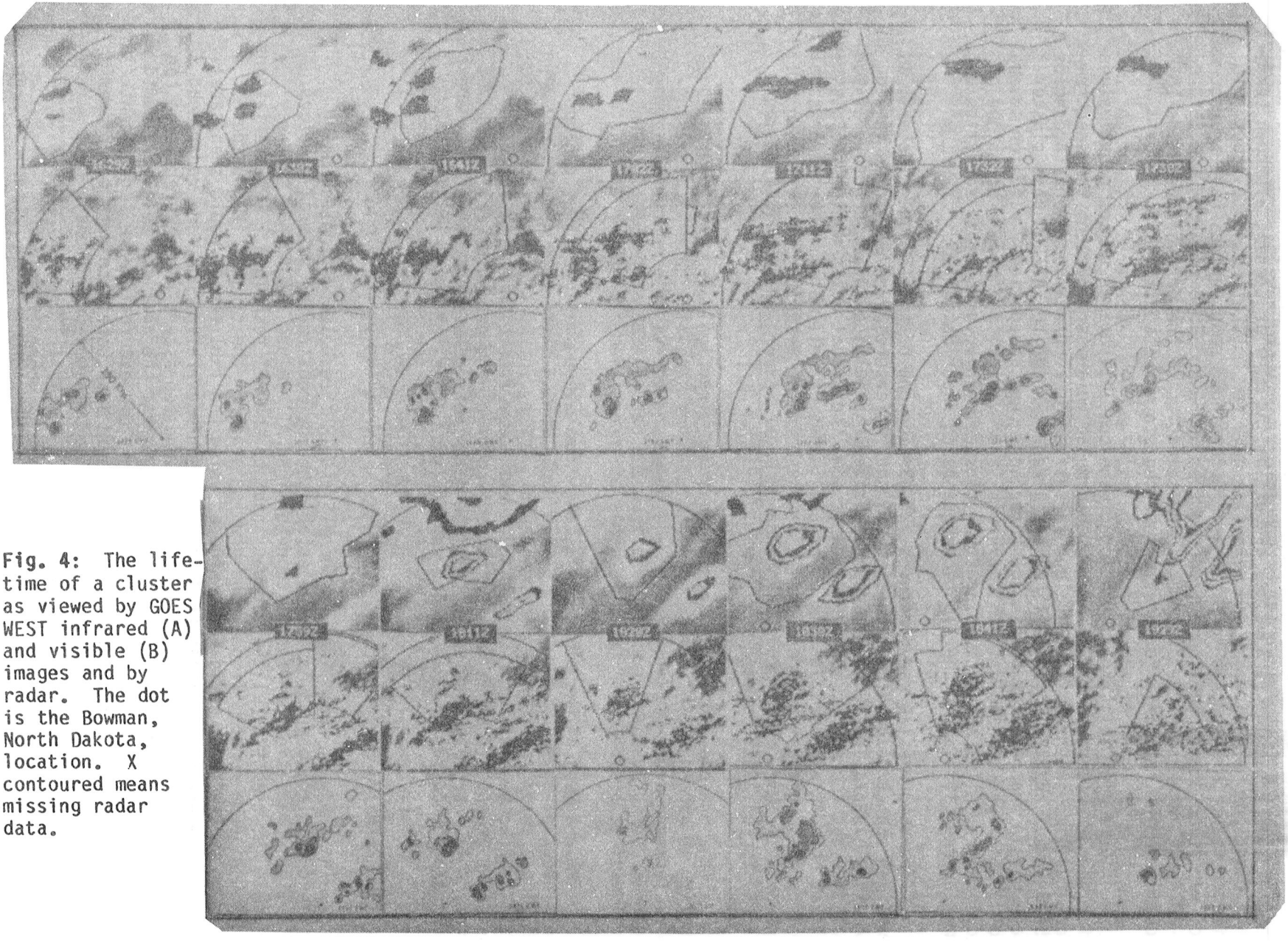

Fig. 4: The lifetime of a cluster as viewed by GOES WEST infrared (A) and visible (B) images and by radar. The dot is the Bowman, North Dakota, location. X contoured means missing radar data.

and of the threshold count values are exhibiting similar trends, although there are time lags between radar and satellite data for most of the time steps. It is important to note that both VIS and IR threshold count values have a spectrum of variation during the storm lifetime from 50.59 to 57.46 and from -20.05°C to -40.45°C, respectively. This makes the selection of one or two thresholds to delineate the rain area for portions of the storm quite difficult.

Figure 3 exhibits the summation of the cumulative area versus count values for the 3-hr storm period. The summed cumulative areas represent the spectrum of Area Time Integral (ATI)[5] values for different count values. The thresholds 54.7 in VIS and 178.9 (≈ -34.15°C) in IR representing the ATI of this cluster are within the range of thresholds throughout the time periods. If, for several clusters, such thresholds do not exhibit large variations, then a technique of delineating ATI's and estimating total cluster rain volumes using satellite data may emerge (similar to the ATI technique using radar data).

The step-by-step radar returns >25 dBz for one of the 12 June clusters, as well as the corresponding satellite VIS and IR features, are displayed in Fig. 4. A visual inspection of the images emphasized the multicellular structure of the cluster and the particular evolution of some individual cells during the cluster's lifetime. An extended discussion of the images as well as of other radar/satellite comparative graphs are presented in a manuscript accepted for inclusion in the preprint volume of the 22nd Conference on Radar Meteorology, 10-13 September 1984, Zurich, Switzerland.

This one case analysis suggests that the direction taken to study the possibility to extend the ATI technique to the use of satellite data is promising. The infrared count value (178.9 or -34,15°C) and the visible count value (54.7) corresponding to the ATI values are situated between the step-by-step count values (defined to match the echo areas of intensities >25 dBz).

An analysis of the cloud top ascent rates showed maximum rates of about one order of magnitude smaller in this North Dakota storm than compared to an Oklahoma storm reported by other authors. The evolution during the storm lifetime of the area of radar echoes and the IR temperature threshold exhibited similar trends. The analysis of the evolution of the echo area (km^2) at 5-dBz threshold intervals, confirmed that the decay rate of strong reflectivity areas decreased much faster than weaker reflectivity areas.

FUTURE PLANS:

The range of variations of the VIS and IR thresholds determined using summed cumulative area has to be established by considering several clusters. If little variations of satellite determined ATI values are found, that may permit the use of satellite data as input to the ATI technique. Such variations might also be reduced if only the growing stage of the cluster is considered. Ten to twelve cases could be considered using the 1981 set of rapid scan satellite data. Comparative analyses of developments of several clouds, and radar-echo parameters will also be performed (i.e., cloud top ascent rates versus echo top ascent rates). Further investigations may extend the analysis to a more humid and warmer climate if the results in this dry midwest region are significant. A possibility will be to explore radar and rapid scan satellite data taken over one extensive region in Oklahoma in 1985 (The Oklahoma Experiment).

[5]ATI: The echo area >25 dBz integrated over the storm lifetime.

JOURNAL PUBLICATIONS:

Doneaud, A. A., S. Ionescu-Niscov, D. L. Priegnitz and P. L. Smith, 1984a: The area-time integral as an indicator for convective rain volumes. J. Climate Appl. Meteor., 23. [In press]

Doneaud, A. A., S. Ionescu-Niscov and J. R. Miller, Jr., 1984b: Convective rain rates and their evolution during storms in a semi-arid climate. Mon. Wea. Rev., 112. [In press]

CONFERENCE PAPER.

Doneaud, A. A., J. R. Miller, Jr., and L. R. Johnson, 1984: An Attempt to Extend the ATI Technique to Estimate Convective Rain Volumes Using Satellite Data. Accepted for presentation and publication in the preprint volume of the 22nd Conf. on Radar Meteor., 10-13 September 1984, Zurich, Switzerland.

Page intentionally left blank

VIII. NATIONAL RESEARCH COUNCIL

RESEARCH ASSOCIATESHIP PROGRAM

Page intentionally left blank

APPLICATION OF THE BOUNDED DERIVATIVE INITIALIZATION METHOD
(F. H. M. Semazzi)

RESEARCH OBJECTIVES:

The objective of this research work is to develop a data insertion scheme based on the Bounded Derivative Method (BDM). The investigation is comprised of three principal phases.

Phase 1. To examine the impact of the BDM as an initialization tool using real data and the GLAS fourth order global barotropic model.

Phase 2. To design and implement a data insertion scheme based on the BDM using the GLAS fourth order global barotropic model.

Phase 3. To extend the treatment in phase 1 and 2 to the GLAS GCM.

SIGNIFICANT ACCOMPLISHMENTS:

Following Semazzi (1983) two constraints on initial data are derived. The first constraint based on the BDM is an equation for calculating initial divergence. The second constraint yields an additional equation of elliptic type for computing the initial height field. This equation is more general than the balance equation first proposed by Charney (1955). It also has more terms which include the contributions of initial divergence and orography.

The comparison in Fig. 1 demonstrates that the BDM effectively suppresses high frequency motions in this case of real data. A comparison between Fig. 1 and Fig. 2 indicates that both the BDM and the Nonlinear Normal Mode method (NNM) have consistent impact on the numerical integration results. This observation has two important implications. First, in a practical sense, it confirms the results of earlier theoretical studies where the two methods were compared. Secondly, the agreement with the well established NNM demonstrates the suitability of applying the BDM to real data, a factor which is of vital importance to the next phase of this work during which the method is applied to the data insertion problem.

CURRENT RESEARCH:

The current research effort is aimed at developing a data insertion scheme based on the BDM. The experiments are of the identical twin kind. The control experiment starts from balanced synoptic data. The second experiment starts from climatology and data is continuously assimilated into the forecast from the control experiment. The insertion data coverage and frequency of insertion are designed to simulate a polar orbiter satellite data source.

FUTURE PLANS:

Phase 3 which is outlined above.

REFERENCES:

Charney, J., 1955: The use of the primitive equations of motion in numerical prediction. Tellus, 7, 22-26.

Semazzi, H. F. M., 1983: On the bounded derivative initialization method. Ph.D thesis (Nairobi University).

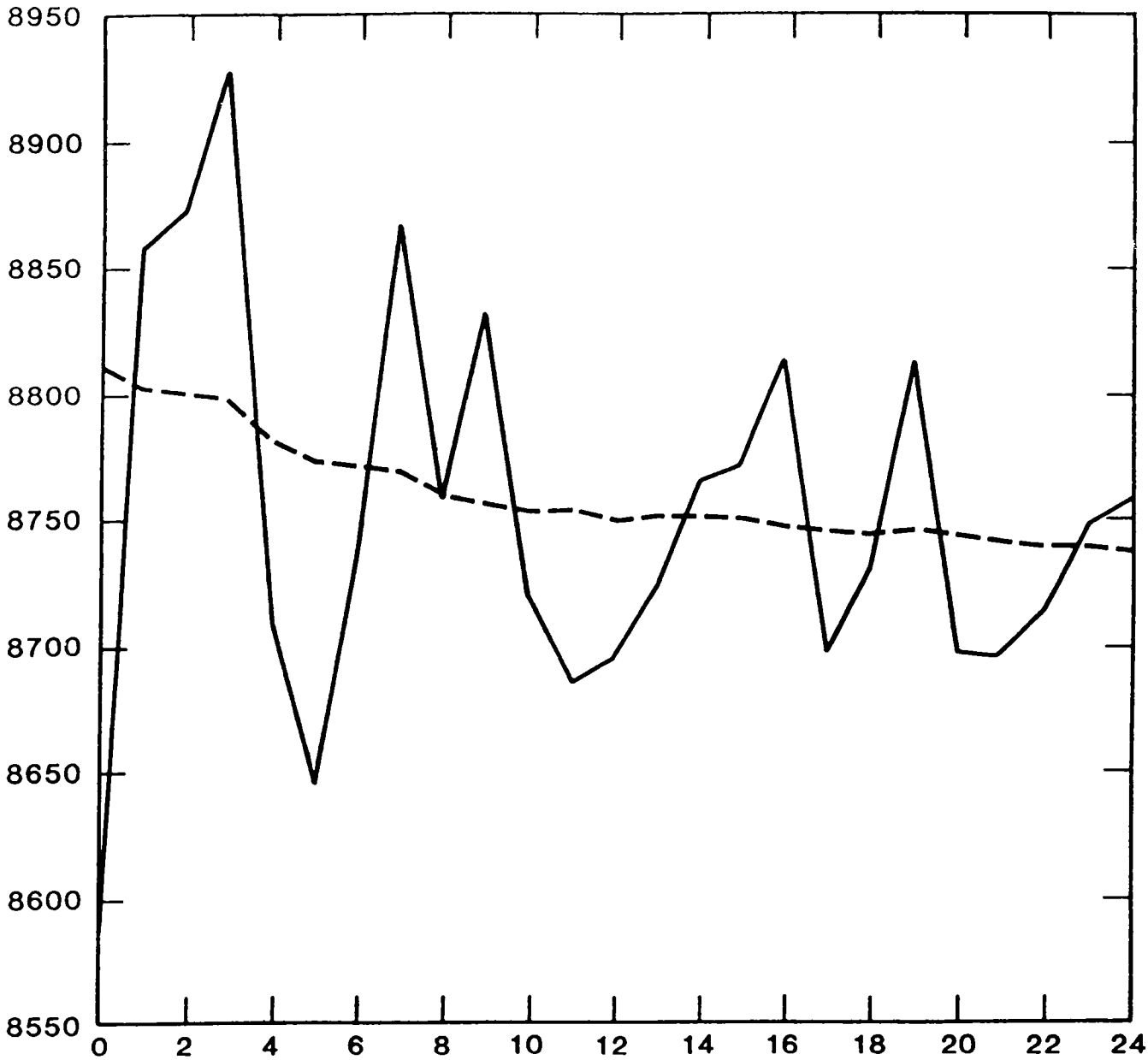

Fig. 1 Height (m) as a function of time (hours) at (60°W, 40°S). Solid curve is the uninitialized case. Dotted curve is the BDM case.

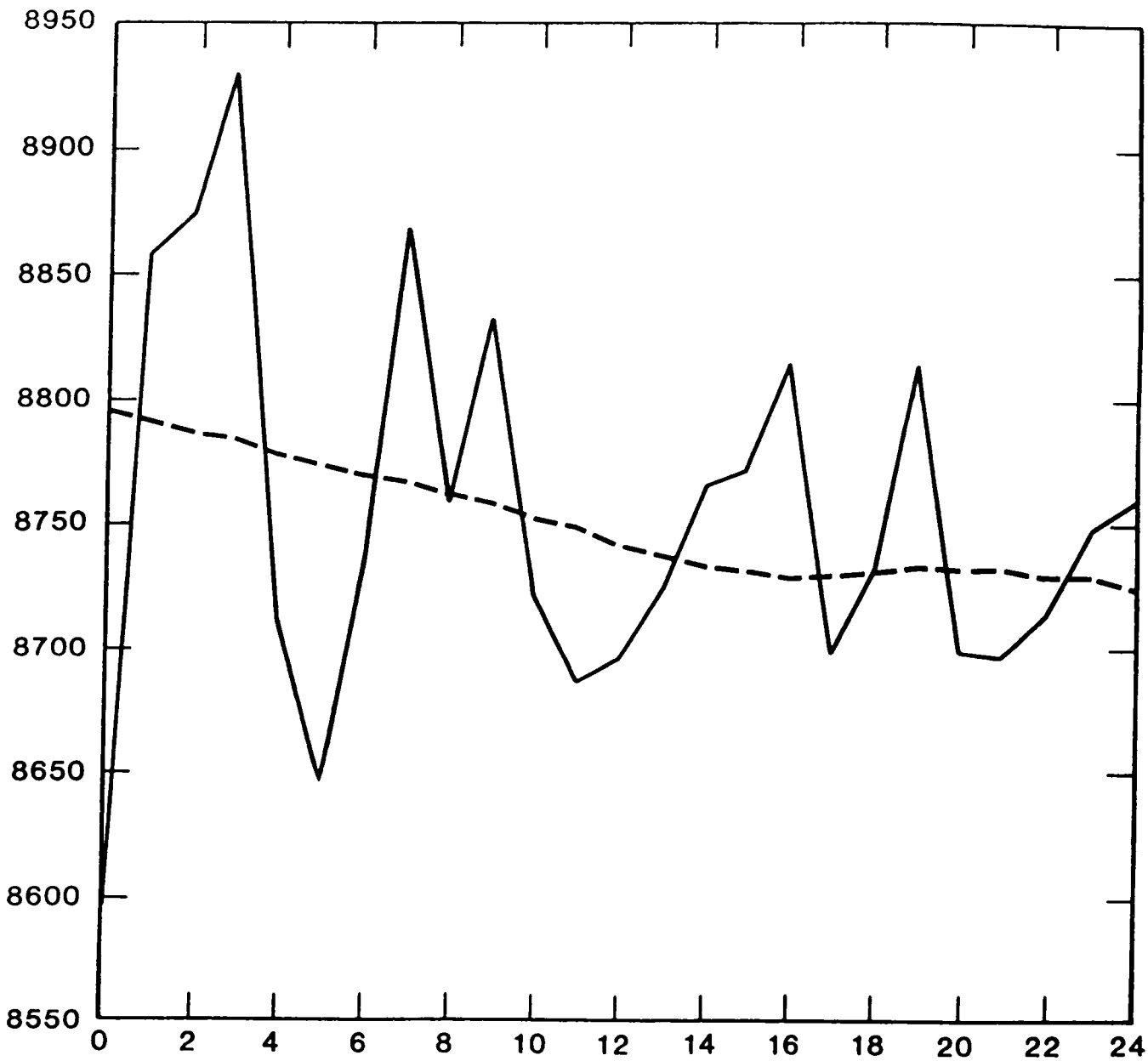

Fig. 2 Height (m) as a function of time (hours) at (60°W, 40°S). Solid curve is the uninitialized case. Dotted curve is the NNM case.

IMPLICIT NUMERICAL METHODS IN METEOROLOGY
(J. Augenbaum-GSFC/RRA)

RESEARCH OBJECTIVE:

The computational efficiency of current primitive equation models - explicit or semi-explicit in time, spectral finite-difference or finite-element in space is limited by a stability criterion on the size of the time step. The major objective of the research (project) is to develop a fully implicit finite-difference model, whose time step is chosen solely to resolve accurately the physical flow of interest. The method is based on an operator factorization which reduces the dimensionality of the implicit approach: at each time step only (spatially) one-dimensional block-tridiagonal linear systems must be solved. The scheme uses two time levels and is second-order accurate in time. Compact implicit spatial differences are used, yielding fourth-order accuracy both vertically and horizontally.

In addition, a significant objective of the project is to develop and implement a fully interactive computer code where the user will have a choice of models, with various levels of accuracy and sophistication, which are imbedded, as subsets of the fully implicit 3D code.

The current design of the code provides for the following options:

1. Solve 3-D baroclinic primitive equations or any 2-D subset, including shallow water and vertical slice models.

2. Temporal discretization: implicit or explicit second-order scheme.

3. Horizontal discretization: fourth-order implicit or explicit, or second-order explicit.

4. Vertical discretization: fourth-order implicit or second order explicit.

5. Grid system: nonstaggered uniform or nonuniform in any direction.

6. Can solve the forced system $L(\overline{W}) = L(\overline{W}_0)$ where $\overline{W}_0$ is any linear combination of Hough harmonics.

7. Interactive input, output, and graphics available.

This research is being carried out in collaboration with Drs. S. Cohn (NYU), D. Dee (PUCRJ/BRAZIL), E. Isaacson (NYU), E. Kalnay (GLAS), and D. Marchesin (PUCRJ/BRAZIL) and with the assistance of G. Hsu (NYU) and Arlinda Silva de Moraes (PUCRJ/BRAZIL).

SIGNIFICANT ACCOMPLISHMENTS:

1. The overall design of the complete code has been formulated so that the explicit 3D version and all 2 dimensional versions are included as subsets of the 3D implicit code.

2. General purpose software packages have been developed to allow the user to interactively specify the options he wants for a given model run. These general purpose software packages have widespread applicability and can easily be integrated into any partial differential equation solver.

3. The explicit 2 and 3 dimensional versions of the code is written and extensive testing and debugging has recently begun.

CURRENT RESEARCH:

Current research centers around two main areas:

1. A detailed mathematical analysis of the stability and accuracy of the implicit scheme.

2. Numerical testing and debugging of the various versions of the code.

Specifically, we are conducting a detailed mathematical and numerical study of the factorization error for a linearized barotropic primitive equation model when large time steps are used. We are also conducting a mathematical investigation to prove the unconditional stability of the 3D implicit scheme for the linearized baroclinic primitive equations.

Testing and debugging of the shallow water version of the code is continuing. This is being accomplished by using equations forced by a right hand side consisting of prescribed linear combinations of Hough harmonics. These forced equations have exact solutions which can be easily computed and compared to the computed solutions to diagnose coding errors. The forced solutions are also being used for accuracy studies of the various numerical schemes.

Testing and debugging of the 3D codes will begin as soon as the shallow water versions are sufficiently debugged. Since the subroutines used in the shallow water version make up most of the 3D code, when the shallow water codes are debugged, the 3D codes will themselves be almost completely debugged.

At this point the model will interface with the GLAS physics and GLAS data sets for direct comparisons and accuracy tests.

FUTURE PLANS:

In the future, a vector version of the implicit scheme will be developed to run on the Cyber 205.

Also, a full documentation of the entire code will be written.

PUBLICATIONS AND REFERENCES:

Augenbaum, J., S. Cohn and D. Marchesin, 1984: The Effects of Compact Implicit Differencing in a Baroclinic Primitive Equation Model. Research Review 1983, NASA Tech. Memo 86053, 87-90.

Augenbaum, J., S. Cohn, D. Dee, E. Isaacson, D. Marchesin and G. Zwas, 1984: A Fully Implict Scheme for the Baroclinic Primitive Equations: Shallow Water Models. (In preparation).

Cohn, S., D. Dee, D. Marchesın, 1982: Baroclinic models with fourth-order vertical accuracy: Preliminary report. Segundo Congresso Brasileiro de Meteorologia, proceedings to appear. Sociodade Brasileiro de Meterologia, Oct., 1982.

Marchesın, D., 1984: Using exact solutions to develop an implicit scheme for the baroclinic primitive equations. Mon. Wea. Rev., 112, 269-277.

INTERANNUAL VARIABILITY IN THE OBSERVED CIRCULATION
(Glenn H. White-GSFC/RRA)

RESEARCH OBJECTIVES:

To increase our understanding of variability in the atmospheric circulation.

SIGNIFICANT ACCOMPLISHMENTS:

a) An observational study, with Prof. B. J. Hoskins, of the relative roles of transient eddies and the time-mean flow in maintaining the momentum balance and in forcing vertical motion has illuminated the role of time-mean secondary circulations forced by transient eddies. These secondary circulations transport westerly momentum from the upper to the lower troposphere in the storm tracks, accelerating surface westerlies and making the time-mean flow more barotropic.

b) An observational study, with Dr. K. C. Mo, of teleconnections in the Southern Hemisphere revealed a zonal wavenumber 3 pattern of low-frequency variability in the wintertime midlatitudes and a land-ocean "seesaw" during summer.

c) An observational comparison of the Northern Hemisphere winters of 1980-81 and 1981-82 found substantial differences in circulation patterns, but little evidence of substantial changes in tropical heating. The circulation changes may have been associated with substantial changes in low-frequency transient eddies in the Pacific, perhaps related to barotropic instability in the exit region of the Asian jet. Changes in the baroclinicity of the low-level flow appeared to be associated with changes in the storm tracks, while changes in the transient eddies appeared to play a minor role in interannual differences in the zonal momentum balance or in the forcing of vertical motion.

CURRENT RESEARCH:

A simulation of the atmospheric circulation by the UCLA general circulation model (GCM) is being compared to observations. Results suggest that the time-mean structure of the Northern Hemisphere wintertime circulation is reproduced fairly well in the GCM and that transient eddies in the GCM are qualitatively similar to observed transient eddies and have similar relationships to the time-mean flow. Low-frequency transient eddies (periods longer than 10 days) are significantly weaker in the GCM than in observations. Blocks appear in the GCM and appear to be supported by transient eddies of baroclinic time scales, as is seen in observations.

FUTURE PLANS:

a) Further investigations into the UCLA GCM simulation will compare the time-averaged zonal momentum budget and omega equation in the model to those observed. Blocking events, interannual variability and the effect of sea-surface temperature anomalies will also be investigated in the GCM. A similar investigation into the simulation of the atmosphere by the GLAS GCM is also planned.

b) Further investigations into interannual variability are planned, using several years of circulation statistics and FGGE analyses. Possible relationships between the baroclinicity of the time-mean flow and the storm tracks and between barotropic instability and interannual variability of the seasonal mean flow will be investigated. FGGE analyses will be used to examine the momentum budget and patterns of vertical motion and diabatic heating.

JOURNAL PUBLICATIONS:

Mo, K.-C., and G. H. White, 1984: Teleconnections in the Southern Hemisphere. Submitted to Mon. Wea. Rev.

White, G. H., and B. J. Hoskins, 1984: An observational study of the role of transient eddies in maintaining the seasonal mean circulation. In preparation.

White, G. H., 1984: Two contrasting Northern Hemisphere winters, 1980-81 and 1981-82. In preparation.

CONFERENCE PUBLICATIONS:

White, G. H., 1983: An observational study of the relative roles of the time-mean flow and transient eddies in interannual variability. Presented at the IAMAP-WMO Symposium on Maintenance of the Quasi-stationary Components of the Flow in the Atmosphere and in Atmospheric Models, Paris, France, Aug. 29-Sept. 2, 1983.

Mo, K.-C., and G. H. White, 1984: Teleconnections in the Southern Hemisphere. Presented at the 1984 Stanstead Seminar, Lennoxville, Quebec, Canada, July 9-13, 1984.

LINEAR STUDIES OF STATIONARY, EXTRATROPICAL ANOMALIES IN THE TROPOSPHERE

(J. L. Kinter III-GSFC/RRA)

RESEARCH OBJECTIVES:

The Pacific-North American pattern (PNA) has received a great deal of attention in the recent literature as one of the dominant spatial modes of variability in the extratropical, winter troposphere of the Northern Hemisphere on time scales of one month to one season. The pattern, with four "centers of action" in the north Pacific and over North America (figure 1), was identified by Wallace and Gutzler (1981, hereinafter referred to as WG) in the monthly mean 500 mb geopotential height anomalies. Horel and Wallace (1981) noticed a similar spatial pattern in correlations of 700 mb geopotential height with equatorial Pacific sea surface temperature and the Southern Oscillation index.

Patterns resembling the PNA have also been identified in general circulation model (GCM) experiments. These have fallen into two categories: experiments with anomalous forcing and those without. Lau (1981) found that the internal variability in a 15-year integration of the medium resolution Geophysical Fluid Dynamics Laboratory spectral model without anomalous forcing has a spatial pattern quite similar to the PNA. In the category of experiments including anomalous forcing, several GCM studies have identified modes of variability quite similar to the PNA resulting from anomalous tropical sea surface temperature (SST) boundary conditions. Most recently, Shukla and Wallace (1983), Blackmon, et al. (1983) and Suarez (1984, personal communication) have noticed PNA-like responses to equatorial Pacific SST anomalies.

In the category of experiments including anomalous forcing, several GCM studies have indicated that there are free and forced modes which may be considered to correspond to the PNA. Simmons et al. (1983) examined the normal modes of the barotropic vorticity equation on the sphere linearized about the zonally varying 300 mb observed climatological mean flow. They found that the fastest growing (unstable) mode resembles the PNA in one phase and another of the WG teleconnections in another phase. Blackmon, et al. (1984) have interpreted their findings regarding observed variability on intermediate time scales (10-30 days) as a possible manifestation of this mechanism.

Alternatively, the PNA may be considered a forced mode response. Using the barotropic vorticity equation on a sphere, linearized about a zonally symmetric basic state, Branstator (1984) showed that variations in the planetary wave response to climatological forcing associated with observed changes in the zonal mean flow have a PNA-like spatial structure. The mechanism causing the observed changes in the basic state is not considered, but may be associated with fluctuations in the Hadley and Walker circulations due to variations in tropical forcing. It is the objective of this project to identify the full physical mechanism for PNA variability.

SIGNIFICANT ACCOMPLISHMENTS:

The work described herein is similar to that of Branstator (1984) in that the same model is used. However, the forcing, rather than being derived as a residual from the observed climatological planetary waves, is topographic

forcing. Further, the variations in the mean state, rather than being co ed from the empirical orthogonal function analysis of the observed, zonal mean zonal winds, are computed by compositing (after WG) the zonal winds only in the 180 degree longitude sector to the west of the PNA region. That is, positive and negative PNA composite zonal winds are averaged in the sector 90E - 180 - 90W to obtain basic states. The steady, linear solution is then computed for each basic state, and the difference of the two is calculated. The resulting difference pattern is shown in figure 2. The solution difference has a correlation coefficient of 0.500 with the observed difference in figure 1. A nonlinear extension of this result, in which the zonal mean flow is prevented from deviating from the observed composite, shows a very similar solution well correlated with the observed composite difference (Figure 3).

CURRENT RESEARCH:

The results with barotropic models are being expanded in three ways. First, a multilevel, primitive equations model is being utilized in an effort to identify the dominant modes of variability in the baroclinic atmosphere and to compare such modes with the PNA. Second, further experiments with the nonlinear barotropic model are planned to examine the roles of free and forced modes in that model's variability. In one experiment, the most unstable mode of Simmons et al. (1983) will be used as the initial condition, and its evolution will be studied. Another experiment is planned in which the zonally symmetric parts of various phases of the most unstable mode will be used as basic states in the nonlinear model to examine the forced solutions for such mean flows. Third, the implications for atmospheric blocking will be explored in experiments designed to measure the degree of Rossby wave focusing achieved by various zonally varying basic states.

FUTURE PLANS:

After these simple model tests have been carried out, the underlying themes will be tested in a GCM. In particular, diagnostic analyses of energy transfers between the basic state and planetary waves under various conditions (e.g., seasonal forcing vs. anomalous forcing) will be instructive and will enhance understanding of the variability of the basic state as well as planetary wave variability.

REFERENCES:

Blackmon, M. L., J. E. Geisler, and E. J. Pitcher, 1983: A general circulation model study of January climate anomaly patterns associated with interannual variation of equatorial Pacific sea surface temperatures. J. Atmos. Sci., 40, 1410-1425.

_____, Y.-H. Lee and J. M. Wallace, 1984: Horizontal structure of 500 mb height fluctuations with long, intermediate and short time scales. To appear in J. Atmos. Sci.

Branstator, G., 1984: The relationship between zonal mean flow and quasi-stationary waves in the midtroposphere. Submitted to J. Atmos. Sci.

Horel, J. D. and J. M. Wallace, 1981: Planetary scale atmospheric phenomena associated with the Southern Oscillation. Mon. Wea. Rev., 109, 813-829.

Lau, N.-C., 1981: A diagnostic study of recurrent meteorological anomalies appearing in a 15-year simulation with the GFDL general circulation model. Mon. Wea. Rev., 109, 2287-2311.

Skukla, J. and J. M. Wallace, 1983: Numerical simulation of the atmospheric response to equatorial Pacific sea surface temperature anomalies. J. Atmos. Sci., 40, 1613-1630.

Simmons, A. J., G. W. Branstator and J. M. Wallace, 1983: Barotropic wave propagation, instability and atmospheric teleconnection patterns. J. Atmos. Sci., 40, 1363-1392.

Wallace, J. M. and D. S. Gutzler, 1981: Teleconnections in the geopotential height field during the Northern Hemisphere winter. Mon. Wea. Rev., 109, 784-812.

JOURNAL PUBLICATION:

Kinter, J. L., 1984: Planetary-scale waves and blocking patterns in barotropic atmospheric models, Part I. In preparation.

CONFERENCE PUBLICATIONS:

Kinter, J. L., 1984: Barotropic studies of stationary, extratropical anomalies in the troposphere. Proceedings of the 1984 Stanstead Seminar (Lennoxville, Quebec, Canada, July 9 - 13, 1984). McGill University, 1984.

Kinter, J. L., 1983: Numerical simulation of anomalous stationary waves in a barotropic atmosphere. IAMAP Symposium on Blocking and Atmospheric Prediction: Programme and Abstracts (Hamburg, F.R.G., August 15-27, 1983). IUGG-IAMAP, 1983, 129.

Kinter, J. L., 1983: Numerical simulation of anomalous stationary waves in a barotropic atmosphere. IAMAP-WMO Symposium on the Maintenance of the Quasi-Stationary Components of the Flow in the Atmosphere and in Atmospheric Models (Paris, France, August 29 September 2, 1983). WMO, 1983, 291-293.

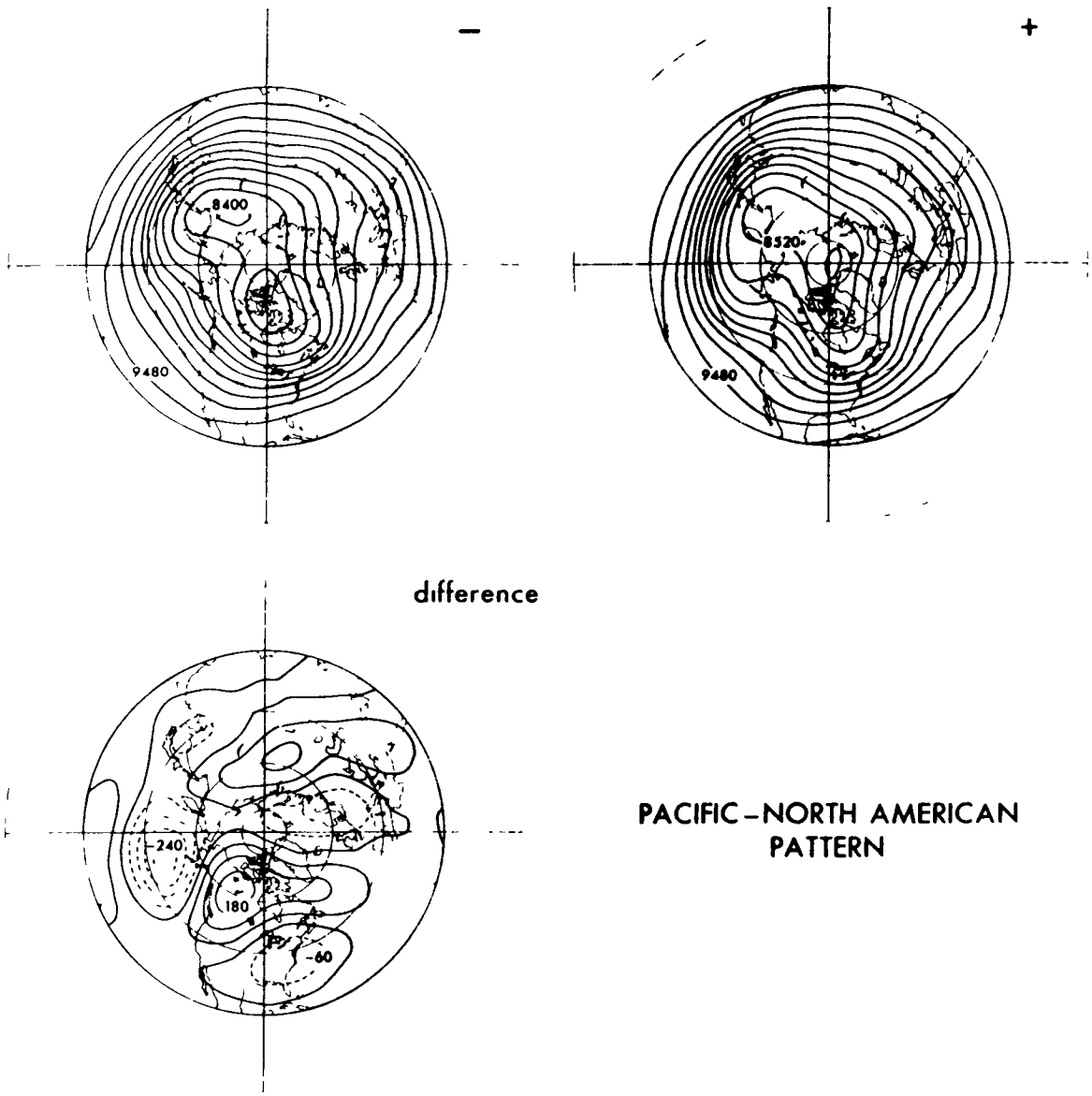

Figure 1 Winter monthly mean, Pacific-North American pattern teleconnection index composite, 300 mb geopotential height. At upper left is the negative index composite, at upper right is the positive index composite (both with a contour interval of 120 geopotential meters), and at lower left is the difference of the two (with a contour interval of 60 geopotential meters).

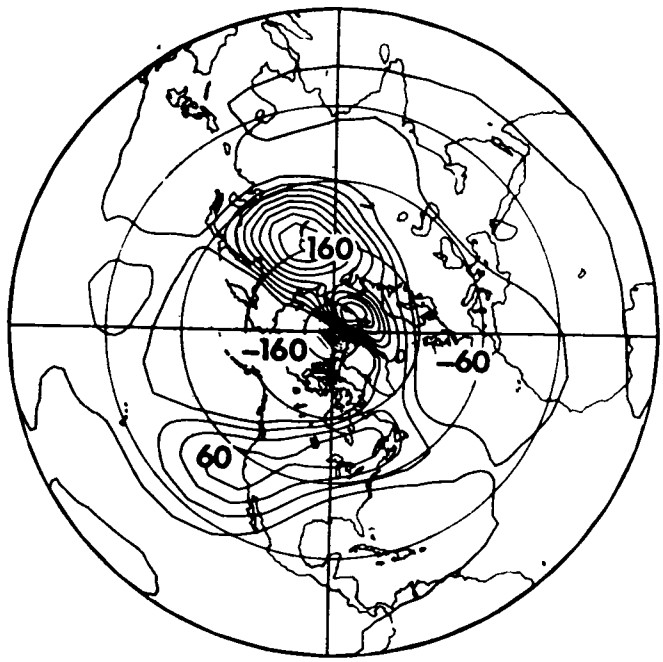

Figure 2 Eddy geopotential height solution of the steady, linear barotropic vorticity equation on a sphere with PNA (positive minus negative) composite sector mean zonal winds as basic state. The sector chosen for the basic state is 90E - 180 - 90W.

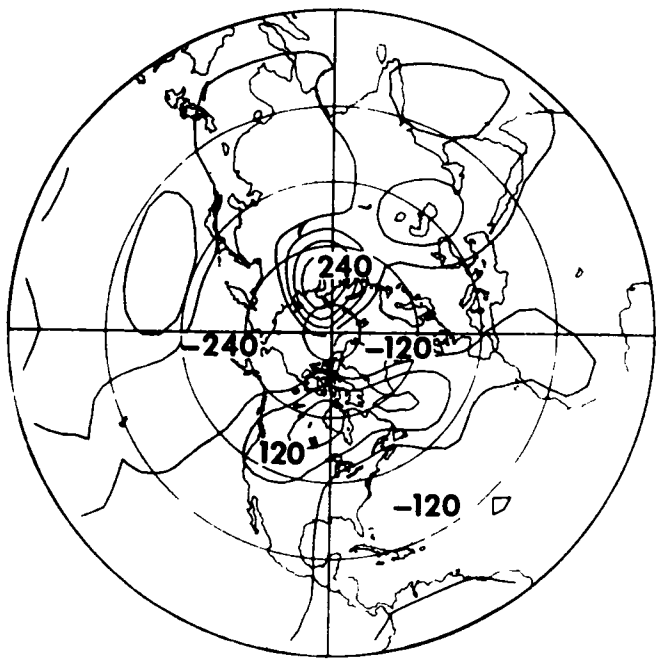

Figure 3 As in figure 2 except for time mean of nonlinear integration of the shallow water equations on a sphere. The zonally symmetric basic state is forced to remain near its initial condition.

MIXED LAYERS AND SATELLITE RETRIEVALS
(R. Boers-GSFC/RRA)

RESEARCH OBJECTIVES.

As part of the process to determine whether it is possible to retrieve boundary layer structure with the current sounding techniques, temperature retrievals were performed for radiosonde profiles that showed temperature inversions. It was found that when temperature inversions exceed 8-10° C a retrieval will indeed show a temperature increase with height over a limited vertical distance. For weaker inversions retrieved temperatures are generally smoothly decreasing with height. It is, however, impossible to determine the actual mixed layer height from the retrievals. A typical inversion profile and retrieval is shown in figure 1.

SIGNIFICANT ACCOMPLISHMENTS:

We investigated whether the water vapor channels could be used in observing mixed layer structure. Temperature inversions are accompanied by significant drops in relative humidity. While this effect is very pronounced in parts of the trade wind regimes with relative humidity drops of up to 60%, it is widespread in other areas of the ocean as well. We performed a simulation experiment in which brightness temperatures were computed for smooth temperature and humidity profiles and compared with those computed from inversion profiles. To simulate different atmospheric conditions a variety of inversion strengths and relative humidity jumps were chosen. The results showed that brightness temperatures for water vapor channels 10-12 were markedly warmer for the inversion profiles than for the smooth profiles. This was due to the enhanced water vapor emission close to the surface relative to the air above the inversion. This enhanced emission results in a maximum of the sensitivity function closer to the surface. An example of the change in sensitivity function for the water vapor channels is shown in figure 2.

We proceeded by examining a set of 800 randomly selected oceanic temperature profiles for the existence of temperature inversions. Approximately half of the profiles contained some type of inversion indicating that it is a commonly found feature. Brightness temperatures were computed for this set of inversion profiles. Based on the computed brightness temperatures a water vapor and temperature retrieval was performed followed by a computation of brightness temperatures from the retrievals. Attempts were made with no success to seek relations between various observed temperature and humidity parameters and the brightness temperature computed form the original profiles. We proceeded by subtracting the brightness temperatures based on the retrievals from the brightness temperatures based on the observed profiles. No signal was found that could systematically differentiate between various types of inversion strengths and humidity drops. The reason for this is that water vapor is a highly variable function of height. Frequently secondary maxima in water vapor content are found well above the mixed layer. Combined with the natural variability of the temperature profiles it produces a very complex functional dependence of water vapor brightness temperature on temperature.

FUTURE PLANS:

Additional tests are planned to discern mixed layer structure with the current sounding techniques. Those tests will involve the determination of atmospheric stability criteria for retrievals to discern the existence of stratification. Also model computations are planned that allow for the development of mixed layer structure in retrievals in accordance with observed brightness temperatures.

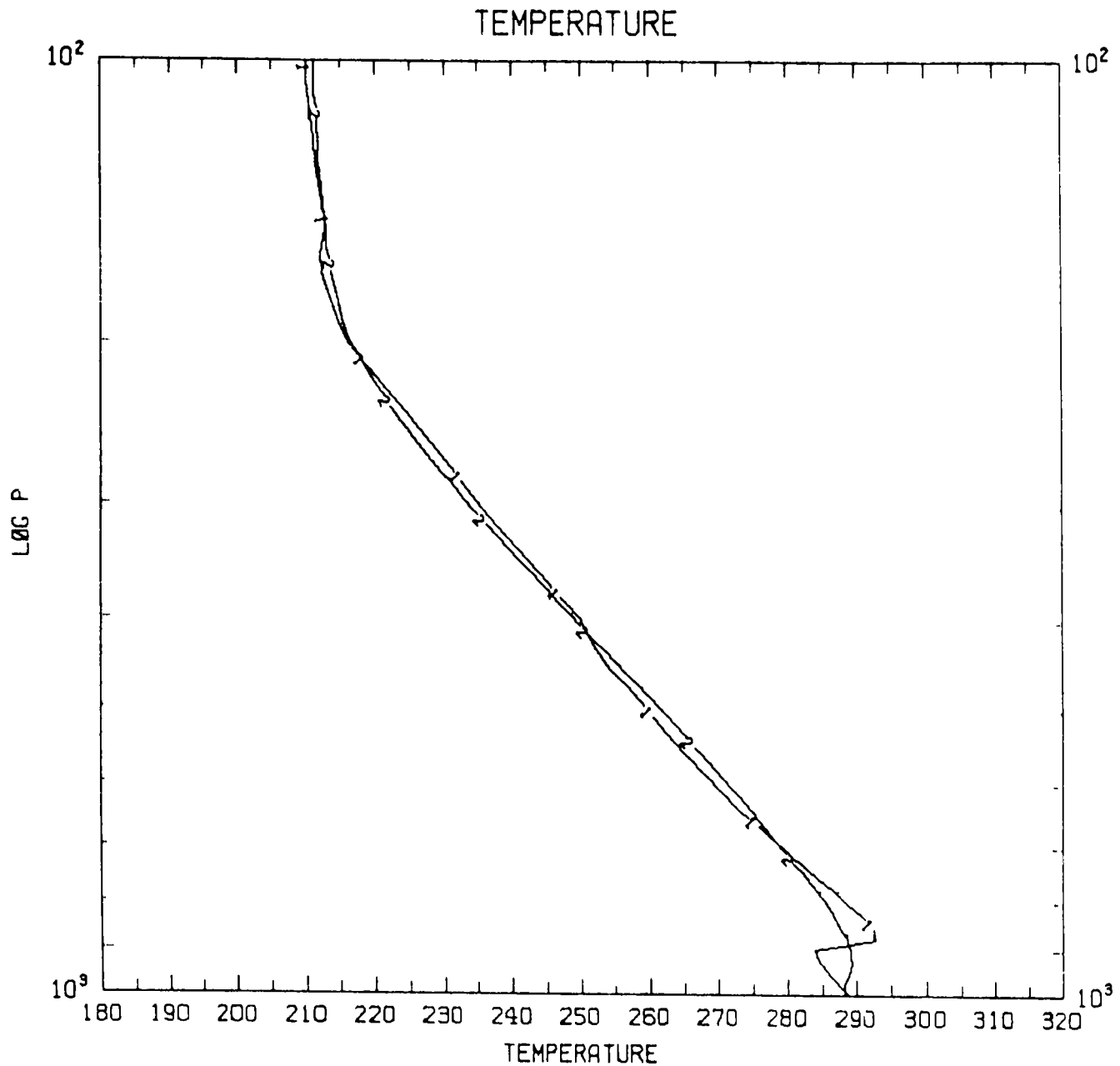

Figure 1. A typical inversion profile (1) with the associated retrieval (2)

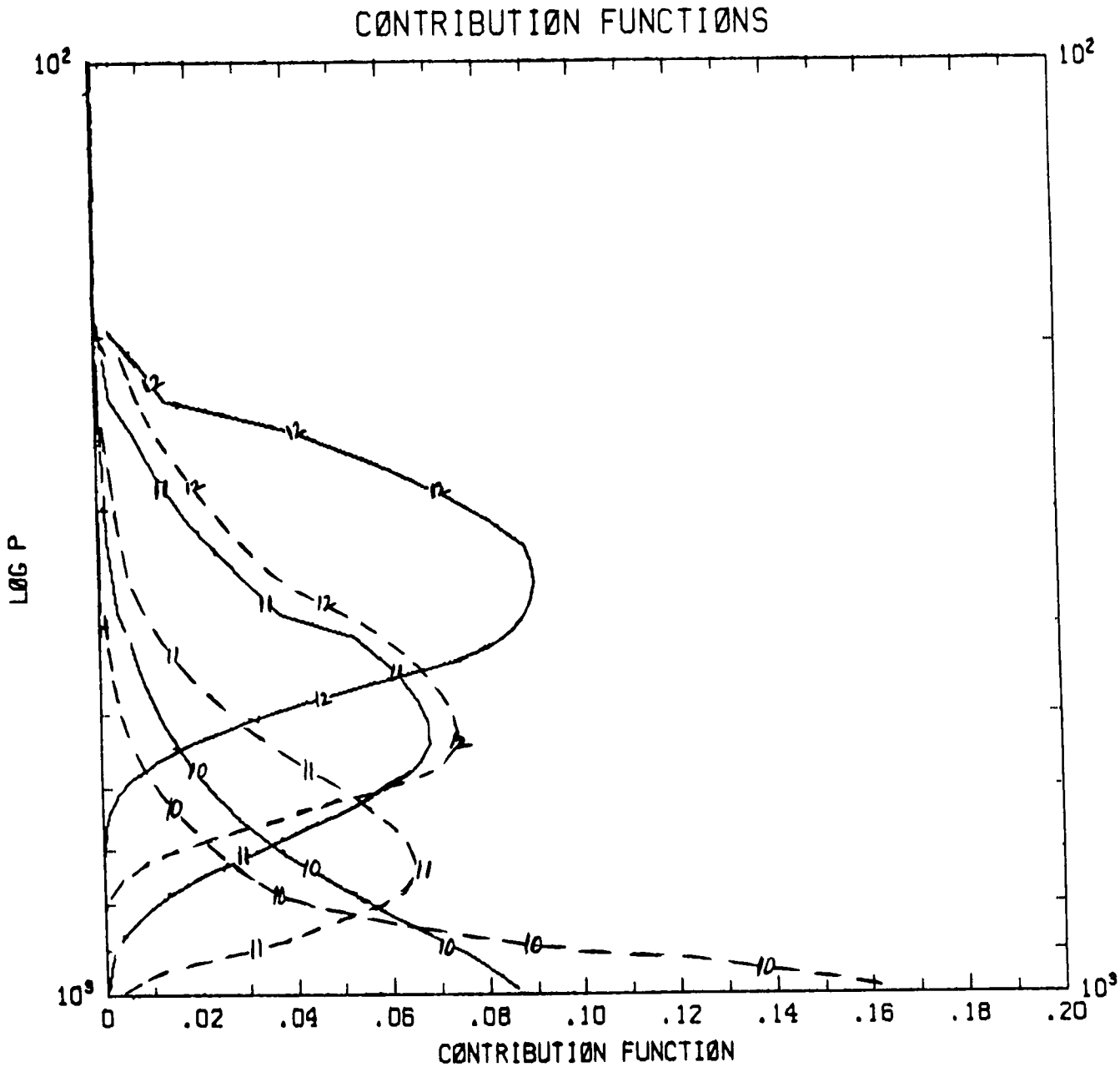

Figure 2. Contribution function for water vapor channels 10, 11, 12 for inversion (_ _ _) and for no inversion (_____).

THE INFLUENCE OF SYNOPTIC SCALES ON LOW-FREQUENCY MODES OF VARIABILITY
(S. D. Schubert)

RESEARCH OBJECTIVES:

An important factor influencing our ability to extend the present day range of useful weather forecasts is our poor understanding of the nature of atmospheric modes having time scales of approximately one week to several months. The basic goal of this research is to study the factors limiting the predictability of these modes. The present analysis centers on the role of synoptic scales in the evolution of low frequency modes.

SIGNIFICANT ACCOMPLISHMENTS:

The initial focus of this study has been on model analysis and predictability studies using an equivalent barotropic empirical orthogonal function (EOF) model described in Schubert (1984b). An extensive set of 10-day forecasts has been produced for the 12 component version of the model. Comparisons with observed data show apparently useful forecasts for individual winters (Schubert, 1984c). However, when averaged over 10 winters, the improvement over persistence was marginal and only one of the EOF's (resembling North Atlantic blocking) showed a statistically significant improvement. These results suggest the need for a more realistic model which includes shorter time scale baroclinic processes and spatial modes capable of efficiently representing the characteristic structures associated with baroclinic instability.

CURRENT RESEARCH:

A natural extension of the equivalent barotropic model is the 2-level model (Lorenz, 1960) written here as

$$\frac{\partial}{\partial t} \nabla^2 \Psi = J(\nabla^2 \Psi + f, \psi) + J(\nabla^2 \tau, \tau) + ... \qquad (1a)$$

$$\frac{\partial}{\partial t} (\nabla^2 - r)\tau = J(\nabla^2 \Psi + f, \tau) + J(\nabla^2 \tau, \psi) + ... \qquad (1b)$$

with an appropriate diagnostic relationship for the divergent wind field. The sum and difference stream function at the 2 levels is given by Ψ and τ, respectively. In its final form this model is written as a set of quadratically nonlinear prognostic equations for the EOF coefficients. The EOF's are computed from 10 winters of the stream function anomaly field at 500 mb (Ψ (500)) and the shear field (τ) defined as (Ψ (200) - Ψ (700))/2. The EOF's are computed separately for data filtered by a band pass filter ($T \lesssim 6$ days) and low pass filter ($10 \lesssim T \lesssim 90$ days). The filter is identical to that described in Blackmon and Lau (1980).

Figure 1a shows an example of the band pass EOF's. The spatial distribution of EOF 2 is dominated by zonal wave numbers 6, 7 and 8 concentrated over the

North Atlantic and the east coast of North America. This mode is very similar to some of the band pass correlation maps of Blackmon et al. (1984). Figure 1b shows the corresponding shear field (τ) for this mode. Note the approximate 90° phase shift indicating a baroclinic structure.

Currently only the barotropic interactions ($J(\nabla^2\Psi,\Psi)$) have been computed for the 25 component EOF model consisting of the first 12 low pass EOF's and the first 13 band pass EOF's. An inspection of these interaction coefficients shows that the second EOF (also the third, which is a 90° phase shifted version of EOF 2) interacts very efficiently with the ninth (North Atlantic blocking) low pass EOF (see Schubert, 1984a for a description of the ninth low pass EOF). The sense of this interaction is to enhance the anticyclonic flow in this region. This is in contrast to the interaction of EOF 9 with the other low frequency modes which tend to destroy the anticyclonic flow.

FUTURE PLANS:

Future work involves a continuation of the EOF model analysis with particular emphasis on the shear components. These results will be used to diagnose the forecasts of the GLAS fourth order general circulation model.

REFERENCES:

Blackmon, M. L. and N.-C. Lau, 1980: Regional characteristics of the northern hemisphere circulation: A comparison of the simulation of a GFDL general circulation model and observations. J. Atmos. Sci., 37, 497-514.

Blackmon, M. L., Y.-H. Lee and J. M. Wallace, 1984: Horizontal structure of 500 mb height fluctuations with long, intermediate and short time scales. J. Atmos. Sci., 41, 961-979.

Lorenz, E. N., 1960: Energy and numerical weather prediction. Tellus, 12, 364-373.

Schubert, S., 1984a: A statistical-dynamical study of empirically determined modes of atmospheric variability. Part I: Data analysis and interpretation. Submitted to J. Atmos. Sci.

Schubert S., 1984b: A statistical-dynamical study of empirically determined modes of atmospheric variability. Part II: Model formulation and analysis. Submitted to J. Atmos. Sci..

Schubert, S., 1984c: Predictability experiments using a low-order empirically corrected dynamical model. NASA Tech. Memo. 86053, 157-163.

JOURNAL PUBLICATIONS:

Schubert, S., 1984: A statistical-dynamical study of empirically determined modes of atmospheric variability. Part I: Data analysis and interpretation. Submitted to J. Atmos. Sci.

Schubert, S., 1984: A statistical-dynamical study of empirically determined modes of atmospheric variability. Part II: Model formulation and analysis. Submitted to J. Atmos. Sci.

TECHNICAL PUBLICATION:

Schubert, S., 1984: Predictability experiments using a low-order empirically corrected dynamical model. NASA Tech. Memo. 86053, 157-163.

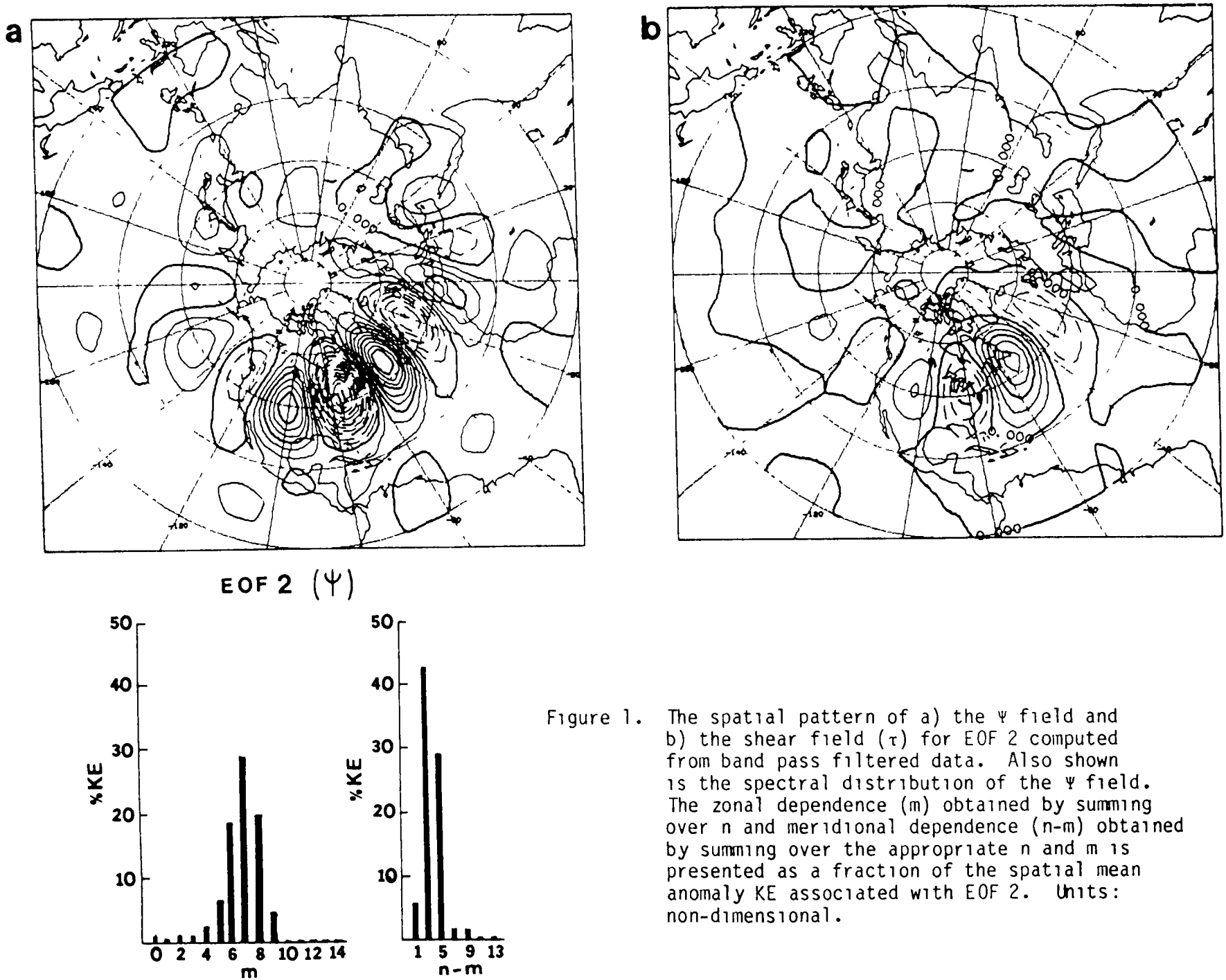

Figure 1. The spatial pattern of a) the Ψ field and b) the shear field (τ) for EOF 2 computed from band pass filtered data. Also shown is the spectral distribution of the Ψ field. The zonal dependence (m) obtained by summing over n and meridional dependence (n-m) obtained by summing over the appropriate n and m is presented as a fraction of the spatial mean anomaly KE associated with EOF 2. Units: non-dimensional.

BIBLIOGRAPHIC DATA SHEET

1. Report No.	2 Government Accession No	3 Recipient's Catalog No
NASA CP-2344		

4. Title and Subtitle	5. Report Date
GLOBAL SCALE ATMOSPHERIC PROCESSES RESEARCH PROGRAM REVIEW	November 1984
	6. Performing Organization Code 911
7. Editors: Barbara A. Worley and Cindy Peslen	8 Performing Organization Report No
9 Performing Organization Name and Address: Global Scale Atmospheric Processes Program, Goddard Space Flight Center, Greenbelt, MD 20771	10. Work Unit No
	11 Contract or Grant No
12 Sponsoring Agency Name and Address: National Aeronautics and Space Administration, Washington, D.C. 20546	13. Type of Report and Period Covered: NASA Conference Publication
	14 Sponsoring Agency Code

15 Supplementary Notes

16. Abstract

This document includes progress reports of scientific research concerning the following areas: Global Modeling; Satellite Data Assimilation and Initialization; Satellite Retrieval Methods; Simulation of Future Observing Systems; Model and Observed Energetics; Dynamics of Planetary Waves; FGGE Diagnostic Studies; and National Research Council Research Associateship Program. These reports were presented at the Global Scale Atmospheric Processes Research Program Review, held 8-10 August 1984 in Greenbelt, Maryland.

17 Key Words (Selected by Author(s))	18 Distribution Statement
Global Modeling Satellite Data Assimilation Future Observing Systems FGGE	Unclassified - Unlimited STAR Category 47

19 Security Classif (of this report)	20 Security Classif (of this page)	21 No of Pages	22 Price
Unclassified	Unclassified	234	A11

For sale by the National Technical Information Service, Springfield, Virginia 22161

GSFC 25-44 (10/77)

☆U S GOVERNMENT PRINTING OFFICE 1984 537-086/ 32

National Aeronautics and
Space Administration

Washington, D.C.
20546

Official Business
Penalty for Private Use, $300

SPECIAL FOURTH CLASS MAIL
BOOK

Postage and Fees Paid
National Aeronautics and
Space Administration
NASA-451

NASA

POSTMASTER: If Undeliverable (Section 158 Postal Manual) Do Not Return